UNIVERSITY OF
CHEMISTRY AND TECHNOLOGY
PRAGUE

Faculty of Chemical Engineering

Department of Chemical Engineering

Chemical engineering contribution to artificial life research

HABILITATION THESIS

AUTHOR | **Ing. Jitka Čejková, Ph.D.**

YEAR | **2019**

To my son and my parents

I hereby declare that this thesis is my own work. Where other sources of information have been used, they have been acknowledged and referenced in the list of used literature and other sources.

Prague, February 27, 2019

Abstract

Artificial life is the study of artificial systems that exhibit the behavioural characteristics of natural living systems. This thesis introduces the field of artificial life with an emphasis on wet artificial life, which aims to synthesize artificial cells from chemical precursors. The challenge of creating an artificial cell composed of all attributes of living counterparts (such as growth and development, homeostasis, movement, energy use) is one that is yet to be solved. Our ambition is to create a system that will at least partly mimic cell behaviour. We focus on the investigation of organic droplets in the presence of aqueous solutions of surfactants. We have found that in a similar way to living cells, these droplets are able to perform chemotactic movements in concentration gradients of chemoattractants, change their shape or behave collectively. Recently we proposed to call such droplets with life-like behaviour "liquid robots". The relation of liquid robots to the origin of the word "robot" will also be discussed. Artificial life is very interdisciplinary, and it will be shown how chemical engineers in particular can contribute to solving the open problems in the field. Droplets defined as liquid robots are a novel concept that could find engineering applications in various areas, such as environmental sensing and remediation.

Contents

Artificial Life can contribute to theoretical biology
by locating life-as-we-know-it within the larger
picture of life-as-it-could-be.
Christopher G. Langton

1 Introduction

1.1 Artificial life

Nature has found one method of organizing living matter, but maybe there are also other not yet discovered options on how to create life. And to study the life as it could be is the objective of an interdisciplinary field called Artificial Life (commonly abbreviated as ALife). The word "artificial" refers to the fact that man is involved in the creation process. The results might be completely unlike natural forms of life, not only because of the chemical composition, but even some computer programs exhibiting the life-like behaviour interest the ALife researchers.

ALife field was established at the first *"Interdisciplinary Workshop on the Synthesis and Simulation of Living Systems"* in Los Alamos in 1987 by Christopher G. Langton [1]. Currently ALife is a radically interdisciplinary field that is not even defined as pure "science" or "engineering" field, it is beyond that [2]. It involves both, experimental and theoretical approaches and the research is fundamental and mainly curiosity driven. Usually the applications are coming as a by-product but they are not the goal. The common characteristic of all so-called "ALifers" (researchers in ALife field) is their open mind. The community of ALifers is very miscellaneous, it contains computer scientists, physicians, chemists, biologists, engineers, experts in robotics, philosophers, artists, and representatives from many other disciplines. As I am actively involved in ALife research several years already, I proudly name myself as ALifer as well, although officially I am a chemical engineer. This thesis aims to introduce the artificial life discipline and discuss the questions such as "How a chemical engineer can contribute to artificial life research". The emphasis will be placed on topics related to my research interests, namely on chemistry and artificial life forms and their life-like behaviour. I will also introduce the concept of liquid robotics.

There are several approaches to defining ALife research. One ALife sorting could be into soft, hard and wet (Figure 1). Some ALifers are working on "soft" ALife aiming to create simulations or other purely digital constructions exhibiting life-like behaviour. "Hard" ALife is related to robotics and implements life-like systems in hardware made mainly from silicon,

steel and plastic. "Wet" ALife uses all kinds of chemicals to synthesize life-like systems in the laboratory. According to this division, my work is related mainly to the wet artificial life, because I aim to study the life-like properties of chemical droplet systems.

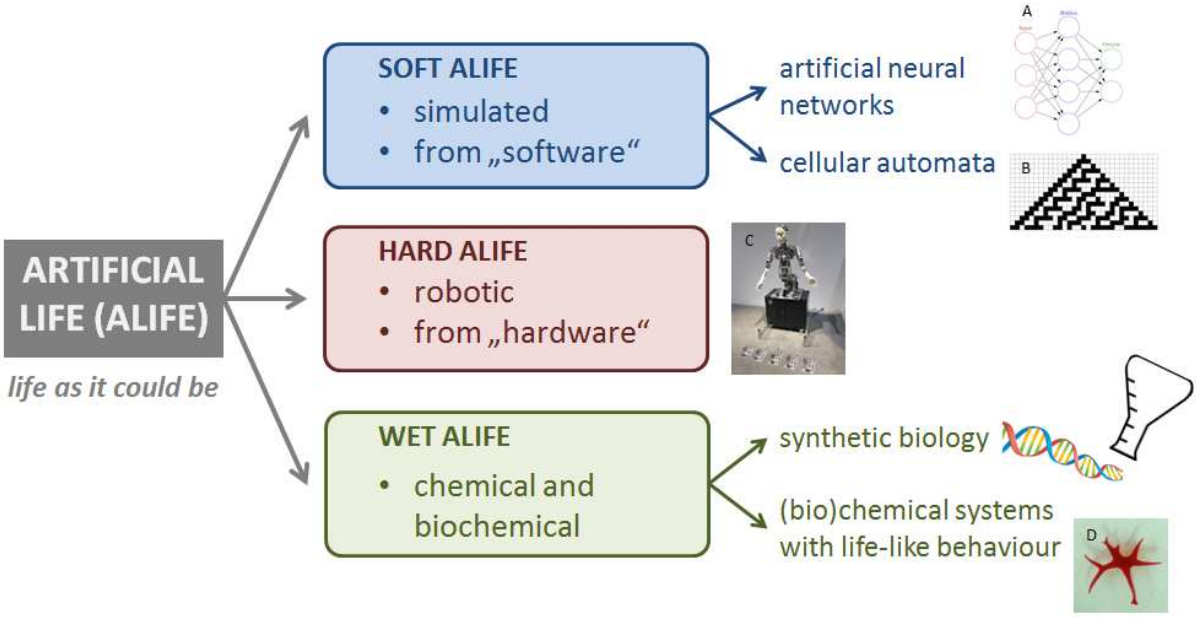

Figure 1. Artificial life research. (A – Artificial neural networks. B – Cellular automaton, rule 30. C – Robot Alter 2 in Miraikan in Tokyo. D – Shape changing decanol droplet.)

ALife is often confused with a related field called Artificial Intelligence (abbreviated as AI). Scientists do not have a rigorous standardized definition of what life is, even definitions of what intelligence is are not unified. However, everyone can feel the difference between life and intelligence intuitively, thus the differences in ALife and AI are also obvious. Roughly speaking what AI is to psychology and the philosophy of mind, ALife is to biology and the philosophy of biology [3]. AI uses the top-down approach to study the cognitive processes such as reasoning, memory, and perception. ALife by using bottom-up approach deals with the study of all processes characteristic for living systems. What is common in both fields is their history, because both have the roots in computer science and that both aim to study natural phenomena by simulating and synthesizing them.

M. Bedau *et al.* proposed 14 open problems in ALife in the year 2000, but none of them have been solved yet [4]. T. Froese and C. Gershenson with their colleagues summarized the ALife research interests and divided them into thirteen themes [5]: origins of life, autonomy, self-organization, adaptation (evolution, development, and learning), ecology, artificial societies, behaviour, computational biology, artificial chemistries, information, living technology, art,

and philosophy. It can be seen that ALife research is very broad and for readers interested in all the above mentioned problems I can recommend one of several comprehensive works on ALife in general (*e.g.* [1, 3, 4, 6-9]). However, in this thesis I will focus mainly on the problems related to my research, *i.e.* chemistry and artificial life forms.

More than 30 years ago the first ALife workshop took place, and every year since that the ALife community has come together. I have participated at four ALIFE or ECAL (European Conference on Artificial Life) conferences and I always enjoy these events. In comparison with other conferences where usually one narrow topic is presented, artificial life conferences are typical with their multidisciplinary and interesting discussions. It fascinates me what kinds of topics are discussed and although very often during the discussions many views on the problem are presented, nobody is wrong and everyone is at least partly right. There are so many basic questions that we are not able answer, such as "What is life?", "How the life originated on Earth?", "What is consciousness?" *etc.* Many of these questions are related not only to science but also to philosophy and each new view or thought can move the current state of knowledge in artificial life further. In 1995 one critic described his feelings from ALife meeting as that he was wondering "whether or not he has gone beyond the lunatic fringe" [10]. Nevertheless, some strictly conservative researchers have similar comments also in these days, because interdisciplinary research is permanently underestimated. In my view the interdisciplinary communities, such as community of ALifers, are needed to move the boundaries in science and technology further.

Figure 2. Photograph from ALIFE 2018 conference in Tokyo.

Moreover each ALIFE conference has a specific topic that usually opens new questions and starts new collaborations. For example ALIFE 2018 in Tokyo (Figure 2) subtitled *"Beyond AI"* focused on the future directions of artificial life research and potential applications. ALIFE 2019 that held this year in Newcastle aims to discuss how ALife research can help to solve societal challenges such as sustainability. In 2021 I will organize in Prague ALIFE 2021 subtitled *"Robots – one century past and ahead"* and on the 100th year anniversary of the word "robot" we will focus on the past, presence and future of robotics. Further I will describe the relation of the origin of the word robot to artificial life research more in details.

1.2 Engineering of artificial life

Let me discuss briefly the history of the word "robot", because this word is one of the key words of artificial life discipline. I will also show how the inception of this term is related to my droplet research. Almost one hundred years ago that the Czech writer Karel Čapek wrote his science fiction drama R.U.R. – *"Rossum's Universal Robots"* [11] (published in November 1920, premiered in Prague on 25 January 1921) where the word "robot" was used for the first time (Figure 3), this play opens many contemporary questions. I am fascinated by Čapek's work in general, nevertheless here I will discuss the chemistry and engineering aspects that appeared in R.U.R. play, although also many other Čapek's works open artificial life questions (*e.g. The Makropulos Secret, War with the Newts*).

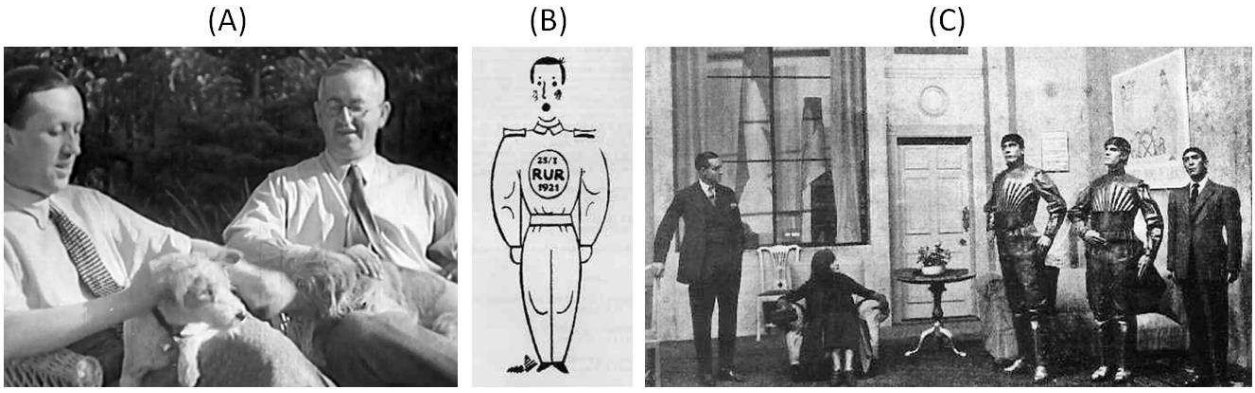

Figure 3. (A) The Czech writer Karel Čapek and his brother Josef that recommended him to use the word "Robot" for artificial people in the play R.U.R – Rossums' Universal Robots. (B) Karel Čapek as a Robot - caricature by his brother, painter Josef Čapek. (C) A scene from the first act of the theatre play R.U.R – Rossums' Universal Robots premiered on 25 January 1921 in Prague. (Public domain images). [12]

The origin of the word "*robot*" comes from the word "*robota*" which means *"corvée"* or *"serfdom"* in the Czech language, *i.e.* forced labour of the kind that serfs had to perform on

their masters' lands. R.U.R. play is about an island factory called Rossum's Universal Robots, where artificial people are fabricated and sent around the world as working machines. At the beginning of the play, the director of the company tells a story about the factory founder, an old mad scientist named Rossum [11]:

> *"Old Rossum* ***attempted by chemical synthesis to imitate the living matter*** *known as protoplasm until he suddenly discovered a substance which behaved exactly like living matter although its chemical composition was different… He wrote the following among his chemical specimens: '****Nature has found only one method of organizing living matter****.* ***There is, however, another method****, more simple, flexible and rapid, which has not yet occurred to nature at all. This second process by which life can be developed was discovered by me today' … Just think: he wrote these words about* ***a blob of some kind of colloidal jelly that not even a dog would eat.*** *Imagine him sitting over a test tube, and thinking how the whole tree of life would grow from it, how all animals would proceed from it, beginning with some sort of beetle and ending with a man. A man of different substance from us. Now, the thing was how to get the life out of the test tubes, and hasten development and form organs, bones and nerves, and so on, and find such substances as catalytics, enzymes, hormones, and so forth … And then old Rossum started on the manufacture of man.*"

However, this old fictional scientist failed. Old Rossum was obsessed to create a man from the synthetic living matter just to prove that God is not needed to create the living beings. The old Rossum's attempts were purely scientific. However, then his nephew, young Rossum, came with an engineering approach. Young Rossum decided to make artificial humans as working machines in the factory and he called them "robots".

> *"A man is something that feels happy, plays the piano, likes going for a walk, and in fact, wants to do a whole lot of things that are really unnecessary… But a working machine must not play the piano, must not feel happy, must not do a whole lot of other things. A gasoline motor must not have tassels or ornaments. And to manufacture artificial workers is the same thing as to manufacture gasoline motors. The process must be of the simplest, and the product of the best from a practical point of view… Young Rossum invented a worker with the minimum amount of requirements. He had to simplify him. He rejected everything that did not contribute directly to the progress of work -- everything that makes man more expensive. In fact, he rejected man and made the Robot… The Robots are not people.*"

In Čapek's play, young Rossum is described as a very progressive engineer. He began to overhaul anatomy and tried to see what could be left out or simplified. He used his engineering knowledge and experience to design and optimize the artificial human beings so that they function with the maximum efficiency. He fabricated each part of the body separately and then combined them together as the car is manufactured from individual parts.

> *"The pestle for beating up the paste. In each one we mix the ingredients for a thousand Robots at one operation. Then there are the vats for the preparation of liver, brains, and so on. Then you will see the bone factory. After that I'll show you the spinning mill.... For weaving nerves and veins. Miles and miles of digestive tubes pass through it at a time."*

Similar approaches are currently used by researchers that aim to fabricate the artificial organs. The human body can be thought as a chemical plant that incorporate a number of subsystems in which enzymatic processes and unit operations are taking place. For example, the heart may be viewed as a pump that distribute the blood through the body, the veins are like pipes, the lungs are adsorbing and desorbing gas via biomembranes, the digestive tract serves as bioreactor engaged in decomposition or synthesis of various substances, the filtration units in the body are represented by kidney, *etc.* The schematic representations of these ideas are shown in Figure 4.

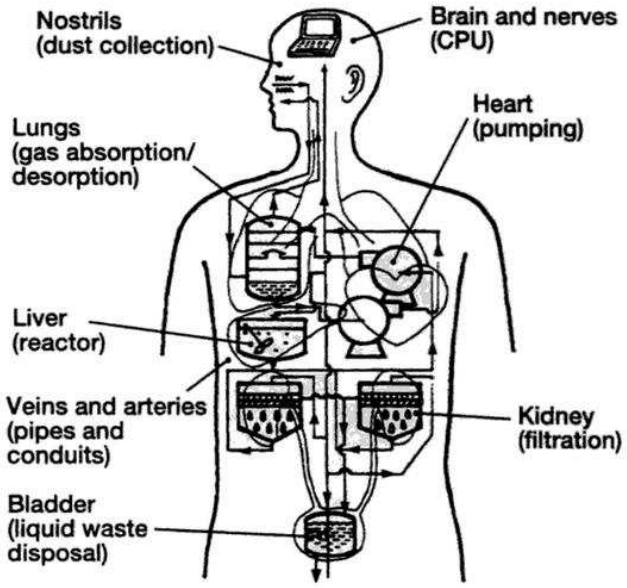

Figure 4. The body as a chemical plant – most of the organs are analogous to common chemical plant systems [13].

The objectives of both old and young Rossums in the play R.U.R. were to create artificial human beings. In our Laboratory of Chemical Robotics established in 2008 by Prof. Štěpánek, we are much more modest. Our objectives of artificial life research are to start with much simpler forms of life – cells. We aim to create artificially small objects with as many possible attributes of living cells. If we compare the idea to fabricate robots as creatures with only those human-like properties that are needed for specific tasks, then we can create robotic counterparts of living cells and we can reject all the unnecessary properties. I started to investigate droplets with few life-like properties and I proposed to call them "liquid robots". We can say that liquid chemical robots are mimicking living cells in the way that they have only a few cell-like properties necessary for the implementation of a specific goal. I am aware that many researchers at the world have similar ideas and objectives. In literature one can find the mismatch of terms, which deal with man-made objects showing life-like cell behaviour. The terms protocell, minimal cell and artificial cell are often used interchangeably. Moreover we created the terms "chemical robot" and "liquid robot". In the next section, I will summarize the differences between these concepts.

1.3 Protocells, artificial cells, liquid robots

The living cell is the basic structural, functional, and biological unit of all known living organisms. Such living cells are found in nature and produced and maintained by homeostasis, self-reproduction and evolution - three characteristics that may define a natural living cell [14]. In contrast, artificial cells are prepared by humans and mimicking the properties, functionalities, or processes of natural cells. Therefore artificial cells (or synthetic cells) are man-made systems with some similarity to living cells. Although there are many laboratories working on the synthesis of artificial cells, the successful preparation of synthetic cells having all features of natural living cells is still a challenging task and an artificial cell that is able to self-produce and maintain itself (so-called autopoietic system) has not been demonstrated yet [15]. The simpler and less problematic task is to synthesize protocells that are not necessarily alive exhibiting only some life-like properties. Protocells can be defined as simplified systems that mimic one or many of the morphological and functional characteristics of biological cells. Their structure and organization are usually very simple and can be orthogonal to any known living system. Protocells are used both as model systems in artificial life research and as model systems for origin of life research. In the latter case, protocells are often defined as hypothetical precursors of the first natural living cells [16].

In principle, there are three main approaches to prepare protocells, which are categorized as the "bottom-up", "top-down" and "middle-out." The bottom-up approach starts with non-

living components assembled to create cell-like structures, whereas the top-down approach to make a minimal cell is based on taking existing microorganisms and removing genes apparently not essential for survival [15]. Some researchers use a middle-out strategy that employs existing biochemical molecules such as enzymes in constructing an artificial cell [17].

All published papers with "artificial cell", "protocell", "chemical robot" in the title describe usually simple particles that have at least one property in common with living cells (Figure 5). Nevertheless, there is formidable challenge to synthesize an artificial cell having all properties typical of living cells, *e.g. (i)* with a stable semi-permeable membrane that mediates the exchange of molecules and energy between internal content and external environment while preserving specific identity, *(ii)* sustaining themselves by using energy from its environment to manufacture at least some components from resources in the environment using metabolism and *(iii)* capable of growth and self-replication including the genetic information [18].

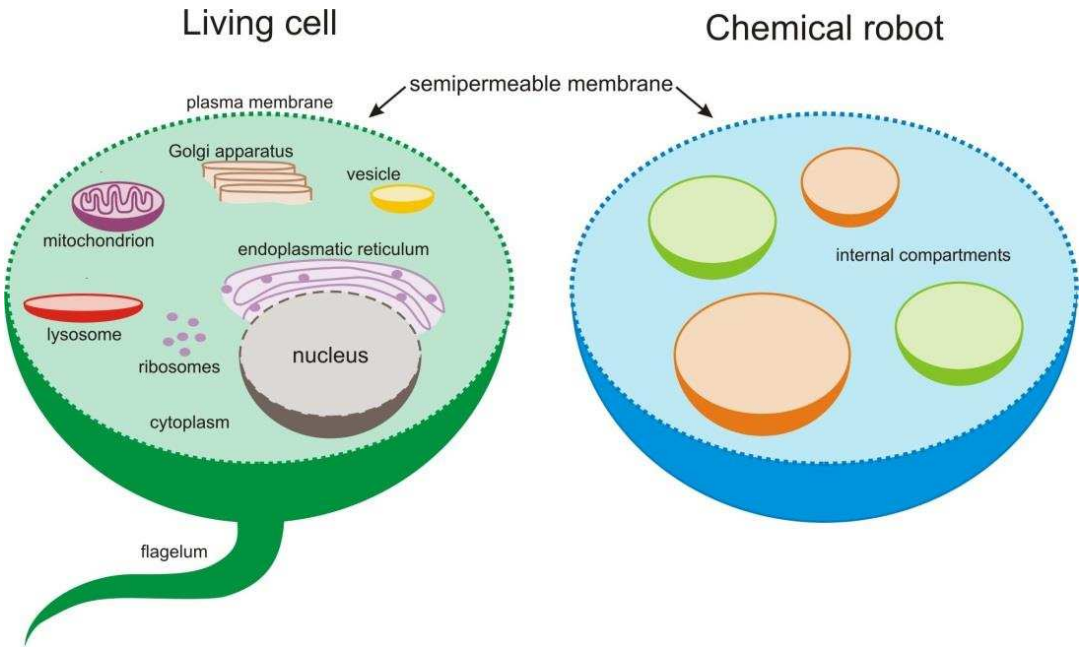

Figure 5. Comparison of a living cell and a chemical robot.

As we focus on the current research on protocells or artificial cells, we can find that they could take different forms (see examples on page 11 and Figure 6). They could be embodied as solid particles [19, 20], coacervates [21], hydrogel microcapsules [22], lipid vesicles [23] or droplets [24, 25]. In principle the research focus using protocells could be the studies of cell-like membranes [26], growth and division [27, 28], or motility [16]. Recently it was shown how

artificial cells can communicate with their living counterparts [29, 30]. However, the majority of research assumes the spheroidal shape of protocells, and there is not much focus on the shape and shape changes of protocells and artificial cells [31], although living cell exhibit a plethora of intriguing shapes. One notable exception is the growth of elongated protocells where the shape plays an essential role in the fission dynamics [27]. The shape changes of liquid robots with cell-like properties in the form of droplets and their relevance to living cells will be discussed in more details in Chapter 4.

In principle, the effort to prepare an artificial cell could be from two main reasons. One group of researchers endeavour to answer the questions about origin of life, they synthesize primitive cells which consists from a protocell membrane that defines a spatially localized compartment, and genetics polymers that allow for the replication and inheritance of functional information. The aim is to create self-replicating for example vesicles and to observe spontaneous Darwinian evolution of protocells in laboratory conditions [27, 32-34]. Such approach could be compared to the old Rossum's attempts in R.U.R. because he wanted to demonstrate that the life can be created by anyone in the lab and that no "higher power" as God is needed.

On the other hand, some researchers want to prepare particles with life-like properties that can mimic the behaviour of living cells, although without the ability to self-replicate or evolve. Such objects can move in their environment, selectively exchange molecules with their surrounding in response to a local change in temperature or concentration, chemically process those molecules and either accumulate or release the product. Such synthetically made objects can find the application for example as smart drug delivery vehicles that can produce the medicine *in-situ*. Such artificial cells could also be called chemical or liquid robots [35]. And such research projects are comparable to the objectives of young Rossum in R.U.R., because his aims were to create only the artificial servants that could help people with many activities.

Similarly as a chemical engineering approach can be used for artificial organs or robots fabrication (Figure 4), the design principles from chemical engineering can be borrowed and transferred also to processes related to artificial cells creation [36]. It shows that the unit operation concept is successful and widely used paradigm not only in chemical engineering. A chemical engineer designing a chemical plant breaks down the whole process into elementary steps as heat or mass exchange. Then the suitable method for each operation has to be chosen (*e.g.* it is needed to decide which method is better for separation in a specific system – distillation or adsorption?) and finally the appropriate apparatus must be

designed and constructed. With the same approach, the complex cell system can be divided into simple subsystems. And such decomposition leads to subtasks that can be solved more easily than the whole problem. The creation of artificial cells contains the steps such a design and synthesis of containers with similar properties as the cell membranes have or looking for autocatalytic reactions mimicking the metabolism of cells. Although the chemical engineer can gain knowledge about design and constructions of plants at school, the field of artificial life is still in its infancy and the design and synthesis of artificial cells is still a challenging task.

Let me summarize this chapter and emphasize my main idea. Many researchers from the wet artificial life field and synthetic biologists aim to create artificial objects that resemble the living cells and very often the term "artificial cells" is used for them, although they do not have all the properties typical for living cells. I claim that using the term "artificial cell" for an entity [37] without all life manifestations is not correct. Similarly as we use the term "robot" for machines mimicking human behaviour just partly, I propose to use the term "liquid robot" [35] for small scale droplets mimicking the behaviour and properties of cells or small organisms only partially. I will use the term "liquid robot" for droplets with life-like behaviour in this thesis because I take the inspiration from nature and I will focus on cell-like behaviour of droplets but not in such a degree to be worthy to call them artificial cells. And I renounce to use the term artificial cell also because of the size of droplets. I study the eye-visible droplets with the volume of units of microliters each, which is more comparable to the size of multicellular organisms such as small insects. And one more reason for using of the term "robot" is the relation to the description of protoplasm (substance for fabrication of the robots) in the play R.U.R.: *"a blob of some kind of colloidal jelly that not even a dog would eat."* This description also very often fits to the chemical systems that I am working with.

I could compare my research on motile liquid robots to the work on testing of self-driving cars. I am interested how our liquid robots move and interact between each other and with the environment, how they sense the changes in their surround and how they can alternatively respond and adapt themselves to these changes. As well as the research on self-driving vehicles is divided in several parts (design, construction, programming, testing, answering the questions about safety, legislation) and nobody can do everything in once, the same approach is needed also in liquid robot research. As well as people programming and testing self-driving cars do not focus on problems such as how to make a car that is able to repair itself or build another car, we do not focus on the self-reproduction or evolution of the liquid robots.

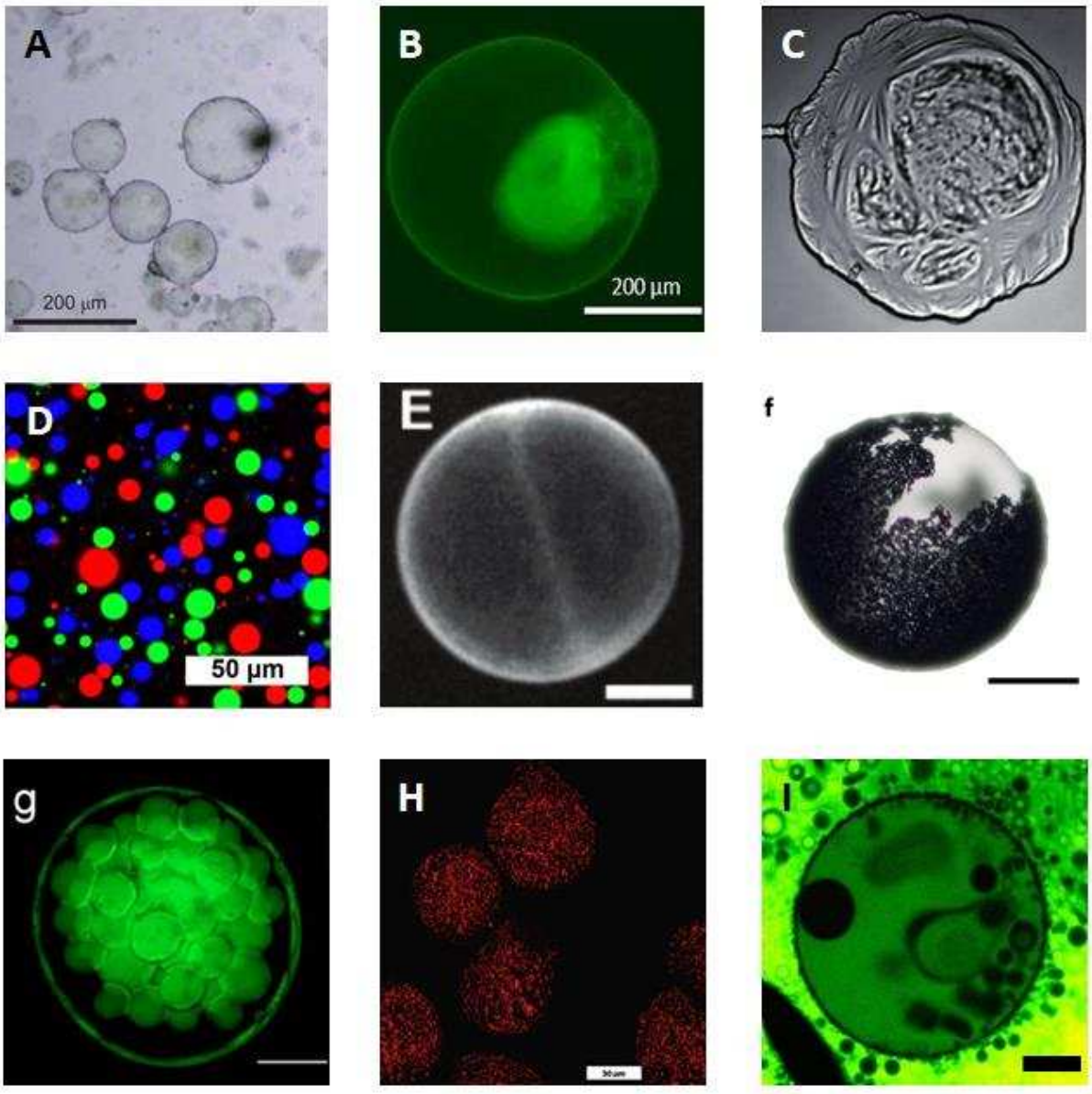

Figure 6. Examples of protocells and artificial cells from literature. (A) Silica nanoparticle-stabilized aqueous protocells [38]. (B) An enzyme-containing protocell assembled from a mixture of DNA and clay particles [39]. (C) Inorganic Chemical Cell: iCHELL, diameter 1.2 mm [40]. (D) Complex copolymer-stabilized coacervate protocells in the form of microdroplets [41]. (E) Self-propelled oil droplet based on fatty acid chemistry, scale bar 100 µm [42]. (F) Synthetic protocell in the form of silica colloidosome, scale bar 100 µm [43]. (G) Assemblies of aqueous droplets in hydrogel as protocell model, scale bar 1 mm [44]. (H) Artificial cells in the form of alginate microcapsules containing immobilised liposomes, scale bar 30 µm [22]. Fatty-acid liposomes compartmentalize inside a clay vesicle, scale bar 10 µm [45].

This thesis will be structured as follows. In Chapter 2, the concept of droplets as liquid robots will be introduced and the state-of-the-art of research in this area summarized. Chapter 3 will focus on the oriented motions of both living and artificial object in concentration gradients (so called biological and artificial chemotaxis). The role of morphological changes in living and artificial systems will be discussed in Chapter 4. Collective behaviour is the main topic of Chapter 5. In Chapter 6, I will present the works where I studied artificial systems, although such research was not directly related to artificial life field. In the end I will outline the future directions in artificial life research.

Imagination is more important than knowledge.
Albert Einstein

2 Droplets as liquid robots

2.1 Droplets

Why I am so fascinated by droplets? Why did I decide to study them? They are present in our everyday life and they seem to be such simple objects. And that is advantageous, because the handling of them is easy and cheap. On the other hand the droplets can exhibit fascinating phenomena that are either overlooked because of their omnipresence or are not visible. Some phenomena can be observed by everyone by naked eye, some are visible only by using for example microscopes. Some processes can attract our attention in the real time, however some phenomena are interesting only when we use the camera and then we change the speed of the movie. One example could be the impact of a rain droplet on a solid surface – in real time nobody can see the beauty of the bouncing, spreading and splashing of the droplet, however we can use the high speed camera and watch the movie slowed down [46]. On the other hand there are many processes that are very slow and in the real time the system could look static. We have already observed a few new interesting phenomena within our previous research [47-49] and I anticipate that my further ALife oriented research on liquid robots will uncover even more new interesting phenomena on various spatial and temporal scales.

Current world-wide research on droplets is intensive from various points of views. The knowledge of interfacial phenomena is important for solving of many problems in industry, agriculture, medicine and other areas. In simple term, the research on droplets is related to almost all processes where liquids are present. The objectives of droplet research could be the understanding of droplet formation, droplet evaporation, coalescence, emulsion formation, spreading on surfaces, movement in microfluidic chips, *etc*. Recently the droplet studies became popular also in the artificial life research, not only in the context of microscopic protocells that would answer the questions of the origin of life [50]. It has been shown that also larger droplets can perform several life-like operations, *e.g*. they can self-propel [42, 51-54], move chemotactically in the gradients of various chemicals [49, 55, 56], self-divide [57-62], change their shape [47, 63] or behave collectively [48, 64, 65].

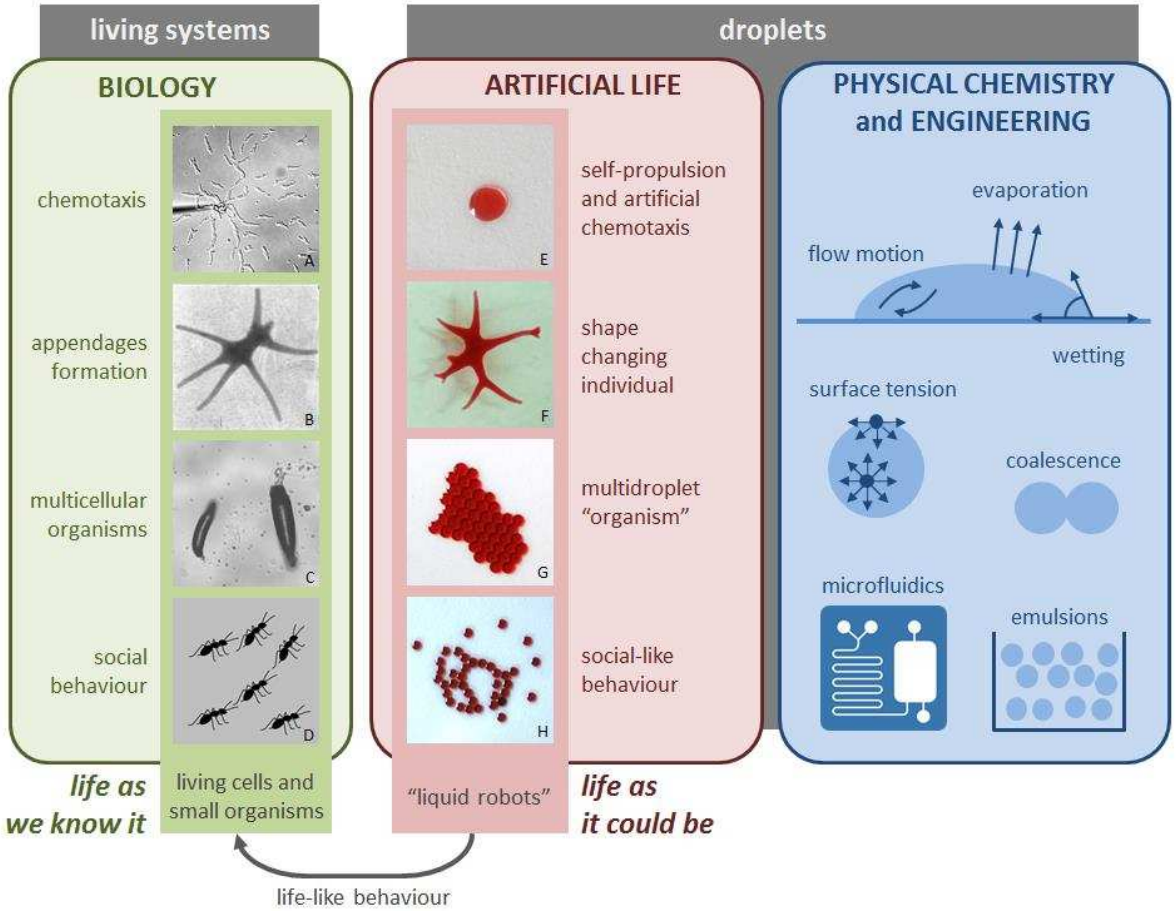

Figure 7. Schematic position of droplet research in various scientific fields. The artificial life studies focusing on life-like behaviour of droplets are related to biology, on the other hand for the explanation of the phenomena observed the experience and knowledge from physical chemistry and engineering are needed. A – Chemotaxis of *Dictyostelium* cells [66]. B - Prosthecate freshwater bacteria *Ancalomicrobium* [67]. C – Multicellular slug stage of the *Dictyostelium* developmental cycle [68]. D – Schematic representation of ants group. E-H – Decanol droplets placed into aqueous solution of sodium decanoate.

Figure 7 shows schematically the position of droplet research in various scientific fields. The artificial life studies focusing on life-like behaviour of droplets are related to biology, on the other hand for the explanation of the phenomena observed the experience and knowledge from physical chemistry and engineering are needed. Although liquid robots are chemically based I am interested in understanding how they move, change their shape, behave in a large group in a complex environment, and what "laws" govern these processes. For my research I use similar approaches to biologists, *i.e.* I observe both a single droplet and population of droplets. I study the droplet as a single entity and also investigate its individual

parts (surface, inner volume) using various microscopic and for biologists common techniques. On the other hand I study the system purely from the physicochemical point of view and I use the methodologies that are standard for engineers. Further, the knowledge and experience from artificial intelligence and robotics and the methodology and terminology from sociology are beneficial for us when studying the collective behaviour in droplet populations.

As this chapter aims to focus on the life-like behaviour of droplets, further I will summarize the existing research on droplets. I will give the overview of my results in this area in the following Chapters 3-5 later. Generally, droplets are liquid entities where a degree of immiscibility is required between at least two phases, so that the cohesion of molecules can give rise to a surface tension that defines the shape of a droplet. We could have for example a water or oil droplet in air, a water droplet in the oil phase or an oil droplet in aqueous solution. The term "oil" refers to the organic liquid. My research primarily focuses on systems consisting of oil droplets in aqueous solutions (namely decanol droplets in aqueous sodium decanoate solution). In oil or aqueous phases we can dissolve various chemical substances or disperse insoluble particles and they in dependence on their hydrophilic/hydrophobic properties preferentially stay in the aqueous or oil phase. However, some molecules, such as amphiphilic surfactants, containing both hydrophilic head and hydrophobic tail prefer to self-assemble on the interphase boundary. The presence of amphiphilic molecules on the droplet surface could protect the droplets from coalescence with other droplets.

The research on droplets with life-like properties is very often related to surface active molecules and it covers the range of droplet sizes from hundreds of nanometres to millimetres. The majority of papers deal with vesicles or liposomes which are in principle droplets in the size of maximally hundreds of micrometres covered with the continuous phospholipid bilayer. The research on sub-millimetre droplets in the form of vesicles and liposomes belongs to the protocell research aiming mainly to answer the question about origin of life, but further here I will summarize only the research on droplets that are in the size with the volume around 1 μL or more and visible by naked eyes.

One of the most studied properties of droplets that can mimic the cell behaviour is their self-propulsion. It has been shown how droplets move on solid substrates [69, 70] or how floating droplets move due to the changes in the surface tension. When a surface active compound is placed into an aqueous system it interacts with the water molecules and lowers the surface tension of the solution. When the surface tension of a liquid is altered, liquid flows from areas of low surface tension to areas of high surface tension along an interface

(this phenomenon is known as the Marangoni flow). The term tensiophoresis has been used in some works for a droplet movement in the gradient of surface tension [71, 72]. The properties of the Marangoni-driven movement are dependent on the size and the shape of the droplets as it has been shown for example in works on pentanol [73] or oleic anhydride fuelled droplets [74]. When the external chemical gradient is present and the self-propelling droplets follow this gradient they can mimic the chemotaxis of living cells. Such artificial chemotaxis was studied *e.g.* in a system based on fatty acid chemistry [42, 54, 56], nitrobenzene droplets containing DEHPA in a gradient of alkaline-earth metal ions [75] or in pH gradients [76]. There are many other examples and their summary you can find in our recent review paper [35]. My research on decanol droplet chemotaxis will be described more in details in Chapter 3.2.

However, there are other approaches how to control the movement of droplets, such as by external magnetic [77, 78] or electric [79] field, but these works are mainly related to manipulation of aqueous droplets in oils, which is the inverse situation to systems that I have worked with. Previous works describe the controlled movement of water droplets on solid surfaces that is based on electro-wetting [80]. Some works are related to meniscus driven movements. Recently, it was shown how an oil droplet is repelled by the meniscus when the water does not include surfactant, and inversely it is attracted to the wall when there is surfactant added in water [81]. Moreover, this paper presents a very simple system consisting of drinking water, plant oil and dishwashing detergent as surfactant. This is an example that liquid droplets are in principle already easily accessible and exploitable. Similarly, very simple system has been introduced where the curvature-driven droplets moved on spiral surfaces [82].

Up until this point I have discussed droplets either not stabilized or stabilized by surfactants. However, not only surfactant molecules can protect the droplets from coalescing. Another way how to stabilize the liquid droplet is to cover the droplet by solid particles. By this approach the so called "liquid marble" is created. Liquid marble preparation is very simple – a small amount of liquid is rolled on the layer of hydrophobic powder consisting of nano- or micro-particles, which spread spontaneously at the liquid / air interface. This process results in a liquid marble formation that has some of the properties of a liquid droplet and at the same time it behaves as a soft solid. Liquid marbles are an alternative to superhydrofobic surfaces, because particles preventing the liquid to wet and contaminate the carrier surface which can be a solid or liquid surface. It has been already shown that liquid marbles can be used for transport of small volumes of liquids [83-85]. We have the experience only with

static liquid marbles [86], we used them as carriers of poorly-water soluble drugs [87, 88] and as micro-bioreactors for spheroid cultivation of HT-29 carcinoma cell line [89]. In Chapter 6.2 it will be shown how we used liquid marbles for artificial tumours cultivation.

2.2 Setups for droplet experiments

The contemporary experimental research on oil droplet life-like behaviour is performed in various geometrical configurations. The most common setup is the use of round Petri dishes with various diameters and depths of the continuous phase (*e.g.* [53]). For droplet movement observations sometimes a circular channel is created, *e.g.* by attaching two rings to the glass substrate (*e.g.* [90]). The space between the inner and outer rings (walls) form in principle an endless channel ideal for self-propelled droplets experiments. Further simple systems are based on rectangular cells or wide channels. Some works deal with the droplet movement in more complex systems such as mazes [49, 91] or arenas with obstacles [92]. Let me mention that one can find an uncountable number of papers on microfluidics, however in those works the droplet motion is due to the flow of external fluid, which is a different scenario in comparison with our experiments. In our experiments the droplets are self-propelled and/or driven by Marangoni flows that arise in the system because of the local chemical changes.

The dimensions of systems for droplet studies vary. Usually the experiments are performed in Petri dishes with diameter of several centimetres. One of the longest straight channels that I have found in literature for self-propelled droplets studies has the dimension of 300 × 15 × 10 mm [93]. Researchers study the self-propulsion of droplets, but to the best of my knowledge, nobody has proven yet the longest distance that the droplet is able to travel in two dimensional space without any collision with the wall or without any other boundary effect. This objective is also written in my "list to do".

The size of individual droplets is usually in order of units or tens of microliters. The reason is to have a system where the surface tension dominates over the gravitational forces. This relationship can be reached when Bond number is lower than one ($Bo = \Delta\rho\ g\ L^2/\sigma$, where $\Delta\rho$ is the difference in density of the two phases, g gravitational acceleration, L characteristic length and σ surface tension). The largest self-propelled droplets that I have found in literature had the volume 50 μL [74, 94].

The droplet motion can be characterized by several parameters, the most common are the directionality and velocity. Additional parameters include the so-called active period and the cruising range, which is defined as the distance (usually in the units of droplet diameters) that a droplet travels during its active period. For chemotactic response it is possible to

evaluate also the so-called induction time, which is defined as the time elapsed between the addition of a chemical signal and the start of the droplet movement. The motion of small droplets (so called micro-swimmers) is usually observed up to one hour [95] or two hours [56]. The exceptions are our work where we observed the droplet dancing several hours [48, 96] and the droplets oscillations in the system of my collaborator S. Tanaka that were recorded even several days [97].

The majority of experiments described in literature were performed "by hand", meaning the droplets were dropped by using pipettes or syringes manually. For production of larger numbers of droplets the microfludic chips can be used. On the other hand there are works where the experiments were performed by using robots. The leading group in research on using artificial intelligence and robotic platforms for performing and even planning of experiments with droplets is the Cronin's Laboratory at University of Glasgow. Their research is oriented on the evolution of droplets. They have already presented 3D-printed fluidic chemorobotic platform with configurable environments [65, 92]. We were collaborating with this laboratory and several other groups within the European project Evobliss that focused on fabrication and implementation of robotic platform "Evobot" for chemical life studies (Figure 8) [98].

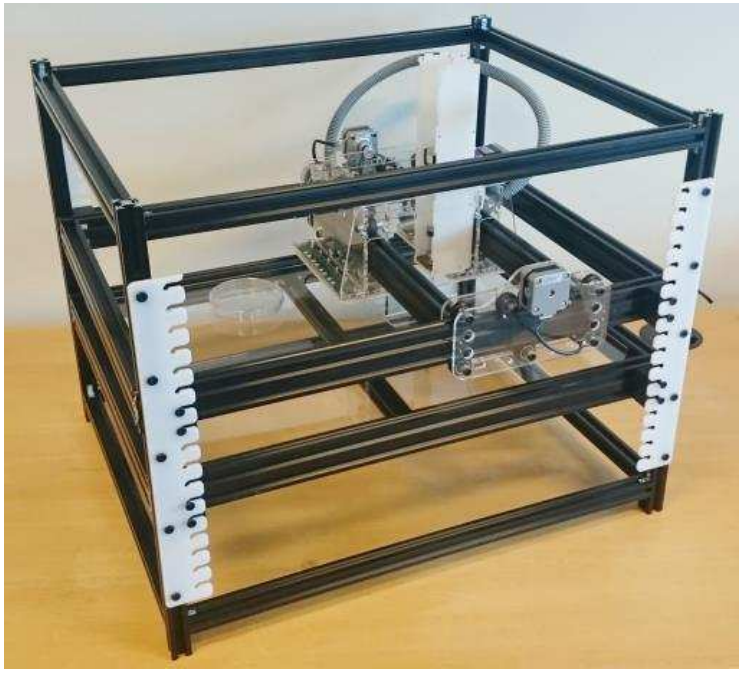

Figure 8. The first prototype of Evobot (designed and fabricated at IT University of Copenhagen).

Related works

- **Čejková J., Banno T., Štěpánek F., Hanczyc M.M. (2017). Droplets as Liquid Robots, *Artificial Life*, 23 (4), 528-549. (Appendix 1)**
- Nejatimoharrami F., Faina A., **Čejková J.,** Hanczyc M., Stoy K. Robotic Automation to Augment Quality of Artificial Chemical Life Experiments. *Proceedings of the Artificial Life Conference 2016*. 04.07.2016, Cancún, Mexico. MIT Press, ISBN: 978-0-262-33936-0, 2016, pp. 634-635.

Plahočím se jen tam, kam chci já, a ne tam, kam ně
někdo pošle. Víc nemůžu od života chtít.
Miroslav Zikmund

3 Chemotaxis

3.1 Chemotaxis in nature

Chemotaxis is a natural way for cells and organisms to perform oriented movement in a chemical gradient. The term comes from Greek words *khemia* (chemistry) and *taxis* (arrangement, order). The movement of cells and organisms could be controlled by other various external forces and then the appropriate response is called according to the force that induced this movement [99]. For example, gravitational force induces gravitaxis (geotaxis), movement in the gradient of cellular adhesion sites or substrate-bound chemoattractants is called haptotaxis, electrotaxis (or galvanotaxis) is the directional movement in response to an electric field, magnetotaxis is movement in magnetic field, phototaxis is the ability to response to light and thermotaxis is migration along a gradient of temperature.

Taxis should not be confused with tropism [12]. The terms geotropism, chemotropism, phototropism *etc.* mean the oriented growth of organisms navigated by appropriate stimulus without the physical motion of the growing object or changing of its position. Another term that is often confused with tactic movement (taxis) is kinesis, which means the increase of motility in response to a stimulus. However, such response is non-directional. For example, chemokinesis represents a situation when the speed or frequency of cell locomotion is determined by substances present in its environment. The presence of chemokinetic mediators can either intensify or suppress the motion activity.

The difference between the terms chemotaxis, chemokinesis and chemotropism is shown in Figure 9. Chemotaxis (Figure 9A) is a response to the gradient of a chemical stimulus by directional movement. In the absence of the gradient of a chemoatractant, cells perform random movement. However, if the gradient of a chemoattractant is present, the cells perform oriented movement towards the area with the highest concentration of the chemoattractant. Such behaviour is called positive chemotaxis. On the other hand, if the cells move away from areas with the highest concentration of harmful substances (chemorepellants), this response is called negative chemotaxis. The most important sign of chemotactic movement is directionality.

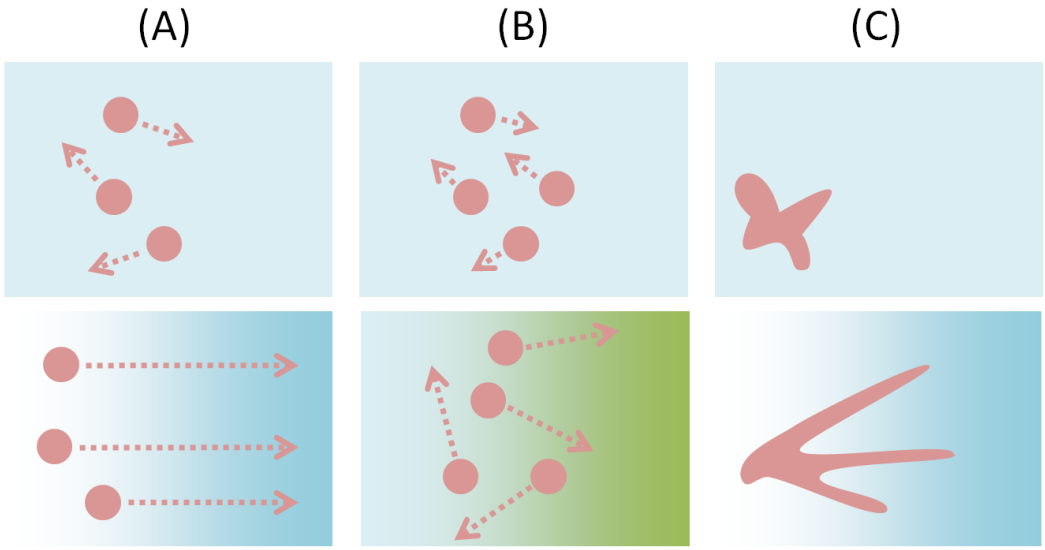

Figure 9. Schematic explanation of the difference between terms chemotaxis, chemokinesis and chemotropism. (A) Chemotaxis - a response by which the direction of locomotion of cells is determined by chemical substances in their environment. (B) Chemokinesis - a response by which the speed of cells moving at random is determined by chemical substances in the environment. (C) Chemotropism - the directional growth of parts of a cell navigated by a chemical stimulus. Upper part – without any stimulus, lower part – in the presence of a chemical gradient. [12]

Chemokinesis (Figure 9B) is a response by randomly moving cells that increase or suppress their moving activity due to the presence of a chemical stimulus, but they do not orient their locomotion in any way. Chemokinesis can be positive if the rate of random movement is increased (this is the case in Figure 9B) or negative if the movement rate is decreased.

Chemotropism (Figure 9C) is an oriented growth response of an organism to a stimulus. The growth response may involve the entire organism or its parts. As in the previous cases, the growth response may be either positive or negative.

All of these kinds of movements are well-known for biological objects, but recently several works focused also on the movement of synthetic objects and several of them are present in the recent book *"Self-Organized Motion: Physiochemical Design based on Nonlinear Dynamics"* edited by S. Nakata *et al.*, where we contributed with Chapter 8: *"Chemotactic droplets serving as chemo-taxi"* [12]. We also compared the biological and artificial chemotaxis in a book chapter titled *"Chemotaxis and chemokinesis of living and non-living objects"* [99]. Further I will discuss similarly as in these book chapters how living cells sense the changes of chemical concentrations in their environment and how they can respond to such changes. Microorganisms and somatic cells use chemoreceptors to detect the

concentrations of chemicals in their environment and consequently very complex intracellular signal transduction pathways are activated leading to the appropriate response. These processes are highly sophisticated, for example *E. coli* chemotaxis signalling pathway can amplify stimuli at least 50-fold, *i.e.* a 1% change in receptor occupancy elicits a 50% change in the rotational bias of the flagellar motors that are used for cellular swimming [100].

The cell motility alone is a very complex process and to explain the mechanism of even chemotaxis or chemokinesis is out of the scope of this thesis. Briefly, many kinds of cellular motions are driven by the actin network beneath the cell membrane. The cell movement is a manifestation of mechanical work, which requires a fuel (ATP) and proteins that convert the energy stored in ATP into motion. There are different modes of cell motility, the cells can swim freely in their environment by using special organelles (*e.g.* flagella), they can perform amoeboid motion and glide smoothly along the surface.

In single cellular organisms chemotaxis plays a crucial role not only for moving towards nutrients, but it is also responsible for collective cell migration [101]. In multicellular organisms chemotaxis is involved in early development (*e.g.* sperm moves towards the egg during fertilization [102]) and subsequent phases of development (*e.g.* lymphocyte migration is essential for the activity of the immune system [103]). Further, chemotaxis of tumour cells is an essential component of tumour dissemination during progression and metastasis [104, 105].

Another reason why the chemotaxis in nature is very important is that it helps cells to communicate between each other and it is involved in quorum sensing and collective behaviour. As an example of such behaviour the slime mould *Dictyostelium discoideum* could serve. *Dictyostelium discoideum* is a biological system that I am familiar with [68, 106, 107] (my diploma thesis under the supervision of Ing. Hana Ševčíková, CSc. focused on *"Studies of atypical aggregation of Dictyostelium discoideum"* [108]) so it is my favourite model system when comparing natural and artificial life. *Dictyostelium discoideum* is a microorganism that under normal conditions consists of independent single amoebas and under unfavourable conditions, these cells become "social" and enter a multicellular developmental program. After the initiation of starvation, pioneer cells release pulses of cyclic adenosine-3',5'-monophosphate (cAMP). Nearby cells sense this compound and start to move chemotactically in the direction where the cAMP concentration rises most rapidly. By using chemotaxis, cells aggregate into multicellular object enabling them to survive unfavourable conditions.

3.2 Artificial chemotaxis

Everyone can imagine a macroscopic robot that can be preprogramed or remotely controlled to perform a target mission or a self-driving car that moves as needed through streets thanks to a navigation system. But how about small liquid robots in the form of droplets, where it is not possible to embed the control panel? How could they operate in their environment? Imagine the situation that we would like to construct a miniaturised robot that will serve for so called intelligent cleaning of areas or surfaces that are difficult to access. The compound that is needed to be disposed of is appearing just time to time, anyway it is dangerous substance and the cleaning robot should be always ready to perform its target mission, *i.e.* deprive the environment of this harmful substance. What are the requirements for such a robot? It must be small enough to reach the areas that we would like to clean. It would be cheap and efficient. There are already published works on solid self-propelled Janus particles that serve as minirobots for cleaning polluted waters [109], but let us introduce the idea of liquid robots in the form of droplets.

How does the liquid robot know where to go? How can it find the pollutant? We can take the inspiration from nature and use the chemotactic principles. Although the cellular sensing and locomotion is much simpler than the processes in higher multicellular organisms, it is still a very complex problem and for the creation of chemical liquid robots even simpler mechanisms are needed. We have studied non-biological positive chemotactic movements of liquid robots in the form of droplets in the concentration gradient of different chemical signal molecules. The movement mechanism is based on the Marangoni effect acting on decanol droplets in an aqueous environment.

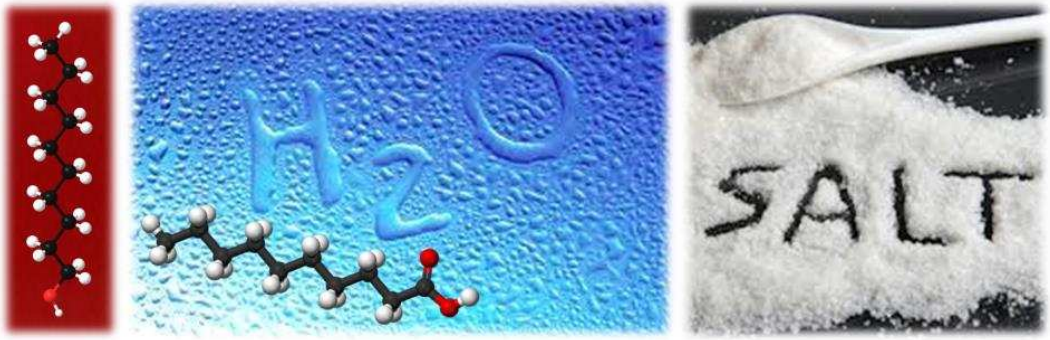

Figure 10. The main substances used for the majority of experiments presented in this thesis. 1-decanol (coloured by Oil Red O), aqueous solution of sodium decanoate (pH 12-13) and sodium chloride.

We have studied the movement of decanol droplets in the presence of sodium decanoate solution [49]. The majority of experiments described in this thesis and related papers were

based on this chemistry: aqueous solution of sodium decanoate (pH around 12, concentration 10mM), decanol droplets coloured by Oil Red O for better visibility and sodium chloride as a chemoattractant (Figure 10). We have found that decanol droplets are able to follow salt or hydroxide additions and mimic the chemotactic behaviour of living organisms [99]. This droplet system has also the ability to reverse the direction of the movement repeatedly, to carry and release a chemically reactive cargo, to select a stronger concentration gradient from two options, and to initiate chemotaxis by an external temperature stimulus. Moreover the droplets are able to follow the salt gradient in complex environments, for example we have shown how the droplet solved the simple maze [110] (https://youtu.be/P5uKRqJIeSs).

Such chemotactic liquid robots can serve as transporters for dissolved chemically reactive payloads or even small physical objects, thus we proposed to use the term "chemo-taxi" [12]. Generally, a taxi is a type of vehicle that conveys passengers between locations of their choice. Let us consider that our decanol droplet could serve as a taxi and as our model passenger a dead fly was chosen. Figure 11 represents the transport of a fly from the right hand side of the glass slide to the left hand side of the glass into the place where in the beginning of experiment small amount of salt was added. In principle this kind of chemo-taxi could serve for the transport of any other small object. We have performed experiments also with other small objects with various sizes and densities and studied their effect on droplet velocity. We have found that the shape and the surface-to-volume ratio of the object are more important factors than its weight [12].

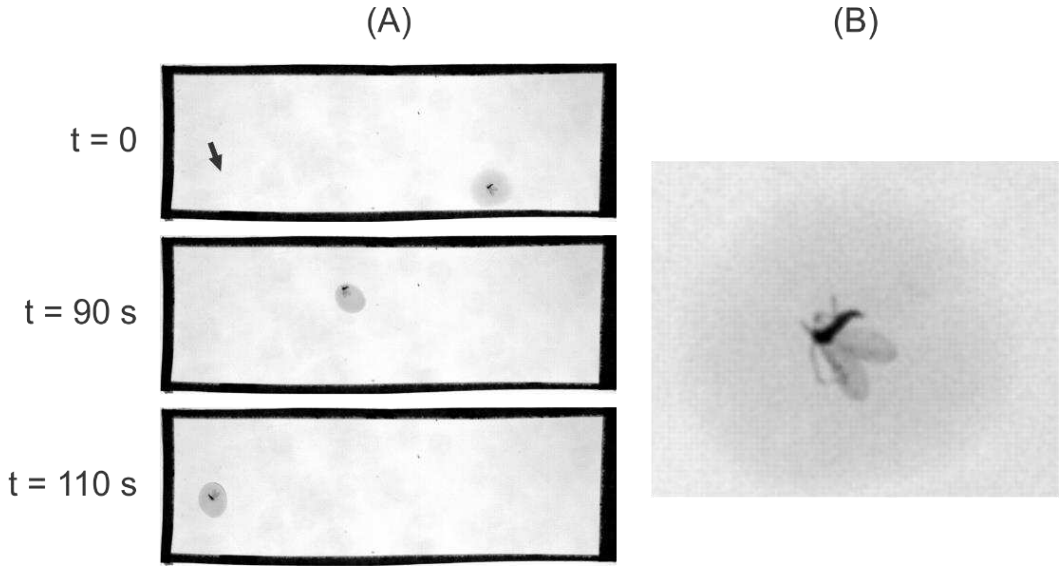

Figure 11. (A) Decanol droplet transporting a fly in the gradient of salt. The black arrow indicates the place of the salt addition at time t = 0. The size of a rectangular slide is 25 × 75 mm. (B) Detail of the droplet carrying a fly. [99]

The idea to have such a "chemo-taxi" could be used for several potential applications in the future. This chemotactic system could be developed to help machine engineers maintain their equipment, because droplets could track down pH, salt or heat gradients to get to the desired destination and lubricate a specific joint or axle. Another application of chemotactic droplets could be for chemical reaction control. The motile reaction containers in the form of the oil droplets could move to another place or closer to other reaction container via the concentration gradient. Gradients are thus one way of controlling reactions and for manipulation of reactants or products. Chemotactic droplets can fulfill various tasks in response to chemical signals in hazardous areas or limited spaces beyond the control of external power sources.

When studying artificial chemotaxis of droplets, I was wondering, is the speed of chemotactic decanol droplets comparable with other systems? To compare the speed of objects whose dimensions vary by orders of magnitude, it is common to express the velocity in the units of body lengths per second. As an example for decanol droplet speed estimation, we can take a 5μL droplet with a diameter 2.1 mm (if the spherical shape is assumed). The average speed of such a droplet in NaCl gradient is around 2 mm/s, thus the chemotactic speed is about one body length per second [49]. Also microswimmers, much smaller self-propelled droplets with a typical diameter of several micrometres, have a speed in the order of one diameter per second [111]. Slightly faster in the inanimate world are self-motile colloidal Janus particles that are able to increase their moving activity in the presence of hydrogen peroxide [109]. Just for the curiosity, the largest artificially made underwater moving objects are submarines with the maximal size of hundred meters moving with a speed around 80 km/h. Such a vehicle moves with the speed about 0.2 body length per second. When they are floating on the surface, their speed is less than half of that when submerged [112].

Figure 12 compares the swimming speed of some non-living objects with that of living entities. As we can see there are big differences in speed depending on the locomotion mechanism. Cell crawling on substrates is very slow in comparison with cell swimming. The crawling of cells on substrates can be divided into the following stages: protrusion of the leading edge of the cell, adhesion of the leading edge, deadhesion at the cell body and trailing edge, and finally, cytoskeletal contraction to pull the cell forward. Such continuous reorganization and turnover of the actin cytoskeleton takes some time and as a result this mode of motion is very slow. For example *Dictyostelium* amoeboid cells move at the rate of 10 μm/min which corresponds to the speed one body length per minute [113]. Similar speed was observed in the motion of the neutrophil chasing down its prey. This is 60 times slower in comparison with artificial chemotaxis of droplets. On the other hand, bacteria equipped by

flagella or other moving organelles can swim very fast. *E. coli* cells have a mean speed of roughly 30 μm/s that means they travel roughly 15 of their 2 μm body lengths every second [114]. To make a picture of the speed of larger living objects, I added the speed of fish and the fastest human swimmer into the figure. The typical speed of fish is 10 body lengths per second (the top speeds of 26 body lengths per second were observed for small haddock and sprats [115]). I have found that decanol droplets motion with an average speed of one body length per second is comparable to the swimming speed of the Olympian Michael Phelps [116]. With his height 193 cm, he can swim 100 m in about 50 seconds, which corresponds also to the speed of around one body length per second.

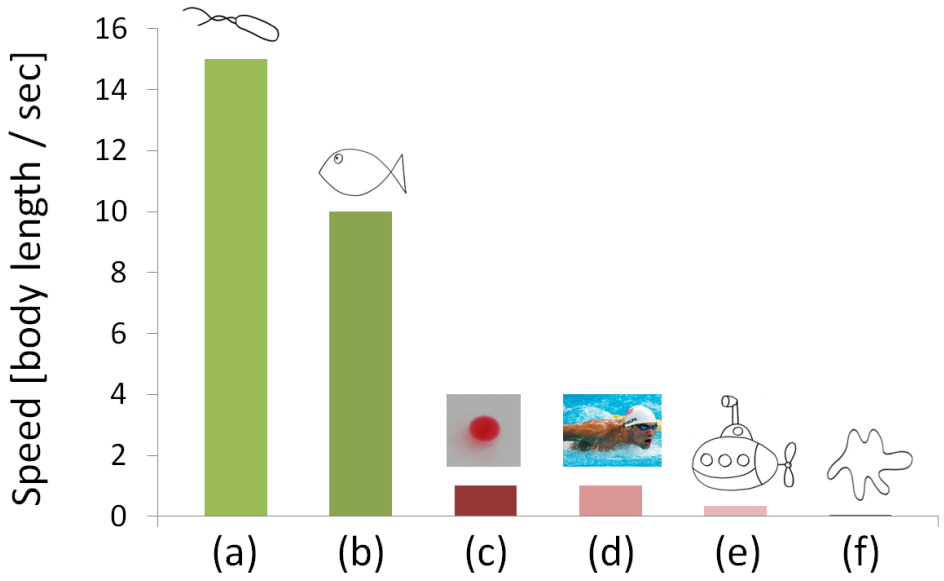

Figure 12. Comparison between the speed of various living and non-living systems in units of body lengths per second. (a) *Escherichia coli*, (b) fish, (c) droplet, (d) swimmer, (e) submarine, (f) amoeboid cell. [12]

Related works

- **Čejková J.,** Nguyenová T.Q., Štěpánek F. "Chemotactic droplets serving as chemo-taxi". In book *"Self-Organized Motion: Physiochemical Design based on Nonlinear Dynamics"* (Nakata S., Pimienta V., Lagzi I., Kitahata H., Suematsu N.J., eds.), str. 182-203, ISBN: 978-1-78801-166-2, Royal Society of Chemistry (2019).
- **Čejková J.**, Tóth R., Braun A., Ueyama D., Lagzi I. "Shortest path finding in mazes by active and passive particles". In book *"Shortest path. Parallel and distributed solvers"* (Adamatzky A., ed.), str. 401-408, ISBN: 978-3-319-77509-8, Springer (2018).

- **Čejková J.,** Holler S., Nguyenová T.Q., Kerrigan C., Štěpánek F., Hanczyc M. M. "Chemotaxis and chemokinesis of living and non-living objects". In book *"Advances in Unconventional Computing, Volume 2: Prototypes, Models and Algorithms"* (Adamatzky A., ed.), str. 245-260, ISBN: 978-3-319-33920-7, Springer (2017).

- **Čejková J., Novák M., Štěpánek F., Hanczyc M. (2014), Dynamics of chemotactic droplets in salt concentration gradients, *Langmuir,* 30(40), 11937–11944. (Appendix 2)**

- **Čejková J. (2013), *Dictyostelium discoideum* – model system not only for biologists, *Chemické listy* 107, 563-600. (Appendix 3)**

- Ševčíková H., **Čejková J.**, Krausová L., Přibyl M., Štěpánek F., Marek M. (2010) A new traveling wave pattern of *Dictyostelium* in the presence of cAMP in the agar. *Physica D* 239, 879-888.

- Hilgardt C., **Čejková J.**, Hauser M. J. B., Ševčíková H. (2008), Streamless aggregation of *Dictyostelium* in the presence of isopropylidenadenosin. *Biophysical Chemistry* 132, 9-17.

Shape matters.
Author unknown

4 Morphogenesis

4.1 Shapes in nature

Living cells, such as bacteria, exhibit immense number of shapes, even eukaryotic cells within the multicellular organisms show enormous diversity in the size, shape, and internal organization. Bergey's Manual of Determinative Bacteriology [117] focuses on morphological diversity of bacterial shapes and sizes. In a paper of Kysela *et al.* [118] readers can find in one paragraph a lot of terms that can be used for bacterial shapes description: *"to the familiar coccoid, rod-shaped, or spirillar types, there are also dendroid, coryneform, cylindrical, bulbiform, fusiform, and vibrioid types. There are uniseriate or multiseriate filaments of cells that are flexible or rigid, flat or round, unbound or bound in hyaline or slime sheaths. Single cells are described as star-shaped, disk-shaped, hourglass-shaped, lemon-shaped, pear-shaped, crescent-shaped, or flask-shaped. Rods can be pleomorphic, straight, curved, or bent, with blunt, pointed, rounded, or tapered ends. Some cells grow appendages such as prosthecae, stalks, or spikes."*

There are several reasons why cells are not simply round shaped and why they exhibit such a huge variety of shapes. For readers interested in this morphological diversity, I recommend excellent Young's review paper [119]. Here I will briefly discuss the important factors for shape, such as *(i)* nutrient uptake, *(ii)* motility, and *(iii)* predation.

Perfectly spherical shape of the cell means the minimal ratio of surface area to volume. Each change in the shape (elongation, flattening, growth of protrusions, *etc.*) leads to the increase of this ratio. The increase of the surface supports better opportunity for diffusion and nutrient uptake. Some cells can adapt to the changes in environmental conditions and change their shape as needed. For example, prosthecate bacteria are spherical or rod-shaped in nutrient-rich conditions, however in nutrient-poor conditions they develop prosthecae (appendages, cell envelope extensions) that facilitate the acquisition of nutrients from the environment [120]. There is also the relationship between shape and movement. For example, highly motile bacteria are usually rods with a specific (optimal) shape and size, and movement through viscous fluids seems to a favour spiral shape. Non-spherical shape also helps bacterium to avoid predation. For example the strategy to avoid phagocytosis and facilitate enhanced attachment to host cell surfaces used by a number of different bacterial and fungal pathogens is to increase cell size and overall surface area [121].

Nature likes patterns, thus not only single cells exhibit a variety of shapes. Simply, the various shaped objects and the pattern forming systems are omnipresent. They are studied across many sciences, not only in biology, but also in physics, chemistry, mathematics, astronomy, and earth science. Here I will focus mainly on branching structures, because our decanol droplets are also able to form branches as will be described in the next section. We can find many examples of branching structures in both living and non-living systems, such as tree crowns [122] and root systems [123] in plants, coral reefs [124], branched organs higher organisms (*e.g.* lung, kidney, prostate, liver, pancreas, the circulatory system and the mammary glands) [125], cancer invasion [126], neuronal cells [127], swarming colonies of bacteria [128], branching of plasmodium of *Physarum polycephalum* [129], evaporation-induced branched structures consisting of nanoparticles [130], crystal growth (*e.g.* snowflakes [131]), electrochemical deposition [132] or viscous fingering in Hele-Shaw cell [133]. Whereas in the chemical and physical systems the mechanism of branching pattern formation is based on physicochemical principles (*e.g.* diffusion, reaction kinetic, viscosity, surface forces play the role), in biological systems the additional levels of complexity are involved. The branching morphogenesis is controlled at molecular scale, when gene expressions and intracellular transduction pathways control for example the cell proliferation and fate, cytoskeleton-driven changes of single-cell shape or collective cell migration.

The growth of branching structures can be affected by various stimuli. In natural systems such an oriented growth is usually called tropism, we distinguish several kinds of tropisms in dependence on the nature of the stimulus [12]. So for example the plant can react to sunlight by phototropism, the roots of plants grow towards useful and away from harmful chemical substances by chemotropism, the response to gravity is called geotropism, changes in temperature cause the thermotropism, *etc.* Further well known kind of tropisms is the so-called electrotropism, when the organism or its parts response to the exogenous electric field. It is known that for example the growth of pollen can be affected by the electric field. However, the literature sources have a high incidence of contradictory findings. In some works the pollen turn towards the anode [134], towards the cathode [135], towards the closest electrode or parallel to the electric field [136]. Recently it has been found that the plant roots can align with an electric field and that the weak electric field makes the tissue of the cut root tip regenerate faster [137]. It is intuitive why plant parts are navigated by light, chemicals (namely oxygen) and temperature, but the description of interactions with electric field are still missing [138]. Various hypotheses are based on the thoughts that the presence of electric field drives the ionic currents essential for the growth.

4.2 Shape-changes of liquid robots

Therefore nature has found important roles for shape change, especially in response to environmental pressures and challenges. The question is, are we able to explore the shape of liquid robots in the form of droplets? In our papers [47, 63] we focused on shape-shifting, multi-arm droplets observable in a simple system consisting again only of decanol, water, sodium decanoate and NaCl on a glass substrate. The evaporation of water from the decanoate solution in this open system induces fantastic shape changes in the droplets: the originally spheroidal decanol droplets develop branching patterns and mimic the appendage growth of bacteria or axon growth.

We have performed detailed parametric study where decanol droplets were floating on the sessile droplet of aqueous decanoate solution containing sodium chloride [47, 63]. In dependence on initial composition of the system and the conditions of evaporation, the growth of branching structures was observed. In dependence on molar ratio between decanol, decanoate and the added sodium chloride three regimes of behaviour were described: *(i)* the disintegration of one decanol droplet into smaller droplets, *(ii)* tentacle-like pattern formation and *(iii)* the absence of any pattern formation. The time when formation of pattern started was dependent on the amount of added sodium chloride.

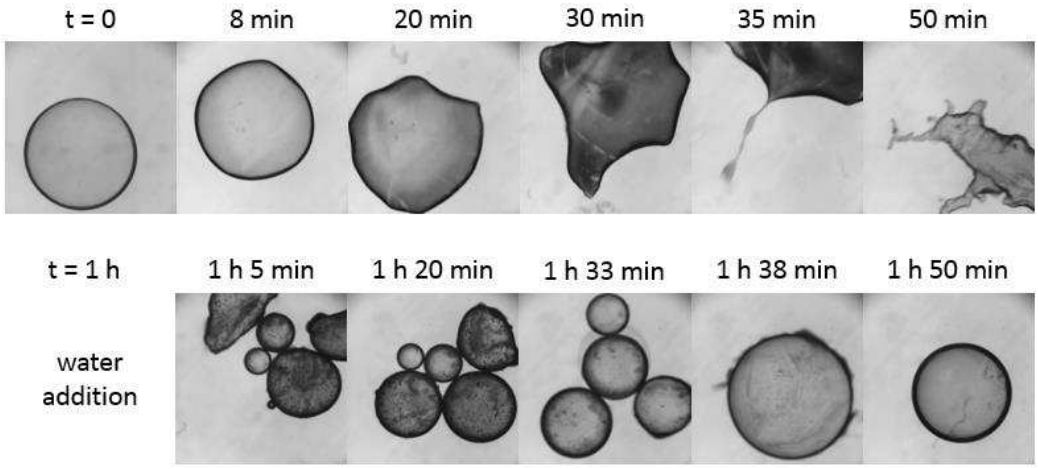

Figure 13. Shape changes of a decanol droplet during water evaporation (time 0 to 50 mins) and then rehydration (time 1 h to 1 h 50 mins) with a return to spheroidal shape. [63]

Since the shape changes described above were driven by the process of water evaporation from the system, we perturb the system back to its initial condition by adding the appropriate quantity of water. Figure 13 shows a microscopic detail of decanol droplet behaviour during the period of evaporation (time t = 0 to 1 hour) and then the return into

spherical shape during the rehydration phase. This experiment confirms that the process of pattern formation is reversible over at least one cycle and that it is possible to control this process by the timing of evaporation and hydration.

We also focused on mutual interactions of two or more droplets during the growth of tentacles. Two particular outcomes were possible: the arms will attract each other and intertwine, or the arms from different droplets would avoid mutual contact. Figure 14 shows the progress of a typical experiment with two droplets. Initially, the droplets come together to form a doublet. Later on they repel each other and start to form tips that elongate into tentacles. It was observed that the tentacles from one droplet were never attracted by the second droplet. The droplets always avoided the contact. In multiple droplet experiments the symmetrical star-shaped beginning of pattern formation was not observed. This contrasts with single droplet experiments, in which case the growth of tentacles was usually more or less symmetrical and there was no preferential direction of tentacles growth.

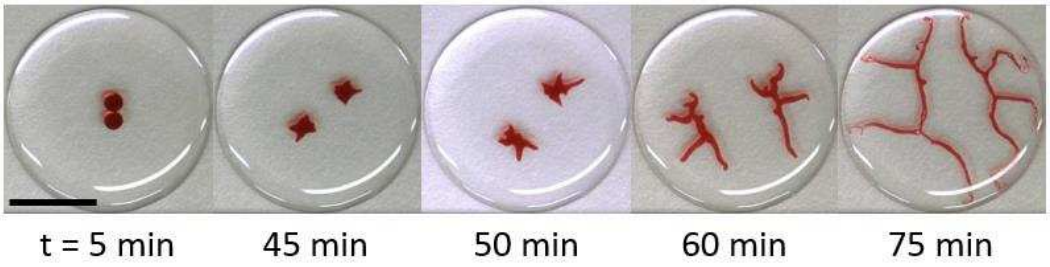

Figure 14. Image sequences of appendages formation in experiments with two decanol droplets. Initial conditions: glass coverslip with a diameter 24 mm, 500 µL of 10mM aqueous decanoate solution, two decanol droplets with the volume 2.5 µL each, 3.2 µL of 6.5M NaCl added. The scale bar corresponds to 10 mm. [63]

Surprisingly, almost all researchers studying origin of life use spherical vesicles as protocells. Maybe they assume that the first cell had the shape of a sphere: without any internal structure, just a membranous bag suspended in liquid. However, phylogenetic studies indicate that the early bacteria on planet Earth were rod-shaped and cocci appear to possess a "dead-end" shape that has arisen many times independently [139]. This indicates that non-spherical droplets could serve well as protocells and it is important to focus on their properties and the process of shape changes. In a similar manner that living cells exhibit a variety of shapes and morphological changes allowing them to live and survive under certain conditions, we suggest that also the study of morphological changes of non-living protocells is a key step in understanding the underlying principles. We hope to use our and other droplet systems as simple artificial life models of living cells to investigate the role of shape and shape change in simple chemical systems, artificial cells and protocells. It may be that

shape provides necessary information or regulation of protocell dynamics and therefore could have a selectable function in future applications.

The observed extensive shape changes in our droplet system, with bifurcation and branching patterns are at least superficially similar to biological neuronal architectures. However, in this moment we cannot speak about functional similarity, because the electrical conductivity of the surrounding bulk electrolyte is now much higher than the conductivity of decanol, so this is the opposite of what happens in neuronal networks. In order to simulate neuronal connections and some signal propagation, we would need the tentacles to conduct electricity better than the surrounding solution. Also, the tentacles now seem to be "self-avoiding", so we would need to somehow convince them to make connections. Anyway we hope our multi-armed droplets could represent "artificial neurons" in future, so in addition, spiking-type behaviour in our system will be tested. A chemistry-based artificial neuron would provide embodiment of unit and population-based self-organization, inter-communication and emergent higher order phenomena that can be fully characterized in terms of chemistry.

We were interested if the growth of the arms from the decanol droplet can be controlled by electric field and if we can observe any kind of electrotropism in a simple chemical droplet system. We focused on the application of DC electric filed on the same pattern forming decanol/decanoate system as in our previous works [47, 63]. Experiments on round and square shaped glass substrates with golden electrodes were performed. The parameters such as Lempel-Ziv complexity (LZ complexity [140]), a maximal number of disconnected components and a maximal number of nodes were evaluated in both control experiments without application of electric filed and experiments, where the voltage was applied to the experimental chamber. We have concluded that direct current applied to decanol droplets in a thin layer of sodium decanoate with sodium chloride does not affect directional growth of the branching droplets, but the current increases complexity of the branching structures [141].

4.3 Chemobrionics

Chemical or silica gardens are tubular precipitation structures that grow during the interaction of metal salt solutions with silicates, carbonates or other selected anions. Their growth characteristics and attractive final shapes derive from a complex interplay between reaction-diffusion processes and self-organization. A classic demonstration experiment in chemistry, the study of chemical gardens gained importance over the years due to their potential to bridge the nanoscopic and macroscopic world, the interesting patterns and motifs that span from them and their association to hydrothermal vents and one hypothesis for the origin of life on Earth. This emerging research topic has been named Chemobrionics

[142]. In 2018 the COST Action Chemobrionics started which I am involved in. The objective of this project is to study the phenomena when biomimetic micro- and nano-tubular precipitates are formed in chemical gardens. It explores the boundaries between chemistry, physics and engineering covering topics such as self-assembly, self-organization, hydrodynamics and materials science.

We are familiar with an organic system where intriguing pattern formation is observed as was described in Chapter 4.2 [47, 63]. From the physico-chemical point of view there are several similarities between purely inorganic chemical gardens and the structures in our organic decanol/decanoate system in presence of salt. Apparently in both inorganic and organic systems tubular growth is based on the self-propagation under fluid advection of reaction zones forming semipermeable precipitation membranes that maintain steep concentration gradients, with osmosis and buoyancy as the driving forces for fluid flow.

The key publication *"From Chemical Gardens to Chemobrionics"* [142] extensively summarizes the state of the art of inorganic chemical gardens. There are also listed several open research questions in Chemobrionics that are related to artificial life. Our aim is to find the answers to questions such as: *"Do chemical gardens, our tentacular structures and biological structures share any similar processes of formation?" "Can these structures teach us about biological morphogenesis, or is the similarity only accidental?" "Are they related to the origin of life?"* We hope that our research on chemical garden-type systems can contribute to the science of chemobrionics and artificial life.

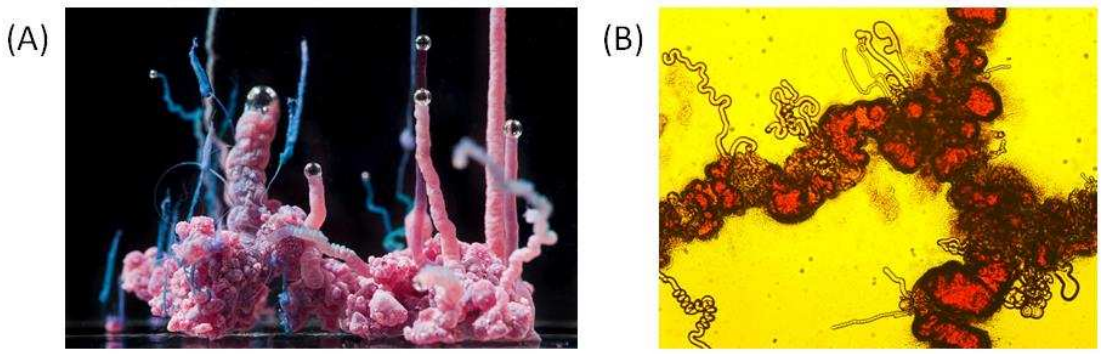

Figure 15. Comparison of (A) a chemical garden (© Stephane Querbes [142]) with (B) a shape changing decanol droplet (© J. Čejková).

Related works

- **Čejková J.,** Hanczyc M.M., Štěpánek F. (2018). Multi-Armed Droplets as Shape-Changing Protocells, *Artificial Life*, 24 (1), 71-79.
- **Čejková J., Štěpánek F., Hanczyc M. (2016). Evaporation-induced pattern formation of decanol droplets, *Langmuir* 32, 4800-4805. (Appendix 4)**

The whole is more than the sum of its parts.
Aristotle

5 Collective behaviour

5.1 Swarming in nature

The mutual interactions between agents are intensively studied in various systems, in both living systems and the inanimate world. A swarm is defined as a complex adaptive system, which is decentralized and self-organized and whose individuals are simple, homogeneous and autonomous. They are able to aggregate together, move *en masse* or migrate towards a common direction [143]. Swarming behaviour is well-known in biology where for example flocks of birds or schools of fish are extensively studied. The swarming has been observed also in bacteria or tumour cell populations [104]. Also in non-living systems this kind of collective behaviour can be implemented, for example in biologically-inspired swarm robotics.

Collective behaviour is a widespread phenomenon present in almost all biological systems at various scales and levels of complexity. Such a self-organization of animals, insects and even cells in the absence of centralized control has various reasons. For example, the commonly assumed advantages of flocking in the animal world are defence against predators, more efficient search for resources, hunting, or improvement in decision making [144]. Collective grouping in cells is important especially for their survival. As it was already noted in the chapter about chemotaxis, the amoeba *Dictyostelium* is an interesting example where free-living single cells can behave collectively when needed. In the absence of nutrients, *Dictyostelium* cells form large aggregates consisting of thousands of cells that transform into multicellular organisms enabling them to survive unfavourable conditions [107].

In living systems, different strategies exist for cell chemotactic movement, including both individual cell migration and the coordinated movement of groups of cells [145]. Cell migration in loosely or closely associated groups (commonly called collective cell migration) can be performed by various mechanisms. The cells can migrate in sheets (*e.g.* cells in carcinoma or in wound healing), in close packed clusters (*e.g.* border cells in *Drosophila* embryos or melanomas), in chains (*e.g. Drosophila* myoblasts or squamous cell carcinoma) or in streams (*e.g.* neural crest cells, mammalian endoderm and in some breast carcinomas). Nevertheless, the main sign of collective cell chemotaxis is the polarization of cells. They typically form the protrusions (such as lamellipodia and filopodia) at the leading edge and the trailing edge is contracted.

In the field of artificial life, the investigation of interactions between multiple man-made objects that behave like living organisms is also of interest. The aim is to find an analogy between the collective behaviour of artificial objects and their living counterparts. Further I will describe the collective behaviour of artificial objects, namely of oil droplets, and its phenomenological similarity with the behaviour of swarming living cells.

5.2 Swarming of liquid robots

Recently several physical and chemical systems consisting of self-propelled units have also shown a kind of collective behaviour [144]. The complex self-organized structures that arise from repeated interactions between individual units were observed for example in the groups of self-propelled catalytic microparticles [146] or camphor boats [147, 148]. However, the investigation of droplet swarming (*i.e.* mutual interactions of multiple liquid droplets) appeared only in few papers up to now. Some authors study the droplets with the volume of several microliters on Petri dishes with the diameter of several centimetres [64, 65, 74, 97], others observe the micrometre-sized droplets and their interactions under the microscope [149, 150]. We have studied the spatiotemporal arrangement of multiple decanol droplets as will be described later.

We can distinguish two categories of droplet experiments that one can find in the literature: droplets that are crawling on solid substrates and droplets that are floating on the surface of another liquid or swimming in another liquid. Regarding droplet interactions on dry solid substrates, it has been for example reported [151] that miscible liquids such as propylene glycol and water deposited on a clean glass cause the motion of neighbouring droplets over a distance, because these droplets are stabilized by evaporation-induced surface tension gradients and they move in response to the vapour emitted by neighbouring droplets. The vapour induced interactions were also described for water droplets containing a volatile fluid that were floating on silicone oil [152]. In systems where the oil droplets were floating in an aqueous pool, various mechanisms for droplets attractions or repulsions were described. In systems containing surfactant the surface tension gradients and Marangoni flows are usually responsible for droplet interactions [153]. In some droplet systems the so-called "Cheerios effect" plays the role [154]. As well as the cereals are attracted because of interfacial deformation and the effect of gravity, similarly liquid droplets can be attracted or repelled [155]. Although some works focus on the interactions between two droplets [74, 153], only a few papers deal with large populations of droplets and their swarming [64, 65, 97].

We were interested in the behaviour of groups of decanol droplets. However, there are too many parameters that potentially control the mutual interactions between droplets: the number of droplets, volume of a single droplet, volume of the aqueous "pool", size and shape of the glass substrate, pH, salinity and decanoate concertation in the aqueous phase,

etc. As one can see, to perform the complete parametric study where all these parameters and their combinations would be systematically investigated is not a simple task. Thus we focused on varying a few parameters, other parameters were usually fixed, as described in an appropriate part related to specific set of experiments. We performed two main kinds of experiments where we studied the behaviour of a group of decanol droplets in both the absence and presence of salt. The salt additions served as chemoattractants. We have focused on two main questions: *(i)* What are the qualitative types of spatial patterns attained by multiple decanol droplets in the absence of salt? *(ii)* Do the clusters of decanol droplets retain the chemotactic ability previously observed for single droplets?

We have observed that decanol droplets floating in the absence of salt chemoattractant on sodium decanoate solution on microscopic slides (system open to the environment) exhibit the collective-like behaviour that can be divided into six stages. Figure 16 shows an experiment with initial conditions as follows. The glass cover slip with the size of 24 × 24 mm was covered by a thin layer of 1000 μL of 10mM sodium decanoate. Then by using of a micropipette, 10 decanol droplets with the volume of 1 μL each were added. Duration of the whole experiment was 10 hours. The left black part of Figure 16 shows the typical image sequence (with the time step 1 hour) from the beginning of an experiment until the moment when water was evaporated completely from the system.

Upper right detail of Figure 16 shows an image sequence with the time step 1 minute of first 48 minutes of the experiment. When the droplets were placed in decanoate solution, they self-propelled on the surface independently, no contact or attraction of droplets was observed. We call this phase as *Phase I – initial phase*. Around 1 minute after the beginning of the experiment they distributed for a while in a regular small square in the middle of the system (*Phase II – regular arrangement*). Thereafter the droplets started to attract each other, touch each other and they formed small groups of droplets. However, these clusters were not stable and exhibited dynamical phenomena. The droplets repelled and attracted each other, they exchanged their positions and they did not stay in one static cluster. The droplets were either independent or members of various multi-droplet groups that were not stable in time (they formed *e.g.* doublets, triplets, small groups, chains, rings, half-rings). Such a dynamical behaviour (*Phase III – oscillatory behaviour*) was observed until time t = 42 min, when the droplets created a close-packed cluster and they did not exchange their positions in this arrangement (*Phase IV – static cluster*). The cluster was more or less static with regular hexagonal arrangement of droplets for almost three hours. The lower right detail of Figure 16 shows the image sequence what happened after time t = 3.5 hour after the beginning of the experiment. Some droplets started to escape from the cluster, they repelled each other and the cluster disintegrated in few seconds (*Phase V – cluster disintegration*).

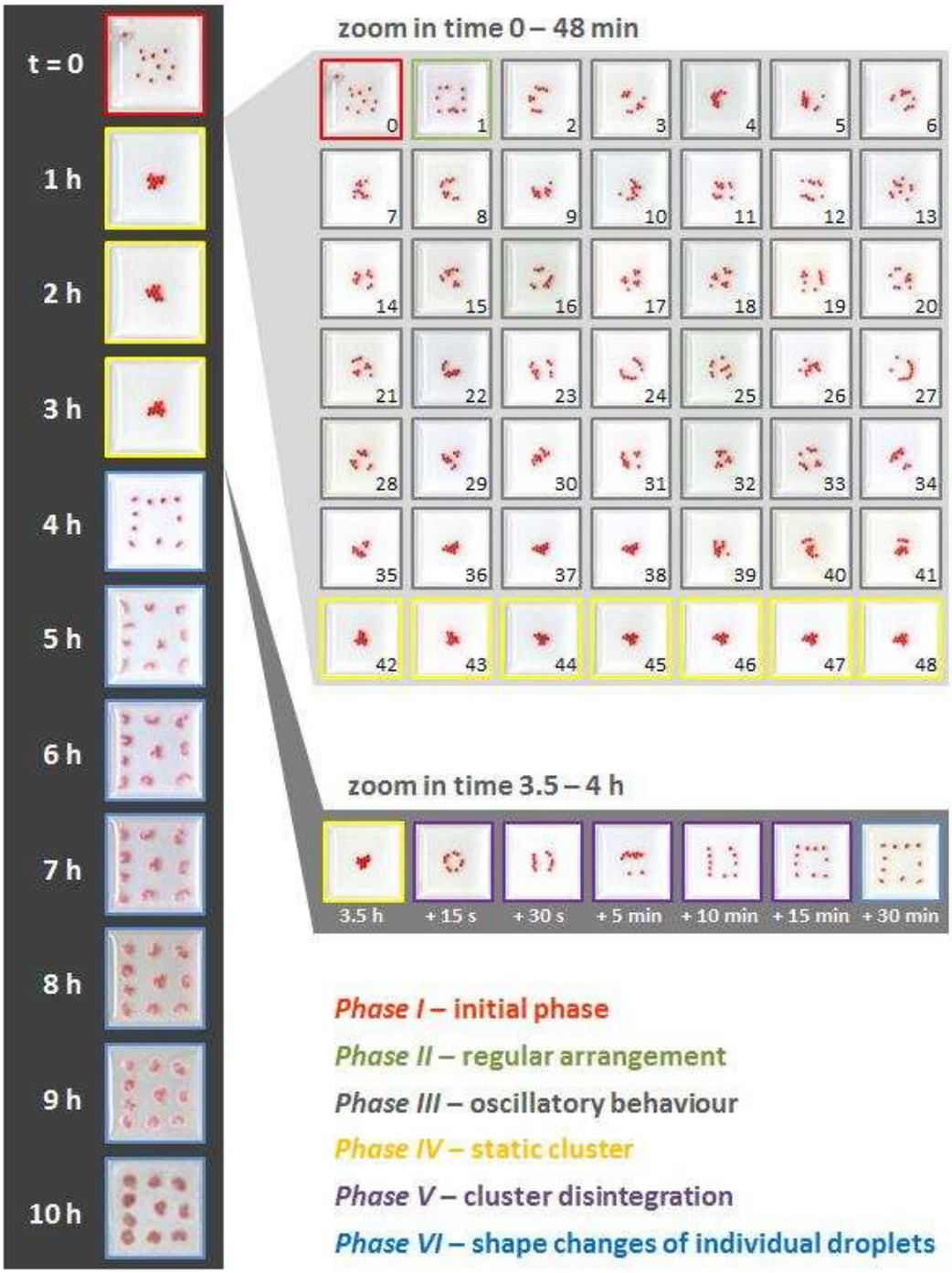

Figure 16. Image sequence showing the droplets behaviour in time. Left black part: The progress of the experiment from the beginning until the end of experiment (until the water was evaporated from the system completely). The time step between images 1 hour. Upper right zoom in time: First 48 minutes of the experiment, the time step of images 1 minute. Lower right zoom in time: Detail of cluster disintegration that started in time 3.5 h (the time step between t=3.5 h indicated in the figure). Initial conditions: glass slide 24 × 24 mm, 1000 µL of 10mM decanoate, 10 µL of decanol divided into 10 droplets (i.e. 1 µL each).

Then the droplets rearranged their positions and finally they arranged regularly in the small square in the middle of the system. Simultaneously the droplets started to change their shape – from round shaped droplets to elongated worm-like structures (*Phase VI – shape changes of individual droplets*). The experiment was over when all water evaporated from the system, *i.e.* approximately in 10 hours. In the end the glass slide was covered by dry leftovers of non-volatile residues.

We have performed several experiments with ten decanol droplets in a square geometry 24 × 24 mm with a thinner and thicker layer (500 µL, 750 µL, 1000 µL) of various concentrated decanoate solutions (5mM, 10mM and 20mM). We have found that there is an effect of the initial volume and concentration of aqueous decanoate solution on the time when individual phases *(I)-(VI)* appear and on the length of these phases ($\tau_{I\text{-}VI}$). Data for fixed number of droplets 10 × 1 µL are shown in Figure 17. We performed also many other experiments and measurements and the results will appear in the paper that is in preparation.

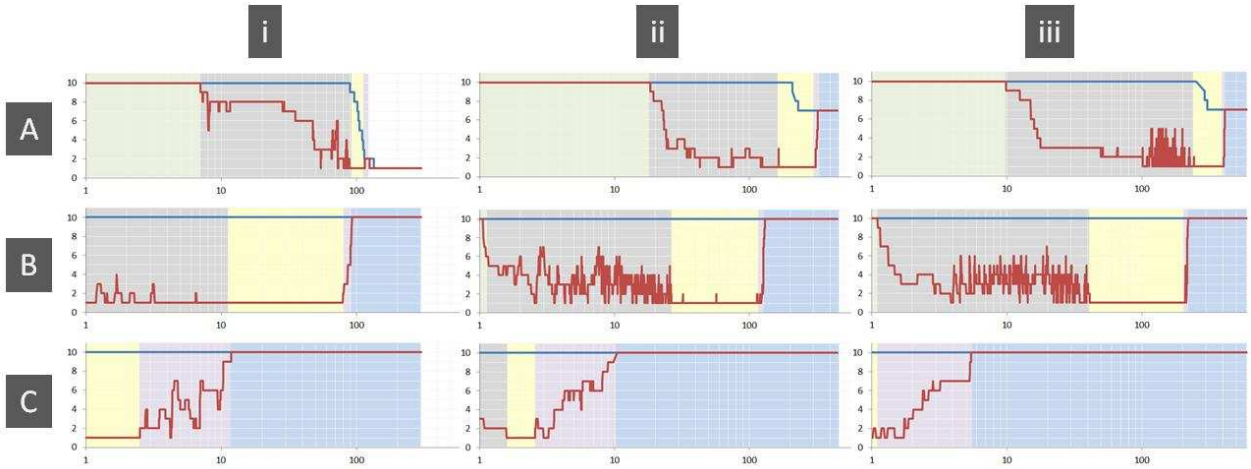

Figure 17. The effect of the initial decanoate volume (i) 500 µL, (ii) 750 µL and (iii) 1000 µL and decanoate concentration (A) 5mM, (B) 10mM and (C) 20mM on the time of individual phases. Glass slide 24 × 24 mm, 10 µL of decanol divided into 10 droplets (*i.e.* 1 µL each). Red curve – number of objects (single droplets, doublets, triplets, *etc.*). Blue curve – number of individual droplets.

We performed similar experiments in the absence of salt also on rectangular glass slides. In this setup, initially the droplets moved randomly, however then they distributed in the middle line of glass slide with almost regular distances between each other. Until this moment they repelled each other, but then the attraction between them dominated and they formed a cluster. As on square shaped substrates fantastic dynamical changes of droplets positions in clusters were observed. We focused on the estimation how the time of

the first cluster formation when all droplets came together (the start of oscillatory phase) is related to the number and size of individual droplets. The number of droplets (2-12) and their volume (1 μL, 2 μL or 5 μL of each droplet) were systematically changed and the time of cluster formation evaluated. The size of glass slide and the initial volume of aqueous solution were fixed (24 × 60 mm glass slide was covered by a thin layer of 2000 μL of 10mM decanoate solution). Figure 18 (A-C) shows the comparison of six droplets clustering for various droplet sizes.

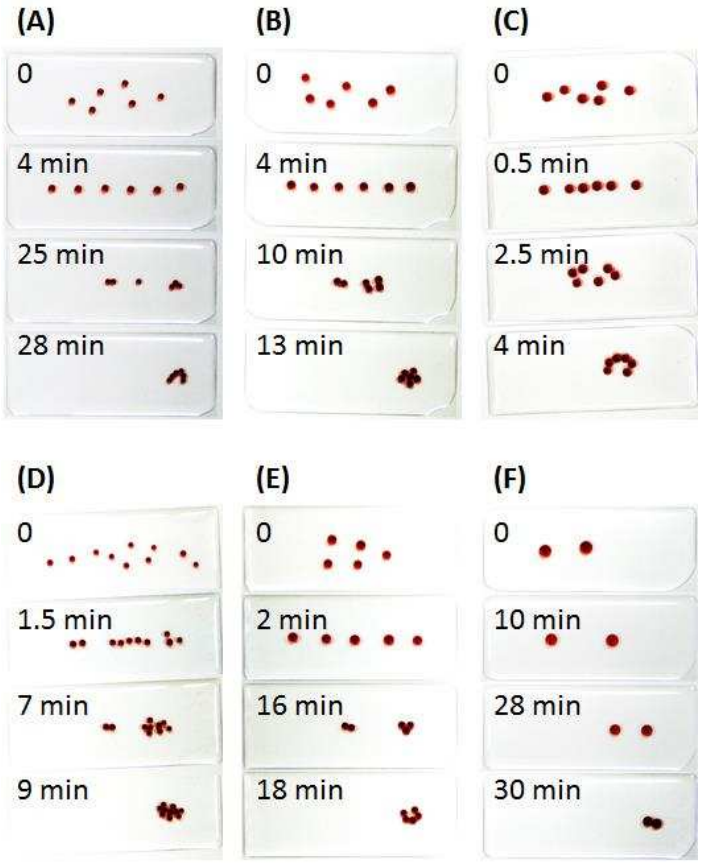

Figure 18. (A-C) Experiments with six decanol droplets. The volume of individual droplets is (A) 1 μL, (B) 2 μL and (C) 5 μL. (D-F) Experiments with 10 μL of decanol divided into (D) 10, (E) 5 and (F) 2 droplets. Initial conditions: the rectangular glass slide 24 × 60 mm, 2 mL of 10mM aqueous decanoate solution. [156]

From these image sequences it is evident that larger droplets reach the line arrangement sooner than smaller droplets. Then the droplets stayed in the middle line for several minutes and later on they started to attract each other, forming pairs, triplets *etc.* These small groups of droplets eventually formed a single cluster. The time of cluster formation in dependence on number of droplets was evaluated and results are summarized in Figure 19A. From these

data one can see following trends. If the number of droplets is the same and N < 10, larger ones cluster sooner than smaller ones. If the number of droplets N is just two, the differences are the most significant. Two 5μL-sized droplets touch each other about 30 minutes after the beginning of experiment, although two 2μL-sized droplets needed almost two hours. On the other hand, two 1μL-sized droplets never merged together within first three hours of the experiments. For N > 10 droplets started to form a cluster almost immediately without any dependence on the droplet size.

It seems that there could be the effect of the total decanol volume in the system on this clustering process, so we also re-plotted the time of cluster formation in dependence on the total decanol volume in the system (Figure 19B). For smaller total volumes of decanol, it needed more time for cluster formation without any significant effect of number and size of droplets. For volumes of decanol around 10 μL it looks like that larger number of smaller droplets clustered sooner (see also Figure 18D-F). Nevertheless this could be because of the distance between droplets (two 5μL-sized droplets need more time to touch each other in comparison of the group of ten 1μL-sized droplets). For larger total decanol volume (more than 20 μL), the droplets clustered almost immediately without the effect of number and size of droplets.

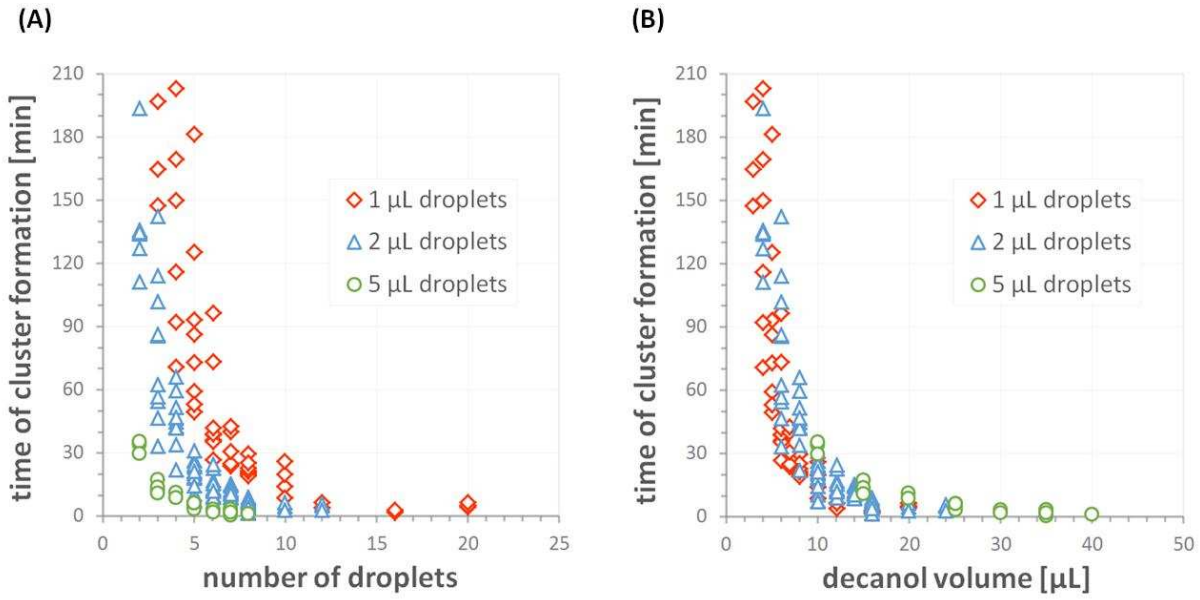

Figure 19. The start time of oscillatory phase of droplets on a rectangular glass slide (A) in dependence on the number of decanol droplets and (B) in dependence on total decanol volume in the system. Individual droplets had the volume 1 μL, 2 μL or 5 μL each. [156]

Independently similar behaviour as we observed in decanol/decanoate system was observed by our collaborator S. Tanaka at Hiroshima University. His system consisting of a mixture of ethyl salicylate (ES) and paraffin liquid floating on the surface of aqueous sodium dodecyl sulphate solution (SDS) in a Petri dish (covered by a lid) has shown qualitatively similar behaviour [64, 97]. Although the systems differ in several parameters, we think that the phenomena observed should be based on the same principles as we have already discussed in our recent publication [48].

The second set of experiments with multiple decanol droplets has focused on the study of the chemotactic ability in the salt gradients. It has been already shown that a single decanol droplet placed in a thin layer of sodium decanoate is able to perform chemotaxis-like oriented movement if a salt concentration gradient is present in the system as was discussed in Chapter 3.2. The main question before performing experiments with multiple droplets was whether the droplets move towards the salt as single droplets, in a chain or in a group? We have investigated not only the chemotaxis of solitary decanol droplets before their clustering, but also the chemotaxis of decanol droplet clusters that have formed spontaneously in the absence of salt discussed above. It has been found that as soon as the droplets that touch each other perceive the salt gradient, they form a close packed group and then move towards the highest salt concentration as a group (see Figure 20). Groups consisting of a larger number of droplets start the chemotactic response sooner than smaller groups, and they also reach the target sooner. In contrast, droplets those are in the state before their clustering they follow the salt gradient individually or in smaller groups (Figure 21).

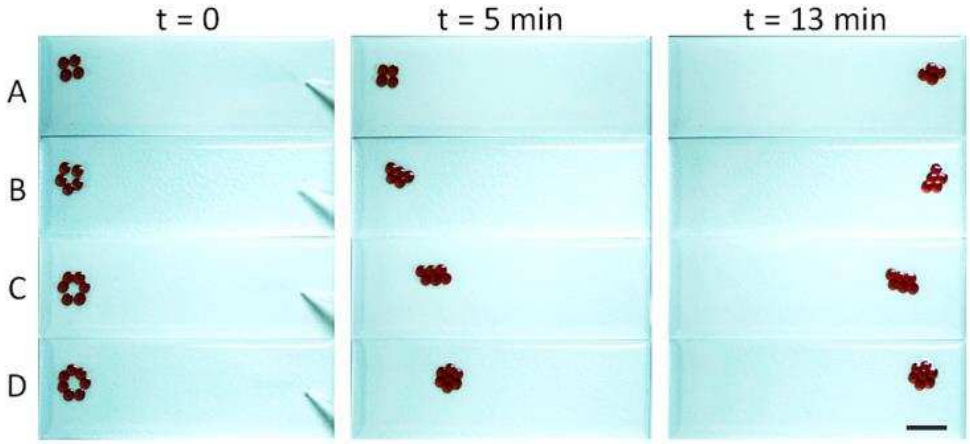

Figure 20. Chemotaxis of multiple decanol droplets after cluster formation: (A) four, (B) five, (C) six and (D) seven. Volume of each decanol droplet is 5 µL. The size of rectangular glass slide is 25 × 75 mm. Volume of aqueous decanoate solution is 1.5 mL. Time t = 0 corresponds to the time, when 1 µL of saturated salt solution (6.5M NaCl) was added as chemoattractant. The scale bar corresponds to 10 mm. [156]

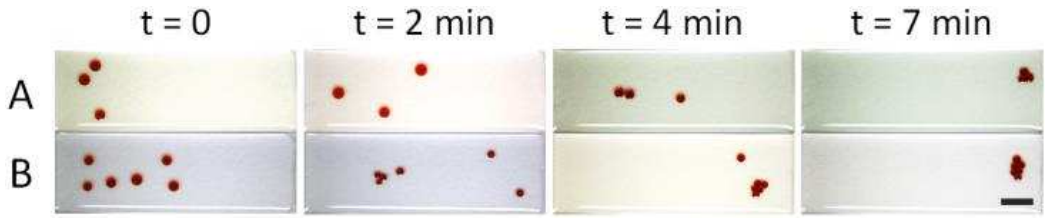

Figure 21. Chemotaxis of multiple decanol droplets before cluster formation: (A) three, (B) six. Volume of each decanol droplet is 5 μL. The size of rectangular glass slide is 25 × 75 mm. Volume of aqueous decanoate solution is 1.5 mL. Time t = 0 corresponds to the time, when 1 μL of saturated salt solution (6.5M NaCl) was added as chemoattractant. The scale bar corresponds to 10 mm. [156]

In the same way as in the populations of living objects or robots, the organization, collective behaviour and swarming of liquid droplets needs to be investigated. Using such approaches, we could design relatively simple and cheap "liquid robots" in the form of droplets that would work together to perform increasingly sophisticated tasks. Examples of potential droplet swarming applications include intelligent cleaning or targeted delivery of chemicals and small objects. Since droplet collective behaviour is an interesting problem, we anticipate that intensive experimental and theoretical study of this problem may help to explain other swarming mechanisms and analogies between collective behaviour of liquid droplets and living swarming systems could be found.

Related works

- **Čejková J., Schwarzenberger K., Eckert K., Tanaka S. (2019). Dancing performance of organic droplets in aqueous surfactant solutions, *Colloids and Surfaces A: Physicochemical and Engineering Aspects,* 566, 141-147. (Appendix 5)**
- **Čejková J.,** Ikegami T. Experimental study of mutual interactions of multiple liquid droplets. *Proceedings of the 2nd International Symposium on Swarm Behavior and Bio-Inspired Robotics.* 29.10.2017, Kyoto, Japan. ISSN:433-5096, 2017, pp. 274-278.
- **Čejková J**., Ikegami T., Štěpánek F. Life-like swarm behavior of multiple chemotactic droplets. *Proceedings of the 14th European Conference on Artificial Life 2017*. 04.09.2017, Lyon, France. MIT Press, ISBN: 978-0-262-34633-7, 2017, pp. 91-95.

I'm still alive.
Pearl Jam

6 Artificial (but not ALife) systems

Although this thesis and my current research focuses mainly on artificial life and life-like behaviour of artificial systems, in this chapter, I will briefly comment on our previous works that were not directly related to artificial life studies, but still some ideas and approaches were borrowed from ALife. Chapter 6.1 will describe the idea of artificial spores. We took the inspiration for it from nature, however finally we created a hybrid system containing living cells as the triggers for rupture of the designed and fabricated so called artificial spores. So it was an artificially made system containing living cells. Similarly, when preparing artificial tumours (see Chapter 6.2) in liquid marbles, the living cells were the key components. Rather than about the study of artificial life we can speak about the engineering of systems that are not created by nature, but artificially from already pre-existing cells that are still alive.

6.1 Artificial spores

Before the description of the artificial spore idea, let me outline the background of this project, where we aimed to design a new kind of controlled release. In many natural systems and also in artificially made systems serving for example for controlled drug delivery several triggers can be used for the release of the content. The typical triggering stimuli are changes in temperature, light intensity, pH, ionic strength, or concentration of signal molecules, either chemical or biochemical (Figure 22) [157]. Our Laboratory of Chemical Robotics has long-term experience with using of superparamagnetic iron oxide nanoparticles (SPIONs) and alternating magnetic field for radiofrequency heating. SPIONs can locally generate heat in a radio-frequency field by the combination of Néel and Brownian relaxation processes. My colleagues have investigated for example radiofrequency induced release kinetics from magnetic hollow silica microspheres [158], radiofrequency heating has also been used as a release mechanism from liposomes encapsulated into hydrogels containing also SPIONs [159-161]. I used the radiofrequency heating for controlled release from thermo-responsive capsules that consisted from poly-N-isopropylacrylamide (PNIPAM) and magnetic nanoparticles [162, 163].

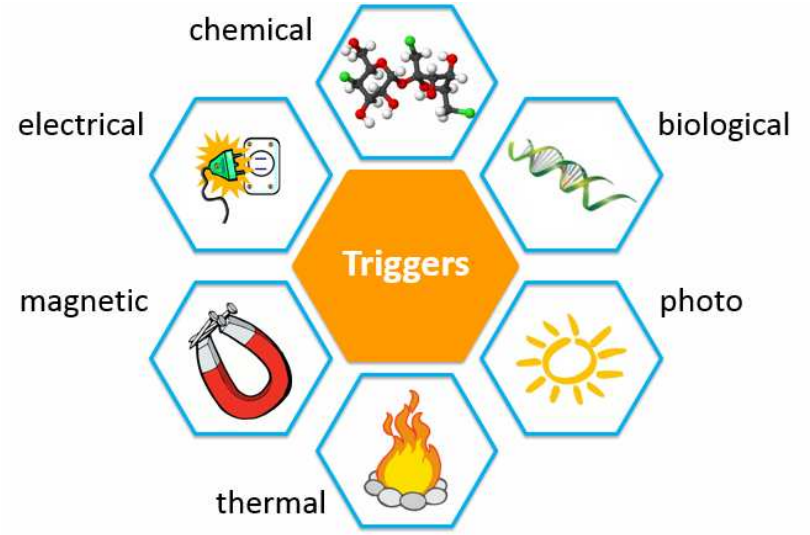

Figure 22. Examples of triggers for controlled release.

The release of the content from the capsules could be by several mechanisms. In the case of core/shell particles, the shell can lose its compactness and then the content of the core can be released. For example (see Figure 23), the pores in a shell can be opened by dissolution or phase transition of the plugs in pores, the phase transition of the whole shell can occur or the shell can rupture because of the increase of internal pressure. The rupture of the shell or whole capsules usually happens because of osmotic pressure. However, in our concept of "artificial spores" we proposed new mechanism, as will be described further.

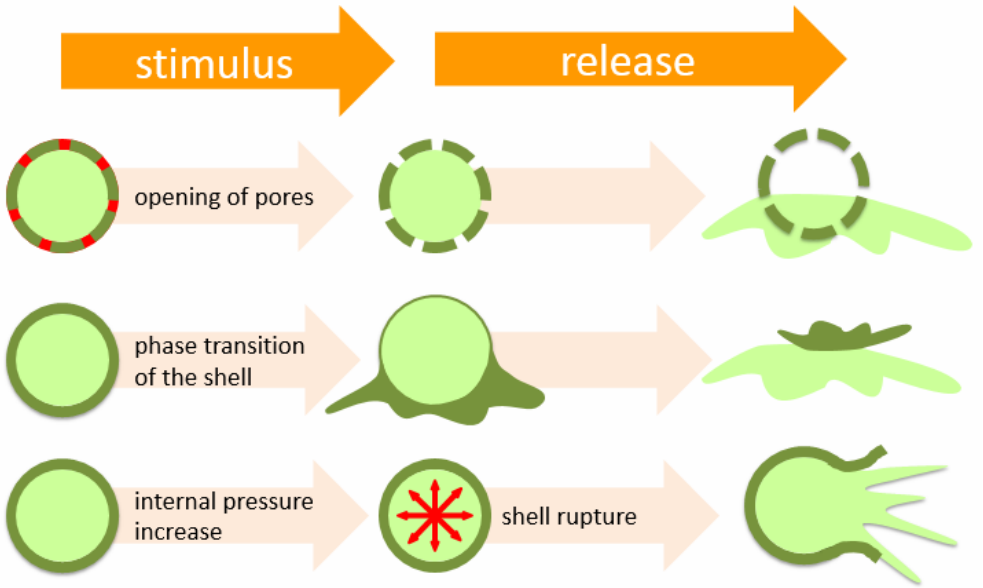

Figure 23. Examples of the controlled release mechanisms.

In biology, a spore is defined as a reproductive structure that is adapted for dispersion and survival for extended periods of time in unfavourable conditions. Once conditions are favourable, spores can develop into new organisms. The activators of such a transformation from spore to cell could be *e.g.* nutrients, temperature, pH, or combination of these parameters. There are several reasons why the spores are formed in the nature:

i. Spores allow organisms to survive for many (in some cases, millions of) years under adverse conditions, thus they serve as storage system for genetic information.
ii. Spores shield cellular components in harsh conditions, and so spores have the protection function.
iii. A spore must somehow "arrive" at a location and be there at time favourable for germination and growth. Some spores have flagella or other organelles that serve for the species dispersion to longer distances and new areas. Therefore spores serve as transporters of genetic information.

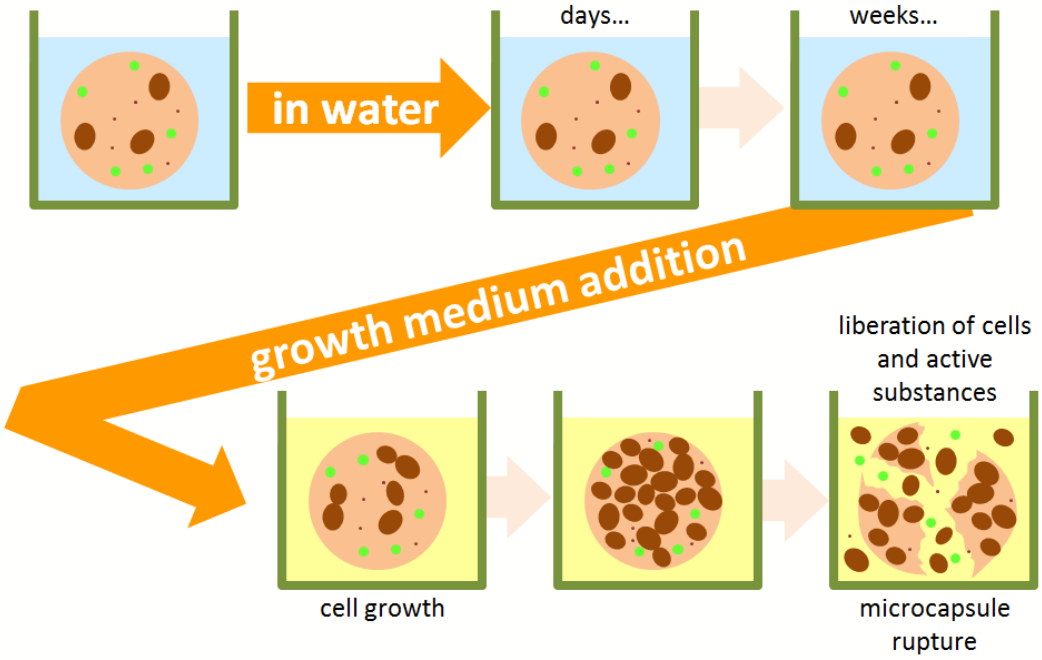

Figure 24. Schematic principle of artificial spore rupture and liberation of an active substance into the environment caused by yeast cell growth in the culture medium. [164]

In our work [165] we adopted the idea of spores and created hybrid alginate microcapsules with embedded yeast cells that are long-term stable and inactive and perform specific target mission only after activation by changing the conditions in their surround. The target aim is

to disintegrate and liberate and disperse the encapsulated content in proper time. The principle of such artificial spores is described in Figure 24. Under unfavourable conditions (absence of nutrients) no cell division of embedded yeast occurs and the composite microcapsules are stable in aqueous medium for extended periods of time without disintegration or release of their content. Once the microcapsules encounter favourable conditions (presence of nutrients, here provided by a culture medium), cell division and growth causes a rupture of the alginate capsule and release of the embedded components. Liposomes loaded with fluorescein represent a model "active" particulate substance that is to be liberated from the composite microcapsules. Additionally, iron oxide magnetic nanoparticles were also embedded within the composite microcapsules to facilitate their manipulation and separation by a magnetic field.

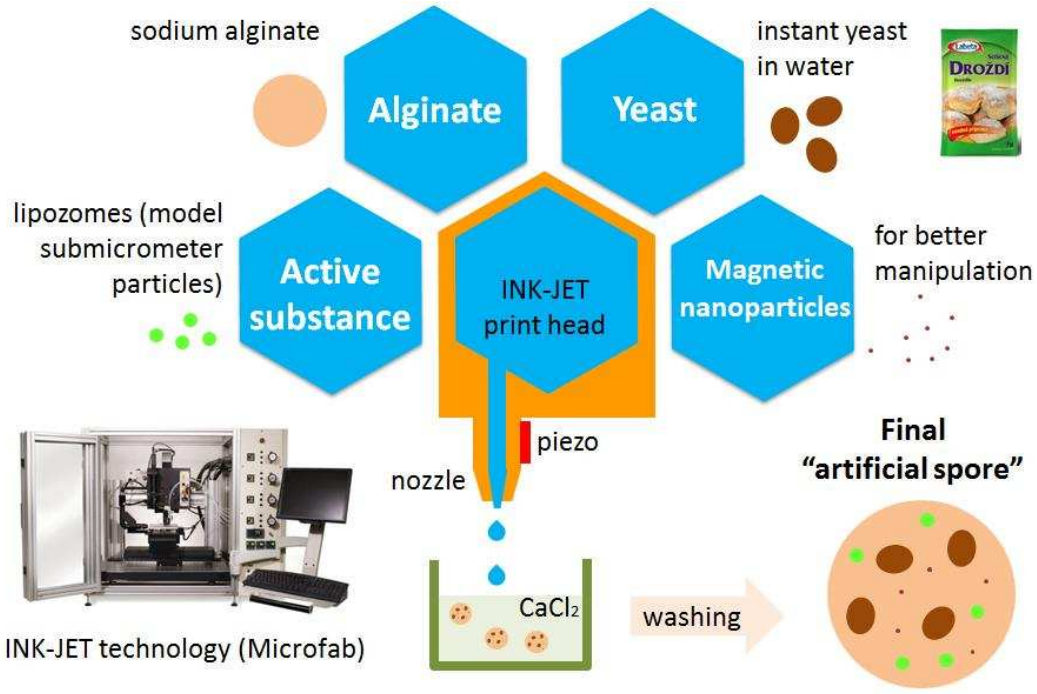

Figure 25. Scheme of artificial spore preparation. Solution of sodium alginate, yeast cells, liposomes and magnetic nanoparticles is by means of Ink-Jet printing technology dropped into $CaCl_2$ solution. Precipitated calcium alginate microcapsules are subsequently washed. [164]

We focused mainly on problem *(i)* described above. Artificial spores were fabricated (see the schematic procedure in Figure 25) and their stability and inactivity for long time were investigated. The ability to activate in suitable conditions (in this case nutrients additions) was studied. Artificial spores cultivated in growth medium showed the ability to disintegrate

and release embedded objects into the surroundings. This mechanism acts as a biological trigger for controlled opening of the microcapsule. Further we concentrated on the protection function of spores (task *(ii)* above) [164]. Artificial spores were coated by solid silica shell and the viability of encapsulated yeast was tested (Figure 26). Although the coating process does not kill the cells, the cell growth in the microcapsules was not sufficient for the microcapsule disruption. Unfortunately this way of protection shell formation seemed to be unsuitable.

Such artificial spores could find applications in biologically triggered controlled delivery *e.g.* of natural fragrances or benign fungicides. Another application of these objects could be as intelligent indicators of storage quality, as was discussed in our paper [165].

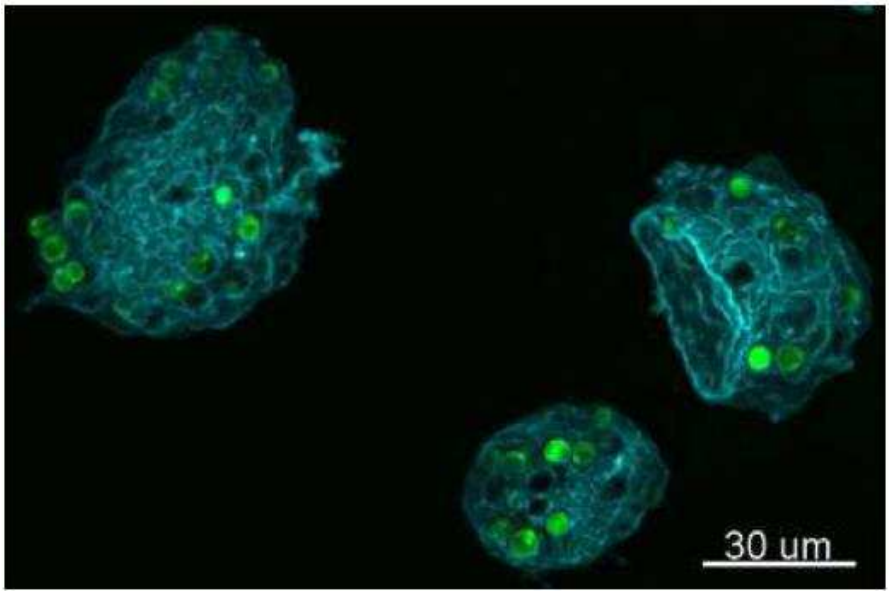

Figure 26. Laser scanning confocal microscopic images of alginate microcapsules with encapsulated yeast cells (viable cells visualized by green colour) and covered by fluorescently labelled silica shell (blue colour). [164]

6.2 Artificial tumours

Artificial life research focuses on questions related to origin of life, origin of a single cell and also origin of multicellularity [166]. Some researchers aim to develop theories and experiments concerning the emergence of multicellularity and organogenesis. Usually they combine genetic engineering and experimental evolution to study the different pathways leading to synthetic multicellular aggregates exhibiting fitness advantage under given environmental conditions. Multicellularity is one of the most significant innovations in the history of life on Earth, but why and how it initiated is still poorly understood [167].

In our previous work, we also created some multicellular objects artificially [89]. However, our aim was not to study the mechanism of cell clustering, adhesion and then cell division in this multicellular object, our ambitions were not to clarify the origin of multicellular clusters. The purpose of our work was to create small tumours, so called spheroids, which could serve later for example for drug testing, because they seem to be ideal as drug screening platforms. Thanks to their three-dimensional structure, spheroids can be used as reliable models of *in vivo* solid tumours. In comparison with their two-dimensional counterparts where the cells grow in a monolayer the spheroids reproduce better the real complexity of cancer microenvironment [168-170].

There are several methods for spheroid cultivation (*e.g.* using low adhesion plates, hanging drop plates or micro-patterned surfaces), however, we have used the novel technique and we have cultivated the HT-29 carcinoma cells in liquid marbles (Figure 27). The parametric study, where the size of liquid marbles and number of inoculated cells were changed, was performed in order to find the optimal conditions for spheroid formation [89]. We have confirmed that liquid marbles [86] can serve as micro-bioreactors for three-dimensional spheroids cultivation. This approach can be used in the future also for artificial life studies related to the origin of multicellularity.

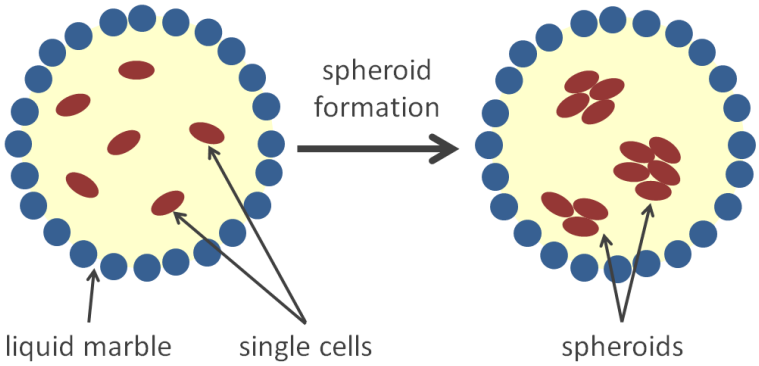

Figure 27. Spheroid cultivation in a liquid marble.

Related works

- **Čejková J.,** Gorný D., Haufová P., Štěpánek F. "Artificial spores" - hybrid alginate microcapsules with encapsulated yeast cells. *Proceedings of the Twelfth European Conference on the Synthesis and Simulation of Living Systems*. 02.09.2013, Taormina, Italy. MIT Press, ISBN: 978-0-262-31709-2, 2013, pp. 818-823.
- **Čejková J., Haufová P., Gorný D., Hanuš J., Štěpánek F. (2013). Biologically triggered liberation of sub-micron particles from alginate microcapsules, *Journal of Materials Chemistry B* 1, 5456-5461. (Appendix 6)**

- Janská P., Rychecký O., Zadražil A., Štěpánek F., **Čejková, J.** (2019). Liquid oil marbles: increasing the bio-availability of poorly water-soluble drugs, *Journal of Pharmaceutical Sciences*. doi: 10.1016/j.xphs.2019.01.026
- **Čejková J.,** Rychecký O. (2017). Tekuté kuličky, *Chemické listy* 111, 109-114.
- **Rychecký O., Majerská M., Král V., Štěpánek F., Čejková J. (2017). Spheroid cultivation of HT-29 carcinoma cell line in liquid marbles, *Chemical Papers* 71(6), 1055–1063. (Appendix 7)**

Artificial life is (not) dead.
Takashi Ikegami

7 Conclusions

Chemical engineering itself is in principle interdisciplinary, because it is built on a foundation of sciences including chemistry, physics, mathematics and biology. Even knowledge in economics is important for chemical engineers. In this thesis I have introduced the field of artificial life which is an even more interdisciplinary research area, and one where chemical engineering approaches could contribute to research. I focused only on a small number of problems that ALife aims to solve, I have presented the projects related to wet ALife and to the creation of synthetic objects with life-like behaviour. The novel concept of droplets as liquid robots was discussed. The research in this area opens several challenges in both chemical engineering and artificial life. From a chemical engineering point of view the challenge is to fully describe the processes observed during phenomena like droplets changing shape or droplets behaving collectively. The droplets exhibit complex dynamics due to the competition of inertial, viscous, and capillary forces coupled with dynamic surface tension. The study of local transport processes at time-evolving interfaces seems to be a non-trivial problem. The complex behaviour of individual liquid robots and their interactions with other robots or the environment is still not well understood and further research is needed, namely studies related to fluid dynamics, phase transitions in the bulk and interfaces and reaction-diffusion driven processes. Further challenges for chemical engineers lie in the design of experimental setups for liquid robotic studies or the scale-up of their production for potential applications.

The idea of liquid robots also opens new avenues in artificial life studies, because it contributes to the never-ending discussion of how to define the system which is alive, life-like and without any attributes of life. Imagine a hypothetical situation where an external observer is shown a living cell and a morphologically equivalent non-living droplet (Figure 28). Would such an observer be able to decide which object is alive and which one is just "life-like"? Similarly, is there any chance to discern any difference between the chemotaxis of living cells and simple non-living droplets? As Karel Čapek wrote in his theatre play R.U.R. discussed in the introduction of this thesis: *"Robot is a man of different substance from us."* With such an approach we can say that droplets mimicking behaviour of living cells are entities that could be called "liquid chemical robots" - artificial cells made from other substances than cells created by Nature. Čapek's idea that robots must be as simple as

possible is fulfilled in our approach of self-propelled droplets as liquid robots. They mimic cells by only sensing chemical gradients, following them by chemotactic response, and eventually changing their shape as well. For the specific purposes (*e.g.* to transport some object to the target destination) it is not necessary for liquid robots to have abilities such as reproduction or evolution.

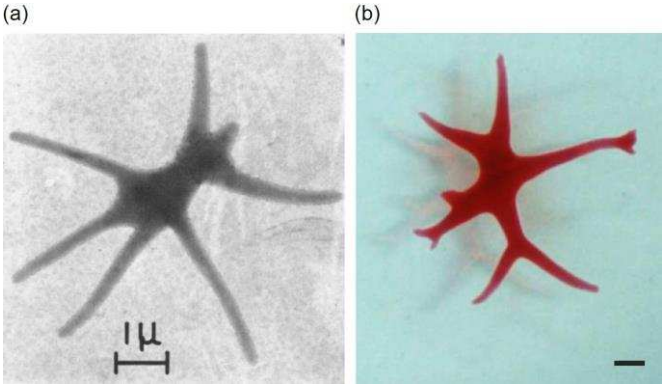

Figure 28. Comparison of a living cell and a morphologically equivalent non-living droplet. (a) Prosthecate freshwater bacteria *Ancalomicrobium* [67]. (b) Decanol droplet (scale bar corresponds to 1 mm) [47].

To conclude, let me discuss the present position and future of ALife. In the book titled *"Artificial Life – An Overview"* [171] from 1997 edited by Christopher G. Langton (the founder of ALife field), it states in the introduction: *"Artificial Life is not yet ready to be constrained by quick and short definitions - the field is still in the process of defining itself, as is proper for any new discipline."* And now, more than 30 years from the establishment of the ALife field, I would say that the field is still evolving and dynamically changing and there is still no unified definition of ALife accepted by all ALifers. Similar to how the AI field have had several "winters" in the past, ALife has also experienced its own "ups and downs". In 2008, at the international conference held in Winchester Takashi Ikegami presented a keynote speech titled *"Artificial life is dead"*. He actually thought so at the time, because of the lack of progress in solving problems in the Alife field. However, now it is not only possible to think about life and ALife phenomena through computer simulations, but also through art, web systems and games. Laboratory facilities have also enabled progress in wet ALife studies. We can speak about a neogenesis of artificial life, which was supported by Ikegami's new statement in 2018: *"Artificial life is not dead"*. Even though ALife is still an unknown field to many people and it has almost no history in the Czech Republic. I believe that with the proper dissemination of activities the situation could change and ALife could attract the attention of not only scientists and students, but also the general public.

8 References

1. Langton C. *Proceedings of the Interdisciplinary Workshop on the Synthesis and Simulation of Living Systems (ALIFE '87), Los Alamos, NM, USA, September 1987*. 1987. Addison-Wesley.
2. Sayama H., *ALife in a larger scientific context.* ALife Roadmap Workshop, ALIFE 2018, Tokyo, 2018.
3. Bedau M.A., *Philosophical aspects of artificial life*, in *Towards A Practice of Autonomous Systems,* Varela and P. Bourgine, Editors. 1992, Cambridge, MA: Bradford Books/MIT Press. p. 494-503.
4. Bedau M.A., et al., *Open Problems in Artificial Life.* Artificial Life, 2000. **6**(4): p. 363-376.
5. Aguilar W., Santamaría-Bonfil G., Froese T., and Gershenson C., *The Past, Present, and Future of Artificial Life.* Frontiers in Robotics and AI, 2014. **1**(8): p. 1-15.
6. Bedau M.A., *Artificial life*, in *Philosophy of Biology*. 2007, Elsevier. p. 585-603.
7. Banzhaf W. and Yamamoto L., *Artificial Chemistries*. 2015: MIT Press.
8. Gershenson C., Trianni V., Werfel J., and Sayama H., *Self-Organization and Artificial Life: A Review.* The 2018 Conference on Artificial Life: A Hybrid of the European Conference on Artificial Life (ECAL) and the International Conference on the Synthesis and Simulation of Living Systems (ALIFE), 2018: p. 510-517.
9. Brooks R.A. *Artificial life and real robots*. in *Toward a Practice of Autonomous Systems: Proceedings of the First European Conference on Artificial Life*. 1992. MIT Press, Cambridge, MA.
10. Smoliar S.W., *Artificial life: Christopher G. Langton.* Arlificial Intelligence 1995. **73**: p. 371-377.
11. Čapek K., *R.U.R. (Rossum's Universal Robots),* 1920, Praha: Aventinum.
12. Čejková J., Nguyenová Q.T., and Štěpánek F., *Chemotactic droplets serving as "chemo-taxi"*, in *Self-Organized Motion: Physiochemical Design based on Nonlinear Dynamics*, S. Nakata, et al., Editors. 2019, The Royal Society of Chemistry. p. 182-203.
13. Furusaki S., Garside J., and Fan L.S., *The Expanding World of Chemical Engineering*. 2002: Taylor & Francis.
14. Luisi P.L., *Toward the engineering of minimal living cells.* The Anatomical Record, 2002. **268**(3): p. 208-214.
15. Walde P., *Building artificial cells and protocell models: Experimental approaches with lipid vesicles.* BioEssays, 2010. **32**(4): p. 296-303.
16. Hanczyc M.M. and Ikegami T., *Protocells as smart agents for architectural design.* Technoetic Arts, 2009. **7**(2): p. 117-120.
17. Ichihashi N., Usui K., Kazuta Y., Sunami T., Matsuura T., and Yomo T., *Darwinian evolution in a translation-coupled RNA replication system within a cell-like compartment.* Nature Communications, 2013. **4**: p. 2494.
18. Monnard P.-A. and Ziock H.-J., *Question 9: Prospects for the Construction of Artificial Cells or Protocells.* Origins of Life and Evolution of Biospheres, 2007. **37**(4): p. 469-472.
19. Dreyfus R., Baudry J., Roper M.L., Fermigier M., Stone H.A., and Bibette J., *Microscopic artificial swimmers.* Nature, 2005. **437**(7060): p. 862-865.

20. Eniola A.O. and Hammer D.A., *Artificial polymeric cells for targeted drug delivery*. Journal of Controlled Release, 2003. **87**(1-3): p. 15-22.
21. Dora Tang T.Y., et al., *Fatty acid membrane assembly on coacervate microdroplets as a step towards a hybrid protocell model*. Nature Chemistry, 2014. **6**(6): p. 527-533.
22. Haufová P., Dohnal J., Hanuš J., and Štěpánek F., *Towards the inkjet fabrication of artificial cells*. Colloids and Surfaces A: Physicochemical and Engineering Aspects, 2012. **410**: p. 52-58.
23. Rasmussen S., et al., *Transitions from Nonliving to Living Matter*. Science, 2004. **303**(5660): p. 963-965.
24. Hanczyc M.M., *Droplets: Unconventional Protocell Model with Life-Like Dynamics and Room to Grow*. Life, 2014. **4**(4): p. 1038-1049.
25. Martino C. and deMello A.J., *Droplet-based microfluidics for artificial cell generation: a brief review*. Interface Focus, 2016. **6**(4): p. 20160011.
26. Morigaki K. and Walde P., *Fatty acid vesicles*. Current Opinion in Colloid & Interface Science, 2007. **12**(2): p. 75-80.
27. Zhu T.F. and Szostak J.W., *Coupled Growth and Division of Model Protocell Membranes*. Journal of the American Chemical Society, 2009. **131**(15): p. 5705-5713.
28. Murtas G., *Early self-reproduction, the emergence of division mechanisms in protocells*. Molecular BioSystems, 2013. **9**(2): p. 195-204.
29. Lentini R., et al., *Integrating artificial with natural cells to translate chemical messages that direct E. coli behaviour*. Nature Communications, 2014. **5**: p. 4012.
30. Lentini R., Yeh Martín N., and Mansy S.S., *Communicating artificial cells*. Current Opinion in Chemical Biology, 2016. **34**: p. 53-61.
31. Banno T., et al., *Deformable Self-Propelled Micro-Object Comprising Underwater Oil Droplets*. Scientific Reports, 2016. **6**: p. 31292.
32. Hanczyc M.M. and Szostak J.W., *Replicating vesicles as models of primitive cell growth and division*. Current Opinion in Chemical Biology, 2004. **8**(6): p. 660-664.
33. Schrum J.P., Zhu T.F., and Szostak J.W., *The Origins of Cellular Life*. Cold Spring Harbor Perspectives in Biology, 2010. **2**(9): p. a002212.
34. Hanczyc M.M., Fujikawa S.M., and Szostak J.W., *Experimental Models of Primitive Cellular Compartments: Encapsulation, Growth, and Division*. Science, 2003. **302**(5645): p. 618-622.
35. Čejková J., Banno T., Štěpánek F., and Hanczyc M.M., *Droplets as Liquid Robots*. Artificial Life, 2017. **23**(4): p. 528-549.
36. Schneider E. and Mangold M., *Modular assembling process of an in-silico protocell*. Biosystems, 2018. **165**: p. 8-21.
37. Biehl M., Ikegami T., and Polani D., *Specific and Complete Local Integration of Patterns in Bayesian Networks*. Entropy, 2017. **19**(5): p. 230.
38. Li M., Harbron R.L., Weaver J.V.M., Binks B.P., and Mann S., *Electrostatically gated membrane permeability in inorganic protocells*. Nature Chemistry, 2013. **5**: p. 529.
39. Kumar B.V.V.S.P., Patil A.J., and Mann S., *Enzyme-powered motility in buoyant organoclay/DNA protocells*. Nature Chemistry, 2018. **10**(11): p. 1154-1163.

40. Cooper G.J.T., Kitson P.J., Winter R., Zagnoni M., Long D.-L., and Cronin L., *Modular Redox-Active Inorganic Chemical Cells: iCHELLs*. Angewandte Chemie, 2011. **123**(44): p. 10557-10560.
41. Mason A.F., Buddingh B.C., Williams D.S., and van Hest J.C.M., *Hierarchical Self-Assembly of a Copolymer-Stabilized Coacervate Protocell*. Journal of the American Chemical Society, 2017. **139**(48): p. 17309-17312.
42. Hanczyc M.M., Toyota T., Ikegami T., Packard N., and Sugawara T., *Fatty Acid Chemistry at the Oil-Water Interface: Self-Propelled Oil Droplets*. Journal of the American Chemical Society, 2007. **129**(30): p. 9386-9391.
43. Rodríguez-Arco L., Li M., and Mann S., *Phagocytosis-inspired behaviour in synthetic protocell communities of compartmentalized colloidal objects*. Nature Materials, 2017. **16**(8): p. 857-863.
44. Bayoumi M., Bayley H., Maglia G., and Sapra K.T., *Multi-compartment encapsulation of communicating droplets and droplet networks in hydrogel as a model for artificial cells*. Scientific Reports, 2017. **7**: p. 45167.
45. Subramaniam A.B., Wan J., Gopinath A., and Stone H.A., *Semi-permeable vesicles composed of natural clay*. Soft Matter, 2011. **7**(6): p. 2600-2612.
46. Rein M., *Phenomena of liquid drop impact on solid and liquid surfaces*. Fluid Dynamics Research, 1993. **12**(2): p. 61-93.
47. Čejková J., Štěpánek F., and Hanczyc M.M., *Evaporation-induced pattern formation of decanol droplets*. Langmuir, 2016. **32**(19): p. 4800–4805.
48. Čejková J., Schwarzenberger K., Eckert K., and Tanaka S., *Dancing performance of organic droplets in aqueous surfactant solutions*. Colloids and Surfaces A: Physicochemical and Engineering Aspects, 2019. **566**: p. 141-147.
49. Čejková J., Novák M., Štěpánek F., and Hanczyc M.M., *Dynamics of Chemotactic Droplets in Salt Concentration Gradients*. Langmuir, 2014. **30**(40): p. 11937-11944.
50. Rasmussen S., et al., *Protocells: Bridging Nonliving and Living Matter*. 2008: The MIT Press.
51. Ueno N., et al., *Self-Propelled Motion of Monodisperse Underwater Oil Droplets Formed by a Microfluidic Device*. Langmuir, 2017. **33**(22): p. 5393-5397.
52. Seemann R., Fleury J.-B., and Maass C.C., *Self-propelled droplets*. The European Physical Journal Special Topics, 2016. **225**(11): p. 2227-2240.
53. Tanaka S., Sogabe Y., and Nakata S., *Spontaneous change in trajectory patterns of a self-propelled oil droplet at the air-surfactant solution interface*. Physical Review E, 2015. **91**(3): p. 032406.
54. Toyota T., Maru N., Hanczyc M.M., Ikegami T., and Sugawara T., *Self-Propelled Oil Droplets Consuming "Fuel" Surfactant*. Journal of the American Chemical Society, 2009. **131**(14): p. 5012-5013.
55. Jin C., Krüger C., and Maass C.C., *Chemotaxis and autochemotaxis of self-propelling droplet swimmers*. Proceedings of the National Academy of Sciences, 2017. **114**(20): p. 5089-5094.
56. Hanczyc M.M., *Metabolism and motility in prebiotic structures*. Philosophical Transactions of the Royal Society B: Biological Sciences, 2011. **366**(1580): p. 2885-2893.

57. Taylor J.W., Eghtesadi S.A., Points L.J., Liu T., and Cronin L., *Autonomous model protocell division driven by molecular replication*. Nature Communications, 2017. **8**(1): p. 237.
58. Zwicker D., Seyboldt R., Weber C.A., Hyman A.A., and Julicher F., *Growth and division of active droplets provides a model for protocells*. Nature Physics, 2017. **13**(4): p. 408-413.
59. Sato Y., Yasuhara K., Kikuchi J.-i., and Sato T.N., *Synthetic cell division system: Controlling equal vs. unequal divisions by design*. Scientific reports, 2013. **3**.
60. Derenyi I. and Lagzi I., *Fatty acid droplet self-division driven by a chemical reaction*. Physical Chemistry Chemical Physics, 2014. **16**(10): p. 4639-4641.
61. Banno T., Kuroha R., Miura S., and Toyota T., *Multiple-division of self-propelled oil droplets through acetal formation*. Soft Matter, 2015. **11**(8): p. 1459-1463.
62. Caschera F., Rasmussen S., and Hanczyc M.M., *An Oil Droplet Division–Fusion Cycle*. ChemPlusChem, 2013. **78**(1): p. 52-54.
63. Čejková J., Hanczyc M.M., and Štěpánek F., *Multi-Armed Droplets as Shape-Changing Protocells*. Artificial Life, 2018. **24**(1): p. 71-79.
64. Tanaka S., Nakata S., and Kano T., *Dynamic Ordering in a Swarm of Floating Droplets Driven by Solutal Marangoni Effect*. Journal of the Physical Society of Japan, 2017. **86**(10): p. 101004.
65. Points L.J., Taylor J.W., Grizou J., Donkers K., and Cronin L., *Artificial intelligence exploration of unstable protocells leads to predictable properties and discovery of collective behavior*. Proceedings of the National Academy of Sciences, 2018. **115**(5): p. 885-890.
66. Kessin R.H., *Dictyostelium: Evolution, Cell Biology, and the Development of Multicellularity* 2001: Cambridge University Press.
67. Staley J.T., *Prosthecomicrobium and Ancalomicrobium: new prosthecate freshwater bacteria*. Journal of bacteriology, 1968. **95**(5): p. 1921-1942.
68. Čejková J., *Slime Mold Dictyostelium discoideum – A Model System Not Only for Biologists* Chemické listy, 2013. **107**: p. 563-600.
69. Chaudhury M.K. and Whitesides G.M., *How to Make Water Run Uphill*. Science, 1992. **256**(5063): p. 1539-1541.
70. Dos Santos F.D. and Ondarçuhu T., *Free-Running Droplets*. Physical Review Letters, 1995. **75**(16): p. 2972-2975.
71. G.K.Kurup and A.S.Basu, *Passive, Label-Free Droplet Sorting based on Chemical Composition using Tensiophoresis*. Micro Total Analysis Systems, 2012.
72. Kurup G.K. and Basu A.S., *Tensiophoresis: Migration and Sorting of Droplets in an Interfacial Tension Gradient*. Micro Total Analysis Systems, 2011.
73. Nagai K., Sumino Y., Kitahata H., and Yoshikawa K., *Mode selection in the spontaneous motion of an alcohol droplet*. Physical Review E, 2005. **71**(6): p. 065301.
74. Horibe N., Hanczyc M.M., and Ikegami T., *Mode Switching and Collective Behavior in Chemical Oil Droplets*. Entropy, 2011. **13**(3): p. 709-719.
75. Ban T. and Nakata H., *Metal-Ion-Dependent Motion of Self-Propelled Droplets Due to the Marangoni Effect*. The Journal of Physical Chemistry B, 2015. **119**(23): p. 7100-7105.

76. Ban T., Yamagami T., Nakata H., and Okano Y., *pH-Dependent Motion of Self-Propelled Droplets due to Marangoni Effect at Neutral pH*. Langmuir, 2013. **29**(8): p. 2554-2561.
77. Lehmann U., Hadjidj S., Parashar V.K., Vandevyver C., Rida A., and Gijs M.A.M., *Two-dimensional magnetic manipulation of microdroplets on a chip as a platform for bioanalytical applications*. Sensors and Actuators B: Chemical, 2006. **117**(2): p. 457-463.
78. Dorvee J.R., Derfus A.M., Bhatia S.N., and Sailor M.J., *Manipulation of liquid droplets using amphiphilic, magnetic one-dimensional photonic crystal chaperones*. Nature Materials, 2004. **3**(12): p. 896-899.
79. Velev O.D., Prevo B.G., and Bhatt K.H., *On-chip manipulation of free droplets*. Nature, 2003. **426**(6966): p. 515-516.
80. Umapathi U., Chin S., Shin P., Koutentakis D., and Ishii H., *Scaling Electrowetting with Printed Circuit Boards for Large Area Droplet Manipulation*. MRS Advances, 2018. **3**(26): p. 1475-1483.
81. Li S., Liu J., Hou J., and Zhang G., *Meniscus-induced motion of oil droplets*. Colloids and Surfaces A: Physicochemical and Engineering Aspects, 2015. **469**(0): p. 252-255.
82. Li S., Liu J., and Hou J., *Curvature-driven bubbles or droplets on the spiral surface*. Scientific Reports, 2016. **6**: p. 37888.
83. Ooi C.H., van Nguyen A., Evans G.M., Gendelman O., Bormashenko E., and Nguyen N.-T., *A floating self-propelling liquid marble containing aqueous ethanol solutions*. RSC Advances, 2015. **5**(122): p. 101006-101012.
84. Bormashenko E., Bormashenko Y., Grynyov R., Aharoni H., Whyman G., and Binks B.P., *Self-Propulsion of Liquid Marbles: Leidenfrost-like Levitation Driven by Marangoni Flow*. The Journal of Physical Chemistry C, 2015. **119**(18): p. 9910-9915.
85. Paven M., Mayama H., Sekido T., Butt H.-J., Nakamura Y., and Fujii S., *Light-Driven Delivery and Release of Materials Using Liquid Marbles*. Advanced Functional Materials, 2016. **26**(19): p. 3199-3206.
86. Čejková J. and Rychecký O., *Tekuté kuličky*. Chemické listy, 2017. **111**: p. 109-114.
87. Janská P., *Synthesis and characterization of oil liquid marbles*. Diploma thesis, University of Chemistry and Technology Prague, 2017.
88. Janská P., Rychecký O., Zadražil A., Štěpánek F., and Čejková J., *Liquid oil marbles: increasing the bio-availability of poorly water-soluble drugs*. Journal of Pharmaceutical Sciences, 2019. doi: 10.1016/j.xphs.2019.01.026
89. Rychecký O., Majerská M., Král V., Štěpánek F., and Čejková J., *Spheroid cultivation of HT-29 carcinoma cell line in liquid marbles*. Chemical Papers, 2017. **6**(71): p. 1055-1063.
90. Oshima S., Nomoto T., Toyota T., and Fujinami M., *Surface Tension Gradient around an Alcohol Droplet Moving Spontaneously on a Water Surface*. Analytical Sciences, 2014. **30**(4): p. 441-444.
91. Lagzi I., Soh S., Wesson P.J., Browne K.P., and Grzybowski B.A., *Maze Solving by Chemotactic Droplets*. Journal of the American Chemical Society, 2010. **132**(4): p. 1198-1199.

92. Parrilla-Gutierrez J.M., Tsuda S., Grizou J., Taylor J., Henson A., and Cronin L., *Adaptive artificial evolution of droplet protocells in a 3D-printed fluidic chemorobotic platform with configurable environments*. Nature Communications, 2017. **8**(1): p. 1144.
93. Satoh Y., Sogabe Y., Kayahara K., Tanaka S., Nagayama M., and Nakata S., *Self-inverted reciprocation of an oil droplet on a surfactant solution*. Soft Matter, 2017. **13**(18): p. 3422-3430.
94. Ikegami T., Horibe N., and Hanczyc M.M., *Potential Memory Effects in Self-Moving Oil Droplets*. International Journal of Unconventional Computing, 2015. **11**(5-6): p. 345-355.
95. Krüger C., Bahr C., Herminghaus S., and Maass C.C., *Dimensionality matters in the collective behaviour of active emulsions*. The European Physical Journal E, 2016. **39**(6): p. 64.
96. Čejková J. and Ikegami T. *Experimental study of mutual interactions of multiple liquid droplets*. in *SWARM 2017: The 2nd International Symposium on Swarm Behavior and Bio-Inspired Robotics*. 2017. Kyoto - Japan.
97. Tanaka S. and Kano T., *Dynamic oscillatory cluster ordering of self-propelled droplets*. arXiv preprint arXiv:1706.00154, 2017.
98. Nejatimoharrami F., Faina A., Cejkova J., Hanczyc M.M., and Stoy K. *Robotic Automation to Augment Quality of Artificial Chemical Life Experiments*. in *Proceedings of the Artificial Life Conference 2016*. 2016. Cancun - Mexico: MIT Press.
99. Čejková J., Holler S., Quyen N.T., Kerrigan C., Štěpánek F., and Hanczyc M.M., *Chemotaxis and chemokinesis of living and non-living objects*, in *Advances in Unconventional Computing,* A. Adamatzky, Editor. 2017, Springer. p. 245-260.
100. Hazelbauer G.L., Falke J.J., and Parkinson J.S., *Bacterial chemoreceptors: high-performance signaling in networked arrays*. Trends in Biochemical Sciences, 2008. **33**(1): p. 9-19.
101. Szabó A. and Mayor R., *Modelling collective cell migration of neural crest*. Current Opinion in Cell Biology, 2016. **42**: p. 22-28.
102. Eisenbach M., *Sperm chemotaxis*. Reviews of Reproduction, 1999. **4**(1): p. 56-66.
103. Zigmond S.H. and Hirsch J.G., *Leukocyte locomotion and chemotaxis*. The Journal of Experimental Medicine, 1973. **137**(2): p. 387-410.
104. Deisboeck T.S. and Couzin I.D., *Collective behavior in cancer cell populations*. Bioessays, 2009. **31**(2): p. 190-197.
105. Roussos E.T., Condeelis J.S., and Patsialou A., *Chemotaxis in cancer*. Nature Reviews Cancer, 2011. **11**(8): p. 573-587.
106. Hilgardt C., Cejkova J., Hauser M.J.B., and Sevcikova H., *Streamless aggregation of Dictyostelium in the presence of isopropylidenadenosin*. Biophysical Chemistry, 2008. **132**(1): p. 9-18.
107. Ševčíková H., Čejková J., Krausová L., Přibyl M., Štěpánek F., and Marek M., *A new traveling wave phenomenon of Dictyostelium in the presence of cAMP*. Physica D: Nonlinear Phenomena, 2010. **239**(11): p. 879-888.
108. Čejková J., *Studies of atypical aggregation of Dictyostelium discoideum cells*. Diploma thesis, Institute of Chemical Technology Prague, 2006.

109. Jurado-Sánchez B., Pacheco M., Maria-Hormigos R., and Escarpa A., *Perspectives on Janus micromotors: Materials and applications*. Applied Materials Today, 2017. **9**(Supplement C): p. 407-418.
110. Čejková J., Tóth R., Braun A., Branicki M., Ueyama D., and Lagzi I., *Shortest Path Finding in Mazes by Active and Passive Particles*, in *Shortest Path Solvers. From Software to Wetware. Emergence, Complexity and Computation*, A. Adamatzky, Editor. 2018, Springer: Cham. p. 401-408.
111. Maass C.C., Krüger C., Herminghaus S., and Bahr C., *Swimming Droplets*. Annual Review of Condensed Matter Physics, 2016. **7**(1): p. 171-193.
112. Zatsiorsky V., *Biomechanics in Sport: Performance Enhancement and Injury Prevention*. 2008: Wiley.
113. Song L., et al., *Dictyostelium discoideum chemotaxis: Threshold for directed motion*. European Journal of Cell Biology, 2006. **85**(9–10): p. 981-989.
114. Berg H.C., *E. coli in Motion*. 2008: Springer New York.
115. Wardle C.S., *Limit of fish swimming speed*. Nature, 1975. **255**: p. 725.
116. Phelps M. and Abrahamson A., *No Limits: The Will to Succeed*. 2008: Free Press.
117. Bergey D., Holt J., and Krieg P., *Bergey's Manual of Determinative Bacteriology*. The Williams Wilkins Co, 1994.
118. Kysela D.T., Randich A.M., Caccamo P.D., and Brun Y.V., *Diversity Takes Shape: Understanding the Mechanistic and Adaptive Basis of Bacterial Morphology*. PLOS Biology, 2016. **14**(10): p. e1002565.
119. Young K.D., *The Selective Value of Bacterial Shape*. Microbiology and Molecular Biology Reviews, 2006. **70**(3): p. 660-703.
120. Wagner J.K., Setayeshgar S., Sharon L.A., Reilly J.P., and Brun Y.V., *A nutrient uptake role for bacterial cell envelope extensions*. Proceedings of the National Academy of Sciences, 2006. **103**(31): p. 11772-11777.
121. Justice S.S., Hunstad D.A., Cegelski L., and Hultgren S.J., *Morphological plasticity as a bacterial survival strategy*. Nature Reviews Microbiology, 2008. **6**(2): p. 162-168.
122. Ford E.D., *Branching, crown structure and the control of timber production*, in *Attributes of trees as crop plants*, M.G.R. Cannell and J.E. Jackson, Editors. 1985, Abbotts Ripton, Institute of Terrestrial Ecology. p. 228-252.
123. Pagès L., *Branching patterns of root systems: quantitative analysis of the diversity among dicotyledonous species*. Annals of botany, 2014. **114**(3): p. 591-598.
124. Chamberlain J.J.A. and Graus R.R., *Water Flow and Hydromechanical Adaptations of Branched Reef Corals*. Bulletin of Marine Science, 1975. **25**(1): p. 112-125.
125. Hannezo E., et al., *A Unifying Theory of Branching Morphogenesis*. Cell, 2017. **171**(1): p. 242-255.e27.
126. Gundem G., et al., *The evolutionary history of lethal metastatic prostate cancer*. Nature, 2015. **520**: p. 353-357.
127. Levitan I.B. and Kaczmarek L.K., *The neuron: cell and molecular biology*. 2015: Oxford University Press, USA.
128. Golding I., Kozlovsky Y., Cohen I., and Ben-Jacob E., *Studies of bacterial branching growth using reaction–diffusion models for colonial development*. Physica A: Statistical Mechanics and its Applications, 1998. **260**(3–4): p. 510-554.

129. Adamatzky A., *Physarum Machines: Computers from Slime Mould*. World Scientific Series on Nonlinear Science: Series A (Book 74). 2010: World Scientific Publishing Company.
130. Crivoi A. and Duan F., *Evaporation-induced branched structures from sessile nanofluid droplets*. The Journal of Physical Chemistry C, 2013. **117**(15): p. 7835-7843.
131. Jiusto J.E. and Weickmann H.K., *Types of Snowfall*. Bulletin of the American Meteorological Society, 1973. **54**(11): p. 1148-1162.
132. Grier D., Ben-Jacob E., Clarke R., and Sander L.M., *Morphology and Microstructure in Electrochemical Deposition of Zinc*. Physical Review Letters, 1986. **56**(12): p. 1264-1267.
133. Saffman P.G. and Taylor G., *The Penetration of a Fluid into a Porous Medium or Hele-Shaw Cell Containing a More Viscous Liquid*. Proceedings of the Royal Society of London. Series A, Mathematical and Physical Sciences, 1958. **245**(1242): p. 312-329.
134. Wang C., Rathore K.S., and Robinson K.R., *The responses of pollen to applied electrical fields*. Developmental Biology, 1989. **136**(2): p. 405-410.
135. Nakamura N., Fukushima A., Iwayama H., and Suzuki H., *Electrotropism of pollen tubes of camellia and other plants*. Sexual Plant Reproduction, 1991. **4**(2): p. 138-143.
136. Malhó R., Feijó J.A., and Pais M.S.S., *Effect of electrical fields and external ionic currents on pollen-tube orientation*. Sexual Plant Reproduction, 1992. **5**(1): p. 57-63.
137. Kral N., Hanna Ougolnikova A., and Sena G., *Externally imposed electric field enhances plant root tip regeneration*. Regeneration, 2016. **3**(3): p. 156-167.
138. Jess W., *Rooted in physics*. Physics World, 2018. **31**(4): p. 38-41.
139. Siefert J.L., and Fox G.E., *Phylogenetic mapping of bacterial morphology*. Microbiology, 1998. **144**(10): p. 2803-2808.
140. Lempel A. and Ziv J., *On the complexity of finite sequences*. IEEE Transactions on information theory, 1976. **22**(1): p. 75-81.
141. Dehshibi M.M., Čejková J., Švára D., and Adamatzky A., *On complexity of branching droplets in electrical field*. arXiv preprint arXiv:1901.05043 2019.
142. Barge L.M., et al., *From Chemical Gardens to Chemobrionics*. Chemical Reviews, 2015. **115**(16): p. 8652-8703.
143. Witkowski O. and Ikegami T., *Emergence of Swarming Behavior: Foraging Agents Evolve Collective Motion Based on Signaling*. PLOS Onene, 2016. **11**(4): p. e0152756.
144. Vicsek T. and Zafeiris A., *Collective motion*. Physics Reports, 2012. **517**(3–4): p. 71-140.
145. Schumacher L.J., Kulesa P.M., McLennan R., Baker R.E., and Maini P.K., *Multidisciplinary approaches to understanding collective cell migration in developmental biology*. Open Biology, 2016. **6**(6).
146. Solovev A.A., Sanchez S., and Schmidt O.G., *Collective behaviour of self-propelled catalytic micromotors*. Nanoscale, 2013. **5**(4): p. 1284-1293.
147. Nishimori H., Suematsu N.J., and Nakata S., *Collective Behavior of Camphor Floats Migrating on the Water Surface*. Journal of the Physical Society of Japan, 2017. **86**(10): p. 101012.
148. Soh S., Bishop K.J.M., and Grzybowski B.A., *Dynamic Self-Assembly in Ensembles of Camphor Boats*. The Journal of Physical Chemistry B, 2008. **112**(35): p. 10848-10853.

149. Dolganov P.V., Demikhov E.I., Dolganov V.K., Bolotin B.M., and Krohn K., *Collective behavior of light-induced droplets in smectic membranes*. The European Physical Journal E, 2003. **12**(4): p. 593-597.
150. Thutupalli S., Fleury J.-B., Schiller U.D., Gompper G., Herminghaus S., and Seemann R., *Hydrodynamics mediated collective motions in populations of microdroplets*. Engineering of Chemical Complexity II, 2014. **12**: p. 125-148.
151. Cira N.J., Benusiglio A., and Prakash M., *Vapour-mediated sensing and motility in two-component droplets*. Nature, 2015. **519**(7544): p. 446-450.
152. Liu D. and Tran T., *Vapor-Induced Attraction of Floating Droplets*. The Journal of Physical Chemistry Letters, 2018. **9**(16): p. 4771-4775.
153. Moerman P.G., et al., *Solute-mediated interactions between active droplets*. Physical Review E, 2017. **96**(3): p. 032607.
154. Vella D. and Mahadevan L., *The "cheerios effect"*. American journal of physics, 2005. **73**(9): p. 817-825.
155. Karpitschka S., et al., *Liquid drops attract or repel by the inverted Cheerios effect*. Proceedings of the National Academy of Sciences, 2016. **113**(27): p. 7403-7407.
156. Čejková J., Ikegami T., and Štěpánek F. *Life-like swarm behavior of multiple chemotactic droplets* in *14th European Conference on Artificial Life 2017*. 2017. Lyon - France: MIT Press.
157. Esser-Kahn A.P., Odom S.A., Sottos N.R., White S.R., and Moore J.S., *Triggered Release from Polymer Capsules*. Macromolecules, 2011. **44**(14): p. 5539-5553.
158. Kovačík P., Kremláčková Z., and Štěpánek F., *Investigation of radiofrequency induced release kinetics from magnetic hollow silica microspheres*. Microporous and Mesoporous Materials, 2012. **159**(0): p. 119-125.
159. Ullrich M., Hanuš J., and Štěpánek F., *Remote control of enzymatic reaction in compartmentalized microparticles: A system for the delivery of unstable actives*. Chemical Engineering Science, 2015. **125**: p. 191-199.
160. Hanuš J., Ullrich M., Dohnal J., Singh M., and Štěpánek F., *Remotely Controlled Diffusion from Magnetic Liposome Microgels*. Langmuir, 2013. **29**(13): p. 4381-4387.
161. Ullrich M., Hanuš J., Dohnal J., and Štěpánek F., *Encapsulation stability and temperature-dependent release kinetics from hydrogel-immobilised liposomes*. Journal of Colloid and Interface Science, 2013. **394**(0): p. 380-385.
162. Čejková J., Hanuš J., and Štěpánek F., *Investigation of internal microstructure and thermo-responsive properties of composite PNIPAM/silica microcapsules*. Journal of Colloid and Interface Science, 2010. **346**: p. 352-360.
163. Čejková J., Tokárová V., Pittermannová A., and Štěpánek F. *Remotely controllable microcapsules for site-specific delivery of a chemical payload*. in *International Conference on Intelligent Robotis and Systems – IROS 2011*. 2011. San Francisco, USA.
164. Čejková J., Gorný D., Haufová P., and Štěpánek F. "*Artificial spores*" *- hybrid alginate microcapsules with encapsulated yeast cells*. . in *Proceedings of the Twelfth European Conference on the Synthesis and Simulation of Living Systems*. 2013. Taormina, Italy: MIT Press.

165. Čejková J., Haufová P., Gorný D., Hanuš J., and Štěpánek F., *Biologically triggered liberation of sub-micron particles from alginate microcapsules*. Journal of Materials Chemistry B, 2013. **1**(40): p. 5456-5461.
166. Solé R., Ollé-Vila A., Vidiella B., Duran-Nebreda S., and Conde-Pueyo N., *The road to synthetic multicellularity*. Current Opinion in Systems Biology, 2018. **7**: p. 60-67.
167. Desnitski A.G., *On the origins and early evolution of multicellularity*. Biosystems, 1993. **29**(2): p. 129-132.
168. Costa E.C., Moreira A.F., de Melo-Diogo D., Gaspar V.M., Carvalho M.P., and Correia I.J., *3D tumor spheroids: an overview on the tools and techniques used for their analysis*. Biotechnology Advances, 2016. **34**(8): p. 1427-1441.
169. Lin R.-Z. and Chang H.-Y., *Recent advances in three-dimensional multicellular spheroid culture for biomedical research*. Biotechnology Journal, 2008. **3**(9-10): p. 1172-1184.
170. Hirschhaeuser F., Menne H., Dittfeld C., West J., Mueller-Klieser W., and Kunz-Schughart L.A., *Multicellular tumor spheroids: An underestimated tool is catching up again*. Journal of Biotechnology, 2010. **148**(1): p. 3-15.
171. Langton C.G., *Artificial life: An overview*. 1997: MIT Press.

9 Appendixes

1. **Čejková J.,** Banno T., Štěpánek F., Hanczyc M.M., *Droplets as Liquid Robots*, Artificial Life, 2017. **23** (4): p. 528-549.

2. **Čejková J.,** Novák M., Štěpánek F., Hanczyc M., *Dynamics of chemotactic droplets in salt concentration gradients,* Langmuir, 2014. **30**(40): 11937–11944.

3. **Čejková J.,** *Dictyostelium discoideum – model system not only for biologists,* Chemické listy, 2013. **107**: p. 563-600.

4. **Čejková J.,** Štěpánek F., Hanczyc M., *Evaporation-induced pattern formation of decanol droplets,* Langmuir, 2016. **32** (19): p. 4800-4805.

5. **Čejková J.,** Schwarzenberger K., Eckert K., Tanaka S., *Dancing performance of organic droplets in aqueous surfactant solutions,* Colloids and Surfaces A: Physicochemical and Engineering Aspects, 2019. **566**: p.141-147.

6. **Čejková J.,** Haufová P., Gorný D., Hanuš J., Štěpánek F. *Biologically triggered liberation of sub-micron particles from alginate microcapsules*, Journal of Materials Chemistry B, 2013. **1**: p. 5456-5461.

7. Rychecký O., Majerská M., Král V., Štěpánek F., **Čejková J.** *Spheroid cultivation of HT-29 carcinoma cell line in liquid marbles,* Chemical Papers, 2017. **71**(6): p. 1055–1063.

Droplets As Liquid Robots

Jitka Čejková*,**
University of Chemistry and Technology Prague

Taisuke Banno†
Keio University

Martin M. Hanczyc‡
University of Trento
University of New Mexico

František Štěpánek**
University of Chemistry and Technology Prague

Abstract Liquid droplets are very simple objects present in our everyday life. They are extremely important for many natural phenomena as well as for a broad variety of industrial processes. The conventional research areas in which the droplets are studied include physical chemistry, fluid mechanics, chemical engineering, materials science, and micro- and nanotechnology. Typical studies include phenomena such as condensation and droplet formation, evaporation of droplets, or wetting of surfaces. The present article reviews the recent literature that employs droplets as animated soft matter. It is argued that droplets can be considered as liquid robots possessing some characteristics of living systems, and such properties can be applied to unconventional computing through maze solving or operation in logic gates. In particular, the lifelike properties and behavior of liquid robots, namely (i) movement, (ii) self-division, and (iii) group dynamics, will be discussed.

Keywords
Robot, droplet, movement, self-division, group dynamics

1 Introduction

The word "robot" was first introduced in 1920 in a famous Czech play *R.U.R.* (Rossum's Universal Robots) [22], where robots are not clanking metal constructions, but humanlike beings made of soft matter. The author of the play, Karel Čapek, describes them as being made of a protoplasm—a substantive essence of living matter. It is described by Domin in the first act as "a blob of some kind of colloidal jelly that even a dog wouldn't eat." At the time the similarities between colloidal materials and the living protoplasm inside cells was already being investigated [27, 37].

Today robots are typically thought of as dynamic electromechanical objects. In contrast, Čapek's robots did not have wheels, electric power, or computer systems to control them. They were based only on chemical principles and consisted of fluidic colloidal substances. Thus we can consider a droplet based on chemical principles and activated through fluid dynamics to be an embodiment of robotics more sympathetic to Čapek's original conception. Such soft-bodied robots might be made from a variety of substances, including liquid droplets [56] and gels [68]. Such chemical and liquid robots could perform autonomous movement through the exploitation of chemical potential without using predefined mechanical parts, but rather using self-organized fluid dynamics.

* Contact author.
** Chemical Robotics Laboratory, University of Chemistry and Technology Prague, Technická 3, Prague 6, 166 28, Czech Republic. E-mail: Jitka.Cejkova@vscht.cz (J.Č.); Franktisek.Stepanek@vscht.cz (F.Š.)
† Department of Applied Chemistry, Keio University, Yokohama, Japan. E-mail: banno@applc.keio.ac.jp
‡ Laboratory for Artificial Biology, Centre for Integrative Biology (CIBIO), University of Trento, Trento, Italy; Chemical and Biological Engineering, University of New Mexico, USA. E-mail: martin.hanczyc@unitn.it

The play *R.U.R.* is famous not only because of the invention of the word "robot"; it was a controversial play that was ahead of its time. Briefly, it was about a mad scientist, Rossum, who discovers how to create artificial life and starts creating artificial human beings. What follows is a factory for making robots, a robot rebellion, and the extinction of the human race. Although the play is almost one hundred years old, it provokes many contemporary questions. In a way, *R.U.R.* also predicted biological engineering, which is now taking halting steps toward creating artificial life. In addition the play used the term "robotka" for female robot, even without gender equality requirements in its time. Only the masculine form "robot" found its way into many languages; the word "robotka" is not used, even in Czech.

The term "robot" derives from the Czech word "robota," which means *forced labor*. In the context of robots in general this meaning still holds. In the context of droplets as liquid robots, we can argue that any force acting on the droplet would induce a response such as movement, division, or release of content. In this article we will develop the idea that forces shape the dynamics of droplets in many different liquid robot contexts.

In another view, droplet-based liquid robots can be considered as a physical embodiment of Braitenberg's *vehicles* [18]. These motile vehicles possess simple environmental sensors linked to actuators at the wheels for movement. In this way Braitenberg's vehicles were capable not only of motion and directed taxis, but also of complex behaviors. It can be argued that mobile droplets possess the basic attributes of vehicles (e.g., sensors, actuators, body), including sensory-motor coupling [46, 51, 57].

The present article is structured as follows. First we introduce droplets in general. Then a literature overview is given to summarize the context of droplet behavior: (i) movement, (ii) self-division, and (iii) group dynamics. This is followed by some examples of droplets moving in mazes or manipulated in logic gates. Finally, liquid marbles are presented as another potential embodiment of liquid-based robotics.

2 Droplets and Vesicles

Droplets are liquid entities for which a degree of immiscibility is required between at least two phases (gas-liquid or liquid-liquid), and the attractive and repulsive interactions between molecules at the interface can give rise to a surface tension, which defines among other things the shape of a droplet. Standard examples include water droplets in air [95], water droplets in oil [5], and oil droplets in water [24]. In addition, molecules can partition preferentially into the water or the oil phase, depending on their hydrophilic or hydrophobic properties. For example, oil-soluble dyes (e.g., Oil Red O, Sudan Black) are used for better visualization of oil phases, while inorganic salts (e.g., NaCl) dissolve preferentially in aqueous phases. However, surfactants, which are amphiphilic molecules containing both hydrophilic and hydrophobic groups, self-assemble on the phase boundary (Figure 1). Surfactants are surface-active compounds that can lower the interfacial tension between the two phases. Droplets can of course form also in the absence of surfactants, but surface-active molecules that self-assemble at the droplet boundary are useful in modulating the interfacial tension of the interface and therefore the properties and behavior of droplets. Another purpose of surfactants is to stabilize droplets by lowering in general the interfacial tension and suppressing droplet coalescence.

When an aqueous droplet is covered by a continuous lipid bilayer in a bulk aqueous phase, it is called a *vesicle* [11]. The self-assembled amphiphilic molecules on the vesicle surface define the vesicle. In principle a vesicle is a water-in-oil-in-water droplet with an aqueous core that can contain water-soluble molecules and a lipid bilayer membrane where oil-soluble molecules can be incorporated. Vesicles are dispersed in the continuous water phase and range in size from tens of nanometers to hundreds of micrometers. For artificially made vesicles using phospholipids or lipids derived from biomembranes, the term *liposomes* is often used, and applications for liposomes range from artificial cells [60] to drug delivery to microcontainers [98].

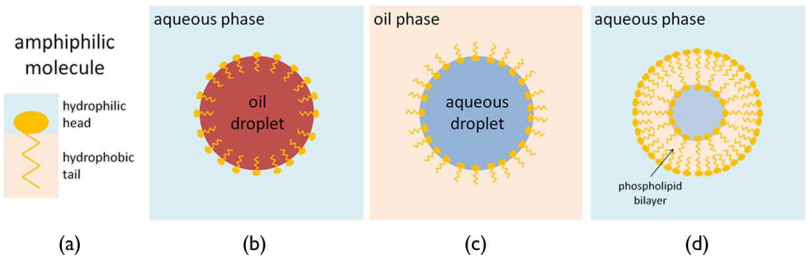

Figure 1. (a) A representation of an amphiphilic surfactant molecule consisting of a hydrophilic head that preferentially partitions in the aqueous phase and a hydrophobic tail that preferentially partitions in the oil phase. Different architectures of surfactants in differently arranged multiphase systems: (b) oil droplet in water phase, (c) aqueous droplet in oil phase, (d) vesicle consisting of a phospholipid bilayer.

Droplets can be produced in various ways. To produce a single droplet or a few droplets, simply dropping liquid from a micropipette or a syringe can be sufficient. Large quantities of droplets can be produced by a wide range of techniques including, for example, atomizers, nebulizers, and homogenizers of various designs. These techniques will produce thousands to millions of droplets dispersed in the continuous phase as emulsions. Typical architectures include oil in water (Figure 1b) or water in oil (Figure 1c) emulsions, but more complex organizations such as double emulsions also exist [36]. The implementation of robotic platforms and microfluidics for the generation and analysis of droplets has been demonstrated [43, 47, 49, 59, 74]. In general, droplets can be produced easily. However, long-term stability is typically achieved through the presence of surfactants, which increase the kinetic stability of the system.

3 Moving Droplets

Droplets can be designed to move and can be controlled by various external forces, and thus the droplets can mimic both the behavior of nonliving objects, such as rocks rolling down a hill, and also the behavior of living cells or small organisms that can move purposefully in response to various stimuli. There are several examples of motion due to applied forces or perceived stimuli: Gravitational force induces gravitaxis (geotaxis), a gradient of chemicals that are soluble in the fluid induces chemotaxis, movement in the gradient of cellular adhesion sites or substrate-bound chemoattractants is called haptotaxis, electrotaxis (or galvanotaxis) is directional movement in response to an electric field, magnetotaxis is movement in a magnetic field, phototaxis is the ability to respond to light, and thermotaxis is migration along a gradient of temperature. These kinds of natural movements are well known for biological objects that have locomotion organelles [23], and in the same way the movement of synthetic objects can be studied for orthologous dynamics. If droplets can become animated and follow one or more of these types of motion, then it would be justified to argue that they are liquid robots, as one of the primary characteristics of robotics is programmed movement. Although it is not common to term moving droplets as robots [56, 92], in the case of solid particles we commonly encounter terms such as swimming micro- or nano-robots [16, 65, 70, 78]. The different types of motion will be presented in the following subsections: Section 3.1 will describe artificial haptotaxis, Section 3.2 will summarize the movement of droplets mimicking chemotaxis, and Section 3.3 will present other examples of oriented movement (such as magnetotaxis or galvanotaxis of droplets).

Figure 2 shows several contexts in which a droplet can be placed and tasked for movement, viewed in vertical cross section. Droplets have been shown to move when placed on a solid surface in air [21] (a), surrounded fully by another liquid (b), or placed in a thin layer of a liquid in contact with both substrate and air [24] (c). When there is an interaction of droplet with solid substrate, the shape of the droplet can change as a result of change in contact angle. Another type of droplet

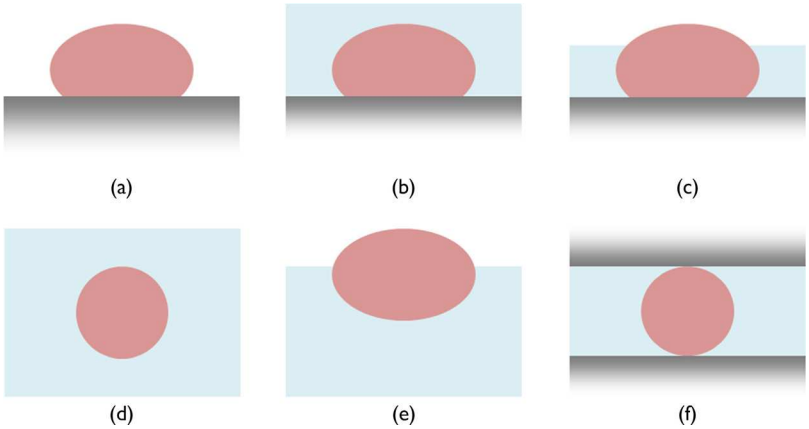

Figure 2. Configuration of droplet movement experiments in a side view: (a) droplet on a solid substrate surrounded by air, (b) droplet on a solid substrate surrounded fully by another liquid, (c) droplet on a solid substrate placed in a thin layer of another liquid, (d) droplet freely swimming in another liquid, (e) droplet floating on the surface of an another liquid, (f) droplet in a channel.

motion is swimming (d), in the case when the droplet and surrounding liquid have similar densities. This will require that viscosity dominate and the droplet move by creating friction with the surrounding fluid. The floating of a droplet on the surface of another liquid (e) happens if the droplet has a lower density than the continuous phase. Both internal droplet dynamics and proximal fluid dynamics in the surrounding fluid may govern droplet movement. Finally, in microfluidics the droplets can move within channels (f). The width of channels and the droplet diameters have similar magnitudes, and the channels are not open to the air. However there can be a configuration where the droplet moves in a channel that is open to the air [62]. Some atypical experimental setups have been used; for example, Sumino et al. have shown rotational motion within a circle normal to the horizontal plane and climbing motion on a stairlike substrate [90].

Studies on oil droplet movement can be performed in various geometrical configurations. Various arenas, shown from the top, are presented in Figure 3. Commonly a round petri dish is used with various depths of the continuous phase [94], where 2D trajectories of droplets are observed and recorded (a). Circular channels can be created, for example, by two rings attached to the glass substrate [76] (b). The space between the inner and outer rings (walls) forms in principle an endless channel ideal for self-propelled droplet experiments. Simple architectures are based on rectangular cells or wide channels (c). Some works deal with droplet movement in more complex systems such as mazes [24, 62] (d).

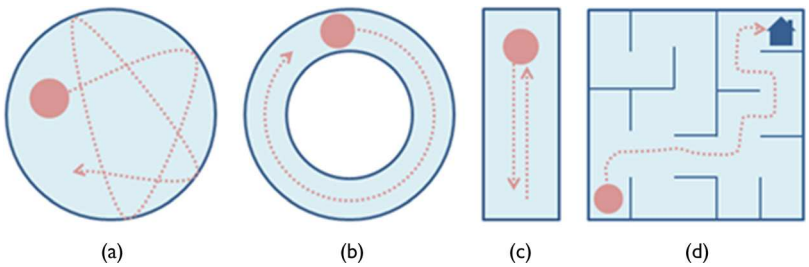

Figure 3. Configuration of droplet movement experiments in a top view: (a) round dish, (b) circular channel, (c) straight channel, and (d) maze.

The droplet movement can be characterized by various parameters; the most common ones are directionality and velocity. Other parameters include acceleration, pause duration, and turning angle [46, 51, 57]. In our article [24] on chemotactic decanol droplets we evaluated also the *induction time*, that is, the time needed for the response to the chemical signal. In the following text, we will summarize experiments according to the designed experimental setup.

3.1 Droplet Movement on Solid Surfaces

In nature, motion induced by an adhesion gradient is called haptotaxis. Droplets can move on solid surfaces without an additional continuous liquid phase if there is any difference in surface properties between the front and the rear of the droplet. This usually results in a difference in contact angle between different parts of the droplet and produces artificial haptotaxis. We present examples below that might be used for various targeted outcomes, such as reversible or irreversible movement.

The classic experiment by the Whitesides group showed how droplets of water can in fact move "uphill" against gravity if the solid surface is patterned with areas that affect the contact angle of the droplet [53]. Droplets consisting of *n*-alkanes and silane molecules behave as *self-runners* on hydrophilic glass or silicon substrates [32]. The mechanism is based on leaving a hydrophobic coating on the hydrophilic substrate, which shifts the center of mass and pushes the droplets towards the exposed hydrophilic area. The movement stops due to depletion of free hydrophilic substrate. It is noted that the droplet trajectories never cross. In another study, reversible self-propelled droplet movements of long-chain alkanes at solid-gas interfaces have been shown [63], with reversibility of movement modulated by temperature changes near the alkane bulk melting temperature.

Cira et al. [21] have shown that miscible liquids such as propylene glycol and water deposited on clean glass cause the motion of neighboring droplets over a distance, because these droplets are stabilized by evaporation-induced surface tension gradients. The droplets move in response to the vapor emitted by neighboring droplets. This kind of movement enables the crossing of droplet trajectories, and no permanent change of substrate surface occurs.

Sumino et al. [90] described oil droplet movement on a glass substrate that is based on a difference in surface tension between the front and the rear of the droplet. This mechanism also allows reversible movement. They have also studied self-running motion of an oil droplet on an acid-treated glass substrate [89]. Similarly, squalene droplets move on a hydrophobic solid substrate [44]. Thus, when using specific substrates and chemical droplets, haptotaxis can be artificially created and studied as long as the system can maintain a differential in surface energy along the droplet with the underlying substrate. This creation and maintenance of a differential in surface energy also underlies the mechanisms of droplet movement presented in the following subsections.

3.2 Chemotactic Droplet Movement

In nature, if a motile cell senses soluble molecules and follows a concentration gradient to the source, or if it moves away from a source of undesirable chemicals (e.g., repellent, toxin), it is displaying a directional movement called positive or negative chemotaxis, respectively [23]. This phenomenon is well known to biologists and intensively studied in living systems. Recently a few laboratories have started to focus on the movement properties of artificial constructs, including the directional movement of nonliving objects in chemical gradients, and such movement is usually called artificial chemotaxis.

Almost all observed movements of droplets in chemical gradients are in fact movements due to gradients of surface tension that are induced by chemical signals. These systems usually involve two immiscible liquids, with one liquid forming the droplet and the other forming the continuous phase (Figure 2b–f). When a surfactant is placed in an aqueous system, it self-assembles at the air-liquid or liquid-liquid interface and lowers the surface tension of the system. Kurup and Basu [35, 61] have used the term *tensiophoresis* for droplet movement due to a gradient of surface tension. When the surface tension of a liquid is altered, liquid and surfactants flow from areas of low surface tension

to areas of high surface tension along an interface. This flow continues until the differential in interfacial tension is null, and this phenomenon is known as *Marangoni flow*.

The Marangoni-type oil droplet movements are driven by thermal or chemical concentration gradients that affect the local interfacial tension. The properties of the movement are dependent on the size and shape of the droplets. Nagai et al. [73] have found that a pentanol droplet with a volume of less than 0.1 μl shows irregular translational motion, whereas intermediate-sized droplets of 0.1–200 μl show vectorial motion. This mode selection is interpreted in terms of competition between the droplet size and the critical wave number in the instability due to the Marangoni effect. In addition, Horibe et al. [51] showed mode-switching for oleic-anhydride-fueled oil droplets that again depended directly on the size (volume) of the droplets. For this system it was also argued that the self-moving oleic-anhydride-fueled oil droplets are an embodiment of homeostasis and therefore contain the basis for sensory-motor coupling. Later, possible memory effects in these self-moving droplets were reported, implying perhaps a limited degree of autonomy [46, 57].

We have studied the movement of 1-decanol droplets in the presence of sodium decanoate solution [24] (Figure 4a). Decanol droplets were able to follow salt additions and mimic the chemotactic behavior of living organisms [23]. This droplet system has also the ability to reverse the direction of movement repeatedly, to carry and release a chemically reactive cargo, to select a stronger concentration gradient from two options, and to initiate chemotaxis by an external temperature stimulus. Again here the interfacial tension between the decanol droplets and the surrounding aqueous solution is governed by the interaction of the decanoate surfactant with the added salt gradients.

A system of oil droplet movement based on fatty acid chemistry has been proposed by Hanczyc et al. [45, 48, 97] (Figure 4b). An oil phase containing oleic anhydride precursor was introduced into an aqueous environment that contained oleate micelles. The products of the precursor hydrolysis were coupled to the movement of the oil droplet and the production of waste vesicles. The oil droplet successfully moved away from this waste product into fresh unmodified solution, displaying a form of chemotaxis. It has been also shown how droplets can move in a pH gradient. In this case the droplets move as they consume the on-board fuel. The droplets move as they generate a local pH gradient through the chemical hydrolysis of the precursor. The self-generated pH gradient then affects the interfacial tension between the droplet and the aqueous environment. As verification of the mechanism, the autonomous motion can be overridden by large external pH gradients imposed on the aqueous environment, resulting in directed chemotaxis. The same chemistry was used by Suzuki et al. [92], who prepared an alginate gel capsule robot with an embedded droplet.

Ban and Nakata [8] have studied nitrobenzene droplets containing di-(2-ethylhexyl)phosphoric acid (DEHPA) in a phosphate buffer solution. In this system, gels containing various alkaline-earth metal ions induced movement of oriented droplets, mimicking chemotaxis. The directional movement was due to the metal ions creating asymmetric convection due to interfacial surface tension differences. In addition the same droplets are responsive to pH gradients [10]. pH-sensitive movement was shown also by Banno et al. [13]. They used *n*-heptyloxybenzaldehyde oil droplets that were self-propelled in the presence of ester-containing cationic surfactant. Later they studied the differences in droplet behavior dependent on surfactant concentration and type and also the phosphate concentration [14]. This group [72] also demonstrated the underwater self-propelled motion of micrometer-sized oil droplets controlled by using chemical reactions, namely pH-induced motion of 4-heptyloxybenzaldehyde droplets using a hydrolyzable gemini cationic surfactant. In this study the droplets moved towards higher pH, where the rate of hydrolysis was increased (Figure 4c).

In the previous examples, the importance of a chemical gradient, either self-generated or externally imposed, is noted for producing an imbalance in the interfacial tension around a droplet, resulting in chemotactic droplet movement. The formation of a chemical gradient that triggers droplet movement can also be controlled by light and is then termed photo-driven chemopropulsion (photo-chemopropulsion) [33]. Photoirradiation in the close proximity of a dichloromethane (DCM) droplet containing 2-hexyldecanoic acid (HDA) and chromoionophore I (CI) (molar ratio HDA : CI ≈ 170 : 1) initiates a rapid pH change in the aqueous channel fluid. This leads to a cascade of events involving, for example, protonation of the 2-hexyldecanoate ion and a change in surface

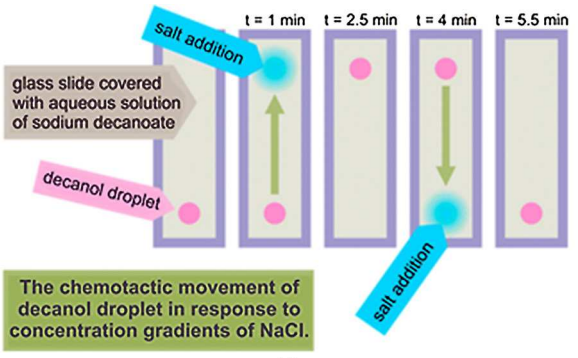

(a)

(b)

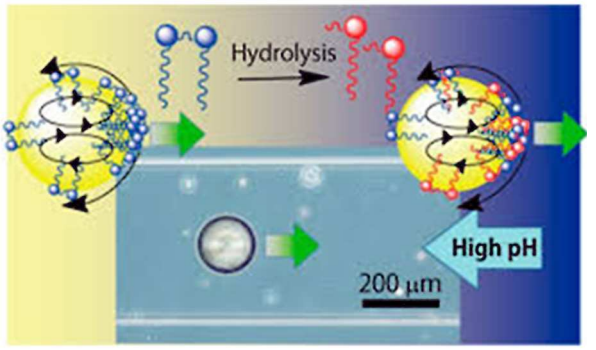

(c)

Figure 4. Examples of moving droplets. (a) Schematic representation of repeatable chemotactic decanol droplet movement in a salt gradient (reprinted with permission from [24]; © 2014 American Chemical Society). (b) Nitrobenzene droplet containing oleic anhydride and Oil Red O as colorant moving in a dish containing both oleate micelles and a pH indicator thymolphthalein (reprinted with permission from [45]; © 2011 The Royal Society). (c) pH-induced self-propelled motion of micrometer-sized oil droplets controlled by using chemical reactions (reprinted with permission from [72]; © 2014, American Chemical Society).

tension of the fluid surrounding the droplet, resulting in a fast movement of the droplet away from the light source.

Directed motion of a nitrobenzene droplet floating in an aqueous solution can be generated by using a laser beam, which causes a local increase of temperature leading to temperature-induced Marangoni convection [82]. With these laser-induced flows the droplet is able to move backward

or forward, depending on whether the laser beam is focused on the top or the bottom part of the droplet. Dixit et al. [30] have shown that water droplets covered by a surfactant or a lipid monolayer immersed in an organic liquid (decanol or mineral oil) can be controlled using infrared light via both the thermocapillary effect and convection. Hu and Ohta [52] have shown the manipulation of aqueous droplets by optically induced Marangoni circulation. For more details about Marangoni-driven swimmers we recommend the recent review article of Maass et al. [67]. Table 1 in [67] summarizes the properties of different droplet systems, namely droplet size, droplet velocity, and active swimming period.

In these experimental systems, it is clear that when the physical mechanism of droplet motion is known, the droplets can be manipulated, resulting in various forms of directional taxis. The systems are typically compositionally very simple, and therefore external control is relatively easy to implement. Precise control may be exerted more efficiently using light/thermal gradients rather than purely dissipative chemical gradients. This type of artificial chemotaxis of droplets should be contrasted with biological systems, which are vastly more complex, and whose taxis mechanisms are complicated. Living cells responding to and then decoupling from external stimuli are common and result in a kind of autonomy. The liquid robots presented here are far less autonomous and perhaps more easily controlled. It is possible that as the degree of complexity in droplets is increased, so will their autonomy. The degree of external control necessary for directed motion can then be experimentally tested.

3.3 Other Types of Droplet Movement

A fully functioning electromagnetic actuation (EMA) system for the manipulation of liquid robots was proposed and fabricated by Zadražil et al. [100]. The system consisted of a custom-made experimental setup using a set of four solenoids and a control algorithm written in LabVIEW software with micro-droplets moving with two degrees of freedom on an air-water interface. The magnetic liquid robots were made from kerosene droplets (stabilized by Tween 65) containing iron oxide nanoparticles (size approximately 10 nm). The EMA system proved to be a robust system for manipulation and navigation of droplets of variable size (diameter 100 μm–1 mm). Furthermore, the LabVIEW-based algorithm was effective in performance and manipulation tasks. Using a video feedback loop to obtain information about the instantaneous droplet position and velocity, the algorithm calculates the currents required in each of the four solenoids such that the resulting magnetic force acting on the droplet drives it in the desired direction. The algorithm is optimized to achieve a "soft landing," that is, to smoothly decelerate the droplet as it approaches the target setpoint without overshooting it. The system allows the user to freely switch between locomotion tasks (user-defined target position, user-defined trajectory, or gamepad control), and so it provides the basis for a wide range of potential future applications involving the use of such liquid robots.

There are additional systems for the two-dimensional magnetic manipulation of droplets, such as manipulation of aqueous droplets suspended in silicone oil [64]. For example, water droplets can be coated with magnetic porous Si nanoparticles in dichloromethane [31] and manipulated with external control. The ability to control the magnetic droplets by external magnetic fields shares some similarities with remote control of traditional mechanoelectrical robots in that no contact between the robot and the operator is necessary.

Overall, most studies of droplet movement analyze lateral motion. There are only a few works that describe vertical motion. As an example, Phan [79] has demonstrated the vertical oscillation of a water droplet between two stationary water-oil interfaces. This mechanism of oscillatory motion is not due to magnetism, but rather to the electrostatic interaction of the droplet with either interface. When in proximity to one interface, the electrostatic potential of the droplet changes and the droplet then travels to the other interface, where the electostatic potential again changes, resulting in repeatable oscillations in the vertical dimension.

Velev et al. [99] have shown a liquid-liquid microfluidic system for manipulating freely suspended water or hydrocarbon droplets, which float on a denser perfluorinated oil and are driven by an

alternating or constant applied electric field. Apart from the influence of applied magnetic or electric fields, the motion of droplets has been observed on a horizontal air-water interface purely due to surface tension effects. For example, it was recently shown how an oil droplet is repelled by a meniscus in pure water but shows the opposite behavior and is attracted to the wall when surfactant is added to the water [66]. The addition of surfactant changes the interfacial energy and therefore the macroscopic behavior of the system. That article also presented a very simple system consisting of drinking water, plant oil, and dishwashing detergent as surfactant. This is a good example of the fact that liquid robots are in principle already easily accessible and exploitable.

Motile droplets as in the examples above can be quite simple in composition. A more intricate system was developed by Sanchez et al. [84]. They observed self-sustained flows in *active gels* in the absence of external forces. Their active gel consisted of substances extracted from living cells; namely, the protein streptavidin served as a scaffold where clusters of kinesin motor proteins were assembled and mediated the bundling of microtubules. Such an active gel was introduced into water, forming water-in-oil emulsions, and autonomous droplet motility was observed due to self-sustained active flows of microtubule bundles at the inner surfaces of droplets. The dynamic properties of this material stemmed from the higher-order assembly of active molecules into emulsion droplets.

4 Droplet Division

The field of robotics continues to develop robots from new materials and with new functionalities. For example, stretchable and deformable electronic devices have been introduced, showing distinct advantages over standard rigid wafer-based systems [81]. Some target functionalities of new types of robots include self-healing, shape change (morphing), reconfiguration, and self-replication. For example, several studies in robotics demonstrate how a robot can replicate by moving, collecting, and assembling another copy of itself from provided parts [91].

With regard to liquid robots, Grzybowski's group has studied the self-division of macroscopic droplets [19]. A droplet of dichloromethane that contained 45–50% 2-hexyldecanoic acid (2-HDA) was placed in a solution of KOH (pH 12). The interfacial reaction between 2-HDA and the base led to the accumulation of the deprotonated 2-HDA at the interface and to the increase of the interfacial area (elongation of the droplet). The droplet divided into two smaller droplets, and they divided further in the same way, until nanometer size was reached. The droplets could divide indefinitely and thus dissolve, or division could be limited under the control of the pH.

Later, Caschera et al. [20] showed that nitrobenzene droplets loaded with cationic surfactant and added to anionic surfactant formed tori, followed by breaking into two or more smaller droplets (Figure 5a). The division event occurs through a temporary minimum in interfacial tension coupled with fluid dynamics as the catanionic system approaches equilibrium. Conditions that support spontaneous droplet fission were tested for several different surfactant pairs. Also, salt-induced droplet fusion in cationic surfactant has been shown, demonstrating a rudimentary fission-fusion cycle capable of the addition of new chemistries or refueling of the droplets.

In addition, Derenyi and Lagzi [28] have shown a self-division of millimeter-sized fatty acid droplets, again governed by surface tension effects. The division was controlled by an autonomous chemical reaction (a pH clock reaction). The pH change affected the protonation state of the fatty acid head groups; the change in fatty acids led to a change of surface tension followed by destabilization and expansion of the droplet. The resulting ringlike structure became unstable (Plateau–Rayleigh instability) followed by the coalescence of some connected protrusions and the division of the unstable droplet. Statistically, the most frequent outcome is the self-division of a droplet into two daughter droplets of the same size.

Both self-propelled motion and division of micrometer-sized oil droplets induced by chemical conversion of the oil components was studied by Banno and Toyota (Figure 5b [12]). Hydrolysis of the surfactant in the system produced a hydrophobic product that added to the mass of the oil droplet, and eventually this resulted in droplet division [15]. From a theoretical and modeling

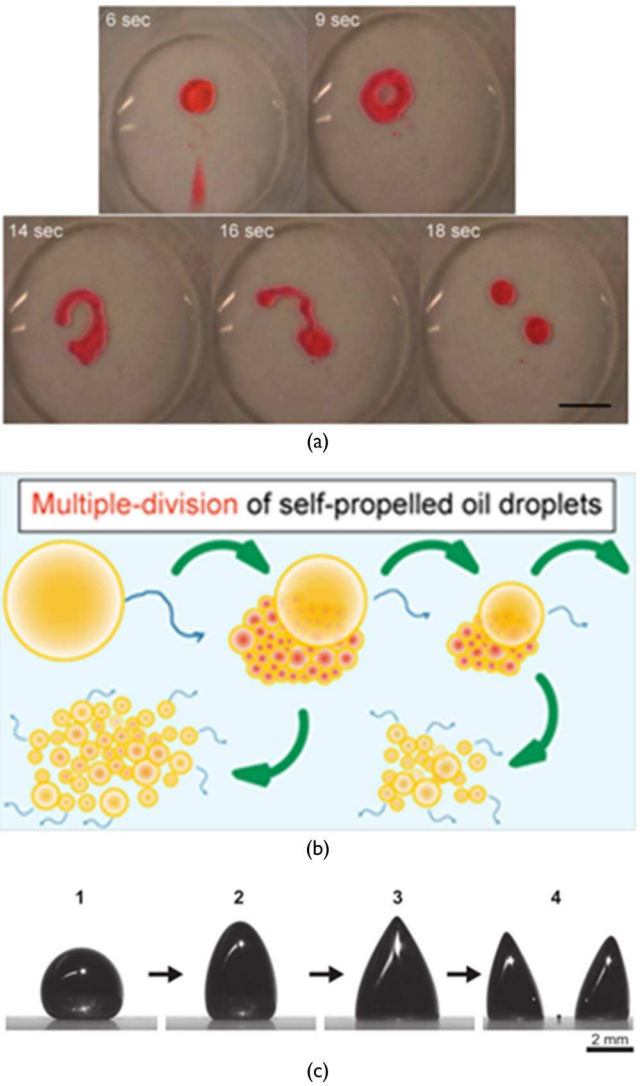

Figure 5. Examples of dividing droplets. (a) Spontaneous droplet division (reprinted with permission from [20]; © 2013 WILEY-VCH Verlag GmbH & Co. KGaA, Weinheim). (b) Schematic illustration of the proposed mechanism for multiple division of self-propelled oil droplets (from [12]; © The Royal Society of Chemistry 2015). (c) Magnetically triggered ferrofluid droplet division on a superhydrophobic surface (reprinted with permission from [95]; © 2013 American Association for the Advancement of Science).

perspective, Schwartz et al. discussed the analogy between cell division (and propulsion) and the division of droplets in the presence of surfactants and determined that the energies required to drive both motion and division are quite small [86]. Their hypotheses are based on the work of Greenspan [40, 41], who studied this problem in the 1970s.

Another self-dividing system was introduced by Sato et al., testing the influence of surface area on the state of the system [85]. Their assumption is that a synthetic cell will divide if the ratio of the surface area to volume increases. Their droplets (formed by a mixture of sorbitan monooleate (Span 80) and polyoxyethylene sorbitan monooleate (Tween 80) with alkaline phosphate buffer solution) were placed in a hydrophobic oil (mineral oil or liquid paraffin with *p*-nitrophenyl palmitate (pNPP)). The aqueous droplets increased their surface area through a hydrolysis reaction. Division occurred

through the increase in surface area, and it was shown that the temperature and viscosity of the microenvironment influenced the division types (e.g., equal versus unequal divisions, and multiple buddings).

Armstrong and Hanczyc [5] revisited a dynamic water-in-oil system first described by Bütschli in 1892. In their experiments, sodium hydroxide was added to olive oil in a Petri dish, and lifelike behavior of aqueous droplets was observed, including droplet group dynamics. Various kinds of droplet division and other behavior modes (explosion, vibration, stardust, galaxies) were observed by Cronin's group when searching the compositional space of the droplets placed in an aqueous phase [43]. Song et al. [87] have shown the splitting of droplets by laser irradiation. It is notable that in [43] the behaviors of droplets were selected over time, resulting in the evolution of droplet composition. This demonstrates that the behavior of droplets is tied to their individual composition. From a robotics perspective, the chemical content of a droplet could be considered as its programming.

On the other hand, droplet division can be manipulated by externally imposed forces. Timonen et al. [95] have shown manipulation and division of magnetic aqueous ferrofluid droplets on a low-friction lotus-leaf–like superhydrophobic surface with an external magnetic field (Figure 5c). A ferrofluid droplet was subjected to increasing magnetic field from a cylindrical permanent magnet. This resulted in a division into numerous daughter droplets that formed different static self-assembled patterns to minimize their total energy. When the magnetic field decreased, the relaxation of conical daughter droplets into spherical ones occurred.

Recently, we have found that decanol droplets surrounded by a decanoate solution containing salt perform intriguing shape changes [26]. Depending on the initial system composition, interesting patterns (e.g., stars, tentacular structures) are observable during the evaporation of the aqueous phase. In addition, the division of droplets can occur. The interesting point is that when the evaporation is completed, the droplets usually return more or less to the original spherical shape. Such reproducible morphological changes in simple droplets, dependent on the initial state of the system, can be used to produce predictable temporal state changes in liquid robotics.

Much like the mechanisms of self-motion, droplet division appears to be achievable if the interfacial tension is reduced. This is often governed by the addition or production of surfactants. Under these conditions a small amount of energy in the form of internal or external fluid dynamics appears to be enough to trigger division events. The division may be noisy, producing several droplets of various dimensions, or well-controlled, transforming one droplet into two daughter droplets of the same size. In all examples provided here we can see the propensity for liquid droplets, either pushed from equilibrium or created far from equilibrium, to produce such dynamics. Such soft-material properties of droplets make them ideal for key aspects of soft robotics, namely self-healing, shape change (morphing), reconfiguration, and self-replication. Consider a robot tasked to pass through a small hole. The droplet can divide, go through in the form of smaller objects, and then coalesce to form the original liquid robot.

Although we have highlighted a few examples from the literature in which the controlled fusion and division of droplets was studied, the development of a functional liquid robot remains a challenging task.

5 Problem Solving by Droplets

5.1 Droplets in Mazes

Above we summarized diverse approaches to animating droplets for both motion and division. Several groups have applied such dynamic liquid robots to solve rudimentary tasks. For example, could a self-moving droplet solve a maze? Maze solving, and finding the shortest path or all paths in mazes, are computational problems that could be solved by using algorithms. There are several types of mazes that could be treated. Here we will consider only 2D perfect mazes (called also simply connected mazes), mazes without any loops or closed circuits and without any inaccessible areas. From each point, there is exactly one path to any other point, and the maze has exactly one solution.

There are several approaches a human might take toward maze solving [7]. Imagine a human being standing at the starting point of a huge perfect maze. Here we will introduce just three simplest options. First, the human can use the algorithm called *random mouse*, meaning to run randomly in the corridors and hope to find the way out. A disadvantage of this algorithm is that it is extremely slow and there is a probability that the human will never reach the exit. A better approach is to use the *wall-follower* algorithm, which is based on keeping one hand in contact with one wall of the maze and following that wall. The solver is guaranteed not to get lost and will eventually reach the exit. The time spent in the maze may depend on the choice of hands; sometimes a left-hand path may be much shorter than a right-hand path or vice versa. If the solver has a chalk, a Trémaux's algorithm can be implemented. In this method the solver makes a random decision where to go from the start point and draws lines on the floor to mark his path. If the solver reaches the endpoint of any corridor, he goes back to the closest crossroad where he chooses any corridor that he has not visited yet. The paths are either unlabeled (which means unvisited yet), marked once, or marked twice (meaning leading to the dead end). These approaches work also for traditional robots, programmed to behave similarly to people.

It is also possible for self-propelled droplets to solve mazes. The self-propelled droplets can implement the random mouse algorithm, with a low probability that the droplet will reach the exit; the time for solving the maze may be long. The wall-follower and Trémaux's algorithms are not applicable to liquid droplets without some further signal that could prompt the liquid robot towards the exit [38].

In all articles where it was shown how chemotactic droplets can solve a maze, the droplets have in fact followed the shortest path predefined by a concentration gradient in the channels of the maze. Therefore diffusion and Marangoni flows are the physical solvers of the maze in principle, and the droplet follows the gradients in order to minimize its free energy [2]. The chemoattractant (i.e., the chemical substance placed at the exit) diffuses and causes a surface tension gradient that a droplet can sense. If the liquid robot is placed anywhere in a perfect maze and follows the steepest gradient, it reaches the source of the chemical signal. The intelligence of liquid robots is not in the ability to find the target, but in the ability to follow the track leading to the target. Note that not all droplets have this ability and not all kinds of droplets can follow the gradient chemotactically.

We have shown that decanol droplets are able to solve a maze containing a thin layer of sodium decanoate solution and locomote to the position with the highest concentration of salt (Figure 6a

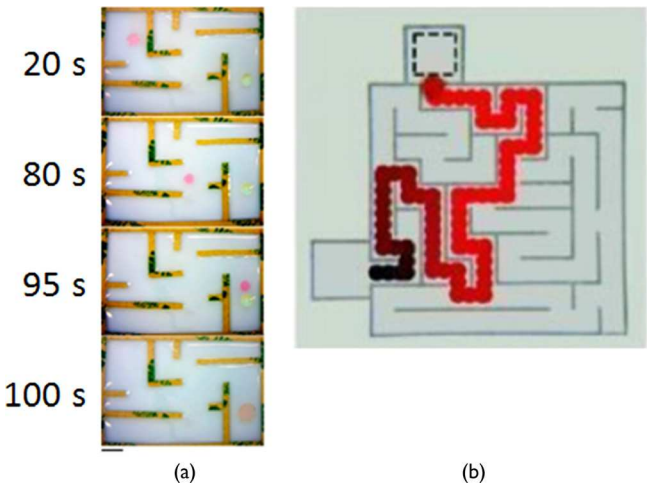

Figure 6. Examples of droplets in topologically complex systems. (a) Chemotactic decanol droplet following salt in a maze (reprinted with permission from [24]; © 2014, American Chemical Society). (b) Maze-solving HDA droplet following HCl gradient (reprinted with permission from [62]; © 2010, American Chemical Society).

[24]). In principle the path was indicated in advance as the salt spread from the source point by diffusion and Marangoni-induced flow along the liquid surface. The decanol droplet representing the liquid robot demonstrates the ability to follow this path without mistake and without exploring alternative paths. In the absence of the gradient of surface tension and determination of the shortest path, the droplet remains at the start point without any long-distance motion or exploratory behavior.

Lagzi et al. [62] have shown maze solving by chemotactic droplets, where oil droplets (mineral oil or dichlormethane) containing 2-hexyldecanoic acid (HDA) were able to move to the area with lowest pH (Figure 6b). As in the case described above, the pH gradient predefined the proper path, and the oil droplets with HDA followed this path. As a control, droplets without HDA have not shown chemotactic ability and have not followed the gradient. In principle, the H^+ ions from the target of the maze were the physical solvers of the maze, while the droplets enabled visualization of the shortest path [2].

Francis et al. [34] presented self-propelled chemotactic ionic liquid droplets that spontaneously travel along the liquid-air interface by release of surfactant-type ions when following HCl, similarly to Lagzi's system. The droplets were placed in any position within the fluidic network, and in every case they spontaneously traveled towards the chemoattractant source.

A further example of solving mazes by droplets is a recent article by Jin et al. [54]. They present self-propelling artificial swimmers in the form of oil droplets in an aqueous surfactant solution driven by interfacial Marangoni flows induced by micellar solubilization of the oil phase. The authors demonstrated that chemotaxis along micellar surfactant gradients can guide these swimmers through a microfluidic maze.

The intelligence of droplets consists in their ability to follow environmental signals; they are not able to solve the maze by themselves. This is not trivial, in that a droplet is able to sense its immediate environment and then link the environmental patterning to self-motion. Using ionic liquids for liquid robots instead of organic compounds will have advantages due to their negligible vapor pressure, low combustibility, and high thermal stability. Further, they are suitable solvents for numerous chemical species and can be used in a wide range of harsh reactions.

5.2 Droplets in Logic Gates

Research in unconventional computing includes analyzing new types of systems for their ability to perform basic logical operations. In some ways these unconventional systems mimic their electronic counterparts, but there are striking differences, including slow processing and high parallelism. It has been already shown that logical arguments could be performed by unconventional systems such as the slime mould *Physarum* [1, 3] or swarms of crabs [42]. A number of articles describe logic gates in chemical media, namely, those based on chemical wave propagation in excitable media (e.g., the Belousov-Zhabotinsky reaction) [88]. In past decades the research on logic gates has also focused on using droplets or bubbles.

Microfluidic computing elements, such as logic gates for logic operations, adders for arithmetic operations, and memory to store information, have been created [69]. Microfluidic chips with logic have been designed, where the presence or state of one droplet was influenced by the state of other droplets, or by the state of the chip. For example, pneumatic membrane valves have been used to open and close different channels and force droplets to execute a certain protocol depending on which valves were activated [29]. This allowed the creation of NOT, NAND, and NOR gates, flip-flops, oscillators, self-driven peristaltic pumps, and a 12-bit shift register. Cheow et al. [55] have demonstrated droplet-based microfluidic AND/OR and NOT logic gates. Logic operations were based on the nonlinear change in hydrodynamic resistance for channels containing droplets. Digital microfluidic logic gates were also shown, for example, by Toepke [96] and Zhao and Chakrabarty [105]. A universal microfluidic logic gate that is capable of conducting all 16 logic operations in one chip was presented by Zhang et al. [101].

The team of Prakash [80] has shown bubble logic processors implemented with nitrogen bubbles in water (with added surfactant 2%(w/w) Tween 20 to stabilize the interfaces) flowing through

PDMS microfluidic chips. Computational models related to bubble logic circuits were presented also by Anandan et al. [4]. Recently Prakash's group demonstrated synchronous water-based ferrofluid droplet generation and propagation in an oil-based carrier fluid between two parallel Teflon-coated glass surfaces [58]. A rotating magnetic field enables parallel manipulation of arbitrary numbers of ferrofluid droplets on permalloy tracks. The limits of synchronization were defined in dependence on frequency and droplet diameter.

Mertaniemi et al. [71] have demonstrated water droplets in air on superhydrophobic substrates, either coalescing or rebounding, depending on the Weber number and impact parameter. Under conditions when droplets rebound (not coalesce), experiments were performed on droplet logic gates (NOT/FANOUT and AND/OR). A toggle flip-flop memory based on controlled droplet collisions was successfully demonstrated, as well as a basis for programmable encapsulated chemistry.

Therefore certain logical operations, also associated with traditional programmed robots, can be implemented with droplet-based liquid robots. So far a substantial amount of external structure—for example, in the construction and architecture of microfluidic channels—is necessary for computing with input and output droplets, with the operations performed by droplets playing a key role in much larger systems. It has not yet been shown that individual droplets regardless of context can execute logical operations of note. Thus we consider the collective behavior and potential interactions of multiple droplets in the next section.

6 Multi-droplet Interactions

Since single droplets are able to demonstrate dynamic properties from self-motion to self-division to maze solving, it is intriguing to ask what types of behaviors can be demonstrated by multiple droplets, including swarms. Some works focus on the behavior of two or more droplets that either touch each other (and form a matrix of "artificial tissue") or are distributed in the environment independently and are able to mimic intracellular communication by means of chemical signals. In the same way as in the populations of living objects or robots, the collective behavior and swarming of liquid robots can be investigated. As Aristotle pointed out, "the whole is more than the sum of its parts"[1]—in terms of droplet behavior a swarm of liquid robots may display more useful properties than individual droplets; a swarm could perhaps perform targeted tasks better, faster, more robustly, or more efficiently.

For a start, we can ask whether two or more droplets influence each other in a measurable way. In [51], we studied in detail the motion of single and multiple self-propelled droplets over the course of minutes. In our experiments we studied the behavior of two droplets placed in one petri dish, and as a control experiment we observed two droplets separately in two petri dishes. We found that in the early part of the experiment (the first 20 minutes) two droplets tended to move close to one another, resulting in a circling effect. Compared to controls, we found that the two droplets influence each other and this influence depended on droplet size (volume).

Multiple droplet behavior may be influenced by attraction or repulsion, but a droplet may change its state through coalescence. Cira et al. [21] have shown that droplets consisting of propylene glycol and water mixtures fuse only if they have the same composition; otherwise they repel each other. In their device, droplets moved down a ramp by gravity. Along the way, a droplet merged only with a container of matched composition (and thus surface tension); otherwise the droplet moved along until it met a container with the appropriate mixture. In such a way the droplets sort themselves through surface tension (Figure 7).

These are examples where the behavior of the systems changes due to the presence of more than one droplet. Perhaps the droplets show some kind of "intelligence," or at least selectivity based on composition. Such purely intrinsic behavior of multiple droplets has great potential for applications

1 "In the case of all things which have several parts and in which the totality is not, as it were, a mere heap, but the whole is something beside the parts,...." (Aristotle, *Metaphysics*, Book 8, part 6).

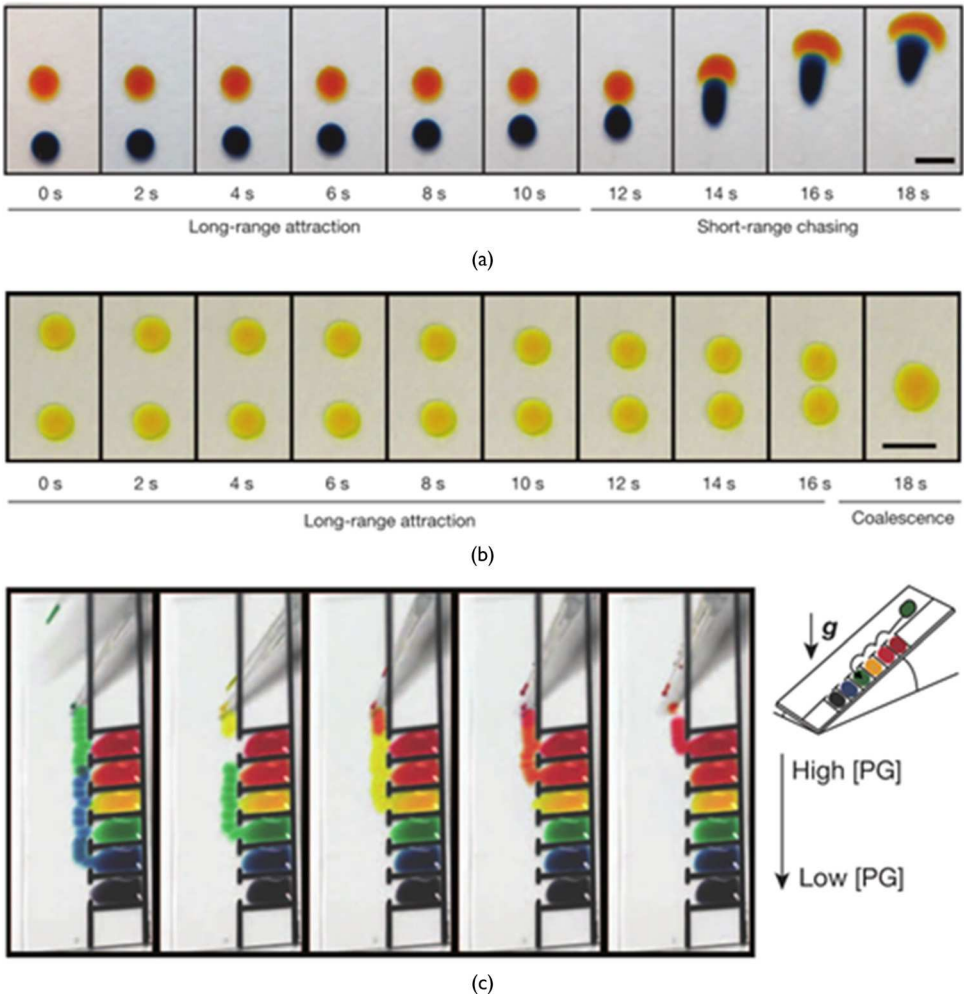

Figure 7. Interaction of two-component droplets consisting of water and propylene glycol mixture. (a) Repulsion of droplets with different compositions. (b) Coalescence of droplets with the same composition. (c) Surface tension sorter. (Reprinted from [21] by permission of Nature Publishing Group.)

of liquid robots where identical droplets may be tasked to work together or specialized droplets may form a working consortium. In this way the system may become more robust and also suitable for diverse targeted outcomes.

7 Liquid Marbles

A special category of droplets, distinct from the liquid-liquid systems depicted in Figure 2, are so-called liquid marbles as defined by Aussillous and Quéré in 2001 [6]. A liquid marble is a liquid droplet encapsulated in a hydrophobic powder that adheres to its surface (Figure 8). Preparation of liquid marbles is a very simple operation—a small amount of liquid is rolled on a layer of hydrophobic powder consisting of nano- or microparticles, which spread spontaneously at the liquid-air interface. This process results in a liquid marble that has some of the properties of a liquid droplet and at the same time behaves as a soft solid. Liquid marbles are an alternative to superhydrophobic surfaces, because particles at the interface prevent the liquid in the marble from

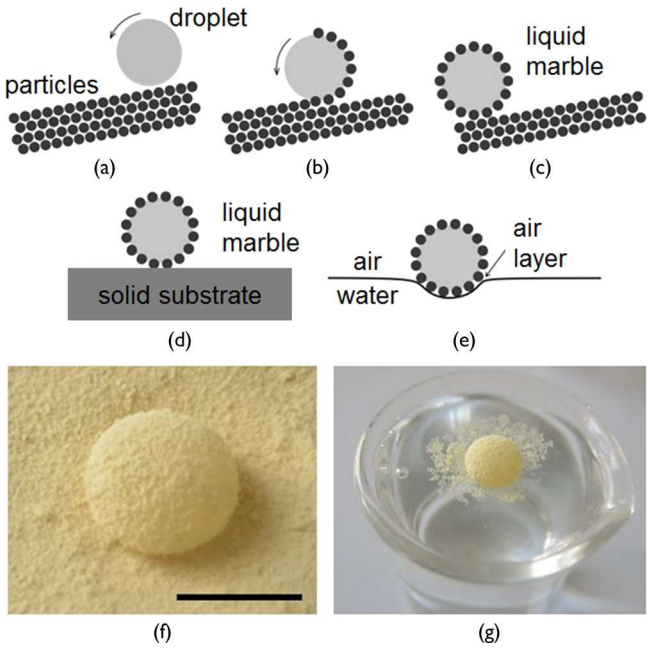

Figure 8. Liquid marbles. (a)–(c) Scheme of liquid-marble preparation process. (d) Scheme of liquid marble on a solid substrate. (e) Scheme of liquid marble floating on the water surface. (f) Photograph of liquid marble (100 μl of water covered by *Lycopodium*). Scale bar corresponds to 5 mm. (g) Photograph of liquid marble from (f) floating on water surface (reprinted with permission from [25]).

wetting the carrier surface. The substrate on which the liquid marble moves can be a solid or even a liquid surface. Liquid marbles can serve, for example, to transport of small volumes of liquids or powders [25, 83].

Like with simple droplets, liquid marbles can be moved using external forces. Ooi [75] summarized methods for manipulation of liquid marbles, mainly by electrostatic and magnetic forces, with other options mentioned (e.g., mechanical, gravitational, irradiation, changes in temperature or pH). Magnetic force could be used for both the manipulation [103] and also for controlled fusion of two liquid marbles [104]. Bormashenko et al. have shown self-propulsion of liquid marbles filled with aqueous alcohol solutions and placed on a water surface [17]. Recently Paven et al. introduced a system whereby laser-driven liquid marbles can push 150 times their own weight [77]. This type of droplet thus also shows potential to be used as a liquid robot and is attracting further interest.

8 Conclusions and Outlook

It is widely accepted that robots are artificial objects that can in some contexts make human life easier. However, the idea of electromechanical robots dominates. In the present review we have described how simple droplets can be an embodiment of liquid robots. These droplet-based robots have the ability to sense gradients and even each other, resulting in directional chemotactic motion and also group dynamics. The composition of individual robots also influences their behavior. Even with such rudimentary abilities, the droplets are able to sense chemical gradients in complex environments and thereby to solve mazes. In addition, droplet-based liquid robots are soft and can deform [9], sometimes to such an extent that the droplets divide into daughter droplets. Moreover, they can change their own shape [26]. Along with fusion, this forms the basis of self-replication and perhaps even evolution. Although multiple droplets in an experiment can perform logical operations, it remains to be seen how individual droplets can also perform logic based on their chemistry.

Like Braitenberg's vehicles, droplet-based liquid robots can be semi-autonomous and self-propelled. And like billiard balls, droplet-based robots can be deterministically controlled by external forces. It is this potential for both external and embedded control that makes liquid robots intriguing and useful as a branch of robotics.

Due to the ability of droplets to change state (e.g., by fission or fusion), the link between chemical composition and function, and the link between environmental information and self-movement, it is possible to design liquid robots that not only perform targeted delivery but also process complex input information—for example, to distinguish the inside from the outside of a tumor and provide controlled doses of therapeutic substances in a manner not available with current theranostics. Beyond medicine, liquid robots as smart materials may allow for the prolonged proper function of machines, organisms, and infrastructure [46, 57].

With regard to potential engineering applications, the area of environmental sensing and remediation is one where droplet-based devices could prove to be valuable and technically feasible. For example, it has been recently demonstrated that droplets can encapsulate chemical species and perform oriented motion in microchip channels, where they can induce phenomena such as the flocculation of a dispersed model pollutant [102]. At the same time, it has to be kept in mind that droplet movement in an actual real-world environment without well-defined channels, in a fluid of uncontrolled composition, and in the presence of macroscopic convective transport is a rather different task.

Although droplets as liquid robots are promising tools for performing various tasks, there is still a long way to go before we can use them in real life. All droplet studies presented in this article were performed in well-defined laboratory conditions, and nobody has yet focused on robustness of droplet systems. For practical application of liquid droplets in biological or environmental use, one must consider the influence of ambient noise on the dynamics of droplets. To transfer liquid robots in the form of droplets from laboratories to real-world conditions is a challenging task in the area of liquid robotics.

A possible way of increasing the robustness of robotic devices in a real-world environment is to proceed from individual robots to robotic swarms [39]. In nature, this is a successful survival strategy used by collective organisms such as swarms of insects, schools of fish, and flocks of birds. Collective phenomena are observable also in cells, as in the multicellular development of *Dictyostelium* cells [50, 93]. The main benefit is that even if a number of individuals are lost, the majority can still complete the mission, thanks to a combination of the statistics of large numbers and mutual communication that leads to the so-called swarm intelligence. Thus, the collective motion of interacting droplet swarms is an area of research that can improve the practical application potential of droplet-based liquid robots.

Acknowledgment

J.Č. was financially supported by the Czech Science Foundation (Grant No. 17-21696Y). M.M.H. was financially supported by the European Commission FP7 Future and Emerging Technologies Proactive (EVOBLISS 611640).

References

1. Adamatzky, A. (2015). Slime mould processors, logic gates and sensors. *Philosophical Transactions of the Royal Society A*, *373*(2046), 20140216.
2. Adamatzky, A. (2017). Physical maze solvers. All twelve prototypes implement 1961 Lee algorithm. In A. Adamatzky (Ed.), *Emergent computation: A festschrift for Selim G. Akl* (pp. 489–504). Cham: Springer International Publishing.
3. Adamatzky, A., & Schubert, T. (2014). Slime mold microfluidic logical gates. *Materials Today*, *17*(2), 86–91.
4. Anandan, P., Gagliano, S., & Bucolo, M. (2015). Computational models in microfluidic bubble logic. *Microfluidics and Nanofluidics*, *18*(2), 305–321.
5. Armstrong, R., & Hanczyc, M. (2013). Bütschli dynamic droplet system. *Artificial Life*, *19*(3–4), 331–346.

6. Aussillous, P., & Quéré, D. (2006). Properties of liquid marbles. *Proceedings of the Royal Society A: Mathematical, Physical and Engineering Science*, *462*(2067), 973–999.
7. Babula, M. (2009). Simulated maze solving algorithms through unknown mazes. In L. Czaja (Ed.), *Proceedings of XVIIIth Concurrency, Specification and Programming Workshop* (pp. 13–22). Krakow.
8. Ban, T., & Nakata, H. (2015). Metal-ion-dependent motion of self-propelled droplets due to the Marangoni effect. *The Journal of Physical Chemistry B*, *119*(23), 7100–7105.
9. Ban, T., Yamada, T., Aoyama, A., Takagi, Y., & Okano, Y. (2012). Composition-dependent shape changes of self-propelled droplets in a phase-separating system. *Soft Matter*, *8*(14), 3908–3916.
10. Ban, T., Yamagami, T., Nakata, H., & Okano, Y. (2013). pH-dependent motion of self-propelled droplets due to Marangoni effect at neutral pH. *Langmuir*, *29*(8), 2554–2561.
11. Banno, T., Kazayama, Y. & Toyota, T. (2014). Giant vesicle formation of novel polymerizable amphiphile associated with its polymerization and hydrolysis in water. *Chemistry Letters*, *43*(11), 1707–1709.
12. Banno, T., Kuroha, R., Miura, S., & Toyota, T. (2015). Multiple-division of self-propelled oil droplets through acetal formation. *Soft Matter*, *11*(8), 1459–1463.
13. Banno, T., Kuroha, R., & Toyota, T. (2012). pH-sensitive self-propelled motion of oil droplets in the presence of cationic surfactants containing hydrolyzable ester linkages. *Langmuir*, *28*(2), 1190–1195.
14. Banno, T., Miura, S., Kuroha, R., & Toyota, T. (2013). Mode changes associated with oil droplet movement in solutions of gemini cationic surfactants. *Langmuir*, *29*(25), 7689–7696.
15. Banno, T., & Toyota, T. (2015). Molecular system for the division of self-propelled oil droplets by component feeding. *Langmuir*, *31*(25), 6943–6947.
16. Behkam, B., & Sitti, M. (2006). Towards hybrid swimming microrobots: Bacteria assisted propulsion of polystyrene beads. In *Proceedings of the 28th Annual International Conference of the IEEE Engineering in Medicine and Biology Society* (pp. 2421–2424). doi:10.1109/IEMBS.2006.259841
17. Bormashenko, E., Bormashenko, Y., Grynyov, R., Aharoni, H., Whyman, G., & Binks, B. P. (2015). Self-propulsion of liquid marbles: Leidenfrost-like levitation driven by Marangoni flow. *The Journal of Physical Chemistry C*, *119*(18), 9910–9915.
18. Braitenberg, V. (1986). *Vehicles: Experiments in synthetic psychology*. Cambridge, MA: MIT Press.
19. Browne, K. P., Walker, D. A., Bishop, K. J. M., & Grzybowski, B. A. (2010). Self-division of macroscopic droplets: Partitioning of nanosized cargo into nanoscale micelles. *Angewandte Chemie*, *122*(38), 6908–6911.
20. Caschera, F., Rasmussen, S., & Hanczyc, M. M. (2013). An oil droplet division–fusion cycle. *ChemPlusChem*, *78*(1), 52–54.
21. Cira, N. J., Benusiglio, A., & Prakash, M. (2015). Vapour-mediated sensing and motility in two-component droplets. *Nature*, *519*(7544), 446–450.
22. Čapek, K. (1920). *R.U.R.* - Rossumovi Univerzálni Roboti [Rossum's Universal Robots]. Prague: Aventinum.
23. Čejková, J., Holler, S., Quyen, N. T., Kerrigan, C., Štěpánek, F., & Hanczyc, M. M. (2017). Chemotaxis and chemokinesis of living and non-living objects. In A. Adamatzky (Ed.), *Advances in unconventional computing* (pp. 245–260). Cham, Switzerland: Springer International Publishing.
24. Čejková, J., Novák, M., Štěpánek, F., & Hanczyc, M. M. (2014). Dynamics of Chemotactic droplets in salt concentration gradients. *Langmuir*, *30*(40), 11937–11944.
25. Čejková, J., & Rychecký, O. (2017). Tekuté kuličky. *Chemické Listy*, *111*, 109–114.
26. Čejková, J., Štěpánek, F., & Hanczyc, M. M. (2016). Evaporation-induced pattern formation of decanol droplets. *Langmuir*, *32*(19), 4800–4805.
27. de Jong, H. B. (1932). Die Koazervation und ihre Bedeutung für die Biologie. *Protoplasma*, *15*(1), 110–173.
28. Derenyi, I., & Lagzi, I. (2014). Fatty acid droplet self-division driven by a chemical reaction. *Physical Chemistry Chemical Physics*, *16*(10), 4639–4641.
29. Devaraju, N. S. G. K., & Unger, M. A. (2012). Pressure driven digital logic in PDMS based microfluidic devices fabricated by multilayer soft lithography. *Lab on a Chip*, *12*(22), 4809–4815.
30. Dixit, S. S., Kim, H., Vasilyev, A., Eid, A., & Faris, G. W. (2010). Light-driven formation and rupture of droplet bilayers. *Langmuir*, *26*(9), 6193–6200.

31. Dorvee, J. R., Derfus, A. M., Bhatia, S. N., & Sailor, M. J. (2004). Manipulation of liquid droplets using amphiphilic, magnetic one-dimensional photonic crystal chaperones. *Nature Materials*, *3*(12), 896–899.

32. Dos Santos, F. D., & Ondarçuhu, T. (1995). Free-running droplets. *Physical Review Letters*, *75*(16), 2972–2975.

33. Florea, L., Wagner, K., Wagner, P., Wallace, G. G., Benito-Lopez, F., Officer, D. L., & Diamond, D. (2014). Photo-chemopropulsion—light-stimulated movement of microdroplets. *Advanced Materials*, *26*(43), 7339–7345.

34. Francis, W., Fay, C., Florea, L., & Diamond, D. (2015). Self-propelled chemotactic ionic liquid droplets. *Chemical Communications*, *51*(12), 2342–2344.

35. Kurup, G. K., & Basu, A. S. (2012). Passive, label-free droplet sorting based on chemical composition using tensiophoresis. In *16th International Conference on Miniaturized Systems for Chemistry and Life Sciences* (pp. 76–78).

36. Giri, T. K., Choudhary, C., Ajazuddin, Alexander A., Badwaik, H., & Tripathi, D. K. (2013). Prospects of pharmaceuticals and biopharmaceuticals loaded microparticles prepared by double emulsion technique for controlled delivery. *Saudi Pharmaceutical Journal*, *21*(2), 125–141.

37. Graham, T. (1861). Liquid diffusion applied to analysis. *Philosophical Transactions of the Royal Society of London*, *151*, 183–224.

38. Grančič, P., & Štěpánek, F. (2013). Swarming behavior of gradient-responsive colloids with chemical signaling. *The Journal of Physical Chemistry B*, *117*(26), 8031–8038.

39. Grančič, P., & Štěpánek, F. (2013). Chemical swarm robots. In S. Kernbach (Ed.), *Handbook of collective robotics: Fundamentals and challenges* (pp. 745–771). Stanford, CA: PAN.

40. Greenspan, H. P. (1977). On the dynamics of cell cleavage. *Journal of Theoretical Biology*, *65*(1), 79–99.

41. Greenspan, H. P. (1978). On fluid-mechanical simulations of cell division and movement. *Journal of Theoretical Biology*, *70*(1), 125–134.

42. Gunji, Y.-P., Nishiyama, Y., Adamatzky, A., Simos, T. E., Psihoyios, G., Tsitouras, C., & Anastassi, Z. (2011). Robust soldier crab ball gate. *Complex Systems*, *20*(2), 93.

43. Gutierrez, J. M. P., Hinkley, T., Taylor, J. W., Yanev, K., & Cronin, L. (2014). Evolution of oil droplets in a chemorobotic platform. *Nature Communications*, *5*, 5571.

44. Haidara, H., Vonna, L., & Schultz, J. (1997). Surfactant induced Marangoni motion of a droplet into an external liquid medium. *Journal of Chemical Physics*, *107*(2), 630–637.

45. Hanczyc, M. M. (2011). Metabolism and motility in prebiotic structures. *Philosophical Transactions of the Royal Society B: Biological Sciences*, *366*(1580), 2885–2893.

46. Hanczyc, M. M., & Ikegami, T. (2010). Chemical basis for minimal cognition. *Artificial Life*, *16*(3), 233–243.

47. Hanczyc, M. M., Parrilla, J. M., Nicholson, A., Yanev, K., & Stoy, K. (2014). Creating and maintaining chemical artificial life by robotic symbiosis. *Artificial Life*, *21*(1), 47–54.

48. Hanczyc, M. M., Toyota, T., Ikegami, T., Packard, N., & Sugawara, T. (2007). Fatty acid chemistry at the oil-water interface: Self-propelled oil droplets. *Journal of the American Chemical Society*, *129*(30), 9386–9391.

49. Henson, A., Gutierrez, J. M. P., Hinkley, T., Tsuda, S., & Cronin, L. (2015). Towards heterotic computing with droplets in a fully automated droplet-maker platform. *Philosophical Transactions of the Royal Society A*, *373*(2046), 20140221.

50. Hilgardt, C., Cejkova, J., Hauser, M. J. B., & Sevcikova, H. (2008). Streamless aggregation of *Dictyostelium* in the presence of isopropylidenadenosin. *Biophysical Chemistry*, *132*(1), 9–18.

51. Horibe, N., Hanczyc, M. M., & Ikegami, T. (2011). Mode switching and collective behavior in chemical oil droplets. *Entropy*, *13*(3), 709–719.

52. Hu, W., & Ohta, A. (2011). Aqueous droplet manipulation by optically induced Marangoni circulation. *Microfluidics and Nanofluidics*, *11*(3), 307–316.

53. Chaudhury, M. K., & Whitesides, G. M. (1992). How to make water run uphill. *Science*, *256*(5063), 1539–1541.

54. Chenyu, J., Krüger, C., & Maass, C. C. (2017). Chemotaxis and auto-chemotaxis of self-propelling droplet swimmers. *Proceedings of the National Academy of Sciences of the U.S.A.*, *114*(20), 5089–5094.

55. Cheow, L. F., Yobas, L., & Kwong, D.-L. (2007). Digital microfluidics: Droplet based logic gates. *Applied Physics Letters*, *90*(5), 054107.

56. Ikegami, T. (2010). Chemical robot: Self-organizing self-moving oil droplet. *Journal of the Robotics Society of Japan*, *28*(4), 435–444.

57. Ikegami, T., Horibe, N., & Hanczyc, M. M. (2015). Potential memory effects in self-moving oil droplets. *International Journal of Unconventional Computing*, *11*(5–6), 345–355.

58. Katsikis, G., Cybulski, J. S., & Prakash, M. (2015). Synchronous universal droplet logic and control. *Nature Physics*, *11*(7), 588–596.

59. Kunstmann-Olsen, C., Hanczyc, M. M., Hoyland, J., Rasmussen, S., & Rubahn, H.-G. (2016). Uniform droplet splitting and detection using lab-on-chip flow cytometry on a microfluidic PDMS device. *Sensors and Actuators B: Chemical*, *229*, 7–13.

60. Kurihara, K., Tamura, M., Shohda, K.-i., Toyota, T., Suzuki, K., & Sugawara, T. (2011). Self-reproduction of supramolecular giant vesicles combined with the amplification of encapsulated DNA. *Nature Chemistry*, *3*(10), 775–781.

61. Kurup, G. K., & Basu, A. S. (2011). Tensiophoresis: Migration and sorting of droplets in an interfacial tension gradient. In *15th International Conference on Miniaturized Systems for Chemistry and Life Sciences* (pp. 1367–1369).

62. Lagzi, I., Soh, S., Wesson, P. J., Browne, K. P., & Grzybowski, B. A. (2010). Maze solving by chemotactic droplets. *Journal of the American Chemical Society*, *132*(4), 1198–1199.

63. Lazar, P., & Riegler, H. (2005). Reversible self-propelled droplet movement: A new driving mechanism. *Physical Review Letters*, *95*(13), 136103.

64. Lehmann, U., Hadjidj, S., Parashar, V. K., Vandevyver, C., Rida, A., & Gijs, M. A. M. (2006). Two-dimensional magnetic manipulation of microdroplets on a chip as a platform for bioanalytical applications. *Sensors and Actuators B: Chemical*, *117*(2), 457–463.

65. Li, D., Choi, H., Cho, S., Jeong, S., Jin, Z., Lee, C., Ko, S. Y., Park, J.-O., & Park, S. (2015). A hybrid actuated microrobot using an electromagnetic field and flagellated bacteria for tumor-targeting therapy. *Biotechnology and Bioengineering*, *112*(8), 1623–1631.

66. Li, S., Liu, J., Hou, J., & Zhang, G. (2015). Meniscus-induced motion of oil droplets. *Colloids and Surfaces A: Physicochemical and Engineering Aspects*, *469*, 252–255.

67. Maass, C. C., Krüger, C., Herminghaus, S., & Bahr, C. (2016). Swimming droplets. *Annual Review of Condensed Matter Physics*, *7*(1), 171–193.

68. Maeda, S., Hara, Y., Yoshida, R., & Hashimoto, S. (2007). Chemical robot—design of self-walking gel. In *Proceedings of 2007 IEEE/RSJ International Conference on Intelligent Robots and Systems*. doi:10.1109/IROS.2007.4399392

69. Marr, D. W., & Munakata, T. (2007). Micro/nanofluidic computing. *Communications of the ACM*, *50*(9), 64–68.

70. Martel, S., & Mohammadi, M. (2010). Using a swarm of self-propelled natural microrobots in the form of flagellated bacteria to perform complex micro-assembly tasks. In *2010 IEEE International Conference on Robotics and Automation*. doi:10.1109/ROBOT.2010.5509752

71. Mertaniemi, H., Forchheimer, R., Ikkala, O., & Ras, R. H. (2012). Rebounding droplet–droplet collisions on superhydrophobic surfaces: From the phenomenon to droplet logic. *Advanced Materials*, *24*(42), 5738–5743.

72. Miura, S., Banno, T., Tonooka, T., Osaki, T., Takeuchi, S., & Toyota, T. (2014). pH-induced motion control of self-propelled oil droplets using a hydrolyzable gemini cationic surfactant. *Langmuir*, *30*(27), 7977–7985.

73. Nagai, K., Sumino, Y., Kitahata, H., & Yoshikawa, K. (2005). Mode selection in the spontaneous motion of an alcohol droplet. *Physical Review E*, *71*(6), 065301.

74. Nejatimoharrami, F., Faina, A., Cejkova, J., Hanczyc, M. M., & Stoy, K. (2016). Robotic automation to augment quality of artificial chemical life experiments. In C. Gershenson et al. (Eds.), *Proceedings of the Artificial Life Conference 2016* (pp. 634–635). Cambridge, MA: MIT Press.

75. Ooi, C. H., & Nguyen, N.-T. (2015). Manipulation of liquid marbles. *Microfluidics and Nanofluidics*, *19*(3), 483–495.

76. Oshima, S., Nomoto, T., Toyota, T., & Fujinami, M. (2014). Surface tension gradient around an alcohol droplet moving spontaneously on a water surface. *Analytical Sciences*, *30*(4), 441–444.

77. Paven, M., Mayama, H., Sekido, T., Butt, H.-J., Nakamura, Y., & Fujii, S. (2016). Light-driven delivery and release of materials using liquid marbles. *Advanced Functional Materials*, *26*(19), 3199–3206.

78. Peyer, K. E., Zhang, L., & Nelson, B. J. (2013). Bio-inspired magnetic swimming microrobots for biomedical applications. *Nanoscale*, *5*(4), 1259–1272.

79. Phan, C. M. (2014). Rechargeable aqueous microdroplet. *The Journal of Physical Chemistry Letters*, *5*(8), 1463–1466.

80. Prakash, M., & Gershenfeld, N. (2007). Microfluidic bubble logic. *Science*, *315*(5813), 832–835.

81. Rogers, J. A., Someya, T., & Huang, Y. (2010). Materials and mechanics for stretchable electronics. *Science*, *327*(5973), 1603–1607.

82. Rybalko, S., Magome, N., & Yoshikawa, K. (2004). Forward and backward laser-guided motion of an oil droplet. *Physical Review E*, *70*(4), 046301.

83. Rychecký, O., Majerská, M., Král, V., Štěpánek, F., & Čejková, J. (2017). Spheroid cultivation of HT-29 carcinoma cell line in liquid marbles. *Chemical Papers*, *71*(6), 1055–1063.

84. Sanchez, T., Chen, D. T. N., DeCamp, S. J., Heymann, M., & Dogic, Z. (2012). Spontaneous motion in hierarchically assembled active matter. *Nature*, *491*(7424), 431–434.

85. Sato, Y., Yasuhara, K., Kikuchi, J.-i., & Sato, T. N. (2013). Synthetic cell division system: Controlling equal vs. unequal divisions by design. *Scientific Reports*, *3*, 3475.

86. Schwartz, L. W., Roy, R. V., Eley, R. R., & Princen, H. M. (2004). Surfactant-driven motion and splitting of droplets on a substrate. *Journal of Engineering Mathematics*, *50*(2–3), 157–175.

87. Song, C., Moon, J. K., Lee, K., Kim, K., & Pak, H. K. (2014). Breathing, crawling, budding, and splitting of a liquid droplet under laser heating. *Soft Matter*, *10*(15), 2679–2684.

88. Steinbock, O., Kettunen, P., & Showalter, K. (1996). Chemical wave logic gates. *The Journal of Physical Chemistry*, *100*(49), 18970–18975.

89. Sumino, Y., Kitahata, H., Yoshikawa, K., Nagayama, M., Nomura, S.-i. M., Magome, N., & Mori, Y. (2005). Chemosensitive running droplet. *Physical Review E*, *72*(4), 041603.

90. Sumino, Y., Magome, N., Hamada, T., & Yoshikawa, K. (2005). Self-running droplet: emergence of regular motion from nonequilibrium noise. *Physical Review Letters*, *94*(6), 068301.

91. Suthakorn, J., Cushing, A. B., & Chirikjian, G. S. (2003). An autonomous self-replicating robotic system. In *Proceedings 2003 IEEE/ASME International Conference on Advanced Intelligent Mechatronics*. doi:10.1109/AIM.2003.1225085

92. Suzuki, A., Maeda, S., Hara, Y., & Hashimoto, S. (2012). Capsule gel robot driven by self-propelled oil droplet. In *IEEE International Conference on Intelligent Robots and Systems* (pp. 2180–2185). doi:10.1109/IROS.2012.6385738

93. Ševčíková, H., Čejková, J., Krausová, L., Přibyl, M., Štěpánek, F., & Marek, M. (2010). A new traveling wave phenomenon of *Dictyostelium* in the presence of cAMP. *Physica D: Nonlinear Phenomena*, *239*(11), 879–888.

94. Tanaka, S., Sogabe, Y., & Nakata, S. (2015). Spontaneous change in trajectory patterns of a self-propelled oil droplet at the air-surfactant solution interface. *Physical Review E*, *91*(3), 032406.

95. Timonen, J. V. I., Latikka, M., Leibler, L., Ras, R. H. A., & Ikkala, O. (2013). Switchable static and dynamic self-assembly of magnetic droplets on superhydrophobic surfaces. *Science*, *341*(6143), 253–257.

96. Toepke, M. W., Abhyankar, V. V., & Beebe, D. J. (2007). Microfluidic logic gates and timers. *Lab on a Chip*, *7*(11), 1449–1453.

97. Toyota, T., Maru, N., Hanczyc, M. M., Ikegami, T., & Sugawara, T. (2009). Self-propelled oil droplets consuming "fuel" surfactant. *Journal of the American Chemical Society*, *131*(14), 5012–5013.

98. Ullrich, M., Hanuš, J., Dohnal, J., & Štěpánek, F. (2013). Encapsulation stability and temperature-dependent release kinetics from hydrogel-immobilised liposomes. *Journal of Colloid and Interface Science*, *394*, 380–385.

99. Velev, O. D., Prevo, B. G., & Bhatt, K. H. (2003). On-chip manipulation of free droplets. *Nature*, *426*(6966), 515–516.

100. Zadražil, A., Čermochová, V., Ullrich, M., Hanuš, J., Štěpánek, F., & McCaskill, J. (2016). Remote manipulation with microlablets and control of enzymatic reaction. In *Design and Manufacture of Functional Microcapsules and Engineered Products*. Engineering Conferences International.

101. Zhang, M., Wang, L., Wang, X., Wu, J., Li, J., Gong, X., Qin, J., Li, W., & Wen, W. (2011). Microdroplet-based universal logic gates by electrorheological fluid. *Soft Matter*, *7*(16), 7493–7497.

102. Zhao, G., & Pumera, M. (2014). Marangoni self-propelled capsules in a maze: Pollutants 'sense and act' in complex channel environments. *Lab on a Chip*, *14*(15), 2818–2823.

103. Zhao, Y., Fang, J., Wang, H., Wang, X., & Lin, T. (2010). Magnetic liquid marbles: Manipulation of liquid droplets using highly hydrophobic Fe_3O_4 nanoparticles. *Advanced Materials*, *22*(6), 707–710.

104. Zhao, Y., Gu, H., Xie, Z., Shum, H. C., Wang, B., & Gu, Z. (2012). Bioinspired multifunctional Janus particles for droplet manipulation. *Journal of the American Chemical Society*, *135*(1), 54–57.

105. Zhao, Y., & Chakrabarty, K. (2010). Digital microfluidic logic gates and their application to built-in self-test of lab-on-chip. *IEEE Transactions on Biomedical Circuits and Systems*, *4*(4), 250–262.

Langmuir

Article

pubs.acs.org/Langmuir

Dynamics of Chemotactic Droplets in Salt Concentration Gradients

Jitka Čejková,*[,†,‡] Matěj Novák,[†] František Štěpánek,[†] and Martin M. Hanczyc[‡,§]

[†]Chemical Robotics Laboratory, Institute of Chemical Technology Prague, Technická 3, 166 28 Prague 6, Czech Republic

[‡]Center for Fundamental Living Technology (FLinT), Department of Physics, Chemistry and Pharmacy, University of Southern Denmark, Campusvej 55, DK-5230 Odense M, Denmark

[§]Centre for Integrative Biology CIBIO, University of Trento, via delle Regole 101, 38123 Mattarello (TN), Italy

Supporting Information

ABSTRACT: The chemotactic movement of decanol droplets in aqueous solutions of sodium decanoate in response to concentration gradients of NaCl has been investigated. Key parameters of the chemotactic response, namely the induction time and the migration velocity, have been evaluated as a function of the sodium decanoate concentration and the NaCl concentration gradient. The ability of the decanol droplets to migrate in concentration gradients has been demonstrated not only in a linear chemotactic assay but also in a topologically complex environment. Additionally, the ability to reverse the direction of movement repeatedly, to carry and release a chemically reactive cargo, to select a stronger concentration gradient from two options, and to initiate chemotaxis by an external temperature stimulus have been demonstrated.

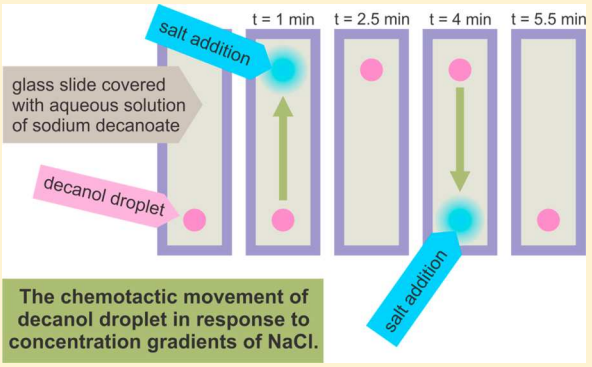

1. INTRODUCTION

The locomotion of live cells is a highly complex process involving various biochemical and biophysical elements.[1] Motion is usually associated with motor proteins that convert chemical energy to mechanical work. The movement of freely living cells can be caused by special organelles for locomotion such as cilia and flagella or by migration over solid substrates by crawling or gliding, i.e., by coordinated changes in shape and adhesivity to a substrate in response to environmental stimuli, using pseudopodia. The latter mechanism is manifested by single-cell organisms such as amoebae, diatoms, and some types of cyanobacteria and human leukocytes.

The swimming and crawling movements of cells can be random or oriented. Cells usually move because this takes them closer to a source of nutrients or further away from a source of harmful compounds. Such extracellular chemical cues (nutrients, pheromones, repellents, toxins) guide the movement of a cell in a particular direction—a process called chemotaxis.[2] Chemotaxis can be positive (movement toward a chemoattractant) or negative (movement away from a repellent). Chemotaxis differs from chemokinesis, in which case the signal substance merely alters the rate or frequency of random motion.[3]

The movement of nonliving objects in concentration gradients (artificial chemotaxis) can be based on several different mechanisms. The movement of asymmetric bimetallic catalytic rods or spheres in the concentration gradient of H_2O_2 has been reported.[4] In this case, a catalytic chemical reaction produces gas bubbles that propel the particles. Similarly, Mano and Heller[5] described a system based on a carbon fiber having a terminal glucose oxidizing microanode and an O_2 reducing microcathode, which was propelled at the H_2O-O_2 interface. It was shown that the diffusiophoretic phenomenon shares similarities with chemotaxis.[6] When a rigid colloidal particle is placed in a solution with nonuniform concentration of a solute that interacts with the particle, the particle can move along the concentration gradient of the solute. It has also been shown that dynamic cytoskeletal components, biomolecular motors (kinesin, myosin), and their associated filaments (microtubule, actin) can be combined *in vitro* with synthetic components to create nanoscale transport systems.[7] Synthetic phospholipid vesicles coated by proteins that initiate actin polymerization displayed the ability to propel lipid vesicles in a similar way as in *Listeria* cells.[8] Hybrid objects containing an artificial component and living organism have also been suggested.[9]

An alternative mechanism of artificial chemotaxis is based on "self-running" objects at interfaces. Alcohol droplets[10] or pieces of camphor[11] on a water surface can move due to a surface tension gradient caused by the gradual dissolution of the object itself. An oil droplet can also move on a solid substrate when the surface underneath the droplet is asymmetrically modified and causes a difference in the interfacial energy between the leading and the trailing edge of the droplet.[12] Grzybowski and co-workers showed a droplet of mineral oil and 2-hexyldecanoic acid in a labyrinth with a pH gradient, where the droplets were able to find the shortest path through the maze.[13]

Received: July 3, 2014
Revised: August 4, 2014
Published: September 12, 2014

The self-propelled motion of a droplet can be coupled with a chemical reaction that occurs at the interface between the droplet and the surrounding medium. The chemical reaction can result in a symmetry breakage due to the accumulation and release of the reaction products, and the droplets can move through the aqueous medium without the need of an air−water or a solid−liquid interface. A system of oil droplet movement based on fatty acid chemistry has been proposed by Hanczyc et al.[14] An oil phase containing oleic anhydride precursor was introduced into an aqueous environment that contained oleate micelles. The products of the precursor hydrolysis were coupled to the movement of the oil droplet and the production of waste vesicles. The oil droplet successfully moved away from this waste product into fresh unmodified solution, displaying a form of chemotaxis. This example mimics the behavior of cells that move away from their metabolic products into regions with fresh nutrients. Similar experiments with different chemicals were performed in ref 15.

In the present work, a new artificial chemotaxis system is introduced, based on decanol droplets moving in aqueous solution of sodium decanoate along concentration gradients of sodium chloride. The parametric dependence of the chemotactic response with respect to background concentration of sodium decanoate and the strength of the NaCl concentration gradient has been investigated. Several scenarios that utilize chemotaxis—namely, migration over a nonlinear path, delivery of a chemically reactive cargo, selection of the direction of motion according to the strength of the chemoattractant source, and temperature-triggered release of the chemoattractant—have been demonstrated.

2. EXPERIMENTAL SECTION

2.1. Materials and Methods. β-Carotene, decanoic acid, decanol, iodine, nitrobenzene, oil red O, paraffin, sodium chloride, and sodium hydroxide were obtained from Sigma-Aldrich. Decanoic acid solutions in the aqueous phase were prepared at the desired concentration (typically 10 mM) in water using 5 M NaOH to raise the pH of the resulting solution, typically to 10−13. Menzel-Gläser microscope slides 76 × 26 mm and 75 × 50 mm (Thermo Scientific) and an adhesive double sided tape (3M 468MP 200MP) were used for the preparation of chemotactic assays.

2.2. Chemotactic Assays. The edges of a microscopic slide were covered with thin strips of adhesive tape to form a shallow pool with a rectangular shape. The pool was filled by 1 mL of decanoate (5 or 10 mM) or water, and then a 5 μL decanol droplet containing oil red O as a colorant was placed at one side of the slide. After approximately 1 min, droplets of NaCl were added to the opposite side. The droplet volume was chosen so as not to alter the liquid level in the pool to an extent that would cause bulk fluid flow or movement of the decanol droplet. (This was verified by adding water droplets without NaCl under otherwise identical experimental conditions and noting that this did not induce any movement of the decanol droplet.) The distance between the decanol and the NaCl droplets was systematically varied to create different concentration gradients. The molar quantity of added NaCl was also systematically varied in the range 5−100 μmol by changing the salt concentration. The movement of the decanol droplet toward higher NaCl concentration was monitored using a PixeLINK camera (PL-A662) and later processed by NIS-Elements software (Laboratory Imaging Ltd., Czech Republic). From the droplet trajectory (X and Y coordinates as a function of time), the induction time and the migration velocity were evaluated.

For temperature-triggered chemotaxis experiments, the NaCl concentration gradient was not formed by adding saline droplets but by liberating small NaCl crystals from a paraffin matrix by the local application of a heat source that melted the paraffin. Fine NaCl grains were first dispersed in molten paraffin, from which small spheres were manually formed upon cooling. The salt-loaded paraffin spheres were then repeatedly washed by deionized water to remove any salt grains that may be at the surface. A single NaCl-loaded paraffin sphere was then carefully placed to one side of the chemotactic assay where it acted as a temperature-responsive salt reservoir.

2.3. Surface Tension Measurements. Surface tension measurements of decanoate solutions with varying concentrations of NaCl and decanol were performed using the Wilhelmy plate method (tensiometer Sigma 703 D, Attension). The purpose of the surface tension measurements was to verify a hypothesis about Marangoni flow as a possible cause of the observed chemotaxis (translation of concentration gradients to gradients of surface tension).

3. RESULTS AND DISCUSSION

3.1. Chemotaxis of Decanol Droplets in Rectangular Cells. Figure 1 shows the trajectory of a 5 μL decanol droplet

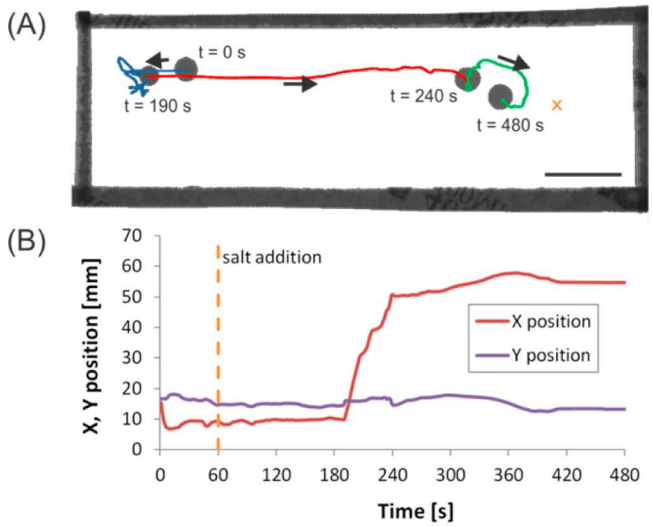

Figure 1. (A) Trajectory of a 5 μL decanol droplet in a rectangular pool (76 × 26 mm) containing 1 mL of 10 mM sodium decanoate. The orange cross indicates the place of salt addition, which occurred at t = 60 s. Scale bar represents 1 cm. (B) The X and Y positions of the droplet as a function of time, evaluated from the trajectory. The orange line indicates the moment of salt addition at t = 60 s.

in 1 mL of a 10 mM decanoate solution contained in a rectangular pool with the size 76 × 26 mm (cf. section 2.2). The droplet started on the left-hand side of the rectangular pool, and its movement was initially random. After 1 min, a 10 μL droplet of a 5 M NaCl solution (i.e., 50 μmol of NaCl) was added to the right-hand side of the microscopic slide. The decanol droplet continued its random movement on the left side of the slide (blue trajectory in Figure 1A), but after a certain induction time it started to follow the salt concentration gradient and performed an almost straight oriented movement to the opposite end of the pool (red trajectory in Figure 1A). Once the decanol droplet reached the area where the salt droplet was added, it has returned to a random, local movement (green trajectory in Figure 1A). A video recording of the entire experiment can be found in Supporting Information Movie 1.

The graph in Figure 1B shows the X and Y coordinates of the decanol droplet as a function of time, evaluated from the droplet trajectory (Figure 1A). Without a salt concentration gradient, the droplet moves locally and randomly, with no apparent directionality. It is interesting to note from Figure 1B that the droplet does not respond by chemotaxis immediately

dx.doi.org/10.1021/la502624f | Langmuir 2014, 30, 11937−11944

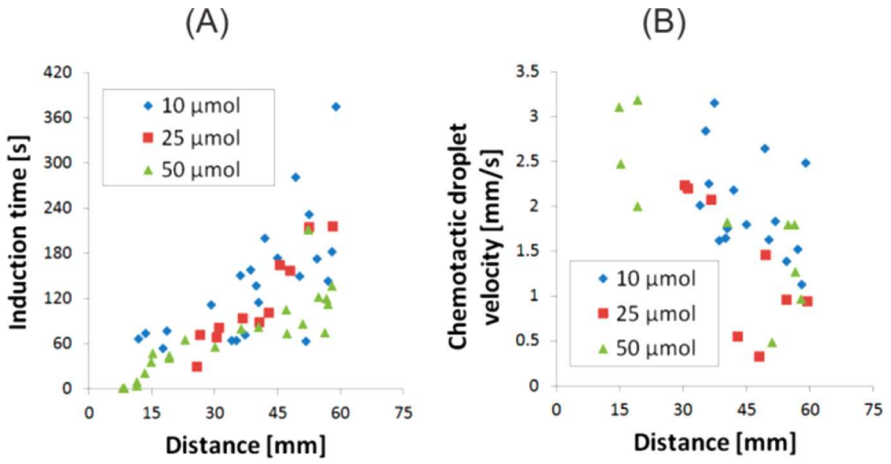

Figure 2. (A) Dependence of the chemotaxis induction time on the initial distance between the decanol and salt droplets for various molar quantities of added NaCl. (B) Dependence of the decanol droplet velocity during chemotaxis on the same parameters as in case (A).

after the salt addition (indicated by a vertical line at t = 60 s). Presumably this lag period corresponds to the time that is necessary for a concentration or interfacial tension gradient caused by NaCl addition to reach the decanol droplet. Once the signal reaches the decanol droplet, the droplet migrates toward the source of the gradient (the point of salt droplet deposition) at an increased speed as indicated by the slope of the X vs time trajectory in Figure 1B.

It can be expected that the induction time, i.e., the delay between NaCl addition and the start of chemotaxis of the decanol droplet, should be related to the time of the "chemical signal" propagation from the NaCl droplet to the decanol droplet. The underlying transport mechanism includes not only the diffusion of NaCl (see Supporting Information) but also convection. In the case of convection the flow can be due to a density difference or due to an interfacial tension gradient. The dependence of the induction time on the molar quantity of added NaCl and on the initial distance between the decanol droplet and the point of salt addition is summarized in Figure 2A (the volume of the added NaCl droplet was kept constant as well as all other parameters of the experiment). Despite the relatively widespread observed induction times, two trends are evident: the induction time increases with increasing distance, and the induction time decreases with increasing salt concentration.

It should be noted that there exists a finite window of NaCl concentrations at which chemotaxis has occurred. Both lower (5 μmol) and higher (100 μmol) salt additions were also tested, but neither has led to chemotaxis. The 5 μmol addition was insufficient to induce a chemotactic response whereas in the case of 100 μmol the decanol droplet responded by a brief jerky movement toward the salt addition point, but only over a short distance. The decanol droplet did not move across the entire slide as in the case of salt additions in the range 10−50 μmol. This behavior bears interesting similarity with one of the best-studied examples of biological chemotaxis, i.e., the migration of *Dictyostelium* amoebae in concentration gradients of cyclic adenosine-3′,5′-monophosphate (cAMP).[16,17] In the absence of cAMP, the cells are not at rest but perform a random motion with an average motility of 4.2 μm/min.[18] At intermediate cAMP gradients, the cells move up the gradient with an average motility of 9 μm/min. In very steep gradients (above 10 nM/μm) the cells again lose directionality and revert to random motion.

The velocity of droplet movement was also evaluated as the slope of the X position vs time (as in Figure 1B) for all distance−concentration combinations, and the results are summarized in Figure 2B. In this case, the chemotactic velocity of the decanol droplet is a decreasing function of the initial distance, but there does not seem to be any systematic dependence on the molar quantity of added NaCl.

The migration speed during chemotaxis is usually considered to be proportional to the concentration gradient of the chemoattractant. However, the results observed here do not fully agree with this assumption. If the gradient is defined as the concentration difference divided by distance, then a 5-fold increase in the quantity of added NaCl (e.g., from 10 to 50 μmol) should have the same effect as a 5-fold decrease in distance (e.g., from 50 to 10 mm). It is evident from Figure 2B that while a change in the droplet distance clearly leads to a proportional change in the chemotactic migration velocity, a corresponding change in the salt concentration does not. This may be due to the salting out of the decanoate surfactant in areas of very high NaCl concentrations. This is sometimes confirmed visually by the appearance of a white turbid substance at the position of highest salt concentration.

3.2. Reversal of Chemotaxis Direction. The ability of the decanol droplet to respond by chemotaxis to repeatedly created salt concentration gradients was investigated (Figure 3, Supporting Information Movie 2). The experimental setup was similar as that discussed in section 3.1, i.e., a 5 μL decanol

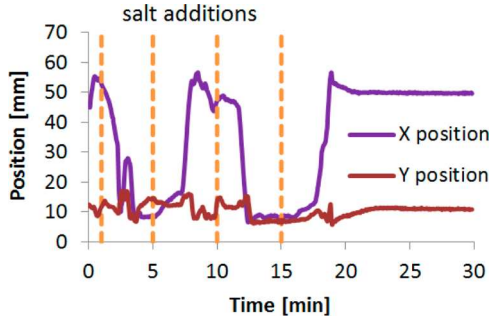

Figure 3. X and Y positions of a 5 μL decanol droplet in a rectangular pool containing 5 mM sodium decanoate solution, subjected to repeated salt additions (each containing 50 μmol of NaCl) at times t = 1, 5, 10, and 15 min.

dx.doi.org/10.1021/la502624f | *Langmuir* 2014, 30, 11937−11944

droplet in a rectangular pool of a sodium decanoate solution. However, instead of a single salt droplet addition, a droplet containing 50 μmol of sodium chloride was added four times at 5 min intervals (specifically, at time t = 1, 5, 10, and 15 min) alternatively to opposite ends of the pool. The interval of 5 min was sufficiently long to include the induction time, chemotactic migration of the decanol droplet toward the salt addition point, and stabilization of the droplet at the final location. The X and Y coordinates of the decanol droplet resulting from the repeated salt additions are shown in Figure 3. Note that although the total molar quantity of the added salt has gradually accumulated to 200 μmol, chemotaxis still took place after the fourth salt addition. Therefore, increased background salt concentration does not appear to be a hindrance to chemotaxis, as long as a concentration gradient is re-established.

3.3. Ink Tracer Experiments. The experiments described above imply that the existence of a salt concentration gradient triggers the chemotactic movement of the decanol droplet, but the underlying interactions can be complex. A key question is whether the observed decanol droplet movement is caused by Marangoni flow due to a surface tension gradient or if there are also other types of flow involved, e.g., due to density difference or contact angle gradient.

The progress of two experiments where an ink tracer was used to visualize the flow pattern in the surrounding aqueous fluid is shown in Figure 4 and in Supporting Information Movie 3. A rectangular pool with 1 mL of a 10 mM decanoate solution was used, and the order in which the decanol and the NaCl solution droplets were added was changed. The initial ink patterns were created by dropping a small amount of ink solution onto the surface of the decanoate pool and then gently mixing the surface layer by a pipet tip (see Supporting Information Movie 3). Neither convective flows nor surface tension changes were observed. Once the decanol droplet was added (time t = 40 s in Figure 4A), the original ink patterns immediately disappeared due to a reduction of surface tension near the decanol droplet and Marangoni flow toward regions of high surface tension, i.e., away from the decanol droplet. Decanol acts as a surfactant, and its effects on the surface tension of 10 mM decanoate solution, measured separately (cf. section 2.3), are summarized in Figure 5A. The addition of a salt droplet colored by blue food dye (time t = 60 s in Figure 4A) did not cause any visible changes in the ink pattern. The salt solution did not attract or repel the ink particles (no diffusiophoresis was observed). However, the salt droplet did not spread uniformly and had a tendency to spread somewhat faster toward the decanol droplet (tear-like blue spot at t = 80 s in Figure 4A). The decanol droplet eventually moved chemotactically to the area of the salt addition (time t = 120 s in Figure 4A).

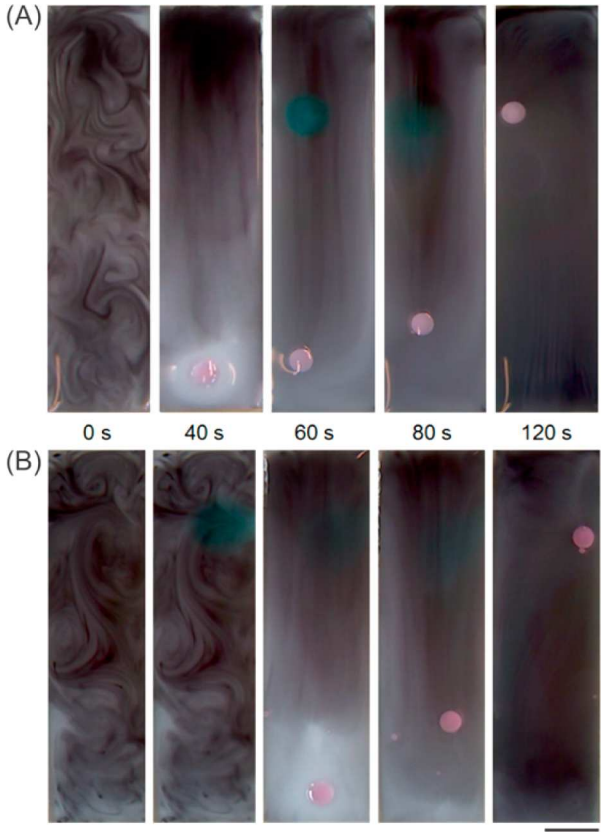

Figure 4. Flow field visualization using ink tracer: (A) decanol droplet addition followed by salt addition; (B) salt droplet addition followed by decanol addition. The decanol droplet was deposited at the bottom end of the rectangular pool and was labeled by a pink color; the salt droplet (deposited at the top end) is blue. Scale bar represents 1 cm.

When the order of the droplet addition was reversed, i.e., adding the salt droplet first and the decanol droplet next (in Figure 4B), no change in the initial ink pattern was observed after salt addition despite the fact that NaCl also slightly reduces the surface tension of decanoate solution (Figure 5B). The salt spot spread uniformly in all directions and did not affect the ink pattern (t = 40 s in Figure 4B). The decanol droplet addition rapidly deleted the ink patterns and repelled the ink to the opposite end of the glass slide (t = 60 s in Figure 4B). The salt started to flow toward decanol (t = 80 s in Figure 4B), and the decanol droplet was transported chemotactically to the zone of the salt droplet addition (t = 120 s in Figure 4B).

Several additional experiments with an ink tracer in a single chamber with and without obstacles were done, and the results are shown in Supporting Information Movie 3. The black ink served as tracer to visualize the convective flow in the aqueous phase. Both direct salt solution addition and salt diffusion from nitrobenzene droplets were tested. The blue spot of salt had a tendency to spread toward the decanol droplet due to directional flow of the aqueous phase. In all cases the shortest path between the decanol droplet and the salt source was highlighted, and the decanol droplet followed this path and moved chemotactically toward the salt. In experiments with nitrobenzene droplets loaded with salt grains, fusion with the decanol droplet occurred.

3.4. Nonlinear Path Experiments. In the experiments described above, it was shown that decanol droplets follow a salt concentration gradient created by direct addition of a salt solution. In order to sustain a concentration gradient for longer periods of time without disturbing the system by repeated external liquid additions, an alternative method of creating the salt concentration gradient has been used—a nitrobenzene droplet loaded with NaCl grains was deposited in the decanoate pool instead of an aqueous droplet with predissolved NaCl (Supporting Information Movie 4). The nitrobenzene droplet (which is immiscible with water) was stationary and allowed a gradual leaching of NaCl to the surrounding solution. This created a salt concentration gradient, which in turn resulted in a chemotactic movement of the decanol droplet toward the nitrobenzene droplet, eventually fusing with it. Independent

dx.doi.org/10.1021/la502624f | Langmuir 2014, 30, 11937−11944

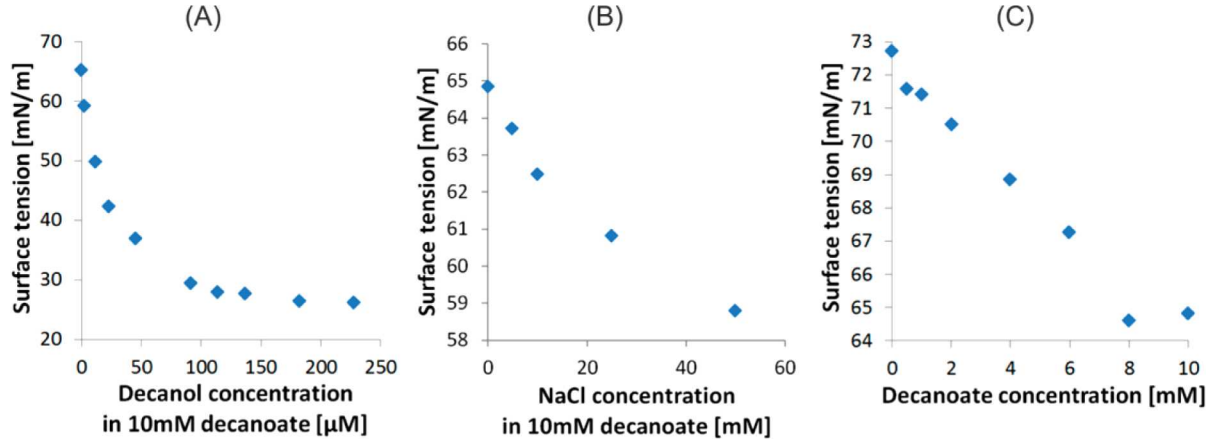

Figure 5. Dependence of the surface tension of 10 mM decanoate solution on (A) decanol and (B) NaCl concentration. (C) Dependence of the surface tension of water on the sodium decanoate concentration.

verification experiments have shown that without NaCl there is no interaction between the nitrobenzene and decanol droplets, i.e., no chemotaxis and no fusion.

The salt concentration gradients created by the nitrobenzene droplet with salt grains were used in scenarios where the chemotaxis of the decanol droplet took place over a nonlinear path in slightly more complex topologies than a straight channel. Two examples of such topologies are shown in Figure 6. In each case, the decanol droplet followed the shortest path toward the source of the salt and eventually fused with the salt-loaded nitrobenzene droplet.

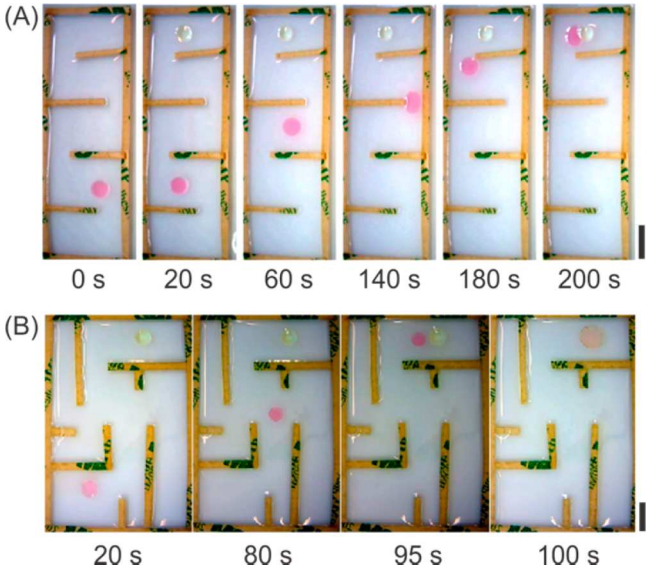

Figure 6. Examples of droplet chemotaxis in a complex topology: (A) nonlinear path in a channel; (B) nonlinear path in a simple "labyrinth" with dead end channels. The decanol droplet has a purple color, and the salt diffuses from a stationary nitrobenzene droplet (yellowish color). Scale bar represents 1 cm.

Although the topology shown in Figure 6B could theoretically allow the decanol droplet to follow an incorrect path into a dead-end channel, there was only one source of the salt gradient. An alternative scenario was therefore realized, where the decanol droplet had two alternatives, i.e., two sources of salt located at an identical distance but in opposite ends of the pool (see Figure 7). The two sources contained a different

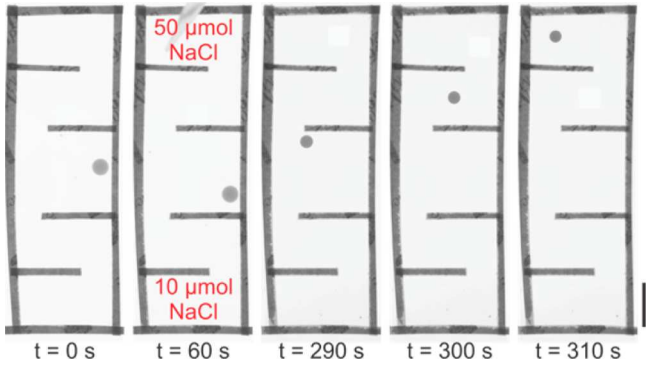

Figure 7. Decanol droplet (middle of the pool at $t = 0$ s) attracted by a stronger salt concentration gradient. Scale bar represents 1 cm.

quantity of NaCl, namely 50 and 10 μmol. The decanol droplet, initially located in the middle of the pool, started to migrate toward the end with a higher concentration of salt. Thus, two important features of chemotaxis, also revealed by living systems, were demonstrated: the ability to follow the chemoattractant in a complex topology and the ability to follow a stronger source of chemoattractant when presented with alternative chemotaxis directions.

3.5. Stimulus-Responsive Release of Chemoattractant. The diffusion of NaCl from the nitrobenzene droplet, discussed in the previous section, was spontaneous. However, in nature, the release of a chemoattractant is often triggered by a change in some environmental variable, for example temperature, which can signal conditions favorable for the next phase of a reproduction cycle. A similar scenario of temperature-triggered release of the chemoattractant has been realized in laboratory conditions as follows. Instead of a nitrobenzene droplet, fine NaCl crystals were encapsulated into a paraffin particle with a melting point of 42 °C as described in section 2.2.

When a single salt-containing wax sphere was deposited into a pool of sodium decanoate at low temperature, the salt could not diffuse from the paraffin particle in the solid state and the system was stationary. However, once the paraffin particle was locally heated to a temperature above its melting point, the previously encapsulated salt was liberated, started to dissolve in the surrounding solution, and triggered the chemotaxis of the decanol droplet, which migrated toward to source of salt

dx.doi.org/10.1021/la502624f | Langmuir 2014, 30, 11937−11944

(Figure 8, Supporting Information Movie 5). As in the case of nitrobenzene, a control experiment without NaCl (only paraffin and heating) did not lead to chemotaxis or thermophoresis.

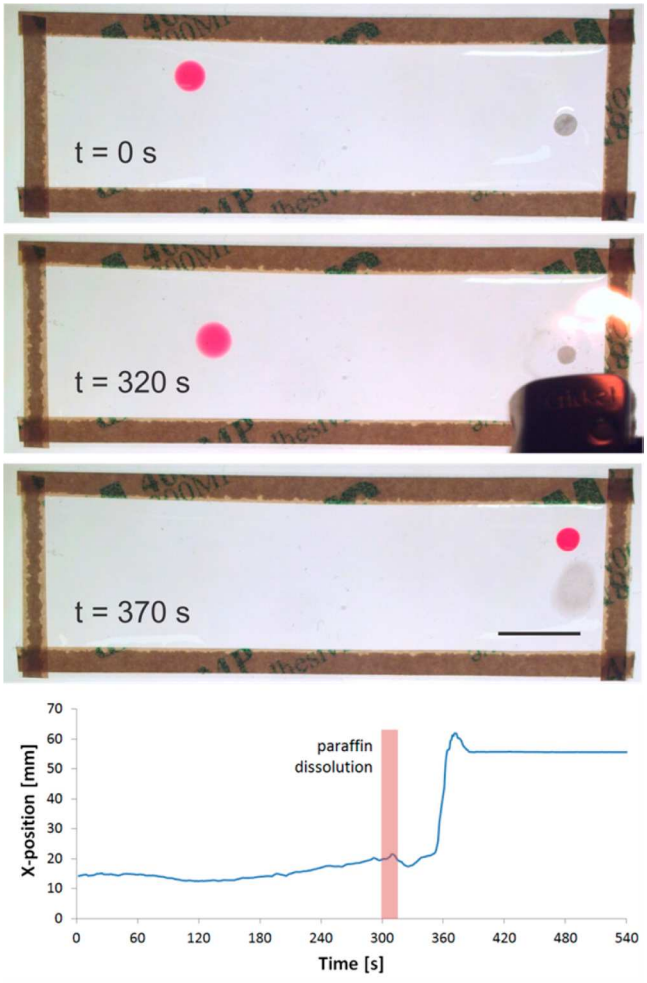

Figure 8. (A) Progress of an experiment with a paraffin particle containing salt grains as a thermoresponsive source of chemoattractant. The chemotactic decanol droplet is marked by a pink color; the paraffin particle is gray. Scale bar represents 1 cm. (B) Trajectory of the decanol droplet, evaluated from the experiment. Local heating of the paraffin particle was applied at t = 300 s for 20 s and resulted in NaCl liberation from the particle.

3.6. Chemotaxis Delivery of a Reactive Payload. It has been shown in the previous sections that a decanol droplet is able to locate a nitrobenzene droplet and fuse with it even in topologically complex environments and that it is able to follow the strongest source of chemoattractant from several alternatives. These are the prerequisites for the laboratory demonstration of a model "search-and-neutralize" mission, whereby the chemotactic droplet carries a payload that will react with the chemoattractant source once the mobile droplet localizes it. Again, an analogy with natural systems can be seen in this scenario, e.g., the chemotaxis of a leukocyte that actively locates and eventually neutralizes a pathogen.

Decanol was saturated with solid iodine to produce a dark orange oil. Independently, β-carotene was added to pure nitrobenzene and mixed to obtain a red oil at 2 mg/mL. Droplets of 10 μL of each solution were added to opposite ends of a channel with a simple obstacle in the middle, filled with 10 mM decanoate (pH 11). The progress of the experiment is shown in Figure 9. After chemotaxis and fusion of the decanol and nitrobenzene droplets, a color change to green indicated that an iodination reaction of β-carotene has taken place.[19]

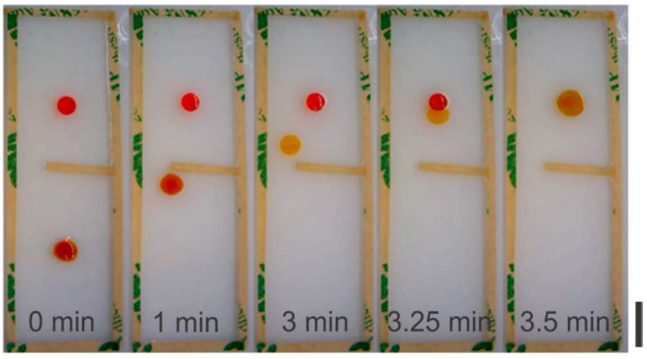

Figure 9. Example of a chemotactic droplet carrying a reactive payload toward the chemoattractant source (iodination assay). The chemotactic decanol droplet moves from the bottom to the top section of the figure and eventually fuses with the stationary nitrobenzene droplet. The chemical reaction is indicated by a color change. Scale bar represents 1 cm.

3.7. Chemotaxis Mechanism and Force Balance. The decanol droplet in a homogeneous solution of decanoate exhibits weak random motion, as shown in Figure 1. This is likely due to the loss of mass of the droplet over time because the droplet itself is slowly being dissolved into to surrounding soapy solution. However, when a salt gradient is introduced to the system, a corresponding surface tension gradient is established (Figure 5). There are several works where it was shown experimentally and theoretically how surface tension gradients give rise to convective flows that result in particle or droplet motion.[20,21] There are two possible theoretical approaches—a fluid mechanics approach based on the solution of the Navier–Skokes equations or a simplified force balance approach whereby the moving object is regarded as a rigid body subjected to the Newton's law of motion. The latter approach, adopted from ref 21, is adopted here.

Let us assume that the decanol droplet has a constant mass. The net force acting on the decanol droplet due to a gradient of surface tension and due to fluid–fluid and wall–fluid friction is

$$m\frac{\mathrm{d}v_{\mathrm{drop}}}{\mathrm{d}t} = F_{\mathrm{A}} - F_{\mathrm{D}} - F_{\mathrm{W}} \quad (1)$$

where m is the droplet mass, v_{drop} is the macroscopic droplet velocity, F_{A} is the surface tension force, F_{D} is the fluid–fluid drag force, and F_{W} is the fluid–wall drag force. If the surface tension force is greater than the frictional and drag forces, locomotion of the droplet can occur.[22,23] Let us now estimate the magnitude of the forces for our system.

In the case of a shallow pool, the total concentration of NaCl in the solution of sodium decanoate is known (50 mM). Since the dependence of surface tension on NaCl concentration was independently measured (Figure 5), the salt concentration gradient can be translated into a gradient of surface tension. Assuming a linear concentration gradient and a pool length of 70 mm, the corresponding macroscopic surface tension gradient is $\partial\gamma/\partial x$ = 173.5 mN/m^2. The diameter of the droplet projection in this setup, obtained through image analysis, is 3.6 mm. By using these values, an order-of-magnitude estimate of

dx.doi.org/10.1021/la502624f | Langmuir 2014, 30, 11937–11944

the force acting on the droplet due to the surface tension gradient can be made. Using the divergence theorem, the integration along the circumference of the droplet can be replaced by

$$F_A = \oint_{\partial A} \mathbf{i}\cdot\mathbf{n}\gamma \,\mathrm{d}l = \int_A (\nabla\cdot\mathbf{i}\gamma)\,\mathrm{d}A = \int_A \left(\frac{\partial\gamma}{\partial x}\right)\mathrm{d}A = \left(\frac{\partial\gamma}{\partial x}\right)A \quad (2)$$

where $A = 10.18 \times 10^{-6}$ m^2 is the projected droplet area and $\mathbf{i} = [1,0,0]$ is a unit vector in the direction of the macroscopic surface tension gradient. The resulting force is $F_A = 1.77 \times 10^{-6}$ N. The force due to a surface tension gradient would be opposed by viscous dissipation in the fluid.

As an order-of-magnitude estimate of these effects, let us consider the droplet to be a rigid sphere and evaluate the Stokes drag force according to

$$F_D = 6\pi\eta r v_{drop} \quad (3)$$

where $\eta = 10^{-3}$ Pa·s is viscosity (assuming equal to that of water for the purpose of the estimate), $v_{drop} = 1.5 \times 10^{-3}$ m/s is a characteristic value of the droplet velocity (cf. Figure 2B), and $r = 1.06 \times 10^{-3}$ m is the characteristic droplet radius computed directly from its volume. The resulting drag force is $F_D = 0.03 \times 10^{-6}$ N, which is significantly lower than the force due to surface tension gradient, although it is in fact an overestimate because the decanol droplet is not fully surrounded by the aqueous phase. Similarly, an estimate of the upper value of the wall friction force can be made by assuming the decanol droplet to be a hemisphere in contact with the glass substrate. In that case, the wall friction would be

$$F_W = \int_A \eta\frac{\partial v_x}{\partial y}\,\mathrm{d}A \approx A\eta\frac{v_{drop}}{h_{drop}} \quad (4)$$

where $A = 10.18 \times 10^{-6}$ m^2 is the projected droplet area, $\eta = 12.0 \times 10^{-3}$ Pa·s is the viscosity of decanol, $v_{drop} = 1.5 \times 10^{-3}$ m/s is a characteristic value of the droplet velocity, and h_{drop} is the characteristic droplet height, calculated from the droplet area and volume ($V = 5$ μL) based on the spherical cap approximation. The resulting force is $F_W = 0.21 \times 10^{-6}$ N, which is larger than the fluid drag force (mainly due to the higher viscosity of decanol compared to water) but still well below the surface tension force. Although simple, this order-of-magnitude calculation supports the hypothesis that in principle the gradient of surface tension has sufficient power to cause the droplet movement. At the same time, it should be kept in mind that other mechanisms such as interaction with the glass substrate can also be involved in the propulsion of the droplet.

4. CONCLUSIONS

A new, relatively simple two-phase system exhibiting artificial chemotaxis has been described. It is based on a decanol droplet in an aqueous solution of sodium decanoate, with sodium chloride as a chemoattractant. The range of concentrations in which the system exhibits chemotaxis has been determined, and the parametric dependence of two important characteristics—the induction time and the migration velocity—on the salt concentration gradient has been systematically investigated. It has been demonstrated that this artificial chemotaxis system bears many qualitative similarities with natural chemotaxis systems, namely (i) the ability to perform chemotaxis repeatedly when the chemoattractant gradients are recreated, (ii) to perform chemotaxis in topologically complex environments, (iii) to select the chemotaxis direction based on the relative strength of alternative chemoattractant sources, (iv) to rest in a dormant state and later respond to a stimuli-responsive chemoattractant release, and finally (v) to deliver a reactive payload toward the chemoattractant source. To the best of our knowledge, this is the first time that an artificial chemotaxis system exhibiting all of the above-mentioned five features has been described. By measuring the concentration dependence of surface tension, order-of-magnitude estimates of the forces acting on the droplet could be made, supporting a hypothesis that a surface tension gradient can be responsible for chemotaxis in this case.

■ ASSOCIATED CONTENT

Supporting Information

Movies 1−5. This material is available free of charge via the Internet at http://pubs.acs.org.

■ AUTHOR INFORMATION

Corresponding Author

*E-mail jitka.cejkova@vscht.cz (J.Č.).

Notes

The authors declare no competing financial interest.

■ ACKNOWLEDGMENTS

This work was supported by the European Commission FP7 Future and Emerging Technologies Proactive: 270371 (COBRA), 318671 (MICREAgents), 249032 (MATCHIT), and 611640 (EVOBLISS).

■ REFERENCES

(1) Lodish, H.; Berk, A.; Zipursky, S. L.; Matsudaira, P.; Baltimore, D.; Darnell, J. Cell Locomotion. In *Molecular Cell Biology*, 4th ed.; W.H. Freeman: New York, 2000.

(2) Eisenbach, M. *Chemotaxis*; Imperial College Press: London, 2004.

(3) Lackie, J. M. *The Dictionary of Cell & Molecular Biology*; Elsevier Science: Amsterdam, 2012.

(4) Fournier-Bidoz, S.; Arsenault, A. C.; Manners, I.; Ozin, G. A. Synthetic self-propelled nanorotors. *Chem. Commun.* **2005**, *4*, 441−443.

(5) Mano, N.; Heller, A. Bioelectrochemical propulsion. *J. Am. Chem. Soc.* **2005**, *127* (33), 11574−11575.

(6) Abecassis, B.; Cottin-Bizonne, C.; Ybert, C.; Ajdari, A.; Bocquet, L. Boosting migration of large particles by solute contrasts. *Nat. Mater.* **2008**, *7* (10), 785.

(7) Agarwal, A.; Hess, H. Biomolecular motors at the intersection of nanotechnology and polymer science. *Prog. Polym. Sci.* **2010**, *35* (1-2), 252−277.

(8) Upadhyaya, A.; Chabot, J. R.; Andreeva, A.; Samadani, A.; van Oudenaarden, A. Probing polymerization forces by using actin-propelled lipid vesicles. *Proc. Natl. Acad. Sci. U. S. A.* **2003**, *100* (8), 4521−4526.

(9) Behkam, B.; Sitti, M. Towards hybrid swimming microrobots: Bacteria assisted propulsion of polystyrene beads. *Proc. 28th IEEE (EMBS Annu. Int. Conf.)* **2006**, 2421−2424.

(10) Nagai, K.; Sumino, Y.; Kitahata, H.; Yoshikawa, K. Mode selection in the spontaneous motion of an alcohol droplet. *Phys. Rev. E* **2005**, *71* (6), 065301.

(11) Nakata, S.; Matsuo, K. Characteristic self-motion of a camphor boat sensitive to ester vapor. *Langmuir* **2005**, *21* (3), 982−984.

(12) Sumino, Y.; Kitahata, H.; Yoshikawa, K.; Nagayama, M.; Nomura, S.-i. M.; Magome, N.; Mori, Y. Chemosensitive running droplet. *Phys. Rev. E* **2005**, *72* (4), 041603.

(13) Lagzi, I.; Soh, S.; Wesson, P. J.; Browne, K. P.; Grzybowski, B. A. Maze solving by chemotactic droplets. *J. Am. Chem. Soc.* **2010**, *132* (4), 1198−1199.
(14) Hanczyc, M. M.; Toyota, T.; Ikegami, T.; Packard, N.; Sugawara, T. Fatty acid chemistry at the oil-water interface: Self-propelled oil droplets. *J. Am. Chem. Soc.* **2007**, *129* (30), 9386−9391.
(15) Toyota, T.; Maru, N.; Hanczyc, M. M.; Ikegami, T.; Sugawara, T. Self-propelled oil droplets consuming "fuel" surfactant. *J. Am. Chem. Soc.* **2009**, *131* (14), 5012−5013.
(16) Ševčíková, H.; Čejková, J.; Krausová, L.; Přibyl, M.; Štěpánek, F.; Marek, M. A new traveling wave phenomenon of *Dictyostelium* in the presence of cAMP. *Phys. D (Amsterdam, Neth.)* **2010**, *239* (11), 879−888.
(17) Kessin, R. H. *Dictyostelium: Evolution, Cell Biology, and the Development of Multicellularity*; Cambridge University Press: Cambridge, UK, 2001.
(18) Song, L.; Nadkarni, S. M.; Bödeker, H. U.; Beta, C.; Bae, A.; Franck, C.; Rappel, W.-J.; Loomis, W. F.; Bodenschatz, E. *Dictyostelium discoideum* chemotaxis: Threshold for directed motion. *Eur. J. Cell Biol.* **2006**, *85* (9−10), 981−989.
(19) Harada, I.; Furukawa, Y.; Tasumi, M.; Shirakawa, H.; Ikeda, S. Spectroscopic studies on doped polyacetylene and β-carotene. *J. Chem. Phys.* **1980**, *73* (10), 4746−4757.
(20) Nakata, S.; Iguchi, Y.; Ose, S.; Kuboyama, M.; Ishii, T.; Yoshikawa, K. Self-rotation of a camphor scraping on water: New insight into the old problem. *Langmuir* **1997**, *13* (16), 4454−4458.
(21) Soh, S.; Bishop, K. J. M.; Grzybowski, B. A. Dynamic self-assembly in ensembles of camphor boats. *J. Phys. Chem. B* **2008**, *112* (35), 10848−10853.
(22) Nakata, S.; Komoto, H.; Hayashi, K.; Menzinger, M. Mercury drop "attacks" an oxidant crystal. *J. Phys. Chem. B* **2000**, *104* (15), 3589−3593.
(23) Haidara, H.; Vonna, L.; Schultz, J. Surfactant induced Marangoni motion of a droplet into an external liquid medium. *J. Chem. Phys.* **1997**, *107* (2), 630−637.

Chem. Listy *107*, 563−600 (2013) Bulletin

HLENKA *Dictyostelium discoideum*: MODELOVÝ SYSTÉM NEJEN PRO BIOLOGY *

JITKA ČEJKOVÁ

Ústav chemického inženýrství, Vysoká škola chemicko-technologická v Praze, Technická 3, 166 28 Praha 6
jitka.cejkova@vscht.cz

Klíčová slova: *Dictyostelium discoideum*, cyklický adenosin-3‘,5‘-monofosfát (cAMP), excitabilní médium, Bělousovova-Žabotinského reakce

Obsah

1. Úvod

Existuje řada chemických a biologických systémů, ve kterých jsou studovány nelineární dynamické jevy, jako jsou oscilace, excitabilita, chaos, tvorba disipativních struktur nebo šíření vln. Na Ústavu chemického inženýrství se během své vědecké kariéry této problematice věnovala Ing. Hana Ševčíková, CSc., které je tento článek věnován. Soustředila se především na výzkum excitability a šíření koncentračních vln ve dvou chemických a jednom biologickém systému. Prvním z nich byla reakce Bělousova a Žabotinského, při níž dochází k oscilacím a vzniku koncentračních vln typu pulsu, které se mohou periodicky šířit systémem[1–8]. Druhý studovaný systém poskytla oxidace kyseliny arsenité jodičnanovými ionty, která tvoří reakční prostředí umožňující šíření koncentračních vln typu fronta[9–14]. Cílem zkoumání biologického systému představovaného populací buněk hlenky *Dictyostelium discoideum*, u něhož dochází k šíření excitačních vln cyklického adenosin-3‘,5‘-monofosfátu (cAMP), bylo posoudit, do jaké míry lze nebo nelze chování biologických systémů pochopit na základě znalostí o chemických systémech[15–19].

Předložená práce je zaměřena pouze na třetí z výše zmíněných systémů, čtenáři tedy budou seznámeni s hlenkou *Dictyostelium discoideum*, detailně bude popsán její zajímavý životní cyklus a princip šíření vln cAMP. Zmíněno bude také využití tohoto modelového systému při studiu některých biologických pochodů (např. chemotaxe, diferenciace buněk, signálních transdukčních drah). Budou ukázány výsledky experimentálního pozorování vývoje hlenky *Dictyostelium discoideum* za přirozených podmínek, podrobněji se zaměříme na agregační fázi vývoje a šíření vln cAMP. Dále budou shrnuty výsledky experimentů výzkumné skupiny Hany Ševčíkové a jejích studentů, které souvisely s ovlivňováním agregace buněk vnějšími stimuly (elektrické pole[16], organické látky[20–23], cAMP[19] a 2‘,3‘-*O*-isopropylidenadenosin (IPA)[18] v agaru).

1.1. Životní cyklus hlenky *Dictyostelium discoideum*

Hlenky jsou eukaryotické mikroorganismy všudypřítomné na vlhkých a stinných místech v půdách mírného pásu[24]. Dosud bylo popsáno asi 60 druhů, z nichž nejvíce studovaným druhem jsou hlenky *Dictyostelium discoideum*. Buňky *Dictyostelium discoideum* mají vlastnosti buněk jak z rostlinné, tak i živočišné říše. Stejně jako rostlinné buňky produkují celulosu a tvoří spóry. S živočišnými buňkami je spojuje schopnost pohybu a kolektivního chování. *Dictyostelium* bylo poprvé pozorováno Oskarem Brefeldem roku 1869. Svůj název získalo podle zesíťovaných struktur během agregace (dicty – zesíťovaný) a vzpřímené plodnice (stelium – věž).

Hlenky jsou buňky měňavkovitého tvaru o velikosti asi 10 μm. Ve své vegetativní fázi života se volně pohybují

** Tento článek bych chtěla jménem svým a jménem zaměstnanců a studentů Ústavu chemického inženýrství VŠCHT v Praze věnovat Hance Ševčíkové, kolegyni, která dokázala vždy ochotně pomoci a měla spoustu elánu do práce, školitelce, která nikdy neztrácela víru v úspěch svých svěřenců, kamarádce, která vždy uměla povzbudit a zvednout náladu, organizátorce, která dokonale připravila každou oslavu či besídku, člověku, který dokázal se vším bojovat. Bohužel boj s těžkou nemocí Ing. Hana Ševčíková, CSc. prohrála dne 23.9.2006. 23.7.2013 by Hanka oslavila své šedesáté narozeniny.*

jako samostatní jedinci, živí se bakteriemi a rozmnožují se dělením. V případě, že se veškerá potrava z jejich okolí vyčerpá, mají buňky *Dictyostelium discoideum* na rozdíl od ostatních druhů z rodiny hlenek pouze dvě možnosti, jak přežít. Buď pohlavním způsobem vytvořit mnohobuněčné makrocysty, nebo nepohlavně vytvořit plodnici nesoucí spóry. Ostatní druhy mohou ještě nepohlavním způsobem vytvářet jednobuněčné mikrocysty. Nejvíce studovaným způsobem je tvorba plodnice a spór, protože jsou na něm ukázány základy vývoje mnohobuněčných organismů a principy mezibuněčné komunikace, díky níž se statisíce buněk začnou chovat jako organizované společenství. V následujícím se zaměříme pouze na tento způsob přežívání hlenek (obr. 1).

Když je v okolí buněk nedostatek živin a buňky začnou hladovět, nastupuje morfogenetická fáze, během níž buňky nepotřebují potravu a čerpají ze zásob nahromaděných během vegetativního období. U hladovějících buněk dochází k inaktivaci genů potřebných pro růst a jsou aktivovány jiné geny – důležité pro morfogenezi. Buňky získávají schopnost syntetizovat a rozpoznávat cAMP, odpovídat na jeho signály a odbourávat ho.

Během rané agregační fáze, která nastává mezi čtvrtou a šestou hodinou od počátku hladovění, některé buňky začnou syntetizovat cAMP a periodicky ho každou pátou až sedmou minutu v pulzech vysílat do okolí. Vyloučený cAMP difunduje k nejbližším buňkám a ty reagují na přísun cAMP díky receptorům citlivým k cAMP dvojím způsobem. Zaprvé se buňky začnou pohybovat proti koncentračnímu spádu (tedy ke zdroji cAMP) pohybem označovaným jako pozitivní chemotaxe a zadruhé buňky začnou produkovat další cAMP, který pak difunduje k buňkám dále od zdroje. Periodickým opakováním těchto dějů se buňky postupně shromáždí v agregačním centru.

Ze 100 000 hladovějících buněk se vytvoří mnohobuněčný, relativně plochý agregát s neostrými hranicemi, který se přemění do tzv. „kupky“ hemisférického tvaru, jež prodělá úchvatné změny. Nejprve se na ní objeví špička, která roste do výšky a připomíná prst (někdy se tato fáze také nazývá „stojící slimák“), poté se skácí na podklad a v podobě plazícího se slimáka (pseudoplasmodium) se stěhuje za světlem, než dosáhne oblasti, kde jsou vhodné podmínky k vytvoření plodnice (houbičky). Zhruba 20 % buněk je určeno k vytvoření stonku, tudíž předurčeno k zániku. Ze zbývajících buněk se ztrátou vody a vytvořením obalu stanou spóry, které ve vrcholu plodnice dokáží přečkat nepříznivé podmínky. Za nějaký čas se spóry uvolní do okolí a v případě dostatku potravy nabobtnají, přemění se v buňky a opět nastává vegetativní fáze životního koloběhu hlenek. Buňky se množí, živí a volně pohybují, dokud se opět nevyčerpá potrava z jejich okolí. Pak jsou hladovějící buňky nuceny znovu agregovat a zopakovat výše popsaný vývojový cyklus.

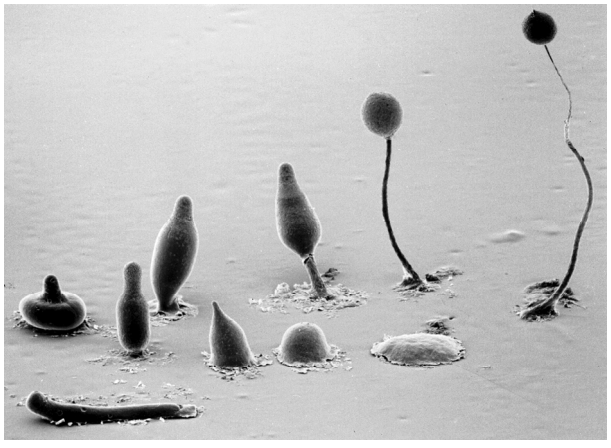

Obr. 1. **Životní cyklus hlenky *Dictyostelium discoideum*.** (Autorem snímků z elektronového mikroskopu je M. J. Grimson a R. L. Blanton, Biological Sciences Electron Microscopy Laboratory, Texas Tech University)

Z uvedeného vyplývá, že hlenku můžeme řadit jak mezi jednobuněčné, tak mezi mnohobuněčné organismy. K vývoji složitého, mnohobuněčného organismu (houbičky) je zapotřebí, aby se populace původně samostatných, identických vegetativních buněk chovala jako spolupracující kolektiv, kde jsou jasně definované úkoly pro všechny členy populace.

1.2. *Dictyostelium discoideum* jako modelový systém

Hlenka *Dictyostelium discoideum* je výborným modelovým systémem, který je zkoumán z různých pohledů v širokém spektru vědních oborů[25]. Zabývají se jím především biologové, např. molekulární, buněční a vývojoví biologové, genetici nebo biochemici. Tento organismus je vhodný k popisu cytokineze, pohyblivosti buněk[26], fagocytózy[27], chemotaxe[28], buněčné diferenciace[29], adheze[30], signálních transdukčních drah, mezibuněčné komunikace, vývoje mnohobuněčného organismu z jednotlivých buněk[31] a dalších dějů. Při pochopení pochodů odehrávajících se u hlenky *Dictyostelium discoideum* můžeme lépe porozumět i pochodům objevujícím se u vyšších organismů. Výhodou studia hlenky *Dictyostelium discoideum* je např. její jednoduchá stavba, krátká reprodukční doba, a tedy možnost připravit velké množství buněk v krátkém čase, dále relativně jednoduchý genetický kód, a tudíž možnost snadno popsat genom a připravit různé mutanty.

Na hlence *Dictyostelium discoideum* se např. pozoruje vzájemná soudržnost buněk a jejich přilnavost k substrátu[32]. Mnoho buněk se dokáže plazivými pohyby přemísťovat na delší vzdálenosti nebo přes překážky. Stejně jako se hlenky dokážou rychle pohybovat během chemotaktické agregace, tak se leukocyty dostávají přes překážky k místům svého působení nebo se nádorové buňky odpojují ze svého primárního místa a přemísťují se do jiných částí těla.

Savčí buňky mají schopnost rozpoznat hustotu buněk ve svém okolí, což hraje důležitou roli při řízení růstu buněk a jejich diferenciaci[33]. Bez této schopnosti by nebylo možné u vyvíjejícího se embrya správné roztřídění zárodečných buněk do různých typů budoucích tkání. Během vývoje si buňky v embryu vyměňují signály, aby si rozdě-

lily, kterou specializovanou funkci bude každá z nich zastávat, jakou polohu zaujme a zda bude dál žít nebo umře či se rozdělí. Studium této diferenciace přímo u savčích buněk je obtížné kvůli jejich složitosti, a proto se tyto procesy zkoumají na jednoduchém organismu jako je hlenka *Dictyostelium discoideum*. Hladovějící buňky *Dictyostelium discoideum* se v určité fázi svého vývojového cyklu diferencují na stonkotvorné a sporotvorné a tím si rozdělují úlohy a umístění v budoucím mnohobuněčném útvaru – plodnici. Některé buňky zahynou a vytvoří stonek a hlavičku houbičky, jiné vytvoří spory a jsou naopak nositelkami života příštích generací hlenky.

Hlenka *Dictyostelium discoideum* je fascinujícím organismem nejen pro biology, ale i pro fyziky a chemiky[34]. Během agregační fáze se objevují obrazce podobné obrazcům vyskytujícím se u reakce Bělousova-Žabotinského. B. P. Bělousov objevil v 50. letech 20. století oscilace koncentrace katalyzátoru (ionty ceru) při oxidační reakci kyseliny citrónové bromičnanem. A. M. Žabotinský později pokračoval ve studiu tohoto typu neobvyklých chemických reakcí a od té doby se skupina takových reakcí označuje jako BZ reakce. BZ reakce jsou hojně zkoumány, jak experimentálně, tak teoreticky matematickým modelováním, protože ukazují řadu typů nelineárního dynamického chování. Biologický systém hlenky *Dictyostelium discoideum* má po formální stránce mnoho společného s chemickým BZ systémem a je tedy studován i z pohledu nelineární dynamiky.

1.3. Šíření excitačních vln

Excitabilní médium je nelineární dynamický systém, který má schopnost šířit vlny a nepodporovat vznik dalších vln, dokud se systém nezregeneruje do původního stavu. Jak bylo zmíněno výše, takovýmto systémem je i vrstva hladovějících buněk *Dictyostelium discoideum*. Než si popíšeme princip šíření vln cAMP u *Dictyostelia discoidea*, definujeme si základní pojmy týkající se excitabilních systémů a jako velice jednoduchý příklad si uvedeme požár v lese.

Prvky excitabilního média se mohou vyskytovat v jednom ze tří stavů: excitabilním, excitovaném a nebo refrakterním. Excitabilní prvky jsou v relativním klidu, ale mohou být vnějšími vlivy převedeny do stavu excitovaného. Na příkladu požáru v lese excitabilní stav odpovídá klidovému období, kdy nic nehoří. Excitací je myšlen impuls, v našem příkladu lesa jeho zapálení, který uvede systém do excitovaného stavu. Excitabilní prvky se dostávají do excitovaného stavu poté, co se staly excitovanými prvky v jejich sousedství. Stromy začnou hořet, až když se na ně přenese oheň z okolních stromů. V excitovaném stavu setrvá systém pouze určité období, potom nastává takzvaná refrakterní fáze. Na jejím počátku je systém vůči dalším impulsům zcela imunní (absolutní refrakterita). Pokud v lese všechno shořelo, nemůže se tam šířit další požár. Následující část refrakterní fáze spočívá v návratu systému do původního stavu, les se regeneruje, začínají růst nové stromy a systém se postupně znovu stává excitabilním, tedy schopným šířit další vlny.

Podle toho, zda se vlny šíří po křivce nebo po ploše, je rozdělujeme na jednorozměrné nebo dvourozměrné. Příkladem jednorozměrné vlny je tzv. mexická vlna, kterou je možno pozorovat na stadionech při různých sportovních utkáních. Dvourozměrné vlny mohou mít různé tvary, základními typy jsou vlny kruhové a spirálové. Kruhové vlny se šíří z jednoho bodu všemi směry, příkladem může být výše popsaný požár v lese. Např. nedopalek cigarety uvnitř lesa může způsobit vznik požáru a jeho následné šíření směrem k hranicím lesa. Spirálové vlny také vznikají v jednom bodě, ale šíří se ve formě spirál. Tímto způsobem se např. šíří patologické vzruchy po srdečním svalu.

Hojně studovaným chemickým excitabilním systémem jsou média Bělousova – Žabotinského. Oscilační barevné změny při těchto redoxních reakcích lze pozorovat buď v míchaném vsádkovém systému, např. v kádince, nebo v nemíchaném médiu, např. na Petriho misce.

Vrstva hladových buněk *Dictyostelium discoideum* nanesených na agar je příkladem biologického excitabilního média. Excitabilní buňky setrvávají v relativním klidu, dokud nejsou vnějšími silami z tohoto stavu vybuzeny. Vnějšími silami je myšlena koncentrační perturbace, čili zvýšení koncentrace signalizační látky (cAMP). Buňka se stává excitovanou po navázání cAMP, který se k ní dostal difusí od sousedních buněk, na povrchové receptory citlivé k cAMP. Buňky v excitovaném stavu mají aktivovaný aparát pro tvorbu dalšího cAMP, který je částečně uvnitř buňky odbouráván enzymem buněčnou fosfodiesterasou a částečně vylučován do okolí buňky. Po několika minutách dosahuje koncentrace extracelulárního cAMP hodnoty řádově 10^{-6} M, buňky jsou vystaveny trvalému stimulu cAMP a dostávají se do stavu absolutní refrakterity. Mají obsazeny všechny receptory, nejsou schopny přijímat signál a ani na něj reagovat. Extracelulární cAMP postupně difunduje k sousedním buňkám nebo je odbouráván extracelulární fosfodiesterasou a jeho koncentrace v okolí buněk klesá. Receptory se stávají znovu citlivými k vnějším podnětům a buňky se pozvolna dostávají opět do excitabilního stavu. Jsou znovu připravené reagovat a vyčkávají na další signál cAMP. Po několika minutách se na receptory naváže další cAMP a cyklus se opakuje.

Výše popsaný mechanismus šíření vln je schematicky znázorněn na obr. 2, kde je postup vlny z hlediska tvaru buněk rozdělen do čtyř fází. Ve fázi A buňky detegují cAMP signál, omezuje se tvorba panožek, buňky se zakulacují a začínají svůj pohybový aparát polarizovat směrem ke zdroji chemoatraktantu. V místech rostoucího gradientu cAMP (fáze B) jsou buňky excitované, protahují se a vykonávají rychlý organizovaný pohyb přímo ke zdroji chemoatraktantu. Zároveň buňka sama produkuje cAMP. Fáze C nastává v místech s nejvyšší koncentrací cAMP (cca 10^{-6} M) a odpovídá počátku refrakterního období. Buňky se zastavují, přestávají vykonávat pohyb ke zdroji cAMP, depolarizují se a začínají opět vytvářet panožky. Ve fázi D gradient cAMP klesá, fosfodiesterasou se postupně odbourává cAMP, receptory se stávají opět aktivními, buňky jsou asymetrické, jakoby rozcuchané, panožky

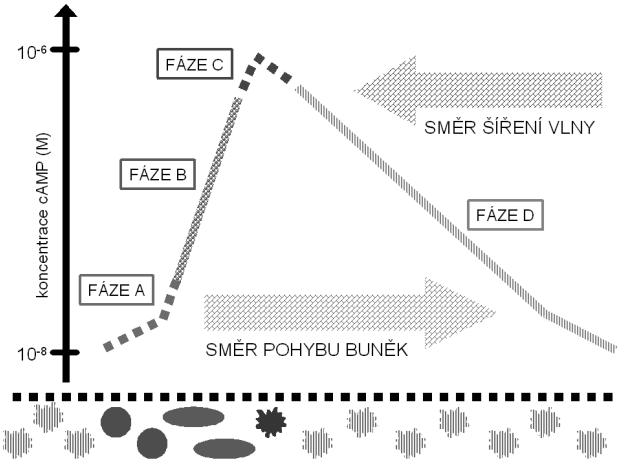

Obr. 2. **Schematické znázornění reakce buněk na přicházející vlnu cAMP**

vyčnívají do všech stran a buňky se pohybují neorganizovaně.

Neorganizovaný migrační pohyb měňavkovitých buněk hlenky se děje náhodně všemi směry rychlostí přibližně 6 μm min^{-1}. Pohyb buněk v přítomnosti gradientu cAMP je orientovaný a děje se ve směru rostoucí koncentrace cAMP. V jeho průběhu se buňka prodlužuje, vytváří dlouhé panožky a pohybuje se řádově rychleji než při pohybu neorganizovaném – rychlostí přibližně 30 μm min^{-1}. Protože je tento pohyb vyvolán přítomností chemické látky v okolí buňky, nazývá se chemotaxí. Během agregace do kupky urazí buňky vzdálenost až 2 cm.

Vrstvou buněk na agaru se šíří kruhové nebo spirálové vlny a to v závislosti na plošné hustotě buněk. Při nižších hustotách se na miskách neobjevují žádné spirály a chemotaktické shlukování je řízeno vysíláním kruhových vln z agregačních center, zatímco při vyšších plošných hustotách dominují na miskách vlny spirálové, vycházející z agregačních center. Spirálové vlny se také mohou tvořit z porušených vln kruhových, a proto je možno během jednoho experimentu pozorovat oba typy vln, nejprve kruhové vlny, které později přecházejí ve vlny spirálové[35].

2. Experimentální studium hlenky *Dictyostelium discoideum*

2.1. Pěstování buněk

Všechny experimenty byly provedeny s axenickým kmenem hlenky *Dictyostelium discoideum* AX2. Buňky byly pěstovány z rozmražených spor (uskladněných při −20 °C) a kultivovány za sterilních podmínek v živném médiu HL5 v temné komoře při teplotě 21 °C za neustálého promíchávání na automatické třepačce. Buňky byly sklízeny v exponenciální fázi růstu.

2.2. Příprava buněk

Suspenze buněk a živného média byla odseparována v centrifuze. K odstředěnému peletu buněk bylo přidáno cca 30 ml fosfátového pufru (14,7 mM KH_2PO_4, 1 mM $Na_2HPO_4 \cdot 12\ H_2O$, pH 6,14), směs byla jemně propláchnuta špičkou pipety a opět vložena do odstředivky. Po dalším promytí byla spočítána koncentrace buněčné suspenze a naředěna fosfátovým pufrem na koncentraci $5 \cdot 10^6$ b/ml. Na jednu Petriho misku (průměr 8,4 cm) s NN−agarem (0,5 % agaru ve fosfátovém pufru, 2 mM kofeinu) bylo naneseno 6,8 ml takto připravené buněčné suspenze. Misky byly ponechány asi 15 min v klidu, během této doby si buňky sedly, a pak byla rychlým otočením misky o 180° slita přebytečná kapalina. Petriho misky byly umístěny do temné komory, kde bylo pozorováno chování buněčné vrstvy.

2.3. Snímání a vyhodnocování experimentů

Základem pro snímání experimentů byl optický přístroj (inverzní mikroskop s fázovým kontrastem nebo makrooptika pro snímání v temném poli), dále kamera a počítač vybavený programem pro obrazovou analýzu Lucia. Misky s buněčnou vrstvou na agaru se začínaly snímat zhruba jednu hodinu od počátku hladovění v časových intervalech 1 min. Celková doba snímání se pohybovala okolo 24 hodin.

Periodický vznik a šíření pulsů cAMP vrstvou buněk byl monitorován pouze nepřímo s využitím tzv. metody temného pole, založené na rozdílných optických vlastnostech buněk v místech s rozdílnými koncentracemi cAMP. cAMP se za přirozených podmínek vrstvou hladovějících agregujících buněk šíří ve formě koncentračních vln. Tyto vlny je možno dosud pozorovat pouze zprostředkovaně optickou metodou temného pole na základě faktu, že buňky vykonávající organizovaný pohyb ke zdroji cAMP mají protáhlý tvar a lámou světelné paprsky pod jiným úhlem než ostatní buňky. Rozdíly v optických hustotách se na snímcích pořízených touto metodou projevují tak, že pohybující se buňky se jeví jako světlé oblasti na tmavém podkladu. S využitím metody založené na izotopovém značení bylo dokázáno[36], že vlny pohybujících se buněk souhlasí s nejvyššími koncentracemi cAMP (10^{-6} M), tedy vlnami cAMP.

2.4. Výsledky experimentálního pozorování vývoje hlenky *Dictyostelium discoideum*

Průběh agregační fáze vývoje hlenky *Dictyostelium discoideum* sledovaný optickou metodou temného pole je zachycen na obr. 3. Několik hodin od počátku hladovění se na snímcích vyskytovala homogenní vrstva buněk. Kolem páté hodiny se na miskách objevovaly první vlny neurčitých tvarů, které se postupně přeměnily v pravidelné spirály. Okolo osmé hodiny se začaly vytvářet hranice teritorií a vrstva se rozpadla na agregační teritoria. V jednotlivých teritoriích se utvořily proudy shlukujících se buněk do

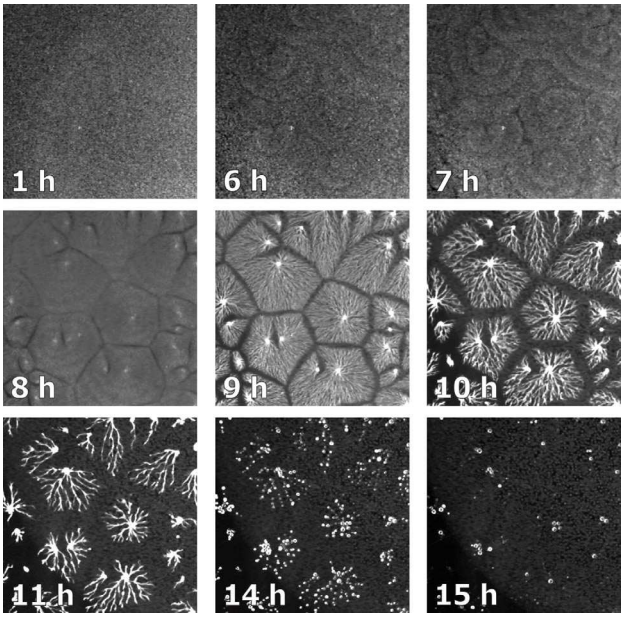

Obr. 3. **Agregační fáze vývojového cyklu hlenky *Dictyostelium discoideum* zaznamenaná technikou temného pole.** V čase 1 h homogenní vrstva hladovějících buněk na agaru, okolo 6 h první vlny cAMP, 7 h pravidelné spirálové vlny cAMP, 8 h rozpad na agregační teritoria, 9–11 h proudy shlukujících se buněk, 15 h kupky, stojící slimáci. Časy uváděny vzhledem k počátku hladovění buněk. Velikost obrázků 1,9 × 1,9 cm

agregačních center. Proudy byly zpočátku velice tenké a dlouhé, ale postupem buněk směrem do centra shlukování mohutněly a krátily se. Zhruba čtrnáct hodin od počátku hladovění byla miska pokryta kupkami, z nichž se většina do 24 h od počátku hladovění přeměnila v houbičky.

Programem Lucia byly obrázky z temného pole upraveny a byly zvýrazněny vlny cAMP (obr. 4). Dále byly vytvořeny časoprostorové grafy a z nich vyhodnoceny parametry šíření vln. Průměrná rychlost šíření vln v čase klesala z počáteční hodnoty 0,31 mm min^{-1} na konečnou 0,17 mm min^{-1}. Perioda šíření vln měla také klesající tendenci, zpočátku se pohybovala kolem 7,3 min a při doznívání vlnění činila asi 4,3 min. Agregační fáze trvala zhruba 3–4 hodiny a ke shromáždění buněk z agregačního teritoria do kupky bylo zapotřebí asi 30 vln.

Na obr. 5 je zachycen vývoj buněk za přirozených podmínek na snímcích z mikroskopu. Po nanesení buněk na agar se vytvořila homogenní vrstva a jednotlivé buňky se pohybovaly náhodně, neorganizovaně, všemi směry. Kolem sedmé hodiny od počátku hladovění se buňky začínaly sdružovat do tenkých řetízků, jejichž spojováním vznikly proudy směřující do agregačního centra. Tento proces trval zhruba do jedenácté hodiny, kdy se vytvořily velké agregáty, které se během dvou hodin rozpadly na kupky. Kupky postupně rostly do výšky a kolem patnácté hodiny se dostaly do stádia stojícího slimáka. Stojící slimáci se skáceli na agar a kolem šestnácté hodiny se po misce pohybovali plazící se slimáci. Kolem dvacáté hodiny se někteří slimáci zastavili a postupně přeměňovali v houbičky. V době 24 hodin od počátku hladovění se vyskytovalo na misce pouze několik houbiček, kolem dvacáté šesté hodiny už byla celá miska pokryta houbičkami a vývojový cyklus byl ukončen.

2.5. Vliv externích stimulů na agregaci hlenky *Dictyostelium discoideum*

Výzkum excitabilního biologického systému hlenky *Dictyostelium discoideum* se v laboratoři Hanky Ševčíkové ubíral několika směry. Velká část výsledků experimentální práce souvisela s vlivem přiloženého elektrického pole na šíření koncentračních vln cAMP během agregační fáze vývoje hlenky[16]. Další oblastí výzkumu byla spolupráce s Ústavem organické chemie a biochemie Akademie věd ČR, kde byly vyvíjeny barevné indikátory cAMP na bázi makrocyklických sloučenin a azopeptidů. Úkolem bylo testovat biokompatibilitu daných látek (organická rozpouštědla[20], pryskyřičné nosiče s navázaným azobarvivem[21], bezfosfátové pufry[22,23]) s buňkami hlenky *Dictyostelium discoideum.*

Dále se skupina Hany Ševčíkové zabývala experimentálním studiem atypické agregace hladovějících buněk *Dictyostelium discoideum* ovlivněných cAMP (cit.[19,37]) a jeho derivátem IPA (cit.[18,37]). Přídavek těchto substancí v různých koncentracích do agaru, nosného substrátu neobsahujícího žádné živiny, na který se nanáší hladové buňky, modifikuje průběh agregační fáze vývoje ve srovnání s průběhem za přirozených podmínek. Navázáním těchto látek na buněčné receptory jsou dosud neobjasněným způsobem vyvolány jiné mechanismy umožňující agregaci a dokončení vývojového cyklu. Dochází tím také

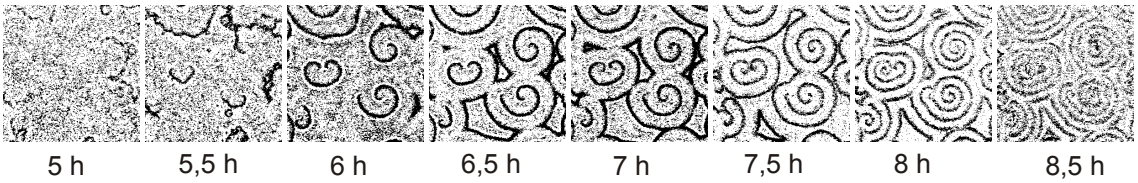

Obr. 4. **Vlny cAMP v průběhu agregační fáze vývoje hlenky.** Snímky pořízené technikou fotografie v temném poli (viz obr. 3) jsou počítačově zpracovány pro získání lepší viditelnosti vln. Časy uváděny vzhledem k počátku hladovění buněk. Velikost obrázků 1,5 × 1,5 cm

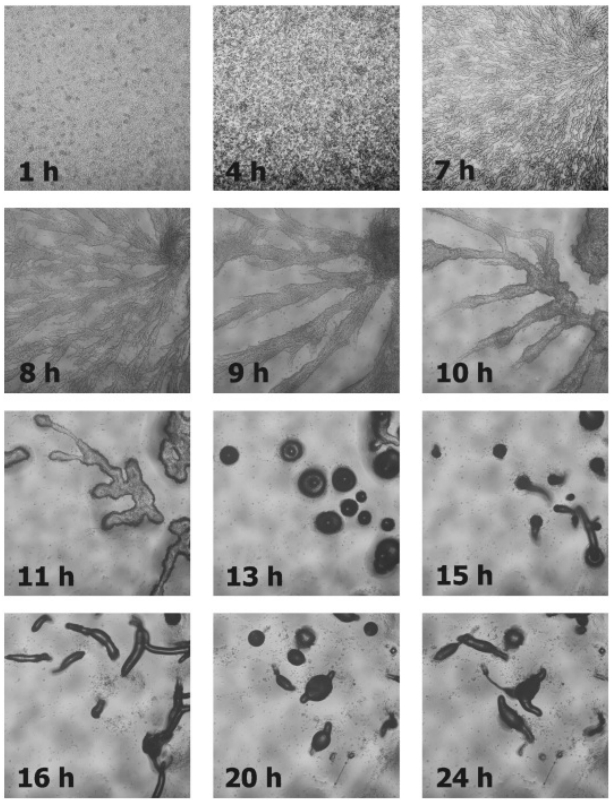

Obr. 5. **Vývoj hlenky *Dictyostelium discoideum* zaznamenaný inverzním mikroskopem s fázovým kontrastem.** V čase 1 h rovnoměrně rozmístěné hladovějící buňky na agaru, od 7 h proudy shlukujících se buněk, 11 h agregáty, 13 h kupky, 15 h stojící slimáci, 16 h plazící se slimáci, 24 h první houbičky. Časy uváděny vzhledem k počátku hladovění buněk. Velikost obrázků 1,75 × 1,75 mm

k ovlivnění excitability, vzniku a šíření koncentračních vln cAMP, chemotaxe, agregace a následného vývoje.

U experimentů s IPA v agaru byla jedním z rozdílů od přirozeného chování tvorba spirálových vln s většími vlnovými délkami. Zatímco za přirozených podmínek se spirálová vlna šíří na ploše několika milimetrů čtverečních (obr. 6A), vlny na agarech obsahujících IPA měly v průměru i několik centimetrů (obr. 6B). Dalším rozdílem bylo netypické druhé vlnění (periodické vysílání malých kruhových vln), které se objevovalo po odeznění spirál, vedoucí k rozpadu buněčné vrstvy na miniteritoria, v nichž se buňky na rozdíl od přirozeného chování shlukovaly atypicky bez tvorby proudů.

Hlavními znaky experimentů s buňkami ovlivněnými cAMP v agaru byly (i) vznik a šíření globální vlny (pro koncentrace cAMP v agaru 0,0625–4,5 mM), (ii) posunutý začátek tvorby excitačních vln (koncentrace menší nebo rovny 1 mM), (iii) vymizení typického cAMP vlnění a netypické shlukování buněk bez tvorby proudů (v koncentračním rozmezí 2–4,5 mM) a (iv) nedokončení vývoje do stádia houbičky (při koncentracích vyšších než 5 mM). Zajímavým poznatkem experimentů s cAMP v agaru byla globální vlna (obr. 6C), která se nikdy neobjevuje u experimentů s přirozenými buňkami. Tato atypická vlna vzniká na misce vždy pouze jedna přibližně ve středu misky a šíří se k okrajům misky přibližně stejnou rychlostí. Čas vzniku globální vlny a rychlost jejího šíření závisí na koncentraci cAMP v agaru. Při nízkých koncentracích cAMP v agaru se globální vlna objevuje dříve a šíří se větší rychlostí než při koncentracích vyšších. Její šíření souvisí s odbouráváním cAMP přidaného do agaru pomocí enzymu fosfodiesterasy.

3. Závěr

Zkoumání průběhu agregační fáze vývoje hlenky *Dictyostelium discoideum* se několik let věnovala Biolaboratoř Ústavu chemického inženýrství VŠCHT Praha založená Ing. Hanou Ševčíkovou, CSc. Na první pohled by se mohlo zdát, že popis dynamického chování hlenky *Dictyostelium discoideum* za přirozených podmínek, i za podmínek pro hlenku v přírodě neobvyklých, s chemickým inženýrstvím nesouvisí, ale ve skutečnosti právě chemicko-inženýrská metodika umožňuje pochopit analogie mezi

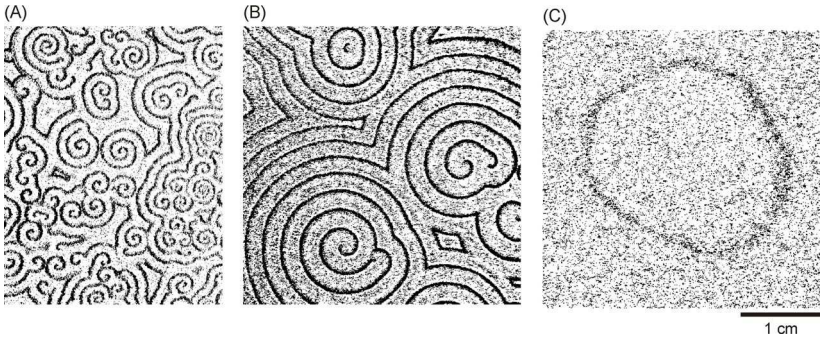

Obr. 6. **Porovnání koncentračních cAMP vln za přirozených podmínek (A) a na agaru s přídavkem 2 mM IPA (B). Globální vlna na agaru s přídavkem 2 mM cAMP (C).** Snímky pořízené technikou fotografie v temném poli počítačově zpracovány pro získání lepší viditelnosti vln

fungováním biologických a chemických systémů.

Studium uvedeného systému zahrnuje stejně jako jiné chemicko-inženýrské práce jak metody experimentální, tak metody matematického modelování. Pro konstrukci experimentálních zařízení se využívají technologie reaktorového inženýrství a pro matematický popis daného systému se aplikují rovnice materiálové bilance. Hojně se uplatňují i základní poznatky o chování autokatalytických reakcí v nemíchaných tenkých vrstvách reakčního média a výsledcích společného působení difuzního transportu složek a autokatalytické reakce.

Hlenka *Dictyostelium discoideum* je intenzivně studovaným mikroorganismem, který prodělává přechod od jednobuněčného organismu k mnohobuněčnému za relativně krátkou dobu. Pro svou jednoduchou stavbu, krátkou regenerační dobu a pro svůj jednoduchý genetický kód je hlenka vhodným modelovým systémem pro studium mnoha biologických pochodů (chemotaxe, cytokineze, signálních transdukčních drah, diferenciace buněk a dalších). Během agregační fáze dochází ke shlukování buněk zprostředkovanému pulzy cAMP, které se šíří vrstvou buněk ve formě koncentračních vln, a proto je agregace hlenky *Dictyostelium discoideum* zkoumána i chemickými inženýry z pohledu nelineární dynamiky.

Hlenka *Dictyostelium discoideum* může posloužit také jako vzor pro inženýry, kteří se snaží navrhnout a vyrobit tzv. chemické roboty[38]. Chemického robota si lze představit jako umělou buňku se schopností autonomního pohybu, látkové výměny, zpracovat absorbované molekuly chemickými reakcemi a cíleně vylučovat produkty. Takovéto inteligentní částice o velikosti v řádu desítek mikrometrů by měly být schopny mezi sebou „komunikovat“ pomocí chemických signálů stejně jako se hlenky dorozumívají pomocí cAMP. Podobně jako hlenky se musí chovat kolektivně, aby přečkaly nepříznivé období, stejně tak je kolektivní chování vyžadováno i u chemických robotů, aby dokázaly vykonat cílovou misi. Mnoho vlastností hlenky *Dictyostelium discoideum* slouží jako zdroj inspirace pro přípravu chemických robotů a ovládat hejna chemických robotů („umělých hlenek“) by našlo uplatnění např. při cíleném doručování a vylučování léčiv.

LITERATURA

1. Ševčíková H., Marek M.: J. Phys. Chem. *88*, 2181 (1984).
2. Ševčíková H., Marek M.: Physica D *39*, 15 (1989).
3. Ševčíková H., Marek M., Muller S. C.: Science *257*, 951 (1992).
4. Kosek J., Ševčíková H., Marek M.: J. Phys. Chem. *99*, 6889 (1995).
5. Ševčíková H., Schreiber I., Marek M.: J. Phys. Chem. *100*, 19153 (1996).
6. Ševčíková H., Kosek J., Marek M.: J. Phys. Chem. *100*, 1666 (1996).
7. Pornprompanya M., Müller S. C., Ševčíková H.: Phys. Chem. Chem. Phys. *4*, 3370 (2002).
8. Pornprompanya M., Müller S. C., Ševčíková H.: Chem. Phys. Lett. *375*, 216 (2003).
9. Ševčíková H., Marek M.: Physica D *13*, 379 (1984).
10. Ševčíková H., Marek M.: J. Phys. Chem. *88*, 2181 (1984).
11. Merkin J. H., Ševčíková H.: Phys. Chem. Chem. Phys *1*, 91 (1999).
12. Forštová L., Ševčíková H., Marek M., Merkin J. H.: Chem. Eng. Sci. *55*, 233 (2000).
13. Forštová L., Ševčíková H., Marek M., Merkin J. H.: J. Phys. Chem. A *104*, 9136 (2000).
14. Forštová L., Ševčíková H., Merkin J. H.: Phys. Chem. Chem. Phys. *4*, 2236 (2002).
15. Lindner J., Ševčíková H., Marek M.: Phys. Rev. E *6304*, 1904 (2001).
16. Šebestíková L., Slámová E., Ševčíková H.: Biophys. Chem. *113*, 269 (2005).
17. Godula T., Ševčíková H., Merkin J. H.: J. Theor. Biol. *240*, 136 (2006).
18. Hilgardt C., Čejková J., Hauser M. J. B., Ševčíková H.: Biophys. Chem. *132*, 9 (2008).
19. Ševčíková H., Čejková J., Krausová L., Přibyl M., Štěpánek F., Marek M.: Physica D *239*, 879 (2010).
20. Čejková J.: Testování biokompatibility organických rozpouštědel s hlenkou *Dictyostelium discoideum.* SVK2004 VŠCHT Praha (2004).
21. Čejková J.: Testování biokompatibility porfyrinů, azobarviv a pryskyřic s hlenkou *Dictyostelium discoideum.* SVK2005 VŠCHT Praha (2005).
22. Pavlík J.: Vliv heterocyklických sulfonových kyselin na agregaci buněk hlenky *Dictyostelium discoideum.* SVK2006 VŠCHT Praha (2006).
23. Šmídová K.: Pozorování buněk *Dictyostelium discoideum* za nestandardních podmínek. SVK2006 VŠCHT Praha (2006).
24. Kessin R. H.: *Dictyostelium: Evolution, Cell Biology, and the Development of Multicellularity.* Cambridge University Press, Cambridge 2001.
25. Annesley S., Fisher P.: Mol. Cell. Biochem. *329*, 73 (2009).
26. Selmeczi D., Li L., Pedersen L.I.I., Nrrelykke S.F., Hagedorn P.H., Mosler S., Larsen N.B., Cox E.C., Flyvbjerg H.: Eur. Phys. J. *157*, 1 (2008).
27. Jin T., Xu X., Fang J., Isik N., Yan J., Brzostowski J.A., Hereld D.: Immunol. Res. *49*, 118 (2009).
28. Rappel W.J., Loomis W. F.: Wiley Interdisciplinary Reviews: Systems Biology and Medicine *1*, 141 (2009).
29. Brown J. M., Firtel R. A.: Dev. Biol. *216*, 426 (1999).
30. Cornillon S., Froquet R., Cosson P.: Eukaryot. Cell *7*, 1600 (2008).
31. Weijer C. J., v: *Systems Biology*, str. 209. Springer, Japan 2009.
32. Fey P., Stephens S., Titus M. A., Chisholm R. L.: J. Cell. Biol. *159*, 1109 (2002).
33. Brazill D. T., Lindsey D. F., Bishop J. D., Gomer R. H.: J. Biol. Chem. *273*, 8161 (1998).
34. Nagano S.: Dev Growth Differ. *42*, 541 (2000).

35. Lee K. J., Cox E. C., Goldstein R. E.: Phys. Rev. Lett. *76*, 1174 (1996).
36. Tomchik K. J., Devreotes P. N.: Science *212*, 443 (1981).
37. Čejková J.: Studium atypické agregace buněk *Dictyostelium discoideum*. Diplomová práce, VŠCHT Praha (2006).
38. www.chobotix.cz, staženo 15.2.2013.

J. Čejková *(Department of Chemical Engineering, Institute of Chemical Technology, Prague):* **Slime Mold *Dictyostelium discoideum* – A Model System Not Only for Biologists**

The slime mould *Dictyostelium discoideum* is an excellent microorganism that allows, as a model system, to study many biological problems, such as chemotaxis, gene expression, adhesion, cell differentiation, cell sorting, multicellular development from single cells, intercellular communication, phagocytosis, motility, programmed cell death and signal transduction. However, the microorganism is also investigated by physicists because of its non-linear dynamic behaviour and pattern formation. These single-celled soil inhabitants are an ideal example for the researchers seeking models of artificial cells and chemical robots or researchers in the swarm robotics field.

LANGMUIR

Article

pubs.acs.org/Langmuir

Evaporation-Induced Pattern Formation of Decanol Droplets

Jitka Čejková,[*,†,‡] František Štěpánek,[‡] and Martin M. Hanczyc[*,†]

[†]Laboratory for Artificial Biology, Centre for Integrative Biology (CIBIO), University of Trento, Via Sommarive 9, I-38123 Povo (TN), Italy

[‡]Department of Chemical Engineering, University of Chemistry and Technology Prague, Technicka 3, Prague 6, 166 28, Czech Republic

Supporting Information

ABSTRACT: Pattern formation in far-from-equilibrium systems is observed in several disciplines including biology, geophysics, and reaction-diffusion chemistry, comprising both living and nonliving systems. We aim to study such nonequilibrium dynamics on the laboratory scale with materials of simple composition. We present a novel system based on a 1-decanol droplet placed in a solution of alkaline decanoate. Previously, we showed the short time scale behavior of this system, which included chemotaxis and maze solving. Here we explore long time scale dynamics of the system (several hours) when open to the environment. We observe dramatic morphological changes in the droplet including long tentacular structures, and we analyze the morphology of these structures at both the macroscopic and microscopic scales across a large range of initial conditions. Such reproducible morphological changes in simple droplets open a path to the exploration of shape-based effects in larger-scale pattern-formation studies.

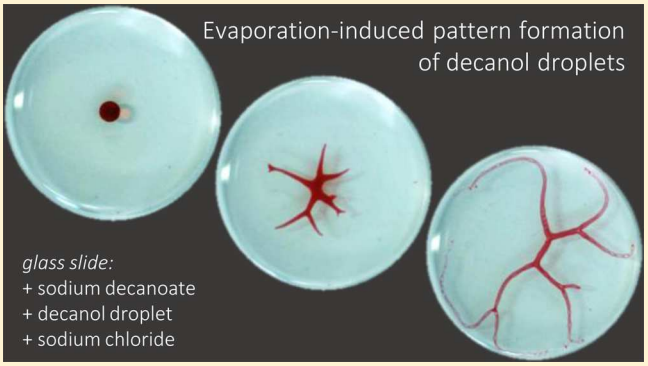

1. INTRODUCTION

In nature, we can observe pattern formation on various spatial and temporal scales; various patterns such as spots, stripes, waves, spirals, and dendrites could appear in both the inanimate word and in biological systems.[1] The spontaneous formation of spatial or spatiotemporal patterns under homogeneous external conditions is a characteristic feature of systems far from equilibrium. Such spontaneous pattern formation is of interest in scientific areas such as hydrodynamics, reaction−diffusion systems, oceanography, meteorology, geophysical and biological morphogenesis, semiconductors, and so forth.

The most familiar patterns observed in the fluid dynamics are Rayleigh−Bénard convection[2] and Taylor vortexes in Taylor−Couette flow.[3] Other well-known examples are patterns formed at interfaces, e.g., snowflakes and ice crystal growth at solid−vapor and solid−liquid interfaces, respectively.[4] Pattern formation in liquid crystals is also studied intensively.[5] Another example of interfacial phenomena is viscous fingering in the Hele−Shaw cell or Saffman−Taylor instabilities.[6] The well-known Belousov−Zhabotinsky reaction−diffusion system[7] displays the famous circular or spiral concentration waves and patterns. Similar patterns are observed in biological systems, for example, in a layer of starving *Dictyostelium* cells.[8,9] The seminal paper by Alan Turing[10] explored how the patterns and structures we observe in nature such as spots and stripes emerge. Although we gave only a few examples of pattern formation, it is obvious that there are plenty of systems where the evolution of patterns in time has been intensively studied both experimentally and theoretically. The present article focuses on a novel type of pattern formation that, to the best of our knowledge, had not been described before.

In our previous work, we have studied the behavior of microliter-sized decanol droplets floating in a thin layer of sodium decanoate solution.[11] We have found that the droplet is able to perform an oriented movement in an externally imposed salt concentration gradient. This phenomenon mimics the chemotaxis of living cells or organisms, which also move directionally in chemical gradients.[12] This observed process is complete within a few minutes. However, in the same system without a macroscopic concentration gradient, we can observe that the decanol droplets undergo intriguing shape changes over much longer time scales. The present article focuses on the pattern formation of decanol droplets in the presence of sodium chloride and sodium decanoate solution that is slowly evaporating under laboratory conditions on the order of hours.

It is known that droplets on solid and liquid surfaces can exhibit complex dynamics as a result of the competition of inertial, viscous, and capillary forces coupled with dynamic surface tension. In oil-in-water systems, several modes of droplet behavior have been defined such as vibrational or fluctuating[13] motion, explosion, stardust or galaxies,[14] blebbing[15] or breathing, and crawling and budding.[16] It has also been shown that droplets

Received: March 18, 2016
Revised: April 26, 2016
Published: April 26, 2016

DOI: 10.1021/acs.langmuir.6b01062
Langmuir 2016, 32, 4800−4805

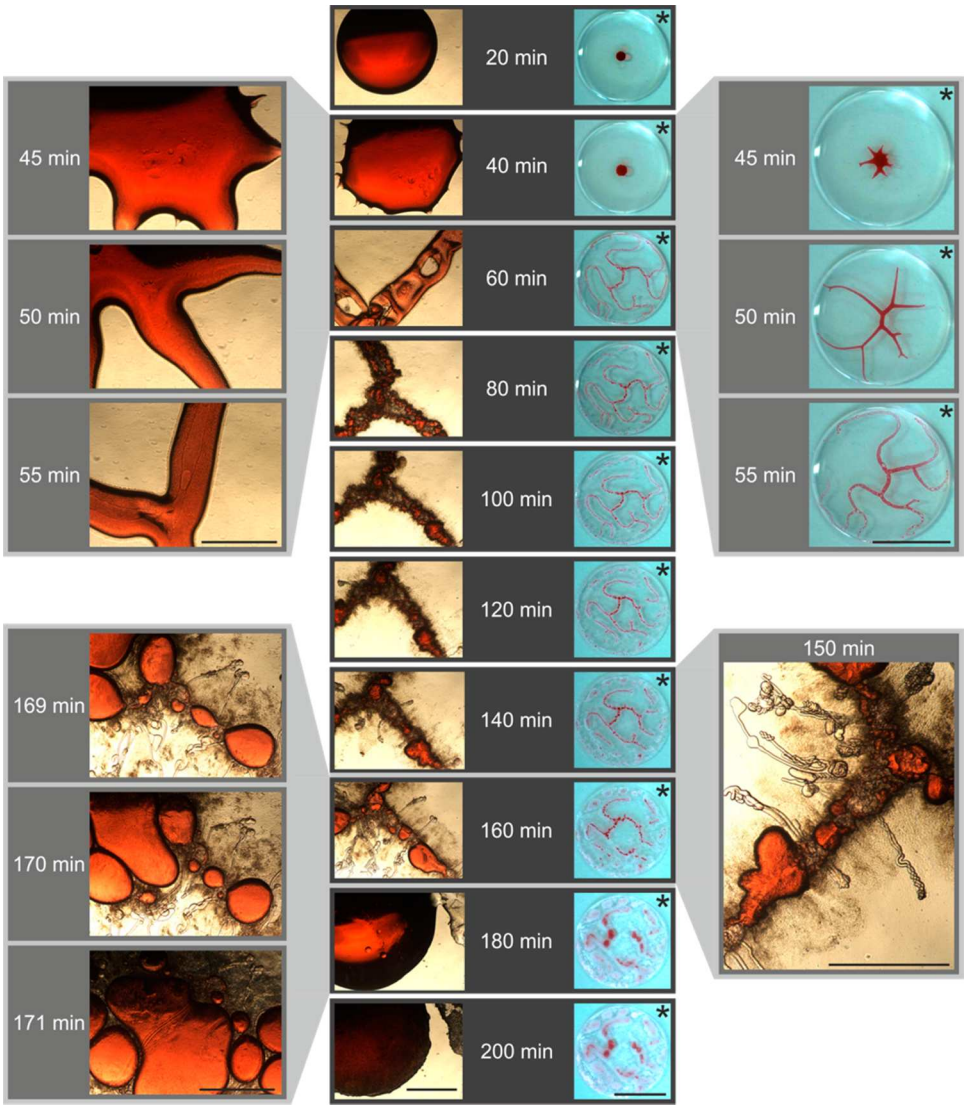

Figure 1. Pattern formation of 2.4 μL decanol droplets on a round cover glass with a diameter of 18 mm. The amount of 10 mM decanoate solution at time $t = 0$ was 250 μL with 1.5 μL of saturated NaCl solution added. Figures marked with an asterisk * were observed on the macroscale, and the scale bar corresponds to 1 cm. Other figures were observed by using an optical microscope, and the scale bars correspond to 1 mm (Supporting Information Movie SM2).

can spontaneously divide or fuse.[17] However, all of these studies focus on droplet shape changes that usually occur on a time scale of milliseconds to minutes. We observe complicated shape change dynamics over the course of several hours in an open system under evaporation.

2. EXPERIMENTAL SECTION

Decanoic acid, 1-decanol, oil red O, sodium hydroxide, and sodium chloride were obtained from Sigma-Aldrich. All chemicals were used without further purification; water was purified by a Millipore Milli-Q system. Sodium decanoate solution was prepared by dissolving decanoic acid in water to a concentration of 10 mM and then using 3 M NaOH to adjust the pH of the resulting solution to 12−13 (the system was not buffered). Sodium chloride solution was prepared at saturation to a final concentration 6.5 M.

The majority of experiments described in the present article were performed as follows (Supporting Information Movie SM1). Aqueous 10 mM decanoate solution (250 μL) was spread over a round cover glass with a diameter of 18 mm. A decanol droplet containing oil red O as a colorant (approximately 2 mg/mL) was placed by a micropipette on the decanoate layer, and then the salt solution was added to the decanoate solution. The amounts of salt and the volumes of decanol droplets were systematically varied as described below. The experiment was performed under laboratory conditions at a temperature of around 23 °C, and the evaporation of water from the decanoate solution occurred as a result of natural convection, i.e., it was not actively controlled. Under these conditions, the complete evaporation of 250 μL of the aqueous phase typically lasted approximately 3.5 h. To inhibit evaporation, we used a partially closed system consisting of a plastic Petri dish with its cover of diameter 10 cm. To enhance evaporation, we applied directional airflow across the system using a hairdryer (Sencor SHS 7551).

The pattern formation of decanol droplets could be clearly seen with the naked eye; however, the experiments were monitored using an ImagingSource video camera (DFK 23U274) from the top view and processed later by the 4.3 version of NIS-Element software (Laboratory Imaging s r.o., Czech Republic). For microscopic observation, an Olympus CK40 microscope with phase contrast was used.

3. RESULTS AND DISCUSSION

When the decanol droplet is placed on the decanoate aqueous surface, it has a round shape, and after approximately 1 min, its diameter decreases. Occasionally, the droplets exhibited a

DOI: 10.1021/acs.langmuir.6b01062
Langmuir 2016, 32, 4800−4805

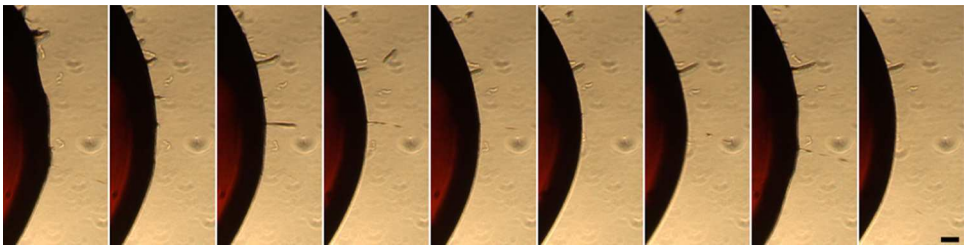

Figure 2. Microscopic image sequence of partial droplet dissolution and the release of small volumes of decanol from droplets about 30 min after the beginning of experiment. The time difference between images is 2 s. Initial conditions: glass slide with a diameter 18 mm, 250 μL of 10 mM decanoate solution, 2.4 μL of decanol, and 1.5 μL of 6.5 M salt. The scale bar corresponds to 100 μm.

Figure 3. Microscopic images of myelin figures formed about 2 h after the beginning of the experiment. Initial conditions: glass slide with a diameter of 18 mm, 250 μL of 10 mM decanoate solution, 2.4 μL of decanol, and 1.5 μL of 6.5 M salt. The scale bars correspond to 100 μm.

pulsatile shrinking/expanding behavior in the first 20 min. We start our measurement after the first 20 min once the size oscillation ceases.

Figure 1 shows an image sequence of pattern formation of a 2.4 μL decanol droplet in 20 min intervals after the addition of 1.5 μL of salt solution (Supporting Information Movie SM2). At the beginning of the experiment, the droplet has a round shape, performs almost no movement, and remains in the middle of the glass slide. At around 40 min from the beginning of the experiment, the first small protrusions on the droplet surface are observable under the microscope (Figure 2). These protrusions bulge and also retract along many points of the droplet circumference. They widely eject small volumes of decanol that detach from the droplet. A few minutes later, several protrusions dominate the others and start to prolong and grow. The droplet adopts a starlike shape with further elongation at the leading edges to form prominent tentacular structures. The tentacles are long and rarely branched. After 1 h, holes appear in the tentacles, with subsequent shrinkage of the tentacles. The tentacles are covered by aggregate structures and eject small amounts of material. After 2 h from the beginning of the experiment, smaller scale protrusions (so-called myelin figures) form from the tentacles often perpendicular to the main tentacle axis that are on the micrometer scale in diameter (up to ca. 30 μm) but can elongate to several millimeters (Figure 3). In addition to standard light microscopy, the myelin figures were imaged by polarized light microscopy, which confirmed their liquid-crystalline nature[18] (Supporting Information Figure 1). Later, when the decanol structures start to swell, the myelin figures shorten and dissolve into the decanol phase. As a result of continuous evaporation of the aqueous phase, small decanol droplets that previously emerged from the disintegration of tentacular structures now coalesce and form larger droplets. After evaporation is complete, the glass slide is covered by dried residues of the myelin structures as well as by other structures including salt crystals and one or several fragments of gelled decanol.

It is known that ionic surfactants exhibit rich phase behavior in saline aqueous solutions. Typically, research on concentration-dependent surfactant/water phases focuses on the equilibrium phase diagrams. The ternary phase equilibria of many amphiphiles in aqueous solutions have been studied in great detail, both experimentally and theoretically. Several papers describing the phase diagrams of decanol−surfactant−water systems have been published, with the surfactants represented by sodium octanoate,[19,20] sodium *N*-lauroylsarcosinate hydrate,[21] dodecyltrimethylammonium with DNA,[22] hexadecyltrimethylammonium bromide,[23] and potassium laurate.[24] All of these works show very complex isothermal phase diagrams from which it is evident that a slight change in the system composition could lead to complicated phase transitions. All of these works focus on equilibrium states; however, the kinetic process through which the nonequilibrium initial state of the pure surfactant and pure water arrives at equilibrium has been subjected to relatively few studies. Several papers describe the process when water is added to the lamellar phase of a surfactant and the so-called myelin figures start to form.[25] In addition, a few papers look at morphological changes in liposomes when the surface area to volume ratio is varied.[26] Evidently, the morphological changes we see are also congruent with an increase in surface area over time.

Here we show that decanol droplets are able to form complex morphological patterns when they are placed on a thin layer of decanoate solution under far-from-equilibrium initial conditions. We performed a systematic mapping of the patterns that formed depending on the initial composition of the system, namely, the molar ratios of decanol, decanoate, and salt. To represent the initial composition in a concise way, we have constructed a triangular diagram, from now on called the initial state diagram, where each point corresponds to a specific molar ratio of decanol, decanoate, and salt in the beginning of the experiment. The number of water molecules was the same in all experiments (each experiment was performed with 250 μL of a 10 mM aqueous solution of decanoate), and thus water is not explicitly shown in this representation. (For more details about the triangular graph

DOI: 10.1021/acs.langmuir.6b01062
Langmuir 2016, 32, 4800−4805

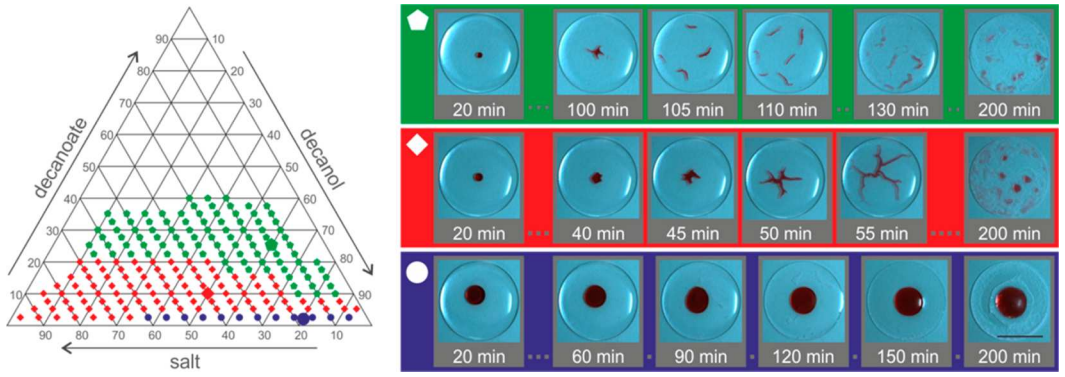

Figure 4. Decanol droplet pattern formation on the cover glass (diameter 18 mm) covered with a thin layer of 250 μL of 10 mM decanoate with varying molar ratios of decanol−decanoate−salt (triangular initial state diagram in the left side). Representative image sequences of three main regimes represented by green pentagons (division), red diamonds (tentacular structures), and blue dots (droplets without extensive morphological patterning) are on the right side. The scale bar corresponds to 1 cm (Supporting Information Movie SM3.)

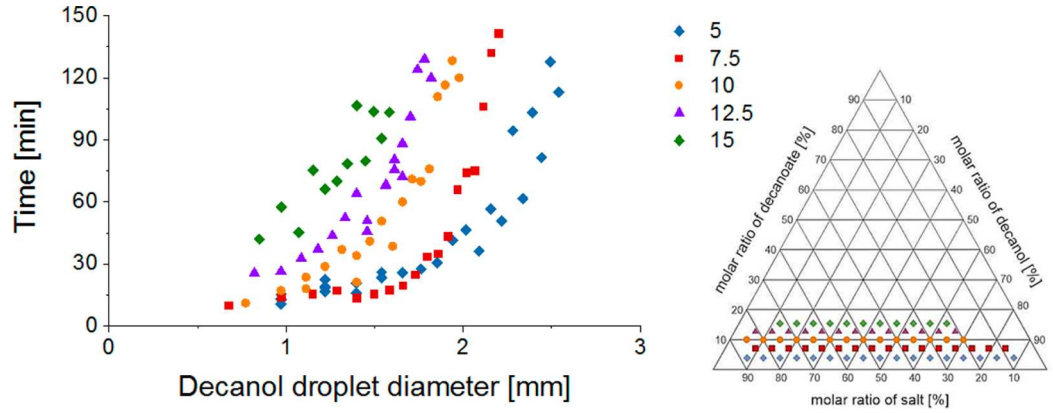

Figure 5. Dependence of time when the first tentacles appear on the decanol droplet diameter for fixed molar ratios of decanoate.

construction, see Supporting Information Figure 2.) Figure 4 shows three main regimes that we have found for this system (Supporting Information Movie SM3). The red diamonds represent the area where decanol droplets behave in the same way as described in Figure 1, with the characteristic formation of tentacles. In the regime depicted by green pentagons, the round droplets start to form small protrusions, but the droplet does not transform into one tentacular structure as in the previous case. Instead, the singular droplet splits into several smaller pieces that maintain an oblong shape. The third type of behavior, observed when the proportion of decanoate in the system is low (represented by blue dots in the graph), is a droplet without tentacle formation. In this situation, no protrusions on the droplet surface appear during the experiment, and the droplet has a round or oval shape and stays in the middle of the glass with minimal movement.

The area in the initial state triangular diagram when droplets form tentacular structures was studied in even more detail. It was found that with increasing size of the droplets, the time for tentacle formation increases in a predictable manner (Supporting Information Movie SM4). Figure 5 shows how the initial time of pattern formation depends on various molar ratios between salt and decanol, whereas the molar ratio of decanoate was constant at 5−15% with a step of 2.5% (corresponding to the cross-section at values of 5, 7.5, 10, 12.5, and 15 for decanoate in the triangular diagram inset in Figure 5). Although experiments were performed without precise control of the experimental conditions (the evaporation conditions changed depending on the conditions in our open-space laboratory), the results show high reproducibility and high predictability of temporal events. In particular, when the decanol droplets start to form tentacles depends on the initial composition of the system. From the graph, it is evident that with the increasing size of decanol droplets (and thus increasing molar ratios between decanol and salt), the time before tentacle formation increases and the lower ratio of decanoate in the system enables earlier pattern formation.

Furthermore, we focused on the final shape of tentacular patterns before their disintegration. We evaluated the number of branches, i.e., the free ends of tentacular structures, and we have found that the droplets form mainly five-branched structures (Figure 6). We suspect that branching is a stochastic process because we have found no systematic dependence of the number of branches on the droplet size or on the composition of the system (Supporting Information Figure 3). We can conclude that three-branched structures are formed only from small droplets (0.5−2.3 μL) and were not observed in the case of larger droplets. To study the branching in more detail, we defined B−N as a ratio between the free ends of tentacular structures and the number of nodes inside the branching structure (Supporting Information Figure 4). Statistically, the most common structures were five-branched with two nodes and four-branched with two nodes.

Although all experiments described in this article were performed on round glass slides, similar behavior and patterning

DOI: 10.1021/acs.langmuir.6b01062
Langmuir 2016, 32, 4800−4805

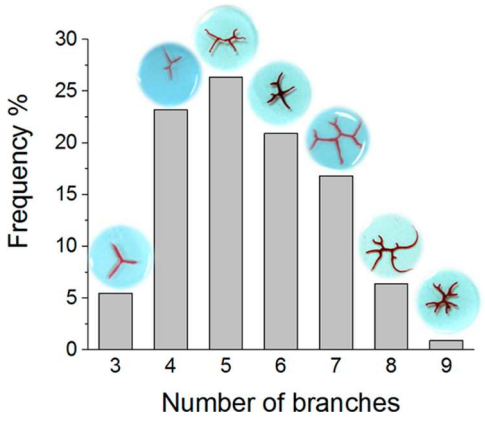

Figure 6. Percentage of droplets in accordance with the number of branches, i.e., free ends of tentacular structures. Evaluated from 220 images.

were observed on semicircular and rectangular cover slides with corresponding surface areas (Supporting Information Figure 5).

All experiments described so far were performed under laboratory conditions and natural convection. However, several reference experiments under accelerated or suppressed water evaporation conditions were also performed in order to assess the effect of the water evaporation rate from decanoate solution on pattern formation. When the evaporation rate was enhanced by applying a constant directional airflow above the glass slide (forced convection), the patterns appeared sooner and had thinner tentacles (Figure 7A). First, tentacular structures appeared about 30 min after the beginning of the experiment and developed very quickly. The experiment was over in approximately 1.5 h, when the glass slide was completely dry. On the contrary, when the glass slide was placed in a Petri dish and covered, evaporation was slowed and the glass slide was completely dry after 30 h. In this case, the start of pattern formation was delayed for several hours, the patterns were different, and no long tentacles were observed (Figure 7B).

Although all experiments described in this article were carried out in the presence of sodium chloride, we have also tested other monovalent salts (specifically, NaBr, NaI, KCl, and KI), and we have found that all of them were able to promote pattern formation that was qualitatively similar to that induced by NaCl. Interestingly, not only salts but also sodium hydroxide was found to induce the tentacular growth of decanol droplets (Supporting Information Figure 6).

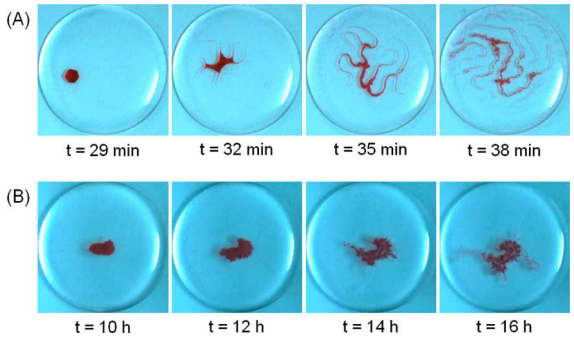

Figure 7. Pattern formation of decanol droplets with a 2.4 μL volume on a round cover glass with diameter 18 mm. The amount of 10 mM decanoate solution at time $t = 0$ was 250 μL with 1.5 μL of saturated salt solution added. (A) Evaporation rate enhanced by applying constant directional airflow. (B) Evaporation slowed by enclosing the glass slide in a covered Petri dish.

Let us note that the initial decanoate concentration was 10 mM, which is under the critical micellar concentration,[27] and the pH of the decanoate solution was between 12 and 13. It is known that the decanoic acid/decanoate system is capable of forming either micelles or vesicles depending on the pH. At high pH, the ionized form dominates and only micelles form.[28] In order to evaluate the role of pH, we also performed experiments with a decanoate solution whose pH was lowered by the addition of HCl to neutral and acidic regions. We have not observed pattern formation in any of these cases, and the droplet remained in the initial circular state.

As a reference, we have also performed experiments without the addition of salt. Such systems have led to the formation of qualitatively different fingerlike branching patterns that share some properties with the well-known Hele-Shaw patterns.[6] However, in Hele-Shaw experiments, fingering occurs when a less viscous fluid displaces a more viscous one confined between two parallel plates. In our case, we place a decanol droplet (more viscous) into thin layer of 10 mM decanoate solution (less viscous), which is opposite to the typical Hele-Shaw experiment. This observation leads us to the hypothesis that during the evaporation of water from the decanoate solution the concentration of decanoate is increasing, reaching and later exceeding its critical micelle concentration (CMC) and thus increasing the viscosity. Originally, a less viscous decanoate solution is converted to a more viscous one, and typical Hele-Shaw fingering can begin. To the best of our knowledge, such an evaporation-controlled Hele-Shaw experiment has not yet been described. The pattern formation of decanol droplets in decanoate without salt is qualitatively different from the patterning in the presence of salt on both macroscopic and microscopic scales, and we will study this problem later separately. For a comparison of decanol droplet pattern formation in the presence and absence of salt, see Supporting Information Movie SM5.

4. CONCLUSIONS

It is well known that numerous open systems in physics (fluids, plasmas, lasers, nonlinear optical devices, and semiconductors), chemistry, and biology (morphogenesis) may spontaneously develop spatial, temporal, or spatiotemporal structures. This report shows patterns formed when a decanol droplet is placed in a slowly evaporating aqueous solution of sodium decanoate in the presence of salt. We have found that some molar ratios of decanol−decanoate−salt lead to the formation of dramatic tentacular structures not described previously. The aim of the present work is to introduce this new phenomenon to the broad scientific community. However, further investigation on the mechanism of pattern formation and an explanatory mathematical model is needed to completely understand this new phenomenon. Because of the very complex nature of the pattern-formation process, experts from various areas can contribute to the explanation of this problem in both experimental and theoretical approaches.

■ ASSOCIATED CONTENT

Supporting Information

The Supporting Information is available free of charge on the ACS Publications website at DOI: 10.1021/acs.langmuir.6b01062.

DOI: 10.1021/acs.langmuir.6b01062
Langmuir 2016, 32, 4800−4805

Links to supporting movies (tentacular pattern formation of decanol droplet, pattern formation in dependence of system composition) and supporting figures (polarized light micrographs of myelin figures, construction of initial state triangular diagram, number of branches of tentacular structures, B-N numbers, patterning on various shaped substrates, pattern formation in presence of other salts) (PDF)

AUTHOR INFORMATION

Corresponding Authors

*E-mail: Jitka.Cejkova@vscht.cz.
*E-mail: Martin.Hanczyc@unitn.it.

Notes

The authors declare no competing financial interest.

ACKNOWLEDGMENTS

This work was financially supported by the European Commission FP7 Future and Emerging Technologies Proactive: 611640 (EVOBLISS), 318671 (MICREAgents), and 318235 (TRUCE).

REFERENCES

(1) Haken, H. *Pattern Formation by Dynamic Systems and Pattern Recognition: Proceedings of the International Symposium on Synergetics*, Schloß Elmau, Bavaria, April 30−May 5, 1979; Springer: Berlin, 2012.

(2) Bodenschatz, E.; Pesch, W.; Ahlers, G. Recent developments in Rayleigh-Bénard convection. *Annu. Rev. Fluid Mech.* **2000**, *32* (1), 709−778.

(3) Fenstermacher, P.; Swinney, H. L.; Gollub, J. Dynamical instabilities and the transition to chaotic Taylor vortex flow. *J. Fluid Mech.* **1979**, *94* (01), 103−128.

(4) Langer, J. Instabilities and pattern formation in crystal growth. *Rev. Mod. Phys.* **1980**, *52* (1), 1.

(5) Buka, A.; Kramer, L. *Pattern Formation in Liquid Crystals*; Springer: New York, 2012.

(6) Saffman, P. G.; Taylor, G. The Penetration of a Fluid into a Porous Medium or Hele-Shaw Cell Containing a More Viscous Liquid. *Proc. R. Soc. London, Ser. A* **1958**, *245* (1242), 312−329.

(7) Zaikin, A.; Zhabotinsky, A. Concentration wave propagation in two-dimensional liquid-phase self-oscillating system. *Nature* **1970**, *225* (5232), 535−537.

(8) Čejková, J. Slime Mold *Dictyostelium discoideum* − A Model System Not Only for Biologists. *Chem. Listy* **2013**, *107*, 563−600.

(9) Hilgardt, C.; Cejkova, J.; Hauser, M. J. B.; Sevcikova, H. Streamless aggregation of *Dictyostelium* in the presence of isopropylidenadenosin. *Biophys. Chem.* **2008**, *132* (1), 9−18.

(10) Turing, A. M. The Chemical Basis of Morphogenesis. *Philos. Trans. R. Soc., B* **1952**, *237* (641), 37−72.

(11) Čejková, J.; Novák, M.; Štěpánek, F.; Hanczyc, M. M. Dynamics of Chemotactic Droplets in Salt Concentration Gradients. *Langmuir* **2014**, *30* (40), 11937−11944.

(12) Čejková, J.; Holler, S.; Quyen, N. T.; Kerrigan, C.; Štěpánek, F.; Hanczyc, M. M. in *Advances in Unconventional Computing*; Adamatzky, A., Ed.; Springer: Berlin, Heidelberg, 2016, pp 261−276.

(13) Horibe, N.; Hanczyc, M. M.; Ikegami, T. Mode Switching and Collective Behavior in Chemical Oil Droplets. *Entropy* **2011**, *13* (3), 709−719.

(14) Gutierrez, J. M. P.; Hinkley, T.; Taylor, J. W.; Yanev, K.; Cronin, L. Evolution of oil droplets in a chemorobotic platform. *Nat. Commun.* **2014**, *5*, 5571.

(15) Sumino, Y.; Kitahata, H.; Seto, H.; Yoshikawa, K. Dynamical blebbing at a droplet interface driven by instability in elastic stress: a novel self-motile system. *Soft Matter* **2011**, *7* (7), 3204−3212.

(16) Song, C.; Moon, J. K.; Lee, K.; Kim, K.; Pak, H. K. Breathing, crawling, budding, and splitting of a liquid droplet under laser heating. *Soft Matter* **2014**, *10* (15), 2679−2684.

(17) Caschera, F.; Rasmussen, S.; Hanczyc, M. M. An Oil Droplet Division−Fusion Cycle. *ChemPlusChem* **2013**, *78* (1), 52−54.

(18) Peddireddy, K.; Kumar, P.; Thutupalli, S.; Herminghaus, S.; Bahr, C. Myelin Structures Formed by Thermotropic Smectic Liquid Crystals. *Langmuir* **2013**, *29* (50), 15682−15688.

(19) Sjöblom, J.; Rosenqvist, K.; Stenius, P. Reversed micellar solutions in the system sodium octanoate/decanol/water: Model calculations and dynamic light scattering measurements. *Colloid Polym. Sci.* **1982**, *260* (1), 82−88.

(20) Friman, R.; Danielsson, I.; Stenius, P. Lamellar mesophase with high contents of water: X-ray investigations of the sodium octanoate-decanol-water system. *J. Colloid Interface Sci.* **1982**, *86* (2), 501−514.

(21) Akter, N.; Radiman, S.; Mohamed, F.; Rahman, I. A.; Reza, M. I. H. Ternary phase behaviour and vesicle formation of a sodium N-lauroylsarcosinate hydrate/1-decanol/water system. *Sci. Rep.* **2011**, *1*, 71.

(22) Bilalov, A.; Leal, C.; Lindman, B. Mixing Oil and Water by a DNA-Based Surfactant. *J. Phys. Chem. B* **2004**, *108* (39), 15408−15414.

(23) Fontell, K.; Khan, A.; Lindström, B.; Maciejewska, D.; Puang-Ngern, S. Phase equilibria and structures in ternary systems of a cationic surfactant (C16 TABr or (C16 TA)2SO4), alcohol, and water. *Colloid Polym. Sci.* **1991**, *269* (7), 727−742.

(24) Berejnov, V.; Cabuil, V.; Perzynski, R.; Raikher, Y. Lyotropic System Potassium Laurate/1-Decanol/Water as a Carrier Medium for a Ferronematic Liquid Crystal: Phase Diagram Study. *J. Phys. Chem. B* **1998**, *102* (37), 7132−7138.

(25) Zou, L.-N.; Nagel, S. R. Stability and Growth of Single Myelin Figures. *Phys. Rev. Lett.* **2006**, *96* (13), 138301.

(26) Peterlin, P.; Arrigler, V.; Kogej, K.; Svetina, S.; Walde, P. Growth and shape transformations of giant phospholipid vesicles upon interaction with an aqueous oleic acid suspension. *Chem. Phys. Lipids* **2009**, *159* (2), 67−76.

(27) Namani, T.; Walde, P. From Decanoate Micelles to Decanoic Acid/Dodecylbenzenesulfonate Vesicles. *Langmuir* **2005**, *21* (14), 6210−6219.

(28) Morigaki, K.; Walde, P.; Misran, M.; Robinson, B. H. Thermodynamic and kinetic stability. Properties of micelles and vesicles formed by the decanoic acid/decanoate system. *Colloids Surf., A* **2003**, *213* (1), 37−44.

DOI: 10.1021/acs.langmuir.6b01062
Langmuir 2016, 32, 4800−4805

Colloids and Surfaces A 566 (2019) 141–

Contents lists available at ScienceDirect

Colloids and Surfaces A

journal homepage: www.elsevier.com/locate/colsurfa

Dancing performance of organic droplets in aqueous surfactant solutions

Jitka Čejková[a,*], Karin Schwarzenberger[b], Kerstin Eckert[b,c], Shinpei Tanaka[d]

[a] University of Chemistry and Technology Prague, Prague, 166 28, Czechia
[b] Helmholtz-Zentrum Dresden-Rossendorf, Dresden, 01328, Germany
[c] TU Dresden, Dresden, 01062, Germany
[d] Hiroshima University, Higashi-Hiroshima, 739-8521, Japan

GRAPHICAL ABSTRACT

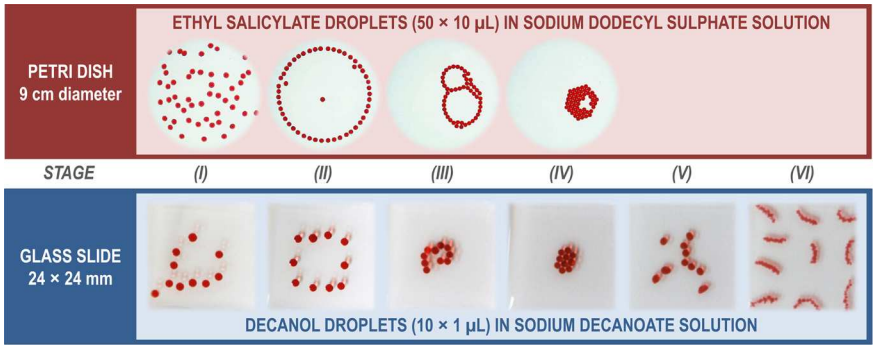

ARTICLE INFO

Keywords:
Droplet
Surfactant
Collective behaviour
Interaction
Artificial life

ABSTRACT

Droplet systems remain the subject of a constant fascination in science and technology. Here we focus on organic droplets floating on the surface of aqueous surfactant solutions. These droplets can exhibit intriguing interactions. Recently we have found independently in two laboratories that we can observe almost the same complex collective behaviour in two different droplet systems. The aim of this paper is to compare both droplets systems, present their differences and show their similar oscillatory behaviour. The first system consists of decanol droplets floating on a sodium decanoate solution. In the second one, the droplets consist of a mixture of ethyl salicylate and liquid paraffin and they are placed on the surface of an aqueous sodium dodecyl sulphate solution. Although the mechanism of these spatio-temporal interactions of droplets is not fully understood yet, we believe that this behaviour is based on the same phenomena.

1. Introduction

Liquid droplets are present in our everyday life. They seem to be so simple objects, nevertheless they can exhibit fascinating phenomena. Some phenomena can be observed by naked eye, some are visible only by using special optical techniques. Some processes can attract our attention in the real time, however some phenomena become pronounced only when the speed of a recorded movie is changed. One example is the impact of a rain droplet on a solid surface [1] – in the real time nobody can see the beauty of the bouncing, spreading and splashing of the droplet as visible by a high speed camera. On the other hand there are many processes that are very slow and in real time the system looks almost static. In this case, playing a recorded movie in fast motion can reveal interesting behaviour. One example can be the shape change of

* Corresponding author.
E-mail address: jitka.cejkova@vscht.cz (J. Čejková).

https://doi.org/10.1016/j.colsurfa.2019.01.027
Received 15 November 2018; Received in revised form 3 January 2019; Accepted 14 January 2019
Available online 15 January 2019
0927-7757/

decanol droplets forming multi-armed structures [2,3]. A further example, namely the dancing of groups of droplets, will be presented in this paper.

The research on droplets is intensive from various points of view, on various spatial and temporal scales. The knowledge of interfacial phenomena at droplets is important for many problems in industry, agriculture, medicine and other areas. Recently, droplet studies also became popular in artificial life research. Whereas biology studies the composition, behaviour and interactions of living cells and organisms (representing *life as we know it*), the artificial life focuses on artificially made systems with life-like properties. In our case we study purely chemical droplet systems (representing *life as it could be*) [4]. Recently we have proposed to use the term "liquid robots" for droplets mimicking the behaviour of living cells or small organisms [5]. It has been shown that organic droplets with a volume of a few microliters floating on aqueous surfactant solutions can exhibit life-like phenomena such as self-propulsion [6–10], sensing of chemical signals and responding to them by chemotactic movement [11,12] or by shape changes [2,3]. The liquid robots can serve as transporters of small objects or chemicals ("chemo-taxi" [13]) even in complex environments such as mazes [14]. However, only few works focus on interactions between multiple droplets [15–19].

We can distinguish two categories of experiments: droplets that are crawling on solid substrates and droplets that are floating on the surface of another liquid or swimming in another liquid. Regarding droplet interactions on dry solid substrates, it has been reported [18] that miscible liquids such as propylene glycol and water deposited on a clean glass cause a motion of neighbouring droplets over a certain distance. These droplets are subject to evaporation-induced surface tension gradients and they move in response to the vapour emitted by neighbouring droplets. The vapour-induced interactions were also described for water droplets, containing a volatile fluid, that were floating on silicone oil [20]. In systems where oil droplets were floating in an aqueous pool, various mechanisms were described for the mutual attraction or repulsion of the droplets. In systems containing surfactant, surface tension gradients and Marangoni flows are usually responsible for droplets interactions [21]. In some droplet systems the so-called "Cheerios effect" plays a central role [22]. Like cereals floating on a liquid surface are attracted because of interfacial deformation and the effect of gravity, liquid droplets can be similarly attracted or repelled [23]. Although some works focus on the interactions between two droplets [17], only few papers deal with large populations of droplets and their swarming [19].

Recently, we have observed that droplets, consisting of a mixture of ethyl salicylate (ES) and paraffin liquid, floating on the surface of an aqueous sodium dodecyl sulphate solution (SDS) in a Petri dish (covered by a lid), exhibit collective behaviour that can be divided into four stages: the random motion state (stage I), the ring structure state (stage II), the cluster oscillation state (stage III), and the final static state (stage IV) [15,24]. Another system (here called D system) consisting of decanol droplets floating on a sodium decanoate solution [25,26] on microscopic slides (system open to the environment) has shown a qualitatively similar behaviour. Moreover, because of water evaporation from the system, we can observe two more stages, namely (V) disintegration of the cluster and separation of the droplets and (VI) shape changes of the droplets [2,3]. Although both systems differ in several parameters, we think that the phenomena observed should be based on the same principles. The present work aims to compare the dynamics during the whole experiments in both systems, especially focussing on the fascinating oscillating behaviour of droplets in a cluster.

2. Experimental

2.1. Chemicals

The ES system consisted of droplets of ethyl salicylate (ES, Tokyo Chemical Industry, Tokyo) that contained 30–90 wt% of paraffin liquid (Sigma-Aldrich, Tokyo). The droplets were dyed with 0.005 wt% Oil red O (Nakarai tesque, Tokyo). The concentration of the aqueous sodium dodecyl sulfate (SDS, Tokyo Chemical Industry) solution was fixed at 35 mM (pH ≈ 7). The chemicals were used as supplied.

The D system was based on the same chemistry as described in our previous work on single decanol droplet chemotaxis [12] and pattern formation [3], *i.e.* a 10 mM sodium decanoate solution in water as the continuous phase, and decanol droplets coloured with Oil red O (approximately 0.2 wt%) as the disperse phase. The sodium decanoate solution was prepared by dissolving decanoic acid at a concentration of 10 mM in water using 3 M NaOH to raise the pH of the resulting solution, typically around 12. All chemicals were purchased from Sigma-Aldrich (Czechia) and used without further purification. Deionised water was produced using an ionex filter (Aqual 25, Czechia).

2.2. Experimental procedure

The experiments with the ES system were performed on glass Petri dishes with a diameter of 86 mm (Schott/Duran, Japan). The volume of the aqueous solution was 30 mL and the volume of each droplet was 10 µL. The standard experiments with the D system were performed on microscopic cover slips with dimensions of 24 × 24 mm (P-Lab, Czechia). The glass slide was covered with a thin layer of 10 mM sodium decanoate solution (0.75 mL). Systematically varying numbers of decanol droplets (5, 6, 7 and 10) with a volume of each droplet of 1 µL were added by means of an electronic micropipette and the droplet behaviour in time was recorded.

2.3. Observation technique

The experiments were monitored using a camera from the top view. An ImagingSource video-camera (DFK 23U274) was used for the D system and a CMOS camera (L-835, Hozan, Osaka) for the ES system. The moment of adding the last droplet to the aqueous solution was taken as time t = 0.

2.4. Particle image velocimetry

To study the flow field during the dynamical evolution of the droplets, the standard experiments with the D system were repeated in a microscopic particle image velocimetry (microPIV) setup. For this purpose, fluorescent polystyrene particles (microParticles GmbH, Berlin, Germany) were suspended in the 10 mM decanoate solution as PIV tracers moving with the fluid flow. These highly monodisperse particles with a size of 7 µm are buoyantly neutral for dilute aqueous solutions due to their density of 1.05 g/cm^3. The whole measurement volume is illuminated by a Nd-YLF laser (Photonics Industries, Ronkonkoma, USA). The fluorescent tracer particles are excited by the laser light (wavelength λ_{ex} = 527 nm) and emit light with a wavelength of λ_{em} = 607 nm. An optical long-pass filter cuts off the laser light and transmits the fluorescent light with longer wavelength. By this, the background scatter light is separated from the particle signal.

The recording optics was built of a Zeiss Stereo Discovery.V8 microscope with PlanApo S 1.0× objective, used at 4.0× zoom level. The resulting field of view amounts to 4.2 mm × 2.6 mm. This high magnification is necessary to obtain a sufficiently small depth of field (0.12 mm for these settings) accounting for the high vertical velocity gradients along the small liquid layer height. Due to the limited field of view, the number of 1 µl decanol droplets was reduced to 3 in the microPIV experiments. To capture the flow field in the fluid layer

Table 1
Comparison of droplets in D and ES systems.

	D system 1-Decanol	ES system Ethyl salicylate
Chemical formula	$C_{10}H_{21}OH$	$C_9H_{10}O_3$
Molar mass	158.28 g/mol	166.17 g/mol
Density	0.825 g/cm^3 (at 25 °C) [27]	1.131 g/cm^3 [28] [a]
Solubility in water [29]	0.021 wt% (at 29.6 °C)	0.037 wt% (at 29.8 °C)
Viscosity	11.8 mPa s (at 25 °C) [27]	2.831 mPa s (at 25 °C) [28]
Interfacial tension against water	8.97 mN/m (at 20 °C)	44.3 mN/m
Concentration	100 % (w/w)	70 % (w/w) [15], 60–90% (w/w) [24]
Colorant	Oil red O	Oil red O

[a] Density was 1.04 g/ml at 70 wt% and 1.07 g/ml at 80 wt%.

directly below the surface of the aqueous solution, the focal plane was approached to the liquid layer from above until the first particles came into focus. The movement of the tracer particles was recorded by a Phantom VEO 410 L camera (1280 × 800 pix) operated at 24 Hz. The tracer records were evaluated with the software DaVis 8.4 (LaVision, Göttingen, Germany). The underlying PIV algorithm calculated velocity vectors in discrete interrogation windows from the cross-correlation of two consecutive images.

3. Results

3.1. Comparison of droplet systems

3.1.1. Differences

The properties of the main droplet components in the D and ES systems are summarized in Table 1. In the D system, the droplets consist only of 1-decanol. Decanol is lighter than the aqueous phase, so the droplets are floating on the surface. For the experiments, glass slides were used which are covered by the aqueous solution. Due to the pinning of the aqueous solution at the edges of the glass slide, a convex meniscus formed so that the decanol droplets did not move to the very boundary of the slide. When Petri dishes were used for the D system, the decanol droplets often went to the glass wall because of gravity effects at the concave meniscus (see Fig. 1A). The concave (resp. convex) meniscus of the aqueous solution leads to differences in the potential energy of the floating droplets at different height levels of the surface. In the ES system the droplets are a mixture of liquid paraffin and ethyl salicylate (ES). ES is heavier than the aqueous SDS solution, so the droplets hang on the aqueous surface due to the balance of surface tension forces and gravity. In the presence of small disturbances, it can happen that droplets fall down to the bottom. Once submerged, the droplets stop moving. To reduce the density, ES was mixed with liquid paraffin. Moreover, glass Petri dishes with a concave meniscus of the aqueous solution are used for the ES system, so droplets heavier than the aqueous phase are not attracted by the dish wall. On the other hand, when experiments with the ES system were performed on microscopic glass slides as in the experiments with the D system, the droplets went to the boundary of the glass substrate (see Fig. 1B).

In the D system the aqueous pool consists of 10 mM sodium decanoate solution. This solution is initially bellow critical micellar concentration (CMC). The ES system was studied with various concentrations of SDS, nevertheless always above CMC. Table 2 below summarizes the main properties of the anionic surfactants used in both D and ES systems.

A further difference is due to the evaporation of water from the aqueous phase. The dishes with the ES system were covered by glass lids (without tight sealing), whereas the D system was open to the environment. In the D system it took 10 h until the evaporation of water from 1 mL of decanoate solution was completed, *i.e.* the rate of evaporation was approximately 0.1 mL per hour (the evaporation plays a role mainly in the final stages). In the covered ES system water evaporation was very slow and its effect was negligible.

Because of the spatial scale of the experiments and probably also because of the differences in the material parameters, the time scale of the observed phenomena was different. In real time observations of the ES system no movement of the droplets was immediately noticeable in the stage III, whereas in the D system the dynamical behaviour was obvious already in the real time observation.

3.1.2. Similarity

Although the experiments with D and ES systems seem to be different, as described above, the behaviour of groups of droplets is surprisingly very similar and not yet understood in full detail. One of the most fascinating phenomena observed in both systems is the oscillating behaviour of droplets in a cluster. The repulsion of droplets from the cluster followed by their return into one group seems to be based on the same principles. Further the behaviour during the whole experiments in both systems will be described.

3.2. Dynamic oscillatory cluster ordering

3.2.1. ES system in Petri dishes

In the ES system we can divide the entire clustering process into four stages: the random motion state (stage I), the ring structure state (stage II), the cluster oscillation state (stage III), and the final static state (stage IV). The duration of each stage depends on the conditions such as ES or SDS concentration or the number of droplets. It typically takes 1–2 h for the stage III to appear. Then it sometimes persists for more than a day [24].

Fig. 2 shows an example of these four stages. Characteristic dynamics are observed in stage II and III. In stage II, droplets form a chain concentric to the dish wall. Within the ring, individual droplets oscillate

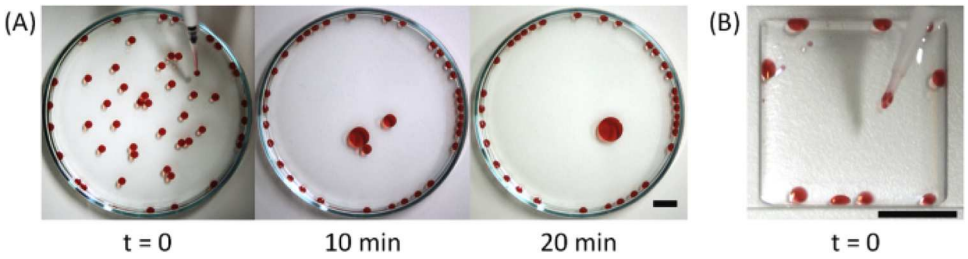

Fig. 1. The effect of the aqueous phase meniscus on the initial distribution of droplets. (A) Petri dish with a diameter of 86 mm filled by 30 mL of 10 mM sodium decanoate solution, 50 decanol droplets with a volume of 10 µL each, scale bar 10 mm. (B) Microscopic glass slide with a size of 24 × 24 mm covered by 1 mL of 35 mM SDS solution, 10 droplets consisting of a mixture of ES and paraffin (1 µL each), scale bar 10 mm.

Table 2
Comparison of continuous phase in D and ES systems.

	D system Sodium decanoate	ES system Sodium dodecyl sulphate
Concentration	10 mM	35 mM [15], 28–69 mM [24]
Surface tension	65 mN/M for 10 mM [12]	37.14 mN/m for 70 mM [9]
pH	11–12	7
Critical micelle concentration (CMC)	80–110 mM [30]	8.08–8.2 mM [31]

between the neighbouring droplets. This ring structure collapses into an oscillating chain structure in stage III. Thereby, the droplets are continuously forming and deforming chains, resulting in an oscillation of the whole structure.

3.2.2. D system on microscopic slides

Qualitatively similar behaviour is observed in the D system so that we can define four initial stages comparable to the ES system. Additionally, because of the evaporation of water from the system, we can observe two more stages, namely disintegration of the cluster and separation of droplets (stage V) and shape changes of droplets (stage VI). The duration of the individual stages (I)–(VI) depends on the initial conditions and on the evaporation rate.

Fig. 3 shows an example of a typical image sequence from the beginning of the experiment until the moment when water was evaporated completely from the D system (see also Supplementary movie 1). At the beginning the droplets were dispersed randomly (stage I). Then they arranged regularly in a small square in the middle of the glass slide (stage II). Few minutes after, the droplets entered into stage III and exhibited a dynamical behaviour. Although they formed a single cluster, they repelled and attracted each other in this group, they exchanged their positions and they did not remain static for a long time. Such a behaviour is qualitatively comparable to stage (III) of the ES system. Around 40 min after the beginning of the experiment, the droplets created a close-packed cluster and further kept their position in this arrangement. The cluster was more or less static. The same behaviour is observed in the ES system as stage (IV). Around 3 h after the beginning of an experiment, some droplets started to escape from the cluster, they repelled each other and the cluster disintegrated (stage V). Then the droplets started to change their shape – from round shaped droplets to elongated worm-like structures. This process in the D system is named stage (VI). The experiment was over when all water evaporated from the system, *i.e.* approximately in 7.5 h. In the end the glass slide was covered by the leftovers of non-volatile residues.

Although the groups of decanol droplets in the D system exhibit interesting complex behaviour during the process of water evaporation from their environment (stages I–VI), we further will focus just on the stages I—IV of the process and compare the behaviour with low number of droplets in the ES system.

3.3. Oscillatory behaviour of low number of droplets

Fig. 4A shows how a chain of six droplets in the ES system oscillated as a cluster. At first, a droplet at the centre of the chain was pushed out of the chain (a–b). The droplet was then attracted by one chain end and attached to it (c–d). Then another droplet at the centre of the chain was pushed out of the chain and attracted by a chain end. This process repeated itself, so that the droplets looked to be juggled continuously. This mode of motion could be seen both in shorter (5 droplets) and longer chains (10–20 droplets). When the droplets form even larger clusters, the motion becomes more complicated (see illustrative example in Fig. 2).

Supplementary movie 2 shows the oscillatory phase in experiments with 5 × 1 µL, 6 × 1 µL and 7 × 1 µL droplets floating on 1000 µL of 10 mM decanoate solution. We performed 10 repeated runs of each experiment indicating a high reproducibility and also showing the similarities in oscillation behaviour. Fig. 4B shows an example how droplets exchanged their positions in the chain during the oscillatory phase in the D system. Such rotations of triplets in the end of chain were observed frequently and are very similar to the juggling of droplets in the ES system.

3.4. Flow visualization by particle image velocimetry

In experiments aiming to observe the flow structure in the decanoate solution fluorescent polystyrene particles with a diameter of 7 µm were suspended as PIV tracers. Then three 1 µL decanol droplets (without any colorant) were placed by a Hamilton syringe on top of the decanoate solution.

Fig. 5 shows PIV images at three different times in the experiment with the D system. The first image (A), corresponding to stage (II), was taken at t = 6 min, where the three droplets were widely separated from each other (only one droplet is visible in the field of view). A radial flow away from the decanol droplet can be observed in the fluid layer near the surface. This flow is due to surface tension gradients caused by the dissolution of a small amount of decanol from the droplet, *i.e.* a solutal Marangoni flow. For this system, a strong decrease of surface tension with decanol concentration was measured in [12], confirming the Marangoni effect as the origin of the flow. Thereby, the drop acts as a source of surface-active material so that the flow is directed to the surrounding regions with higher surface tension.

The second image (Fig. 5B) depicts two droplets during the transition to stage (III) at a time t = 20 min. Here, the droplets repeatedly approached each other and diverged again in the field of view. Due to the low number of droplets, no pronounced oscillations of a whole cluster were obtained. However, the oscillatory movement of the droplets also provides information on the cluster dynamics. The average of the velocity magnitude over all PIV vectors in the field of view is plotted in Fig. 5(D) (blue diamonds) together with the distance between both droplets (orange circles) in a time frame around 22 min (1320 s–1372 s). This graph indicates that the movement of the droplets to and from each other is correlated to the magnitude of the Marangoni

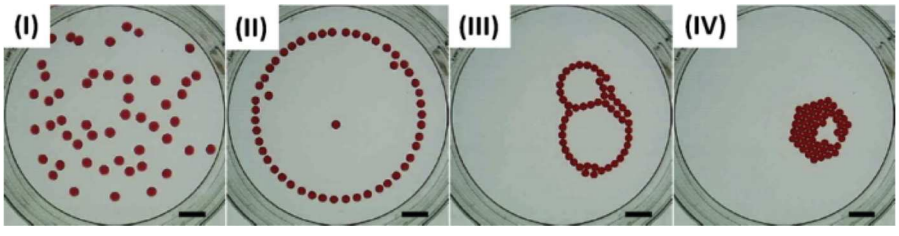

Fig. 2. Modes of droplets motion in the ES system of N = 50. (I) Random, intermittent motion. (II) Ring of droplets where droplets vibrate between others. (III) Characteristic cluster oscillation. (IV) Final static crystal. The scale bar is 10 mm [15].

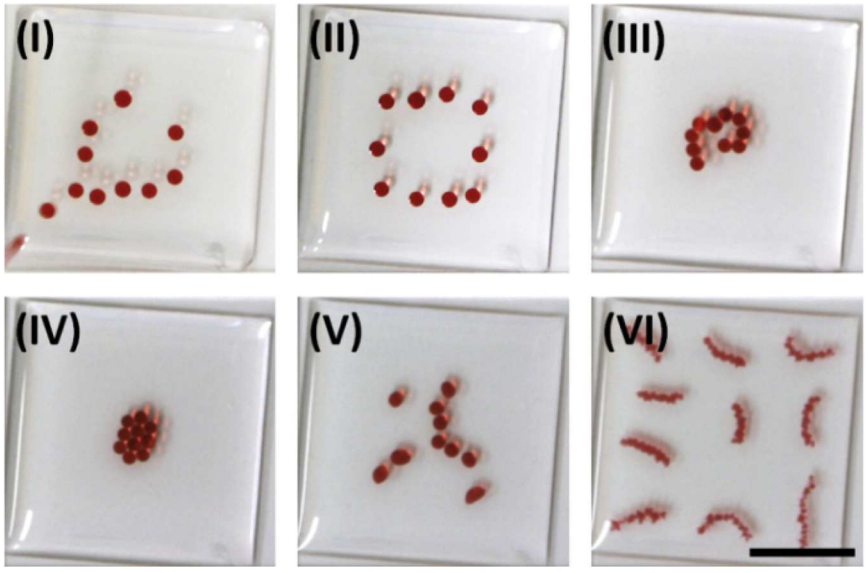

Fig. 3. Modes of droplets motion in the D system of N = 10. (I) Random motion. (II) Regularly ordered square of droplets. (III) Characteristic cluster oscillation. (IV) Static crystal. (V) Cluster disintegration. (VI) Shape changes of decanol droplets. The scale bar is 10 mm. (See Supplementary movie 1).

flow. Note that the distance data (orange curve) is plotted inversely (see second vertical axis) to make the visual comparison between both curves easier: When the two droplets approach, the distance decreases and the velocity increases, *i.e.* both curves rise. It can be seen from this plot that the distance curve is leading (starts to rise and to decrease a bit earlier). When the droplets approach each other, they act as a common, larger source of surfactant. This enhances the surface tension difference to the surrounding, resulting in a stronger Marangoni flow. The same effect can be noted by comparing the velocity fields at the different stages in Fig. 5A–C, where the velocity magnitude likewise increases with the cluster formation.

In the third velocity field at t = 34 min (see Fig. 5C), the three droplets were clustered and stayed together for the rest of the recording (another 10 min) which is characteristic for stage (IV). Fig. 5E displays the average velocity in the field of view during a time span of 100 s (2250 s–2350 s) where no pronounced motion of the droplets occurred. The position of the droplets at 2250 and 2350s is almost identical. Although only two droplets are captured in the field of view at this time, the static cluster of three droplets still is preserved as verified by visual inspection. This plot shows that the Marangoni velocity slightly decreases with time since the system slowly approaches equilibrium. The red dotted curve is smoothed (moving average over 10 s) to illustrate this trend more clearly.

Even in this static cluster, the magnitude of convection is not constant but prone to strong oscillations. Repeated decay and re-amplification is a known phenomenon of solutal Marangoni convection. It can be caused by the re-distribution of adsorbed surfactant by the convection [32] or the temporary consumption of driving concentration gradients by the local convective mixing [33]. Such effects can contribute to the complex dynamics observed at the droplets.

4. Discussion

We have observed and compared intriguing phenomena in groups of simple organic droplets in two different systems, namely time-dependent spontaneous cluster formation of originally solitary distributed droplets and their oscillatory behaviour. The two systems were compared – decanol droplets in decanoate solution (D system) and ethyl salicylate droplets mixed with paraffin in sodium dodecyl sulphate solution (ES system). In both systems the surface tension forces are comparable to gravitational forces because the Bond number is of the order of one ($Bo = \Delta\rho\, g\, L^2/\sigma$ Bo= $\Delta\rho\, g\, L^2/\sigma$, where $\Delta\rho$ is the difference in density of the two phases, g gravitational acceleration, L the characteristic length, *i.e.* droplet diameter and σ surface tension). For 1 µL

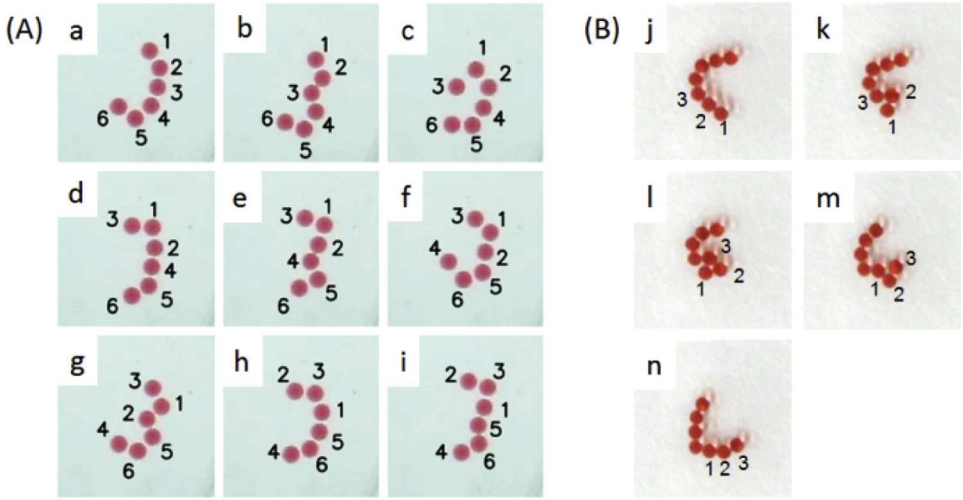

Fig. 4. (A) Dynamic states of a cluster consisting of six ES droplets (the volume of each droplet was 10 µL). The elapsed time from the first picture was: (a) 0 s, (b) 40 s, (c) 60 s, (d) 90 s, (e) 120 s, (f) 150 s, (g) 180 s, (h) 210 s, and (i) 240 s. (B) Dynamic states of a cluster consisting of six decanol droplets (the volume of each droplet was 1 µL).

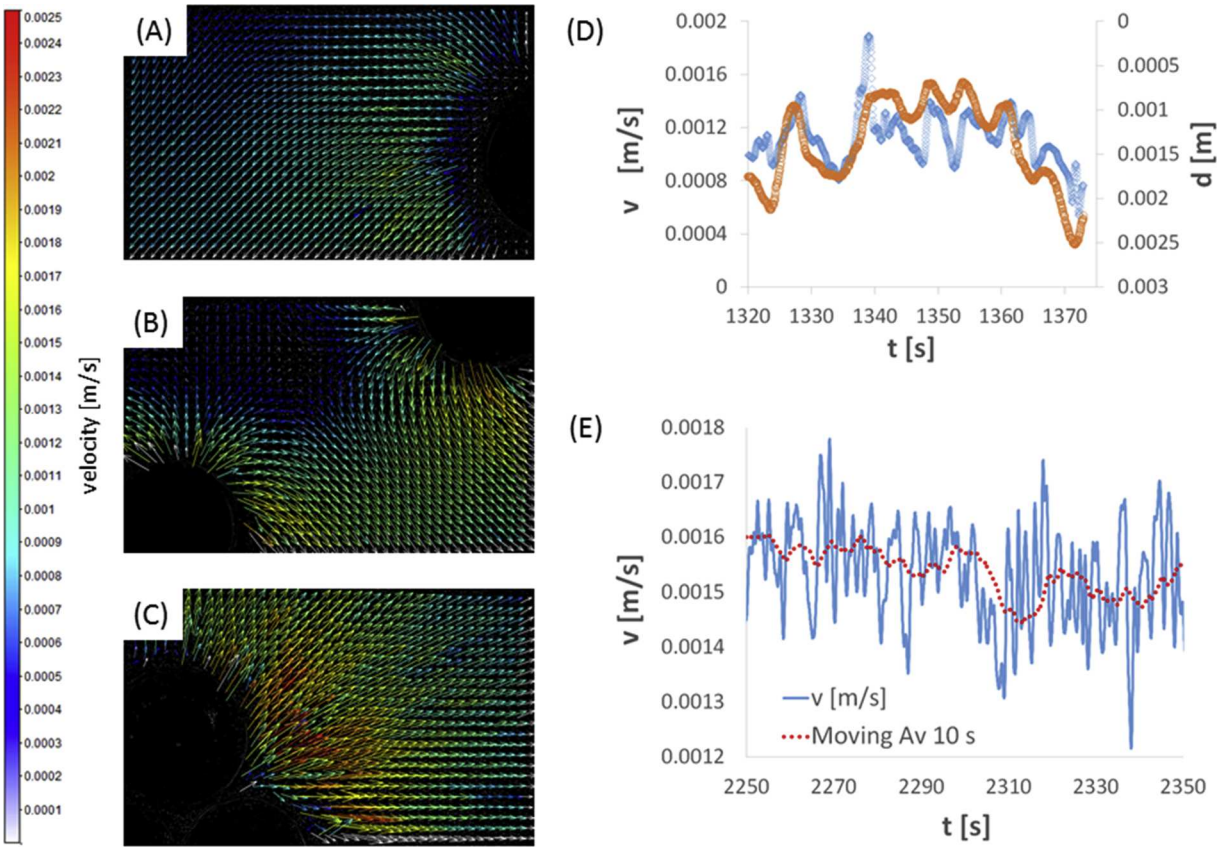

Fig. 5. (A)–(C): PIV velocity field (field of view 2.6 × 4.2 mm) around decanol droplets in different stages: (A) stage (II) where one of the separated droplets is visible, (B) transition to stage (III) with oscillatory movement of two droplets, (C) stage (IV) with a static cluster of three droplets. (D) Temporal evolution of mean velocity magnitude (blue diamonds) over whole field of view around two decanol droplets with changing distance (orange circles). (E) Temporal evolution of mean velocity magnitude at a static cluster (blue curve) with moving average (red dotted curve) over 1 s. (For interpretation of the references to colour in this figure legend, the reader is referred to the web version of this article.)

decanol droplets in 10 mM decanoate solution *Bo*= 0.66 and for 10 µL ES droplets with liquid paraffin (70% w/w, density 1.04 g/mL) in 35 mM SDS solution *Bo*= 1.03. These values of the Bond number represent the relative significance of the droplet weight to the surface tension force showing that the surface forces significantly contribute to the system state.

In both systems the same scenario was observed when many droplets were placed onto the surface of an aqueous solution. At the beginning of an experiment the droplets self-propelled, moved randomly and repelled each other, no attraction was observed. This probably is caused by the droplet dissolution and the formation of Marangoni flows from each droplet. After a certain time, the droplets lost their motility and, driven by gravitational force, approached the potential minimum of the surface of the aqueous solution. However, they still repelled each other and distributed in ordered structures with regular distances between them. Later on the droplets started to attract each other and arranged in one cluster. Then the droplets entered into the dancing phase when the dynamic oscillatory behaviour was observed. However, after some time, the droplets formed one static cluster with a regular hexagonal arrangement. The reason why the droplets switch between these modes (repulsion *vs.* attraction) is not fully clear yet. We believe that the changes of surface tension gradients followed by Marangoni flows are involved in this process.

From the PIV measurements it is obvious that the Marangoni convection influences the droplet interaction. The radial flow at two neighbouring droplets leads to the formation of a stagnation point between both droplets where the fluid velocity becomes zero as visible in Fig. 5B. The resulting stagnation pressure causes a repulsion of the droplets. While approaching the equilibrium, the surface tension gradients in the region between the droplets and accordingly the stagnation pressure caused by the Marangoni flow are reduced. Due to this, attractive interactions resulting from the height difference in the fluid layer due to the meniscus at the border or the capillary attraction between the droplets ("Cheerios effect") begin to dominate from stage (III) to (IV).

The works on droplets frequently use various colourants for a better visibility of the droplets. A question that recently appeared in some papers [19,34] is if and how the dye affects the droplet behaviour. Thus we also performed control experiments with colourless droplets. In the D system the dye Oil red O only serves to increase the visibility of the droplets in the camera records and has no influence on the droplet dynamics. This was verified by repeated experiments without dye and by measuring the surface tension of pure and coloured decanol and the interfacial tension between pure and coloured decanol and decanoate solution. No effect of Oil Red O was observed even when decanol was saturated by the dye. On the other hand, in the ES system Oil Red O had to be used in low concentrations (below 0.005 wt%), because higher concentrations of the dye affect the dynamics and slow down the droplets motion.

5. Conclusions

In this paper two droplet systems were compared. We focused on the behaviour of groups of organic droplets floating on aqueous solutions of surfactants. Although these systems are different in several parameters (chemical composition, physicochemical properties, concentration, size of the system, closed *vs.* open system, *etc.*), similar dynamics were observed. The cluster oscillation resembling a dancing

performance is the most interesting stage that needs to be studied in more detail in the future. We assume that an experimental model systems consisting of a large number of droplets can be the bridge between mathematical simulations and experiments with living objects, when the collective behaviour is studied. As an example we can mention that the formation of groups and their disintegration in our droplet experiments (stage III) correspond to patterns obtained in simulations of friendship formation in human society [35]. Another example could be the comparison of slime mould *Dictyostelium* clustering with the stage IV of the droplet systems described in this paper. *Dictyostelium* is a microorganism that under normal conditions consists of independent single amoebas and under unfavourable conditions, these cells become "social" and enter a multicellular developmental program [36]. Of course, this comparison is just on a qualitative level, there is no immediate analogy in the mechanism of clustering. Whereas in cell clustering complicated intercellular communication and intracellular processes are involved, the droplet clustering is based on physicochemical principles. Note that there is an intrinsic difference between a group of living beings and a group of liquid droplets. In the first one, the interactions are information-based, whereas in the second one, the interactions are force-driven. Our future work will focus on a detailed explanation of the observed phenomena and also on using such droplet systems as an unconventional tool for collective behaviour studies.

Acknowledgments

J.Č. was supported by Czech Science Foundation (17-21696Y). S.T. was supported by JSPS Grants-in-Aid for Scientific Research (JP17K05613). K.E. was supported by the Helmholtz Recruitment Initiative Fellowship.

Appendix A. Supplementary data

Supplementary material related to this article can be found, in the online version, at doi:https://doi.org/10.1016/j.colsurfa.2019.01.027.

References

[1] M. Rein, Phenomena of liquid drop impact on solid and liquid surfaces, Fluid Dyn. Res. 12 (2) (1993) 61.
[2] J. Čejková, M.M. Hanczyc, F. Štěpánek, Multi-armed droplets as shape-changing protocells, Artif. Life 24 (1) (2018) 71–79.
[3] J. Čejková, F. Štěpánek, M.M. Hanczyc, Evaporation-induced pattern formation of decanol droplets, Langmuir 32 (19) (2016) 4800–4805.
[4] C. Langton (Ed.), Proceedings of the Interdisciplinary Workshop on the Synthesis and Simulation of Living Systems (ALIFE' 87), Addison-Wesley, Los Alamos, NM, USA, 1987September 1987.
[5] J. Čejková, T. Banno, F. Štěpánek, M.M. Hanczyc, Droplets as liquid robots, Artif. Life 23 (4) (2017) 528–549.
[6] N. Ueno, T. Banno, A. Asami, Y. Kazayama, Y. Morimoto, T. Osaki, S. Takeuchi, H. Kitahata, T. Toyota, Self-propelled motion of monodisperse underwater oil droplets formed by a microfluidic device, Langmuir 33 (22) (2017) 5393–5397.
[7] C. Jin, C. Krüger, C.C. Maass, Chemotaxis and autochemotaxis of self-propelling droplet swimmers, Proc. Natl. Acad. Sci. U. S. A. 114 (20) (2017) 5089–5094.
[8] T. Banno, Y. Tanaka, K. Asakura, T. Toyota, Self-propelled oil droplets and their morphological change to giant vesicles induced by a surfactant solution at low pH, Langmuir 32 (37) (2016) 9591–9597.
[9] S. Tanaka, Y. Sogabe, S. Nakata, Spontaneous change in trajectory patterns of a self-propelled oil droplet at the air-surfactant solution interface, Phys. Rev. E 91 (3) (2015) 032406.
[10] M.M. Hanczyc, T. Toyota, T. Ikegami, N. Packard, T. Sugawara, Fatty acid chemistry at the oil-water interface: self-propelled oil droplets, J. Am. Chem. Soc. 129 (30) (2007) 9386–9391.
[11] J. Čejková, S. Holler, N.T. Quyen, C. Kerrigan, F. Štěpánek, M.M. Hanczyc, Chemotaxis and chemokinesis of living and non-living objects, in: A. Adamatzky (Ed.), Advances in Unconventional Computing, Springer, 2017, pp. 245–260.
[12] J. Čejková, M. Novák, F. Štěpánek, M.M. Hanczyc, Dynamics of chemotactic droplets in salt concentration gradients, Langmuir 30 (40) (2014) 11937–11944.
[13] J. Čejková, Q.T. Nguyenová, F. Štěpánek, Chemotactic droplets serving as "chemotaxi", in: S. Nakata, V. Pimienta, I. Lagzi, H. Kitahata, N.J. Suematsu (Eds.), Self-Organized Motion: Physiochemical Design Based on Nonlinear Dynamics, The Royal Society of Chemistry, 2019, pp. 182–203.
[14] J. Čejková, R. Tóth, A. Braun, M. Branicki, D. Ueyama, I. Lagzi, Shortest path finding in mazes by active and passive particles, in: A. Adamatzky (Ed.), Shortest Path Solvers. From Software to Wetware. Emergence, Complexity and Computation, Springer, Cham, 2018, pp. 401–408.
[15] S. Tanaka, T. Kano, Dynamic Oscillatory Cluster Ordering of Self-Propelled Droplets, (2017) https://arxiv.org/abs/1706.00154.
[16] S. Thutupalli, J.-B. Fleury, U.D. Schiller, G. Gompper, S. Herminghaus, R. Seemann, Hydrodynamics mediated collective motions in populations of microdroplets, Engineering of Chemical Complexity II vol. 12, (2014), p. 125.
[17] N. Horibe, M.M. Hanczyc, T. Ikegami, Mode switching and collective behavior in chemical oil droplets, Entropy 13 (3) (2011) 709–719.
[18] N.J. Cira, A. Benusiglio, M. Prakash, Vapour-mediated sensing and motility in two-component droplets, Nature 519 (7544) (2015) 446–450.
[19] L.J. Points, J.W. Taylor, J. Grizou, K. Donkers, L. Cronin, Artificial intelligence exploration of unstable protocells leads to predictable properties and discovery of collective behavior, Proc. Natl. Acad. Sci. U. S. A. 115 (5) (2018) 885–890.
[20] D. Liu, T. Tran, Vapor-induced attraction of floating droplets, J. Phys. Chem. Lett. 9 (16) (2018) 4771–4775.
[21] P.G. Moerman, H.W. Moyses, E.B. van der Wee, D.G. Grier, A. van Blaaderen, W.K. Kegel, J. Groenewold, J. Brujic, Solute-mediated interactions between active droplets, Phys. Rev. E 96 (3) (2017) 032607.
[22] D. Vella, L. Mahadevan, The "cheerios effect", Am. J. Phys. 73 (9) (2005) 817–825.
[23] S. Karpitschka, A. Pandey, L.A. Lubbers, J.H. Weijs, L. Botto, S. Das, B. Andreotti, J.H. Snoeijer, Liquid drops attract or repel by the inverted Cheerios effect, Proc. Natl. Acad. Sci. U. S. A. 113 (27) (2016) 7403–7407.
[24] S. Tanaka, S. Nakata, T. Kano, Dynamic ordering in a swarm of floating droplets driven by solutal Marangoni effect, J. Phys. Soc. Jpn. 86 (10) (2017) 101004.
[25] J. Čejková, T. Ikegami, Experimental study of mutual interactions of multiple liquid droplets, SWARM 2017: The 2nd International Symposium on Swarm Behavior and Bio-Inspired Robotics 2017, Kyoto - Japan, 2017, pp. 274–278.
[26] J. Čejková, T. Ikegami, F. Štěpánek, Life-like swarm behavior of multiple chemotactic droplets, in: C. Knibbe (Ed.), 14th European Conference on Artificial Life 2017, MIT Press, Lyon - France, 2017, pp. 91–95, , https://doi.org/10.7551/ecal_a_018.
[27] A.S. Al-Jimaz, J.A. Al-Kandary, A.-H.M. Abdul-Latif, Densities and viscosities for binary mixtures of phenetole with 1-pentanol, 1-hexanol, 1-heptanol, 1-octanol, 1-nonanol, and 1-decanol at different temperatures, Fluid Phase Equilib. 218 (2) (2004) 247–260.
[28] Y.-W. Sheu, C.-H. Tu, Densities and viscosities of binary mixtures of ethyl acetoacetate, ethyl isovalerate, methyl benzoate, benzyl acetate, ethyl salicylate, and benzyl propionate with ethanol at T = (288.15, 298.15, 308.15, and 318.15) K, J. Chem. Eng. Data 51 (2) (2006) 545–553.
[29] R. Stephenson, J. Stuart, Mutual binary solubilities: water-alcohols and water-esters, J. Chem. Eng. Data 31 (1) (1986) 56–70.
[30] T. Namani, P. Walde, From decanoate micelles to decanoic acid/dodecylbenzenesulfonate vesicles, Langmuir 21 (14) (2005) 6210–6219.
[31] F.E. Stanley, A.M. Warner, E. Schneiderman, A.M. Stalcup, Rapid determination of surfactant critical micelle concentrations using pressure-driven flow with capillary electrophoresis instrumentation, J. Chromatogr. A 1216 (47) (2009) 8431–8434.
[32] R. Tadmouri, N.M. Kovalchuk, V. Pimienta, D. Vollhardt, J.C. Micheau, Transfer of oxyethylated alcohols through water/heptane interface: transition from non-oscillatory to oscillatory behaviour, Colloids Surf. A: Physicochem. Eng. Aspects 354 (1) (2010) 134–142.
[33] K. Schwarzenberger, S. Aland, H. Domnick, S. Odenbach, K. Eckert, Relaxation oscillations of solutal Marangoni convection at curved interfaces, Colloids Surf. A: Physicochem. Eng. Aspects 481 (2015) 633–643.
[34] R.J.G. Löffler, J. Gorecki, M. Hanczyc, Better red than dead: on the influence of oil Red O dye on complexity of evolution of a camphor-paraffin droplet on the water surface, The 2018 Conference on Artificial Life: A Hybrid of the European Conference on Artificial Life (ECAL) and the International Conference on the Synthesis and Simulation of Living Systems (ALIFE) (2018) 574–579, https://doi.org/10.1162/isal_a_00106.
[35] T. Kano, K. Osuka, T. Kawakatsu, A. Ishiguro, Mathematical analysis for non-reciprocal-interaction-based model of collective behavior, J. Phys. Soc. Jpn. 86 (12) (2017) 124004.
[36] H. Ševčíková, J. Čejková, L. Krausová, M. Přibyl, F. Štěpánek, M. Marek, A new traveling wave phenomenon of Dictyostelium in the presence of cAMP, Physica D 239 (11) (2010) 879–888.

Journal of Materials Chemistry B

RSC Publishing

PAPER

View Article Online
View Journal | View Issue

Cite this: *J. Mater. Chem. B*, 2013, **1**, 5456

Biologically triggered liberation of sub-micron particles from alginate microcapsules†

Jitka Čejková, Petra Haufová, Damian Gorný, Jaroslav Hanuš and František Štěpánek*

Received 20th March 2013
Accepted 8th August 2013

DOI: 10.1039/c3tb20388c

www.rsc.org/MaterialsB

A new method for triggering the burst liberation of encapsulated sub-micron particles from carrier particles using embedded microorganisms has been developed. Triggering mechanisms such as those based on chemical, light, thermal, or magnetic stimuli are known, but man-made particles are not yet able to replicate the concept of "dormancy" found in biological systems in the form of spores or seeds that survive in an inactive state and start to grow only once favourable environmental conditions are encountered. An engineered particle system that mimics this property by embedding viable yeast cells into synthetically made alginate microcapsules is reported in the present work. Cell growth and division is used as a triggering mechanism for stimuli-responsive release of the encapsulated content. The hybrid living/artificial capsules were formed by an inkjet printing process and the mechanism of biologically triggered release was shown using fluorescently labelled liposomes.

1 Introduction

The controlled release of active substances (*e.g.* drugs, fragrances, probiotics, nutrient preservatives) from man-made capsules is of considerable interest in many fields of science and technology.[1] A variety of chemical and physical methods have been developed to release the capsule contents, *cf. e.g.* a review by Esser-Kahn *et al.*[2] The release triggers are frequently based on mechanical, chemical, electrical, thermal, photo, or magnetic stimuli. While these stimuli are well-defined in terms of their timing and the threshold value of a physical quantity that characterises each stimulus (*e.g.* voltage, temperature, concentration, *etc.*), release triggers occurring in nature are often more complex and comprise the simultaneous occurrence of several stimuli – for example, the combination of specific temperature, humidity, light conditions and nutrients is necessary for seed germination, *etc.*

The use of actual living microorganisms or their spores offers itself as a possible way of achieving such complex triggers even in synthetically made particles. To achieve this, a necessary condition is the ability to fabricate composite microcapsules that incorporate the chosen microorganism or its spores, and to ensure their viability. In the specific case of yeast cell encapsulation into alginate gel, currently available encapsulation techniques include microfluidic approaches,[3] electrostatic droplet generation,[4] spinning disk atomization[5] or simply dropping an alginate solution into $CaCl_2$ using a syringe.[6,7] At present, the main reasons for microbial cell encapsulation into various matrixes include cell protection from negative environmental influences such as shear forces, phagocytosis or digestion. Immobilized microbial cells also can be handled more easily and separated from a solution.[8]

In most current applications of immobilised cells, microcapsule rupture due to internal pressure of proliferating cells is usually not of interest. In the case of cell-based biosensor applications, the cell division and capsule disintegration would be outright undesirable. Cases where the capsules rupture due to CO_2 formation when they are placed in a growth medium have been reported[9] and the surfactant Tween-20 has been used to improve the permeability of the capsule for easier CO_2 liberation.[6] A silica coating can also enhance the mechanical resistance of capsules.[10] A case where the cell division is a wanted process has been reported by Hamad *et al.*[11] who fabricated composite multi-cell/shellac microcapsules that contained living yeast cells. Cell release from the microcapsule after incubation in a cultivation medium has been demonstrated. However, to the best of our knowledge, the use of cell growth as a trigger for the release of another active substance also embedded within the carrier particle has not been reported in the literature as yet.

The present paper describes the preparation of hybrid alginate microcapsules capable of releasing an encapsulated payload – fluorescently labelled liposomes in this case – as a result of rupture caused by proliferating cells. The schematic structure and mechanism of action of the microcapsules is shown in Fig. 1. Under unfavourable conditions (absence of nutrients, low temperature) cell division does not occur and the microcapsules are stable in aqueous medium for extended periods of time without disintegration or release of their

Institute of Chemical Technology Prague, Department of Chemical Engineering, Technicka 5, Prague 6, 166 28, Czech Republic. E-mail: frantisek.stepanek@vscht.cz; Tel: +420 22044 3236

† Electronic supplementary information (ESI) available. See DOI: 10.1039/c3tb20388c

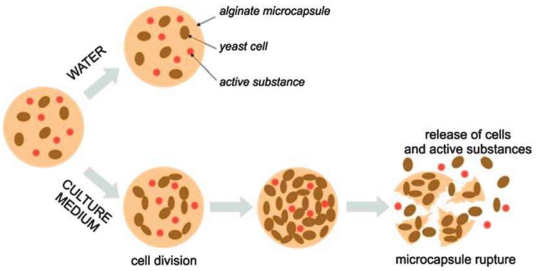

Fig. 1 Schematic principle of microcapsule rupture and liberation of an active substance into the environment caused by yeast cell growth in the culture medium.

content. Once the microcapsules encounter favourable conditions (presence of nutrients, higher temperature), cell division and growth causes an eventual rupture of the alginate capsule and release of the embedded liposomes. Additionally, magnetic iron oxide nanoparticles were also embedded within the composite microcapsules to facilitate their manipulation and separation by a magnetic field. Liposomes loaded with fluorescein represent a model "active" particulate substance that is to be liberated from the composite microcapsules. Calcium alginate hydrogel was chosen as the matrix material in which the three types of internal components (yeast cells, liposomes, magnetic nanoparticles) were embedded due to its ability to form microcapsules by means of an inkjet printing process, which has been demonstrated in our previous work.[12,13]

2 Materials and methods

2.1 Materials

Sodium alginate, calcium chloride ($CaCl_2$), fluorescein diacetate (FDA), yeast extract and glucose were purchased from Sigma-Aldrich. Instant yeast cells (Labeta a.s., Czech Republic) were suspended in deionised water in various concentrations (1 mg of dry powder corresponds to 3×10^7 cells). Hydrophilic iron oxide nanoparticles were prepared according to a synthesis method described in ref. 14. Fluorescently labelled liposomes (molar ratio of DPPC : cholesterol was 2 : 1) were synthesized in the same way as described in ref. 15. Deionised water was produced using an ionex filter (Aqual 25).

2.2 Microcapsule formation

All microcapsules were produced by inkjet printing.[16] A piezoelectric drop-on-demand print-head type M5-ABP-01-80-6MX supplied by Microfab, Inc. (Plano, Texas, USA) was used, coupled with a control unit type JetDrive III and a pressure controller type CT-PT-01 also supplied by Microfab, Inc. 2 ml of aqueous solutions of 2% (w/w) sodium alginate and 2 ml of aqueous suspension of yeast cells were mixed and printed into approximately 50 ml of aqueous solution of 2% (w/w) $CaCl_2$ where a rapid ionic cross-linking of the microdroplets occurred. The receiving $CaCl_2$ solution was constantly agitated to avoid coalescence of microdroplets after impact. To prepare magnetic microcapsules, one half of the cell suspension was replaced by citrate-stabilized iron oxide nanoparticle dispersion in water (15 mg ml^{-1}). The solution for printing of magnetic capsules containing liposomes was obtained from a sodium alginate solution, the cell suspension, the iron oxide nanoparticle solution and a liposome solution in the volume ratio 4 : 1 : 1 : 2. Cross-linked calcium alginate microcapsules were separated from the $CaCl_2$ solution by using a filter or magnet and suspended in deionized water in which they were stored at room temperature until further use. In this state the composite microcapsules were stable for up to 4 months without any significant loss of yeast cell viability.

2.3 Microcapsule characterization

The microcapsules were characterized by means of an inverted optical microscope (Olympus CK40) and a laser scanning confocal microscope – LSCM (Olympus Fluoview FV1000). The particle size was evaluated by laser diffraction (Horiba Partica LA 950/V2). The viability of yeast cells was confirmed by using the standard fluorescein diacetate solution method.

2.4 Yeast cell division and microcapsule disruption study

For a study of the cell division and disintegration of microcapsules, the composite microcapsules were placed into a Petri dish containing a culture medium (consisting of glucose at a concentration of 10 g l^{-1} and yeast extract at a concentration of 5 g l^{-1}) and monitored using an optical microscope for 24 hours. The cell growth curves were measured by means of a visible spectrophotometer (Specord 205 BU, Analytik Jena, Germany); the wavelength used for the measurement of optical density was 600 nm (OD 600).

3 Results and discussion

3.1 Microcapsule characterization

The drop-on-demand inkjet technology was used for the formation of calcium alginate microcapsules with embedded yeast cells by ejecting droplets of a sodium alginate precursor into a pool of calcium chloride solution. The shape of the formed microcapsules was mostly spherical, however, some of them were distorted (flattened) due to droplet deformation upon landing into the $CaCl_2$ solution.[5] Fig. 2(A) and (B) show the composite alginate microcapsules with two different cell concentrations; both spherical and flattened capsules are evident irrespective of the cell concentration used.

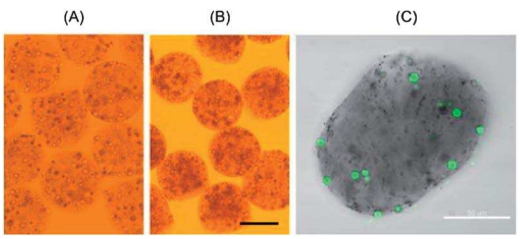

Fig. 2 Magnetic alginate microcapsules with various cell concentrations. Optical microscopy images: (A) 2.25×10^8 cells per ml and (B) 3.75×10^8 cells per ml. (C) Laser scanning confocal microscopy image (single slice in the *x–y* plane) of a 1 month old magnetic alginate microcapsule with 2.25×10^8 cells per ml labelled by FDA. Scale bars represent 50 μm.

The mean size of freshly precipitated capsules measured in $CaCl_2$ solution by means of static light scattering was 61 μm; in water the mean size increased to 79 μm due to swelling of calcium alginate. This is provoked by the relaxation of the polymer network at the presence of osmotic pressure. Swelling of the calcium alginate beads in water occurs until the osmotic pressure equals the forces of the cross-linking bonds that maintain the structure of the polymer network.[17]

The viability of yeast cells in the composite microcapsules was confirmed by using fluorescein diacetate (FDA).[18] This colourless compound exhibits no fluorescence, however, it is known that it diffuses through the cell membrane and living cells are able to hydrolyse it by their enzymatic apparatus and transform FDA into fluorescein. Typically, 2 ml of microcapsule suspension were incubated with a few droplets of FDA in acetone for 20 minutes, then washed and observed under a LSCM. By this test it was proven that the cells are able to retain their viability during the inkjet printing process. Fig. 2(C) shows a microcapsule after one month of its fabrication and storage in water that was incubated with FDA. The green spots correspond to living cells, which confirms that the cell viability is preserved for many weeks. The viability tests also excluded that the magnetic iron oxide nanoparticles have a harmful effect on yeast cells. Viable yeast cells clearly exist in the composite microcapsules in the presence of inorganic nanoparticles.

3.2 Yeast cell growth in microcapsules

The hybrid microcapsules with embedded yeast cells were stored in water for a few weeks and no microcapsule changes or cell division in capsules was observed. Radical changes occurred only after incubation with a growth medium containing yeast extract and glucose. For the preparation of the culture medium we have used water instead of phosphate buffer, which is normally used, due to the fact that the phosphate buffer would precipitate calcium ions and reverse the alginate crosslinking.[19]

To observe the division of encapsulated yeast cells, composite microcapsules were suspended in a Petri dish with the growth medium and placed under a microscope at laboratory temperature (~25 °C). Images in 1 minute intervals were grabbed for at least 24 hours and compiled into a movie (see ESI S1†). A series of experiments starting from capsules containing different initial cell concentrations with and without magnetic nanoparticles were performed. Typical results are summarized in Fig. 3 and 4 for microcapsules containing iron oxide nanoparticles and yeast cells at a concentration of 3.75×10^8 cells per ml.

Fig. 3 shows the evolution of microcapsule structure in time under static conditions in a Petri dish with a cultivation medium. During inkjet fabrication of the microcapsules, no cell loss was observed and the cell number per microcapsule was therefore determined by the cell concentration in the initial alginate solution. Time $t = 0$ h corresponds to the moment of placing microcapsules into the cultivation medium. About two hours after incubation, first buds on the cells appeared but no extensive budding was observed yet. Around the time $t = 7$ h, the cell division was highly developed and around $t = 15$ h the alginate microcapsules were almost full of cells. At time $t = 18$ h the first ruptures of the composite microcapsules started. Due to the extensive cell division all microcapsules eventually disintegrated and essentially no original round microcapsules were evident at time $t = 24$ h. Only clusters of yeast cells were present in the Petri dish.

The growth kinetics was also evaluated by using visible spectrophotometry, when the growth curves of cells in alginate

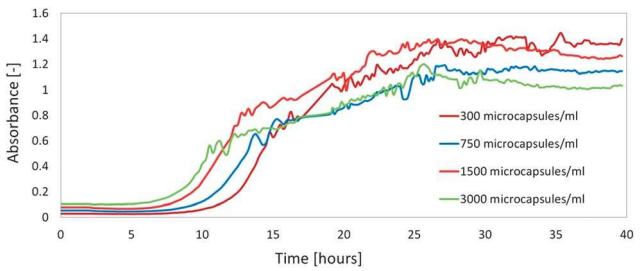

Fig. 4 Growth curves of yeast cells in the microcapsules (initial concentration 3.75×10^8 cells per ml) for various concentrations of microcapsules in the growth medium. The curves correspond to different microcapsule dilutions as indicated in the legend.

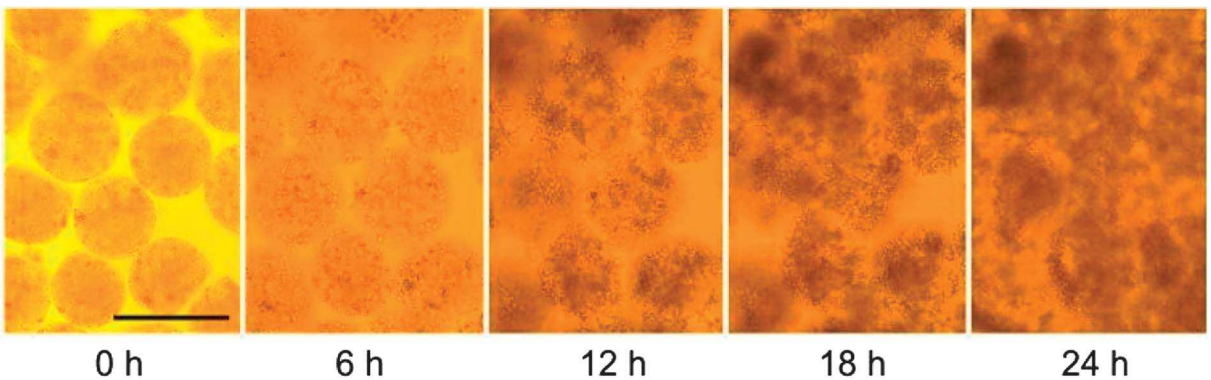

Fig. 3 Yeast cell division in alginate microcapsules incubated in a Petri dish with culture medium. The initial concentration of yeast cells in the microcapsules was 3.75×10^8 cells per ml. Scale bar represents 100 μm.

microcapsules were measured as a function of optical density at the wavelength of 600 nm. These two types of experiments differ in conditions. Observation by microscope was under static conditions without any mixing whereas microcapsules in the spectrophotometer cuvettes were intensively stirred using a magnetic stirrer in order to keep them suspended. Mixing might affect the microcapsule disintegration, therefore the capsules in cuvettes disintegrate somewhat earlier than on the Petri dishes.

Fig. 4 shows the changes in optical density of microcapsule suspension at 600 nm. During the first few hours no changes were evident, because yeast cells were still in the lag phase of their growth, they adapted themselves to the growth conditions and rarely divided. At about $t = 7$ h, the cells entered into the exponential growth phase and at about $t = 12$ h since the addition of nutrients the microcapsules ruptured. Despite mixing, the measured absorbance started to fluctuate at this stage. Nevertheless, a continuous increase of absorbance is evident until approximately $t = 24$ h, which indicates continuing cell division. After the time $t = 24$ h, the absorbance no longer increased as the cells entered into the stationary phase due to lack of nutrients.

To confirm that the disruption of alginate microcapsules was caused solely by the growth of encapsulated yeast cells, a blind experiment was performed. When alginate microcapsules without yeast cells were prepared and placed into the growth medium, no decomposition of the microcapsules was observed. Such a blind experiment excluded the growth medium as a possible factor causing the microcapsule rupture and confirmed the role of the dividing cells. To exclude the effect of yeast cells and the presence of their metabolites on the decomposition of alginate microcapsules, another blind experiment was performed. Alginate microparticles without embedded yeast were placed into a growth medium together with freely suspended yeast cells. Again, no microcapsule disintegration was observed, the cells have grown outside the microcapsules and did not affect the alginate integrity.

3.3 Mimicking spore behaviour

To demonstrate the concept of "artificial spores" or "artificial seeds", additional experiments with switching between favourable/unfavourable conditions and drying of microcapsules were performed. In biology, a spore is defined as a reproductive structure that is adapted for dispersion and survival for extended periods of time under unfavourable conditions. Once conditions are favourable, spores can develop into new organisms. The activators of such a transformation from a spore to a cell could be *e.g.* nutrients, temperature, pH, or combination of these parameters. The interesting property of this transformation is that once the conditions are suitable for germination, the spores enter a lag phase and activate specific genes that trigger signal pathways leading to swelling and cell emergence. Once a spore has swollen, germination becomes irreversible, but during the lag phase activated spores can return to dormancy.[20]

The experiment mimicking the spore response to changes in conditions was performed in a spectrophotometer equipped with heating/cooling facility. The growth curves were measured and temperature changes applied. The experiment started under unfavourable conditions, where microcapsules were stored in water (without nutrients). The first change consisted of placing the capsules in the culture medium at a temperature of 30 °C (corresponding to time $t = 0$ h in the growth curves in Fig. 5). For the first few hours the yeast cells embedded in the microcapsules were still dormant. Once they entered the exponential phase of their growth, the temperature was rapidly decreased to 8 °C. Such a temperature shock stopped the cell growth, resulting in a return to dormancy. During this time no change of optical density was observed, corresponding to no division of cells. When the temperature was increased back to 30 °C, rapid cell growth was restarted and the next temperature decrease again caused an interruption of cell division. An example of three repetitions of heating/cooling is shown in Fig. 5(A). Fig. 5(B) shows the possibility to "freeze" the cell growth in microcapsule for almost two days and then restart growth by a return to favourable conditions.

3.4 Cell growth triggered liberation of active substances from microcapsules

As was shown above, composite microcapsules are stable in water, whereas after cultivation in a growth medium they are able to disintegrate. To demonstrate that capsule disintegration can be used for the release of a previously encapsulated payload, the liberation of fluorescently labelled liposomes was observed using a laser scanning confocal microscope. Fig. 6(A) shows the composite particles directly after their fabrication. The fluorescence signal is obtained only in the microcapsules, which confirms the presence of liposomes. In Fig. 6(B), the same microcapsules were imaged one day after fabrication and storage in pure water. Again, the fluorescence signal comes only from microcapsules, no liberation of liposomes from microcapsules occurred. On the other hand, Fig. 6(C) confirms that after cultivation of the microcapsules in a growth medium, the cells divide and cause the rupture of capsules, liberating the encapsulated substances into the surroundings. After one day

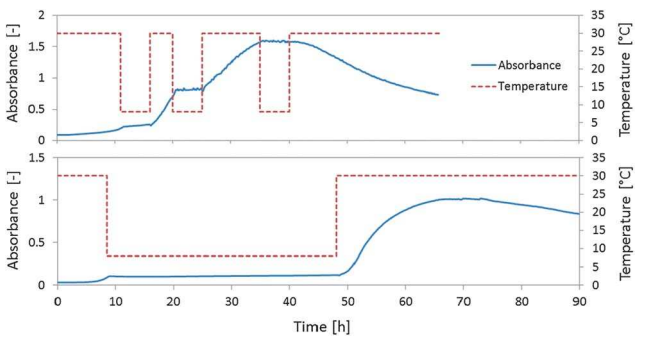

Fig. 5 Control of yeast growth by temperature modulation (interruption of growth by temperature decrease and resumption of growth by temperature increase). (A) Three interruptions of cell growth at times 11–16 h, 20–25 h, and 35–40 h. (B) One cell growth interruption for almost two days (8–48 h).

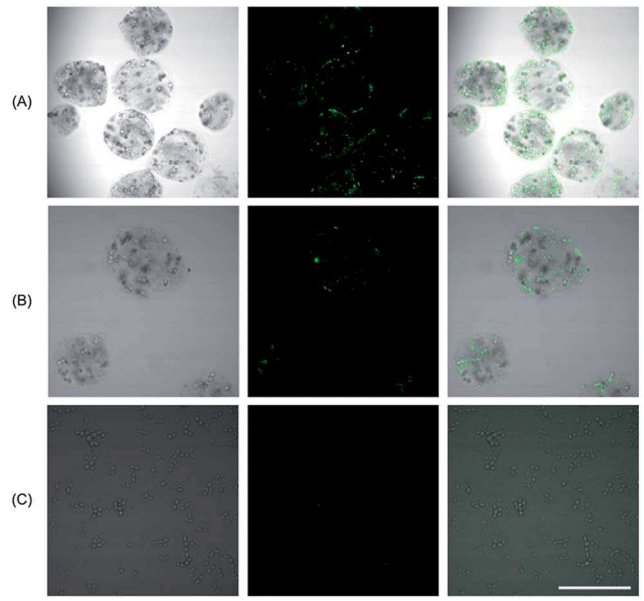

Fig. 6 Alginate microcapsules with fluorescently labelled liposomes. (A) Freshly prepared microcapsules in water. (B) Microcapsules after one day in water. (C) Disintegrated microcapsules after one day of incubation in a culture medium. (Left column – optical image, middle column – fluorescence signal, right column – superposition of both signals. The scale bar represents 100 μm.)

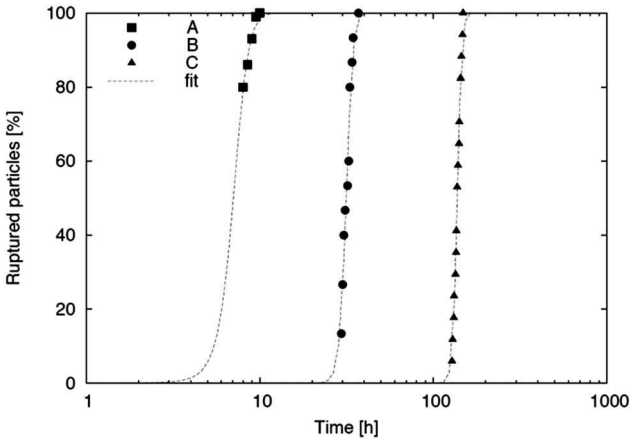

Fig. 7 Time of rupture of microparticles containing (A) 40–60, (B) 10–20 and (C) 3–6 cells per particle.

Table 1 Values of regression parameters from eqn (1) for three different cell concentrations in the microcapsules

Sample	b [h^{-1}]	t_m [h]
A	1.38 ± 0.27	7.05 ± 0.24
B	0.72 ± 0.07	31.46 ± 0.13
C	0.25 ± 0.01	137.15 ± 0.18

of incubation in culture medium no compact microcapsules were present, only clusters of cells were evident and the fluorescence signal was detectable from the whole medium in a diluted way because the liposomes were released during the microcapsule disintegration. Microcapsule disintegration appears to be a "binary" event in the sense that partial rupture was rarely observed; once a microcapsule ruptured, it did so completely and the fluorescent signal from liberated liposomes was present uniformly in the background rather than clustered as would be the case if, *e.g.*, some partially ruptured microcapsules prevailed in the system.

Having established that the liposome release by capsule rupture can be triggered by the cell division, the possibility to control the timing of rupture by the initial concentration of cells in the microcapsules was investigated. Three batches of microcapsules were prepared, with initial cell concentrations of 40–60 cells per particle, 10–20 cells per particle, and 3–6 cells per particle (obtained by dilutions of the initial yeast cell suspension in the alginate solution). The microcapsules were placed into a culture medium under favourable growth conditions and recorded in time. Once the microcapsules started to rupture, the percentage of fractured capsules as a function of time was evaluated by image analysis. The results are summarised in Fig. 7 and the obtained dependence of the fraction of ruptured particles as a function of time was fitted by a sigmoidal function of the form

$$f(t) = 1/[1 + \exp(-b(t - t_m))] \quad (1)$$

where t_m is the mean rupture time and b is a rate constant. The values of b and t_m evaluated by non-linear regression of the data plotted in Fig. 7 are summarised in Table 1. As can be seen from both the figure and the table, there is a systematic dependence of the rupture time on the initial cell concentration, which offers the possibility to control the timing of the release.

4 Conclusions

Composite hydrogel microcapsules with embedded yeast cells that can act as a biological trigger for controlled opening of the microcapsules and locally liberate sub-micrometer objects have been fabricated. Additionally, magnetic nanoparticles were added into the microcapsules to enable manipulation by an external magnetic field. The composite capsules were stable in aqueous media for up to several months and retained their viability. Once favourable conditions were encountered – *i.e.* the presence of nutrients and a suitable temperature – the proliferation of yeast cells within the microcapsule leads to its eventual disintegration and the liberation of other embedded objects, namely fluorescently labelled liposomes. It has been shown that the biologically triggered release can be used not only for a one-off rupture of the microcapsules, but also for a repeated interruption and 'restart' of the growth processes due to variations in external conditions. This behaviour contrasts with that of traditional man-made triggered release systems where irreversible processes tend to dominate. Systems based on biologically triggered release could find applications in fields such as controlled release of bactericides or fungicides, or the detection of potential food contamination due to inappropriate storage conditions. The principle of biologically triggered release can potentially be applied using other microorganisms than yeast cells, which

would offer flexibility in the range of environmental conditions under which the composite capsules can operate, and also in the range of particle sizes (obviously, the initial particle must be large enough to contain at least several cells, as well as space for the payload that is to be liberated).

Acknowledgements

Financial support from the European Research Council (grant number 200580-Chobotix) and the European Union 7th Framework Program (Grant Agreement 318671-MICREAgents) is gratefully acknowledged.

Notes and references

1 X. Yan, J. Li and H. Möhwald, *Adv. Mater.*, 2012, **24**, 2663–2667.
2 A. P. Esser-Kahn, S. A. Odom, N. R. Sottos, S. R. White and J. S. Moore, *Macromolecules*, 2011, **44**, 5539–5553.
3 C. J. Martinez, J. W. Kim, C. Ye, I. Ortiz, A. C. Rowat, M. Marquez and D. Weitz, *Macromol. Biosci.*, 2012, **12**, 946–951.
4 V. A. Nedović, B. Obradović, I. Leskošek-Čukalović, O. Trifunović, R. Pešić and B. Bugarski, *Process Biochem.*, 2001, **37**, 17–22.
5 Y. Senuma, C. Lowe, Y. Zweifel, J. G. Hilborn and I. Marison, *Biotechnol. Bioeng.*, 2000, **67**, 616–622.
6 K. Koyama and M. Seki, *J. Biosci. Bioeng.*, 2004, **97**, 111–118.
7 H. N. Chang, G. H. Seong, I.-K. Yoo, J. K. Park and J.-H. Seo, *Biotechnol. Bioeng.*, 1996, **51**, 157–162.
8 J. K. Park and H. N. Chang, *Biotechnol. Adv.*, 2000, **18**, 303–319.
9 S. Cheong, J. Park, B. Kim and H. Chang, *Biotechnol. Tech.*, 1993, **7**, 879–884.
10 T. Coradin, E. Mercey, L. Lisnard and J. Livage, *Chem. Commun.*, 2001, 2496–2497.
11 S. A. Hamad, S. D. Stoyanov and V. N. Paunov, *Soft Matter*, 2012, **8**, 5069–5077.
12 J. Dohnal and F. Štěpánek, *Chem. Eng. Sci.*, 2011, **66**, 3829–3835.
13 P. Haufová, J. Dohnal, J. Hanuš and F. Štěpánek, *Colloids Surf., A*, 2012, **410**, 52–58.
14 V. Tokárová, A. Pittermannová, J. Čech, P. Ulbrich and F. Štěpánek, *Soft Matter*, 2012, **8**, 1087–1095.
15 M. Ullrich, J. Hanuš, J. Dohnal and F. Štěpánek, *J. Colloid Interface Sci.*, 2013, **394**, 380–385.
16 J. Dohnal and F. Štěpánek, *Powder Technol.*, 2010, **200**, 254–259.
17 G. Pasparakis and N. Bouropoulos, *Int. J. Pharm.*, 2006, **323**, 34–42.
18 G. Adam and H. Duncan, *Soil Biol. Biochem.*, 2001, **33**, 943–951.
19 R. Yao, R. J. Zhang, J. Luan and F. Lin, *Biofabrication*, 2012, **4**, 025007.
20 P. Van Dijken and P. Van Haastert, *BMC Cell Biol.*, 2001, **2**, 25.

Chem. Pap. (2017) 71:1055–1063
DOI 10.1007/s11696-016-0026-2

ORIGINAL PAPER

Spheroid cultivation of HT-29 carcinoma cell line in liquid marbles

Ondřej Rychecký[1] · Monika Majerská[1] · Vlastimil Král[1,2] · František Štěpánek[1] · Jitka Čejková[1]

Received: 26 July 2016 / Accepted: 24 November 2016 / Published online: 5 December 2016

Abstract The ability to simulate the 3D structure of a human body is essential to increase the efficiency of drug development. In vivo conditions are significantly different in comparison to in vitro conditions. A standardly used cell monolayer on tissue culture plastic (2D cell culture) is not sufficient to simulate the transfer phenomena occurring in living organisms, therefore, cell growth in a 3D space is desired. Drug absorption, distribution, metabolism, excretion and toxicity could be tested on 3D cell aggregates called spheroids, decrease the use of animal models and accelerate the drug development. In this work, the formation of spheroids from HT-29 human colorectal adenocarcinoma cells was successfully achieved by means of the so-called liquid marbles, which are liquid droplets encapsulated by a hydrophobic powder. During the cultivation in the medium inside the liquid marbles, cells spontaneously formed spherical agglomerates (spheroids) without the need of any supporting scaffold. The study focused on the influence of different parameters—namely liquid marble volume, seeding cell density and time of cultivation—on the final yield and quality of spheroids. This work has shown that using liquid marbles as microbioreactors is a suitable method for the cultivation of HT-29 cells in the form of spheroids.

Keywords Liquid marble · HT-29 · Spheroid · Microbioreactor

Introduction

Liquid marble is a droplet of fluid encapsulated by a hydrophobic powder. The particles spontaneously cover the droplet surface. Due to the hydrophobicity of its shell, a liquid marble could be rolled on a solid surface as a glass sphere and also it could be deformed as a foam ball (Eshtiaghi and Hapgood 2012). Although the term liquid marble was used for the first time by Aussillous and Quéré in Nature in 2001, liquid marbles could be found in nature since ages, e.g. the first rain droplet is spontaneously covered with solid soil particles after long drought (Aussillous and Quere 2001). Another example of liquid marbles in nature is aphids and their honeydew droplets covered by powdery wax (Pike et al. 2002). Preparation of liquid marbles is very simple—a small amount of liquid (in the order of tens or hundreds of microliters) is rolled on a layer of hydrophobic powder consisting of tiny particles, which spread spontaneously at the liquid–air interface (Fig. 1). Prepared liquid marbles have some of the properties of a liquid droplet and they also behave as a soft solid (Aussillous and Quéré 2006). During rolling on a surface, liquid marble does not lose any amount of liquid content. It is possible to roll a liquid marble on solid surfaces, it can even float on water or another liquid surface. Liquid marbles behave as deformable spheres as they move. Due to their properties, liquid marbles could find application in several fields, for example as gas sensors (Tian et al. 2010),

Presented at the 43rd International Conference of Slovak Society of Chemical Engineering held in Tatranské Matliare on May 23–27, 2016.

✉ Jitka Čejková
jitka.cejkova@vscht.cz

[1] Department of Chemical Engineering, University of Chemistry and Technology Prague, Technická 3, 166 28 Prague, Czech Republic

[2] Laboratory of Structural Biology, Institute of Molecular Genetics of the ASCR, v. v. i., Flemingovo nám. 2, 166 37 Prague, Czech Republic

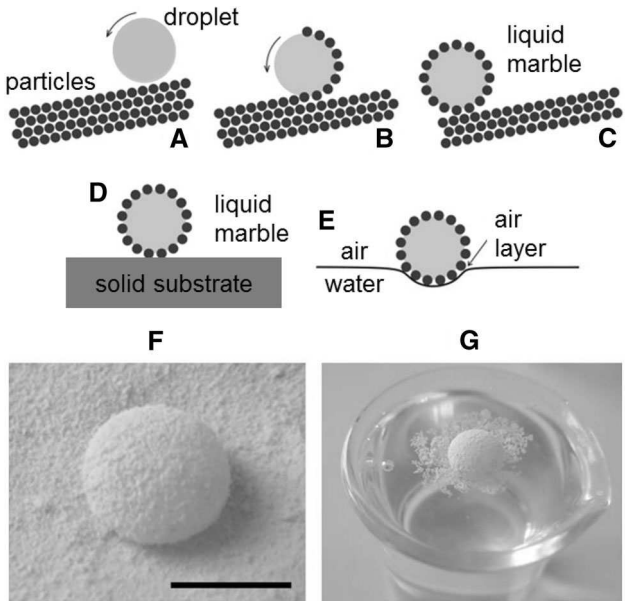

Fig. 1 **a–c** Scheme of liquid marble preparation process. **d** Scheme of liquid marble on a solid substrate. **e** Scheme of liquid marble floating on a water surface. **f** Photograph of liquid marble (100 µl of water covered by lycopodium grains). *Scale bar* corresponds to 5 mm. **g** Photograph of liquid marble from **f** floating on a water surface

microreactors or bioreactors for cell cultivation. One of the first biological applications of liquid marbles was blood testing, specifically human blood typing (Arbatan et al. 2012b). Using of liquid marbles as microreactors for blood testing or other biological applications has many advantages. First of all, a small amount of samples and reagents is needed. Then biohazard risk is also reduced, because liquid core is separated from environment by a powder shell. Moreover, controlling or adding some reagent is easy and can be done by coalescence of two marbles or by a syringe injection.

In the beginning of a drug testing, first biological studies are done in vitro on 2D cell cultures that frequently determine the initial but crucial 'stop/go' decisions on the progression of the development of a drug. But 2D cell cultures are a very simplistic approximation of a biological system. They neglect spatial organization. In 2D, cells are exposed on one side to hard plastic and on the other side to fluid environment with limited cell–cell contact. In vivo, cells are surrounded by other cells and extracellular matrix. Cell–cell and cell-extracellular matrix interactions play a crucial role in a cell life. They influence not only cell proliferation, apoptosis, migration, communication and gene expression but also diffusion of nutrients, respiratory gases or drugs (Campbell et al. 1985; DiPersio et al. 1991). On the opposite end of experimental systems are animal models. Their disadvantages are that they are very expensive, time-consuming, raise ethical questions and also they are just another models of a human body. Moreover, it can be difficult to study some processes in such complex systems. As a result, 3D cell cultures are currently being developed to provide cells with a third dimension to better mimic in vivo microenvironment.

Due to the increasing popularity of 3D cell culture approach, more and more methods are being developed for their preparation. In general, there are two main types of 3D cell cultures: scaffold-based cultures and scaffold-free cultures. Materials used for scaffold fabrication have to be biocompatible, bioadhesive and sometimes even biodegradable when applied in regenerative medicine. On one hand, scaffolds provide physical support to cells for their proliferation and differentiation. Porous scaffolds allow nutrients, oxygen and drugs to reach cells and also waste from cells can be withdrawn from the cell environment. On the other hand, scaffolds represent foreign elements in 3D cell cultures and their microstructure (porosity, pore size, pore shape and interconnectivity) and mechanical properties can modulate cell behaviour (Yeung et al. 2005; Harley et al. 2008). In the scaffold-free approach, a 3D cell culture grows without any support into clusters of spherical shape called spheroids. This type of 3D cell culture is mostly used in studies of solid tumour behaviour. The reason for this is that like in the solid tumours, a necrotic core is developed inside spheroids with their increasing size. In bigger spheroids (200 µm) there is a limited diffusion of nutrients and oxygen into the core and cells start to die (Curcio et al. 2007). Moreover, when they reach certain size above 500 µm they can contain necrotic core which is characteristic for many tumours due to poor vascularization of tumour tissue (Alvarez-Pérez et al. 2005; Fennema et al. 2013). Spheroids have, therefore, a great potential to speed up a drug development process and also to decrease the number of animals used for drug testing. During cell cultivation, spherical agglomerates (spheroids) are formed in the liquid core of marbles without any support (Fig. 2). Spheroids, as a type of 3D cell cultures, represent a bridge between simplistic in vitro 2D cell cultures and in vivo animal models. Due to the addition of a third dimension, they simulate conditions in a biological system more accurately than 2D cell cultures in the form of a cell monolayer.

Liquid marbles were used as microbioreactors for cell cultivation or oocyte in vitro maturation in small volumes (Ledda et al. 2016). Embryonic bodies were prepared in liquid marbles during cultivation of embryonic stem cells

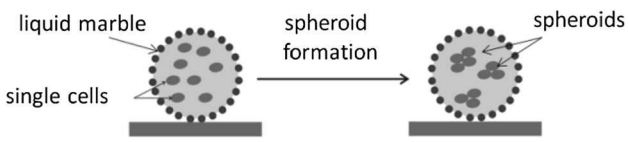

Fig. 2 Spheroid cultivation in a liquid marble

which are key in regenerative medicine (Sarvi et al. 2013). Liquid marbles were also used for the cultivation of murine-derived embryonic stem cells (Oct4b2) and the cell development was monitored by optical-fluorescent microscope due to the expression of oct4-green fluorescent protein (Oct4-GFP). The research was focused on the quality of embryonic bodies by changing parameters, such as the volume of encapsulated medium or cell density (Sarvi et al. 2015). Cell line Hep G2 (hepatocellular carcinoma) was cultivated inside liquid marble, which encouraged the formation of 3D cell structure (Arbatan et al. 2012a). In addition, floating liquid marbles were used for the cultivation of olfactory ensheathing cells (OECs) which have potential for repairing paralysed spinal cord (Vadivelu et al. 2015).

In 2012, the third most common worldwide cancer was colorectal cancer with nearly 1.4 million new patients. Moreover, according to prognosis in 2035 this number will be almost doubled (Ferlay et al. 2015). HT-29 is a human colorectal adenocarcinoma cell line that express carbonic anhydrase IX (CA IX) antigen, a very promising therapeutic marker. In a healthy human body, expression of this antigen is strictly restricted to gastrointestinal tract, but its overexpression and increased activity was observed in many types of hypoxic tumors (Pastorekova et al. 1997; Robertson et al. 2004). Moreover, CA IX can be targeted by monoclonal IgG M75 antibody (Zavada et al. 2000). This system is called active targeting and can be used for cancer targeted drug delivery systems (McDonald et al. 2012).

Cultivation of HT-29 colorectal carcinoma cell line in the form of spheroids in liquid marbles is described for the first time in this paper. Parameters, such as the volume of liquid marbles, number of inoculated cells and cultivation time, were studied to determine optimal conditions for spheroid cultivation and their harvest.

Experimental

Materials

HT-29 human colon adenocarcinoma cell line (ATCC® HTB-38™) was obtained from the American Type Culture Collection (ATCC). Polytetrafluoroethylene particles (PTFE; 35 μm), Dulbecco's Modified Eagle's Medium (DMEM) D6429, foetal bovine serum (FBS) F0804, antibiotic antimycotic solution (A/A) A5955 and Trypan Blue solution T8154 were all purchased from Sigma-Aldrich. Phosphate buffer solution (PBS), 0.02% EDTA solution in PBS and 0.5% trypsin solution in PBS were purchased from the Institute of Molecular Genetics of the ASCR, v.v.i.

Cell cultivation

HT-29 cell line was cultivated in DMEM medium supplemented with 10% FBS and 1% A/A. Before the preparation of liquid marbles, cells were incubated in 5% CO_2 atmosphere at 37 °C until 70–80% confluency.

Liquid marble preparation

Preparation of liquid marbles involved several steps (Fig. 3). First, a layer of PTFE powder was prepared. Then a liquid droplet (suspension of the growth medium with cells) was dropped onto this layer. By gentle shaking particles covered the surface of the aqueous droplet and a liquid marble was formed. The prepared liquid marble was transported into an incubator. During the incubation, spheroids were formed inside the liquid marble.

Various volumes of cell suspensions and various initial concentrations of cells were tested. Table 1 summarizes these parameters. For better orientation in this paper we decided to use a terminology as follows. We marked our samples by two numbers. The first belongs to the volume of liquid marble in μl and the second to the number of inoculated cells in thousands of cells. For example, sample 300/40 means that the liquid marble had the volume of 300 μl and 40,000 cells were inoculated into one marble.

Spheroid harvest

The liquid marbles with encapsulated cells were incubated up to several days and then the formed spheroids were harvested. For spheroid analysis, spheroids had to be removed from the liquid marble. To remove all cells from the liquid marble, the liquid marbles had to be washed three times with PBS. A spheroid pellet was obtained by centrifugation for 3 min at 250 rpm.

Cell proliferation in liquid marbles

In cell proliferation study, standard procedure of trypsinization was used to obtain single cells from the spheroids. The time of the trypsinization was typically 15–30 min depending on the size and the amount of spheroids. The number of cells was calculated using a hemocytometer (Improved Neubauer, Hausser Scientific). The cell viability was determined by the Trypane Blue staining method.

Liquid marble and spheroid characterization

Optical microscope (Olympus CK40) was used for capturing images of the formed spheroids. The static images of liquid marbles were captured by a digital camera (Olympus

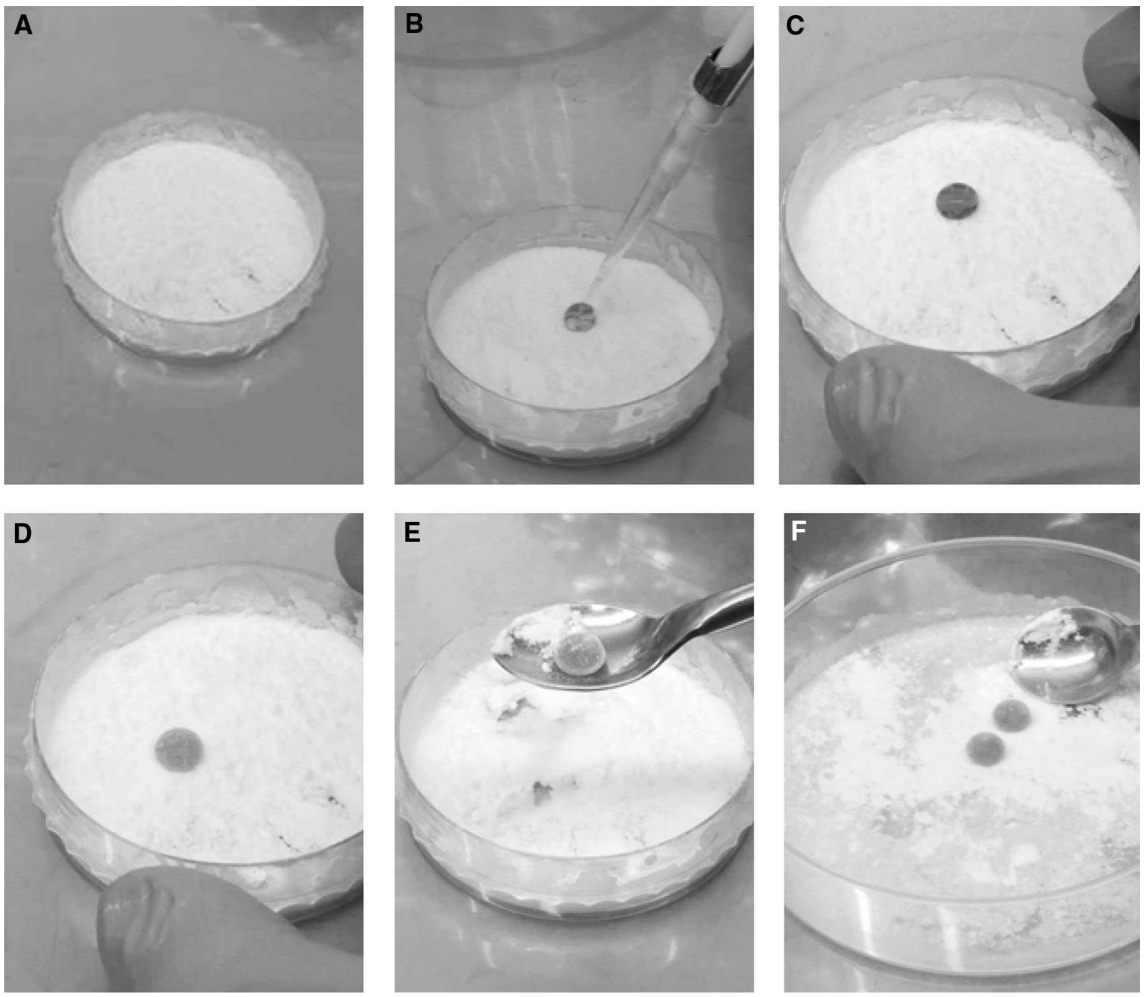

Fig. 3 Liquid marble preparation. **a** Petri dish with PTFE powder. **b** Dropping of liquid medium onto the layer of PTFE powder. **c** Gentle shaking with the dish. **d** Liquid marble covered by PTFE powder. **e** Transportation of the liquid marble by a spoon to another Petri dish. **f** Two prepared liquid marbles

Table 1 Summary of liquid marble samples for spheroid cultivation

Sample	Liquid marble volume/(μl)	Number of cells in one liquid marble	Concentration of inoculate/(cells μl^{-1})
10/1	10	1000	100
10/10	10	10,000	1000
50/1	50	1000	20
50/10	50	10,000	200
100/1	100	1000	10
100/10	100	10,000	100
300/10	300	10,000	33
300/40	300	40,000	133

E-620). Dynamic images were observed with a camera (PixeLINK PL-A662) with time-lapse setting. NIS-Elements imaging software (Laboratory Imaging s r.o., Czech Republic) was then applied for the determination of spheroid number and spheroid parameters (diameter and shape). Only spheroids with a diameter larger than 50 μm were considered (for comparison, the typical diameter of a single HT-29 cell is 14 μm). Spheroid size distributions were evaluated.

Results and discussion

Liquid marble preparation

The first step of this work was to find out optimal conditions for the preparation of liquid marbles that could serve as microbioreactors for cell encapsulation and spheroid cultivation. Therefore, initial experiments were performed without the presence of any cells to find out how to prepare stable liquid marbles with a lifespan of days.

Several powders were tested as a possible coating material for liquid marbles. Soil grains, lycopodium grains,

graphite powder and polytetrafluorethylene (PTFE) powder (the mean particle size of 35 μm) were used for the encapsulation of the liquid growth medium. In accordance with our expectations, the most suitable coating material was the hydrophobic PTFE powder. PTFE powder with the particle size of 35 μm was chosen also by Sarvi et al. (2013) in their study. They were testing two types of PTFE powders (the particle size of 35 and 100 μm) for embryonic spheroid cultivation. They observed that in comparison with a liquid marble shell consisting of 100 μm particles, a shell consisting of 35 μm particles was less adhesive and encouraged cells to form more uniform and compact spheroids.

Cell proliferation in liquid marbles

To determine suitable conditions for spheroid cultivation, liquid marbles of different volumes and with different numbers of inoculated cells were prepared and the number of viable cells was studied during the cultivation (Fig. 4a). Liquid marble nomenclature based on the ratio of liquid marble size and the number of cells in the time of inoculation (as described in the "Experimental" section) will be used in the following text. Let us note that the ratios (sample names) show rounded numbers, real values are summarized in Table 2. This table also contains information about inoculation cell density [C_0 (cells μl^{-1})], maximal cell density [C_{max} (cells μl^{-1})] and the ratio of maximal cell density to inoculation cell density ($R = C_{max}/C_0$).

Aim of this proliferation study was to determine the most suitable day for a spheroid harvest. We decided that it would be a day when the number of viable cells in a liquid marble would reach its maximum. Therefore, measurements of cell viability were stopped after a growth curve maximum was reached. Data of cell viability from Table 2 were obtained from three separate liquid marbles. Liquid marbles with the same numbers of inoculated cells were compared (10/10, 50/10 and 100/10). On the 3rd day of the cultivation, cell numbers were almost the same, (17,300 ± 3800, 19,800 ± 3500 and 18,300 ± 2300), but measurements on the 7th day proved that the smaller liquid marbles could not supply cells with enough nutrients. In the sample 10/10, the number of cells declined on 7100 ± 3900. These results proved our expectations that larger liquid marbles could supply cells with more nutrients for longer time.

To obtain information about the dynamics of cell growth, the data were plotted in a graph (Fig. 4b), where all numbers of cells were divided by the number of inoculated cells. Due to sufficient medium supply, the highest number of cultivated cells in a single liquid marble, which was almost 3.6×10^5 cells, was obtained in the biggest liquid marble (300/40, Fig. 4a). However, the highest proliferation rate was observed in the sample 50/1, which was 38 times higher than the original number (Fig. 4b). This acceleration was achieved due to the lowest inoculation cell density (12 cells μl^{-1}), but in comparison with other cases, the maximum cell number was just 23,000 ± 6000 cells per liquid marble. The highest cell density, 1928 cells μl^{-1}, was found in the case 100/10 (C_{max} in Table 2). The lowest growth rate and the total number of cells were observed in samples with the smallest volume (10/1 and 10/10). Due to the lack of nutrients, cells did not proliferate as much as in the other cases, and their growth reached the maximum on the 3rd day.

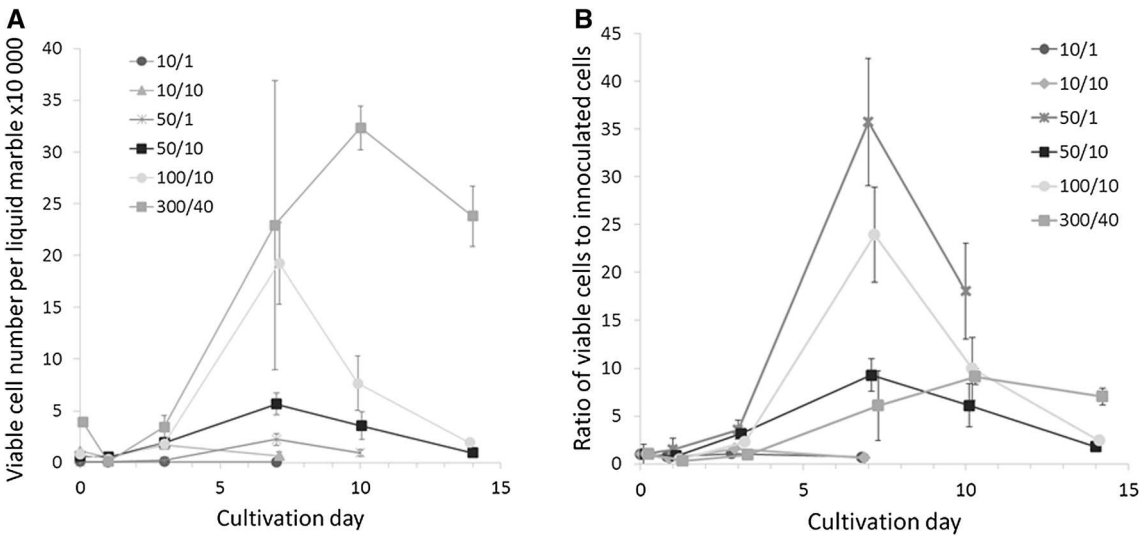

Fig. 4 **a** Number of viable cells encapsulated inside a liquid marble during the cultivation. **b** Proliferation rate of cells inside a liquid marble during the cultivation

Table 2 Dependence of the number of viable cells per liquid marble on the cultivation time and initial conditions

Sample	Day of cultivation						C_0*	C_{max}*	R
	0	1	3	7	10	14			
10/1	1000 ± 400	700 ± 400	1000 ± 400	700 ± 300			100 ± 40	100 ± 40	1
10/10	11,100 ± 1300	5500 ± 2800	17,300 ± 3800	7100 ± 3900			1110 ± 130	1730 ± 380	1.6
50/1	600 ± 700	1000 ± 700	2300 ± 700	23,000 ± 6000	11,600 ± 3200		12 ± 14	460 ± 120	38.3
50/10	6200 ± 2500	5300 ± 1000	19,800 ± 3500	57,800 ± 10,600	38,100 ± 14,100	11,000 ± 2700	124 ± 50	1156 ± 212	9.3
100/10	8100 ± 900	3500 ± 500	18,300 ± 2300	192,800 ± 39,700	79,900 ± 26,300		81 ± 9	1928 ± 397	23.8
300/40	39,400 ± 4200	11,300 ± 2300	35,900 ± 12,000	238,800 ± 144,500	358,400 ± 32,500	277,400 ± 33,800	131 ± 14	1195 ± 108	9.1

* C_0 (cells μl^{-1}), C_{max} (cells μl^{-1})

It was concluded that samples 50/10, 100/10 and 300/40 were the most suitable candidates to be bioreactors for spheroid cultivation, because they had the highest number of viable cells from all tested samples and high growth rates at the same time. Although sample 50/1 had the highest growth rate, the cell density during the cultivation was still low in comparison with the other cases. We anticipated that the higher the number of viable cells was, the higher the spheroid harvest could be. Therefore, the most suitable day for harvesting of spheroids is at the curve maximum, it means the 3rd day for the samples 10/1 and 10/10, the 7th day for the samples 50/1, 50/10 and 100/10 and the 10th day for the sample 300/40.

Spheroid characterization

The proliferation study discussed above focused only on the total numbers of viable cells present in liquid marbles. Results from this study did not say anything about spheroid development, their amount at the time of harvest or about their parameters, such as shape or size distribution. However, this information is essential for further spheroid applications. To better understand spheroid development, 100/10 liquid marbles were prepared and the growth of spheroids was observed at different times (2, 4.5 and 24 h and then 3 and 8 days after inoculation) under an optical microscope (Fig. 5).

The first observation of a liquid marble content was done 2 h after the inoculation (Fig. 5a). At this time, the cells were still separated in the suspension. The second monitoring was performed 4.5 h after the inoculation, when few small clusters consisting of several cells were already formed (Fig. 5b).

24 h after the inoculation, the cells formed clusters consisting of a few tens of cells, but their shape was non-spherical and non-uniform (Fig. 5c). Clusters with almost spherical shape were harvested on the 3rd day of cultivation (Fig. 5d). The aggregates seemed almost ready for the harvest, but they were not stable. During the manipulation, we had to treat them very carefully to prevent their breakage.

The final harvest was made on the 8th day after the inoculation (Fig. 5e). Spheroids were nicely spherical and stable due to the building of a strong extracellular matrix and only few single cells were observed in the suspension.

According to our findings about the number of viable cells inside the liquid marbles and the spheroid development in time, we have chosen the 8th day of cultivation as the optimal one for harvesting of spheroids from the liquid marbles. Figure 5 provides qualitative information about the formed spheroids. The size distribution of the formed spheroids can be found in Fig. 6.

Figure 6 compares the number of harvested spheroids at the 8th day after inoculation obtained from different types

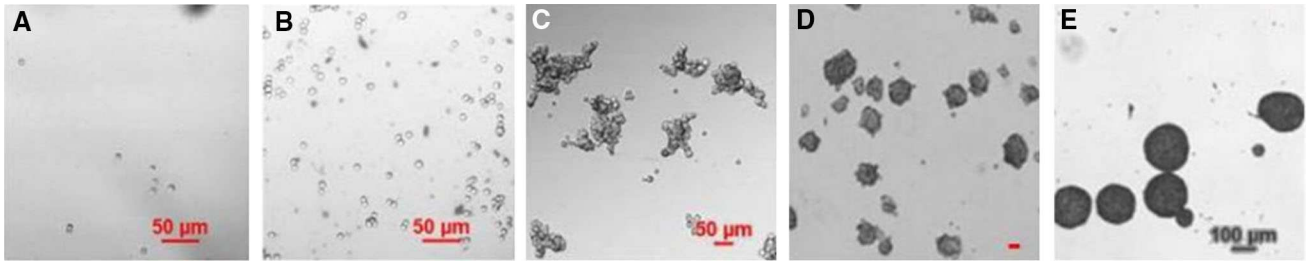

Fig. 5 Optical microscope images of a content of 100/10 liquid marbles **a** 2 h, **b** 4.5 h, **c** 1 day, **d** 3 days and **e** 7 days after inoculation. *Scale bars* represent 50 µm (in **a**–**d**) and 100 µm (in **e**)

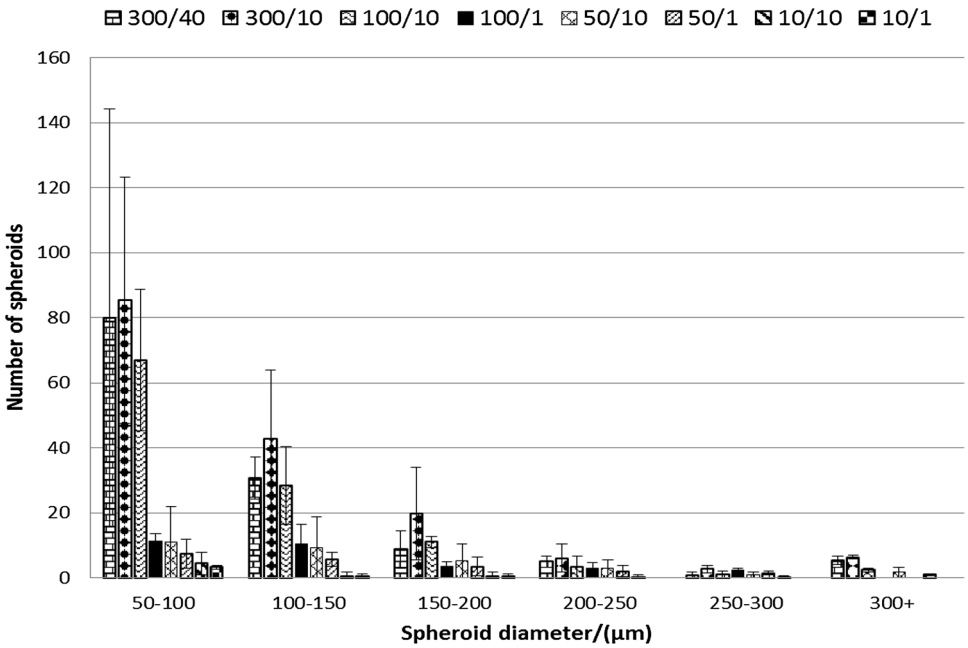

Fig. 6 Comparison of harvested spheroids obtained 8 days after inoculation from different types of liquid marbles. Spheroid size distribution according to number

of liquid marbles (various volumes of liquid marbles and numbers of inoculated cells). For every type of a liquid marble, four liquid marbles were analysed. This graph represents the size distribution according to the number of spheroids in each category. In this representation the highest harvest from one liquid marble (it means the total number of spheroids in the size range of 50–300 µm) was obtained from the largest liquid marbles, such as 300/40 or 300/10, but also 100/10 had a large harvest. In the rest of the samples, there was a visibly smaller yield. These results are in accordance with our observations from the cell proliferation study, where the samples 300/40 and 100/10 contained much more cells than the rest of the samples around the 8th day of the cultivation. Intuitively, a larger number of cells should form a larger number of spheroids. Sarvi et al. (2013) came to the same conclusion. They studied the influence of cell seeding number on the embryonic spheroid formation while keeping the size of liquid marbles constant (300 µl) and found out that the highest number of inoculated cells (20,000 cells) led to the formation of the highest number of spheroids.

The primary results from image analysis are based on number distributions (Fig. 6). Figure 7 shows the volume fraction of spheroids in each size category. If we look at the number distributions, we can see that in all samples almost 50% of all spheroids inside the liquid marble represent spheroids with the size of 50–100 µm. Nevertheless, from the volume distribution we can see that the largest peaks represent spheroids larger than 300 µm. Assuming constant density of all cells, the graph in Fig. 7 represents also the mass distribution. It tells us that the majority of cells inside the liquid marbles are part of large spheroids. This phenomenon was mainly pronounced in the case of the 10/10 samples, where most of the cells aggregated into one big spheroid.

Although the largest liquid marbles (300 µl) contained the highest number of spheroids, during manipulation or cultivation many marbles broke. A crack, shown in Fig. 8a,

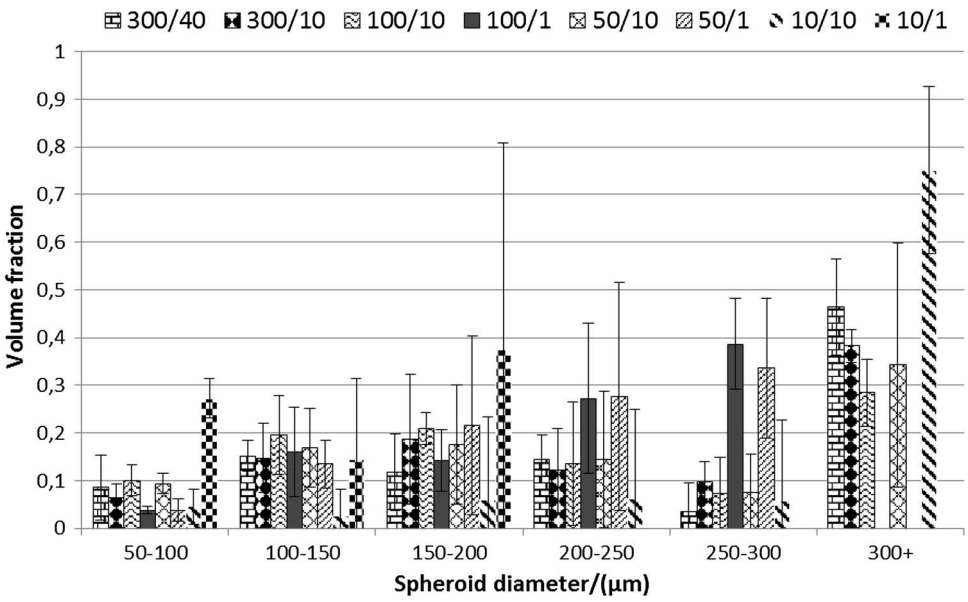

Fig. 7 Spheroid size distribution from Fig. 6 expressed according to volume

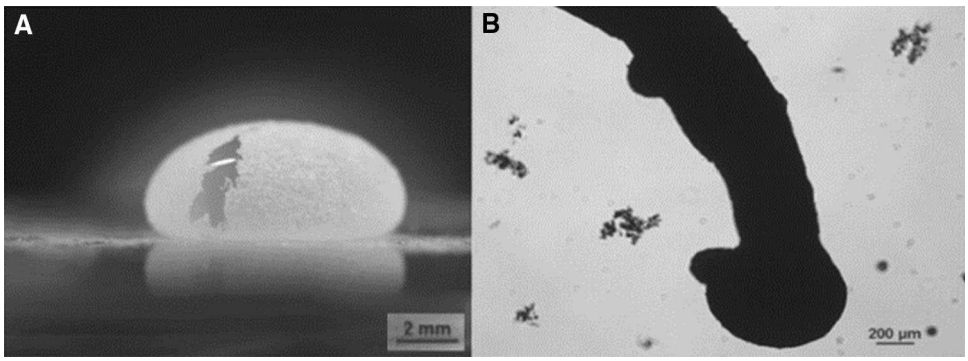

Fig. 8 **a** Photograph of a breakage of a 300 µl PTFE liquid marble shell. **b** Optical microscope image of a non-spherical agglomerate formed inside of a 300 µl liquid marble

could lead to the collapse of a liquid marble. Manipulation with a smaller volume was easier. Another disadvantage of large marbles was that non-spherical agglomerates were formed inside them, as shown in Fig. 8b. This huge cluster was made due to the flat bottom of a liquid marble, and thus cells behaved more similarly to a conventional 2D cell culture. In liquid marbles with a smaller volume, agglomerates with non-spherical shape were not observed.

Conclusions

The cultivation of HT-29 colorectal carcinoma cell line in the form of spheroids (cell agglomerates) inside liquid marbles was presented for the first time in this study. To determine optimal conditions for spheroid formation, different types of liquid marbles were prepared and parameters, such as the number of viable cells, the proliferation rate, the number of spheroids and the spheroid size distribution, were determined during the cultivation. Due to easier manipulation and high spheroid harvest, liquid marbles of the volume of 100 µl and with 10,000 inoculated cells were chosen as the most suitable ones for spheroid cultivation. However, the most predictable harvest of spheroids was reached when liquid marbles of the volume of 10 µl with 10,000 inoculated cells were used for spheroid growth. In this case, most of the cells formed one big spheroid. The main challenges for further spheroid studies will be the preparation of spheroids with a uniform size and co-cultivation of two cell lines in the form of spheroids inside liquid marbles.

Acknowledgement Financial support from specific university research (MSMT No. 20-SVV/2016) and from AZV (16-34342A) is gratefully acknowledged.

References

Alvarez-Pérez J, Ballesteros P, Cerdán S (2005) Microscopic images of intraspheroidal pH by ^{1}H magnetic resonance chemical shift imaging of pH sensitive indicators. MAGMA 18(6):293–301. doi:10.1007/s10334-005-0013-z

Arbatan T, Al-Abboodi A, Sarvi F, Chan PPY, Shen W (2012a) Tumor inside a pearl drop. Adv Healthc Mater 1(4):467–469. doi:10.1002/adhm.201200050

Arbatan T, Li L, Tian J, Shen W (2012b) Liquid marbles as micro-bioreactors for rapid blood typing. Adv Healthc Mater 1(1):80–83. doi:10.1002/adhm.201100016

Aussillous P, Quere D (2001) Liquid marbles. Nature 411(6840):924–927

Aussillous P, Quéré D (2006) Properties of liquid marbles. Proc R Soc A Math Phys Eng Sci 462(2067):973–999. doi:10.1098/rspa.2005.1581

Campbell A, Wicha MS, Long M (1985) Extracellular matrix promotes the growth and differentiation of murine hematopoietic cells in vitro. J Clin Investig 75(6):2085–2090. doi:10.1172/JCI111928

Curcio E, Salerno S, Barbieri G, De Bartolo L, Drioli E, Bader A (2007) Mass transfer and metabolic reactions in hepatocyte spheroids cultured in rotating wall gas-permeable membrane system. Biomaterials 28(36):5487–5497. doi:10.1016/j.biomaterials.2007.08.033

DiPersio CM, Jackson DA, Zaret KS (1991) The extracellular matrix coordinately modulates liver transcription factors and hepatocyte morphology. Mol Cell Biol 11(9):4405–4414. doi:10.1128/MCB.11.9.4405

Eshtiaghi N, Hapgood KP (2012) A quantitative framework for the formation of liquid marbles and hollow granules from hydrophobic powders. Powder Technol 223:65–76. doi:10.1016/j.powtec.2011.05.007

Fennema E, Rivron N, Rouwkema J, van Blitterswijk C, de Boer J (2013) Spheroid culture as a tool for creating 3D complex tissues. Trends Biotechnol 31(2):108–115. doi:10.1016/j.tibtech.2012.12.003

Ferlay J, Soerjomataram I, Dikshit R, Eser S, Mathers C, Rebelo M, Parkin DM, Forman D, Bray F (2015) Cancer incidence and mortality worldwide: sources, methods and major patterns in GLOBOCAN 2012. Int J Cancer 136(5):E359–E386. doi:10.1002/ijc.29210

Harley BAC, Kim H, Zaman MH, Yannas IV, Lauffenburger DA, Gibson LJ (2008) Microstructure of three-dimensional scaffolds influences cell migration behavior via junction interactions. Biophys J 95(8):4013–4024. doi:10.1529/biophysj.107.122598

Ledda S, Idda A, Kelly J, Ariu F, Bogliolo L, Bebbere D (2016) A novel technique for in vitro maturation of sheep oocytes in a liquid marble microbioreactor. J Assist Reprod Genet. doi:10.1007/s10815-016-0666-8

McDonald PC, Winum J-Y, Supuran CT, Dedhar S (2012) Recent developments in targeting carbonic anhydrase IX for cancer therapeutics. Oncotarget 3(1):84–97. doi:10.18632/oncotarget.422

Pastorekova S, Parkkila S, Parkilla AK, Opatovsky R, Zelnik V, Saarnio J, Pastorek J (1997) Gastroenterology 112(2):398–408. doi:10.1053/gast.1997.v112.pm9024293

Pike N, Richard D, Foster W, Mahadevan L (2002) How aphids lose their marbles. Proc R Soc Lond B 269(1497):1211–1215. doi:10.1098/rspb.2002.1999

Robertson N, Potter C, Harris AL (2004) Role of carbonic anhydrase IX in human tumor cell growth, survival, and invasion. Cancer Res 64(17):6160–6165. doi:10.1158/0008-5472.CAN-03-2224

Sarvi F, Arbatan T, Chan PPY, Shen W (2013) A novel technique for the formation of embryoid bodies inside liquid marbles. R Soc Chem Adv 3(34):14501–14508. doi:10.1039/C3RA40364E

Sarvi F, Jain K, Arbatan T, Verma PJ, Hourigan K, Thompson MC, Shen W, Chan PPY (2015) Cardiogenesis of embryonic stem cells with liquid marble micro-bioreactor. Adv Healthc Mater 4(1):77–86. doi:10.1002/adhm.201400138

Tian J, Arbatan T, Li X, Shen W (2010) Liquid marble for gas sensing. Chem Commun 46(26):4734–4736. doi:10.1039/C001317J

Vadivelu RK, Ooi CH, Yao R-Q, Tello Velasquez J, Pastrana E, Diaz-Nido J, Lim F, Ekberg JAK, Nguyen N-T, St John JA (2015) Generation of three-dimensional multiple spheroid model of olfactory ensheathing cells using floating liquid marbles. Sci Rep 5:15083. doi:10.1038/srep15083

Yeung T, Georges PC, Flanagan LA, Marg B, Ortiz M, Funaki M, Zahir N, Ming W, Weaver V, Jamney PA (2005) Effects of substrate stiffness on cell morphology, cytoskeletal structure, and adhesion. Cell Motil Cytoskelet 60(1):24–34. doi:10.1002/cm.20041

Zavada J, Zavadova Z, Pastorek J, Biesova Z, Jezek J, Velek J (2000) Human tumour-associated cell adhesion protein MN/CA IX: identification of M75 epitope and of the region mediating cell adhesion. Br J Cancer 82(11):1808–1813. doi:10.1054/bjoc.2000.1111